

**PH.D. DISSERTATION**

**Design-Build-Operate Energy Information Modeling for  
Occupant-oriented Predictive Building Control**

**Jie Zhao**

Center for Building Performance and Diagnostics

School of Architecture

Carnegie Mellon University

Pittsburgh, Pennsylvania, United States

February 23, 2015

Doctoral Committee

**Khee Poh Lam**, Ph.D., RIBA, Professor (Chair)

School of Architecture, Carnegie Mellon University

**Vivian Loftness**, FAIA, LEED AP, University Professor,

School of Architecture, Carnegie Mellon University

**B. Erik Ydstie**, Ph.D., Professor,

Chemical Engineering, Electrical Engineering (Courtesy), Carnegie Mellon University

# **Design-Build-Operate Energy Information Modeling for Occupant-Oriented Predictive Building Control**

A Dissertation Submitted in Partial Fulfillment of the Requirements for  
the Degree of Doctor of Philosophy in Building Performance and Diagnostics  
in the School of Architecture, Carnegie Mellon University

by

**Jie Zhao**

Center for Building Performance and Diagnostics

School of Architecture

Carnegie Mellon University

Pittsburgh, Pennsylvania, United States

Copyright © Jie Zhao, 2015. All rights reserved.

# Copyright Declaration

---

I hereby declare that I am the sole author of this thesis.

I authorize Carnegie Mellon University, Pittsburgh, PA, USA to lend this thesis to other institutions or individuals for the purpose of scholarly research.

I authorize Carnegie Mellon University, Pittsburgh, PA, USA to reproduce this thesis by photocopying or by other means, in total or in part, at the request of other institutions or individuals for the purpose of scholarly research.

*The dissertation is dedicated to my wonderful, loving, and  
supportive wife – Shu Wang, and my beloved parents Chunqiu  
Zhao and Ruiying Yang.*

# Acknowledgement

---

The completion of this dissertation is and will always be one of the most important episodes in my life. I would like to express my sincerely gratitude to the following people.

I would like to give my deepest appreciation to my PhD advisor and committee chair – Professor Khee Poh Lam. For the past four and half years, I have learned so much from him about in-depth knowledge, research methods, teaching skills, and social etiquette, but more importantly, he shows me how an optimistic attitude can make a difference in our daily life. Also, I would never forget his generous support for me to travel around the world to present our research in conferences. The experience is extremely important to me academically and socially.

I would like to thank my PhD committee member Professor Erik Ydstie from Chemical Engineering department. I learned very important concepts and algorithms about model predictive and adaptive control theories from his class that were used in my research. He also helped me with several critical technical problems during the hardest time of my dissertation work.

I would like to thank my PhD committee member Professor Vivian Loftness. She taught me about the human aspects of the built environment. I also learned from her that looking at a bigger picture using the system integration thinking is as important as focusing on solving a specific problem in the built environment.

I would like to give my sincere gratitude to Richard Piacentini, Jason Wirick, Craig Power, Jason Fabus, Emily Kalnicky, and everyone else who have participated and helped in my case study at the Phipps Conservatory and Botanical Gardens. The case studies would not be possible without their generous and continuous support for the past four and half years.

I also want to thank Bertrand Lasternas, Ray Yun, Omer Karaguzel, Haopeng Wang, Alejandra Munoz Munoz, Jihyun Park, Tajin Biswas, Flore Marion, Shalini Ramesh, Meiwei Qi, Xuan Luo, Yogi Venkata Gopalan, Bing Dong, Samira Ahmadi, Yuebin Yu, Yun Gu, Mike Mihuc from OSIssoft, Juan Du and Xue Yang from Chemical Engineering, and Bill Collinge from the University of Pittsburgh, for their valuable direct or indirect contributions to my dissertation work. Their guidance, assistance, and inspirations are greatly appreciated.

I would like to give special thanks to Sophie Wodzack from CMU Global Communication Center, who gave me valuable comments and suggestions on the writing of my dissertation.

In addition, I would like to express my appreciation to the professors who have taught me and/or worked with me during the past four and half years. I gained much of knowledge and practical experience from them. They are Volker Hartkopf, Omer Akin, David Kosbie, Nina Baird, Gerry Mattern, Ramesh Krishnamurti, Steve Lee, John Folan, Carolyn P. Rosé from Computer Science, Shamena Anwar and Jeffrey Kupfer from Heinz School, as well as the teaching staff at the CMU Intercultural Communication Center.

Last but not least, I would like to acknowledge my wonderful friends who have made my life so amazing in the US. They are Woobok Lee, Boyuan Li, Freddie Croce, Yanfei Wang, Lingwei Zhan, I Shan Tam, Rui Zhang, Yang Hu, Rongpeng Zhang, Avigail Oren and Kevin Seal, Xiaonan Liu, Yuan Tian and Ryan Huang, Ziad and Niveen Ewais, Ruizhe Liu, Chen Ling, Jue

Yuan, Chao Ding, Liming Zhang, Mingming Wu, Kristen Magnuson, and all the friends in the Intelligent Workplace and School of Architecture.

The studies in this dissertation are primarily funded by National Science Foundation (NSF) Emerging Frontiers in Research and Innovation (EFRI) in Science in Energy and Environmental Design (SEED) (Award #: 1038139). Some equipment in the occupant behavior case studies is funded by the Energy Efficient Buildings Hub Consortium (Subtask 6.4 Award# EE0004261) and Phipps Conservatory and Botanical Gardens.

# Abstract

---

Green buildings aim to save land, energy, water, and material, as well as to create a healthy and comfortable environment for their occupants throughout the life-cycle. One of the primary goals for the design of green buildings is reducing operating energy costs. Mainly due to the energy performance requirements of various green building rating systems, building energy modeling (BEM) is being increasingly used in the building industry, which definitely improves building energy efficiency through code and standard compliances. However, as a scientific and standardized method, using BEM can provide far more benefits than just code and standard compliances. BEM can be used for many other purposes at different stages of the building life-cycle.

This dissertation has developed and demonstrated the concept of Design-build-operate Energy Information Modeling (DBO-EIM) infrastructure, which can be used at different stages of the building life-cycle to improve energy and thermal comfort performance. The whole process is tested using a medium-size office building in Pittsburgh, PA.

At the design stage, for the purpose of design decision making a parametric BEM process is demonstrated in the test-bed building. The case study results show that the proposed design case building has better energy performance than the baseline, design alternatives, and various benchmark buildings. At the commissioning and early operation stages, an EnergyPlus model calibration method is introduced using empirical data that are collected from the test-bed building. The final calibrated model has a mean biased error of 1.27% and a coefficient of



variation of the root mean squared error of 6.01%. This calibration method provides a scientific and systematic framework to conduct high accuracy EnergyPlus model calibration. At the operation stage, on the basis of the calibrated EnergyPlus model, an occupant-oriented mixed-mode EnergyPlus predictive control (OME<sup>+</sup>PC) system is developed. Given the Pittsburgh weather context and current operation assumptions, the simulation results suggest a potential 29.37% reduction in annual HVAC energy consumption. In addition, OME<sup>+</sup>PC enables building occupants to control their thermal environment through an internet-based dashboard.

Several important research findings are also concluded from the studies in the DBO-EIM development process that may benefit future work in the building science realm, including the development of an occupant behavior modeling method, the integration of the real-time building operation data collection system, an passive cooling control simulation study, and an occupant subjective thermal comfort field study.

In order to show the applicability of the Design-build-operation Energy Information Modeling infrastructure, the process is demonstrated again in a generic Department of Energy prototype medium office EnergyPlus model. Step-by-step instructions and computation time are documented to facilitate future studies.

In summary, this dissertation has demonstrated that an original design stage EnergyPlus model can be updated and utilized through the entire DBO-EIM process. Compared to typical building operation, implementing this process can achieve better energy performance and maintain occupant thermal comfort.

# Table of Contents

---

Acknowledgement ..... I

Abstract ..... IV

Table of Contents ..... VI

List of Figures ..... XI

List of Tables ..... XVIII

Chapter 1. Introduction ..... 1

    1.1. Background ..... 1

    1.2. Literature review ..... 4

        1.2.1. Occupant behavior in buildings ..... 4

        1.2.2. BEM for design decision making and standard compliance..... 10

        1.2.3. BEM model calibration..... 11

        1.2.4. Building energy model-based predictive control ..... 14

        1.2.5. Summary of literature review ..... 19

    1.3. Objectives and hypothesis..... 23

    1.4. Dissertation chapter overview..... 24

Chapter 2. Design-build-operate energy information modeling (DBO-EIM) infrastructure and energy modeling at the design stage ..... 26

VI

2.1. Overview .....	26
2.2. Case study on BEM for design decision making .....	29
2.2.1. Creation of energy models .....	31
2.2.2. Building load analysis .....	34
2.2.3. Building energy use intensity analysis .....	36
2.2.4. Indoor temperature analysis .....	38
2.3. Summary .....	38
Chapter 3. Design-stage EnergyPlus model calibration .....	40
3.1. Overview .....	40
3.2. Test-bed building model creation and data collection .....	44
3.3. Weather information for EnergyPlus input .....	45
3.4. Occupant behavior and schedule modeling .....	46
3.4.1. Experiment design .....	46
3.4.2. Nominal classification algorithms .....	49
3.4.3. Numeric regression algorithms .....	53
3.4.4. Pilot study at the Intelligent Workplace .....	56
3.4.5. Case study at the Center for Sustainable Landscapes .....	62
3.5. Daylight/Lighting and equipment operation calibration .....	77
3.6. Passive/Active HVAC system operation calibration .....	87

3.6.1. Active HVAC system model calibration .....	87
3.6.2. Passive HVAC system model calibration .....	89
3.6.3. Passive/Active HVAC system calibration result .....	90
3.7. Whole building energy model calibration result.....	95
3.8. Summary .....	98
Chapter 4. Occupant-oriented mixed-mode EnergyPlus predictive control (OME <sup>+</sup> PC) .....	100
4.1. Overview .....	100
4.2. Baseline EnergyPlus model-based building control .....	101
4.3. EnergyPlus Predictive Control (E <sup>+</sup> PC) .....	104
4.3.1. E <sup>+</sup> PC problem description.....	104
4.3.2. E <sup>+</sup> PC implementation.....	107
4.3.3. Result comparison between baseline and E <sup>+</sup> PC.....	110
4.4. Mixed-mode passive/active E <sup>+</sup> PC (ME <sup>+</sup> PC).....	117
4.4.1. CO <sub>2</sub> concentration as a constraint .....	118
4.4.2. ME <sup>+</sup> PC design and implementation.....	120
4.4.3. Result comparison between E <sup>+</sup> PC and ME <sup>+</sup> PC .....	122
4.5. Occupant-oriented ME <sup>+</sup> PC (OME <sup>+</sup> PC) .....	127
4.5.1. Occupant subjective feedback data collection .....	128
4.5.2. Real-time BAS data collection.....	130

4.5.3. Occupant subjective feedback and thermal environment data analysis .....	131
4.5.4. OME <sup>+</sup> PC design and implementation .....	139
4.5.5. Result comparison between ME <sup>+</sup> PC and OME <sup>+</sup> PC .....	145
4.6. Summary .....	148
Chapter 5. Conclusions .....	151
5.1. Summary of findings.....	151
5.1.1. Hypothesis testing results .....	151
5.1.2. Other research findings .....	153
5.2. Contributions.....	155
5.3. Future work.....	156
References .....	158
Appendices.....	169
A. Modeling process at the design stage.....	169
B. Model calibration process at the construction, commissioning and early operation stages	171
C. OME <sup>+</sup> PC development process at the operation stage .....	173
C.1. Software platform.....	173
C.2. Configure EnergyPlus model .....	174
C.3. Configure BCVTB files .....	177
C.4. Configure data transfer in Matlab/Simulink.....	182

C.5. Configure outside data input sources in Matlab/Simulink .....	184
C.6. Update control algorithms in Matlab/Simulink.....	185
C.7. Run the co-simulation model in Matlab/Simulink .....	190
C.8. Demo development results .....	193

# List of Figures

---

Figure 1 the potential value of BEM in the building life-cycle. ....	2
Figure 2 Measured/Design EUI by LEED level, with medians (Frankel and Turner, 2008). ....	12
Figure 3 DBO-EIM Infrastructure. ....	28
Figure 4 Satellite map of the CSL building (Source: Google Map <a href="https://www.google.com/maps/@40.4320873,-79.9487346,991a,35y,39.17t/data=!3m1!1e3">https://www.google.com/maps/@40.4320873,-79.9487346,991a,35y,39.17t/data=!3m1!1e3</a> ). .	30
Figure 5 Photos of the CSL building (left: exterior, right: interior). ....	30
Figure 6 Baseline (on the left) and PDC (on the right) models in the DesignBuilder program. ..	33
Figure 7 Calculated building cooling and heating design loads of the six models. ....	35
Figure 8 Annul EUI of the design stage energy models. ....	37
Figure 9 Annual EUI of various benchmark and the CSL proposed design case models. ....	38
Figure 10 Input assumptions and output results of the building energy model. ....	41
Figure 11 EnergyPlus whole building energy model calibration method. ....	43
Figure 12 Screen shot of the CSL building model in the DesignBuilder program. ....	44
Figure 13 Dry bulb temperature comparison between the AMY2013 and TMY weather data. ..	45
Figure 14. Plug Load meter data and ground truth data collection architecture (The images of Fitbit <sup>®</sup> , Plugwise <sup>®</sup> , and ZigBee <sup>®</sup> are from (Fitbit, 2013a), (Plugwise, 2013), and (ZigBee, 2014)). .....	48

Figure 15 True value and predicted value of Occupant #1 in a typical work day. ....	59
Figure 16 True value and predicted value of occupancy schedule in a typical work day. ....	62
Figure 17 The statistics of weekdays and weekends (holidays) in the study.....	63
Figure 18 The statistics of participants in the study (number of people is shown in the graph). .	64
Figure 19 The statistics of metered office appliances in the study. ....	65
Figure 20 Attributes and class value parallel coordination plots of occupant C (Value on the y-axis: power consumption data and types of behavior).....	67
Figure 21 Attributes and class value parallel coordination plots of occupant F (Value on the y-axis: power consumption data and types of behavior).....	68
Figure 22 C4.5 decision tree models of occupant C's behavior. ....	69
Figure 23 C4.5 decision tree models of occupant F's behavior.....	69
Figure 24. Comparison of ground truth and model predicted value for occupant F.....	70
Figure 25. Average weekday occupancy schedule with 95% confidence interval at the CSL building. ....	71
Figure 26. Average occupancy schedule comparison for different weekdays at the CSL building. ....	72
Figure 27. Total attribute weights comparison by appliance type. ....	74
Figure 28. Group schedule predictions and the ground truth comparison in a typical week.....	76
Figure 29. Group schedule predictions and the group truth comparison in a typical weekday....	76
Figure 30 The inverse calibration procedure. ....	78



Figure 31 Interior equipment hourly power input schedule (The calibrated interior equipment power density is $29\text{W/m}^2$ ).....	80
Figure 32 Interior lighting hourly power input schedule (The calibrated lighting power density is $29\text{W/m}^2$ ).....	80
Figure 33 Exterior lighting hourly power input schedule (The calibrated exterior total lighting power 600W). ....	81
Figure 34 Exterior equipment hourly power input schedule (The calibrated total exterior equipment power is 2560W).....	81
Figure 35 Interior equipment hourly power consumption output.....	82
Figure 36 Interior lighting hourly power consumption output. ....	83
Figure 37 Exterior equipment hourly power consumption output.....	83
Figure 38 Exterior lighting hourly power consumption output. ....	84
Figure 39 Interior equipment monthly energy consumption output. ....	85
Figure 40 Interior lighting monthly energy consumption output.....	85
Figure 41 Exterior equipment monthly energy consumption output.....	86
Figure 42 Exterior lighting monthly energy consumption output. ....	86
Figure 43 Heating season zone air temperature setpoints comparison. ....	91
Figure 44 Cooling season zone air temperature setpoints comparison.....	91
Figure 45 Swing season zone air temperature setpoints comparison. ....	92
Figure 46 Heating season zone air temperature comparison. ....	93

Figure 47 Cooling season zone air temperature comparison. ....	93
Figure 48 Swing season zone air temperature comparison. ....	94
Figure 49 Monthly HVAC energy consumption calibration result. ....	95
Figure 50 Total annual EUI comparison for the CSL building. ....	97
Figure 51 Air loop HVAC diagram and control/sensing points. ....	103
Figure 52 Baseline control implementation schema. ....	104
Figure 53 E <sup>+</sup> PC implementation schema. ....	107
Figure 54 E <sup>+</sup> PC receding horizon mechanism. ....	109
Figure 55 Outdoor temperature and control variables of the baseline and E <sup>+</sup> PC in the heating season. ....	111
Figure 56 Energy performance of the baseline and E <sup>+</sup> PC in the heating season. ....	112
Figure 57 Thermal comfort performance of the baseline and E <sup>+</sup> PC in the heating season. ....	112
Figure 58 PMV distribution in unoccupied hours. ....	114
Figure 59 PMV distribution in occupied hours. ....	114
Figure 60 Outdoor temperature and control variables of the baseline and E <sup>+</sup> PC in the cooling season. ....	115
Figure 61 One week plot of energy performance of the baseline and E <sup>+</sup> PC in the cooling season. ....	116
Figure 62 One day plot of energy performance of the baseline and E <sup>+</sup> PC in the cooling season. ....	117

Figure 63 Thermal comfort performance of the baseline and E <sup>+</sup> PC in the cooling season. ....	117
Figure 64 ME <sup>+</sup> PC implementation schema.....	120
Figure 65 Window opening control logic. ....	121
Figure 66 Outdoor temperature and control variables of E <sup>+</sup> PC and ME <sup>+</sup> PC in the swing season. .....	123
Figure 67 One week plot of the power consumptions of the active mode baseline, mixed-mode baseline, E <sup>+</sup> PC, and ME <sup>+</sup> PC in the swing season. ....	124
Figure 68 One week total HVAC energy consumption of the active mode baseline, mixed-mode baseline, E <sup>+</sup> PC, and ME <sup>+</sup> PC in the swing season. ....	125
Figure 69 Thermal comfort performance of E <sup>+</sup> PC and ME <sup>+</sup> PC in the swing season. ....	126
Figure 70 PMV distribution in unoccupied and occupied hours in the swing season. ....	127
Figure 71 Internet-based occupant subjective feedback data collection system.....	129
Figure 72 PI system data collection system architecture for the CSL building. ....	131
Figure 73 Statistics of occupants' effective voted instances during the experiment period. ....	132
Figure 74 Marginal plot of air temperature vs. comfort vote of Subject A. ....	133
Figure 75 Marginal plot of relative humidity vs. comfort vote of Subject A. ....	133
Figure 76 Marginal plot of clothing insulation vs. comfort vote of Subject A.....	134
Figure 77 Marginal plot of air temperature vs. comfort vote of Subject B. ....	135
Figure 78 Marginal plot of relative humidity vs. comfort vote of Subject B. ....	135
Figure 79 Marginal plot of clothing insulation vs. comfort vote of Subject B. ....	136

Figure 80 Marginal plot of air temperature vs. comfort vote of Subject C. ....	137
Figure 81 Marginal plot of relative humidity vs. comfort vote of Subject C. ....	137
Figure 82 Marginal plot of clothing insulation vs. comfort vote of Subject C. ....	138
Figure 83 OME <sup>+</sup> PC implementation schema. ....	139
Figure 84 Weather forecast data acquisition schema. ....	141
Figure 85 Scatter plot of the measured data versus predicted value (A – global solar radiation, B – direct solar radiation). ....	143
Figure 86 Thermal comfort performance of different zones in OME <sup>+</sup> PC in the swing season..	146
Figure 87 Outdoor temperature and control variables of ME <sup>+</sup> PC and OME <sup>+</sup> PC in the swing season. ....	147
Figure 88 One week plot of the power consumptions of ME <sup>+</sup> PC and OME <sup>+</sup> PC in the swing season. ....	147
Figure 89 Different control schemes, as well as their methods and outcomes. ....	150
Figure 90 DOE prototype medium office building model. ....	175
Figure 91 MLE+ co-simulation function block. ....	182
Figure 92 Complete control system model in Simulink. ....	187
Figure 93 Block B of the control system model in Simulink. ....	188
Figure 94 Block C of the control system model in Simulink. ....	189
Figure 95 Block C-2 of the control system model in Simulink. ....	190
Figure 96 PMV simulation results of the demo model. ....	194



# List of Tables

---

Table 1 Occupants’ “active” influence in buildings. ....	5
Table 2 Direct approach of occupant behavior recognition and modeling studies in the building field. ....	8
Table 3 Indirect approach of occupant behavior modeling studies in the building field.....	9
Table 4 Summary of the studies with direct contributions. ....	21
Table 5 Baseline, design alternatives (DAs), and proposed design case (PDC) model assumptions. ....	32
Table 6 ASHRAE 90.1-2007 baseline building energy model assumptions. ....	32
Table 7 Alternative design building energy model assumptions. ....	33
Table 8 Occupant individual behavior ground truth. ....	48
Table 9 An example of the training dataset for the individual behavior learning. ....	49
Table 10 An example of the training dataset for the group schedule learning. ....	54
Table 11 Occupant behavior recognition result (percentage of correctly classified instances / kappa statistic). ....	58
Table 12 Occupancy schedule prediction result (correlation coefficient / relative absolute error). ....	60
Table 13. Occupant individual behavior data mining result. ....	66

Table 14. Group schedule data mining results with different algorithms over the 28 appliances.	73
Table 15. Group schedule data mining results with different datasets. ....	75
Table 16 Lighting and equipment energy calibration statistical results. ....	87
Table 17 HVAC equipment parameter calibration. ....	88
Table 18 Summary of window open conditions (Source: ALC WebCtrl Logic as of July 30, 2014). ....	90
Table 19 Summary of calibration errors in different seasons. ....	94
Table 20 Errors of total annual EUI compared with measured data for the three models.....	97
Table 21 Assumptions for the baseline and E <sup>+</sup> PC controls. ....	101
Table 22 One week HVAC energy consumption comparison for the CSL building.....	112
Table 23 Result comparison of the global and direct solar radiation machine learning models.	142
Table 24 Thermal comfort and clothing insulation preferences in OME <sup>+</sup> PC.....	145
Table 25 Energy modeling objectives and tasks.....	170
Table 26 Data points should be streamed via BAS on the hourly basis. ....	172
Table 27 Summary of the demo development process. ....	193

# Chapter 1. Introduction

---

## 1.1. Background

Green buildings aim to save land, energy, water, and material, as well as to create a healthy and comfortable environment for their occupants throughout the building life-cycle. This concept has been well acknowledged in the US and around the world. For example, a widely used green building rating system - Leadership in Energy and Environmental Design (LEED) enjoyed an over 100% market growth rate from 2000 to 2011 in the US (Zhao and Lam, 2012).

Reducing operating energy cost is one of the primary goals for the design of green buildings. As an evidence of this, the Energy and Atmosphere (EA) section in LEED 2009 New Construction and Major Innovation (LEED 2009 NC) uses energy cost savings, rather than actual energy consumption savings as a prerequisite (10% improvement than baseline) and point calculation method. The EA section also has the highest possible credit points (35 out of 110 for LEED 2009 NC and 33 out of 110 for LEED V4) among all the seven sections. Mainly due to the energy performance requirements of LEED and other green building rating systems, such as EnergyStar and BREEAM (Lam *et al.*, 2013), the whole building energy modeling (BEM) is being increasingly used in the building industry (Vaughn, 2011). The popularity of BEM can definitely help the building industry move towards energy efficiency through code and standard compliances. However, as a scientific and standardized method, the benefits of using BEM are far more than just for code and standard compliances during the design stage. BEM can be used for many other purposes at different stages of the building life-cycle.



Figure 1 shows the potential value of BEM in the entire building life-cycle. Typically, there are six forms of input for creating a BEM model: (1) location & weather, (2) geometry & material, (3) lighting, (4) heating, ventilation, and air conditioning (HVAC), (5) appliance, and (6) occupant. The occupant behavioral input assumption, highlighted with a different color in Figure 1, is known for highly impacting BEM results and is difficult to model. Detailed literature review on occupant behavior in buildings is given in Section 1.2.1.

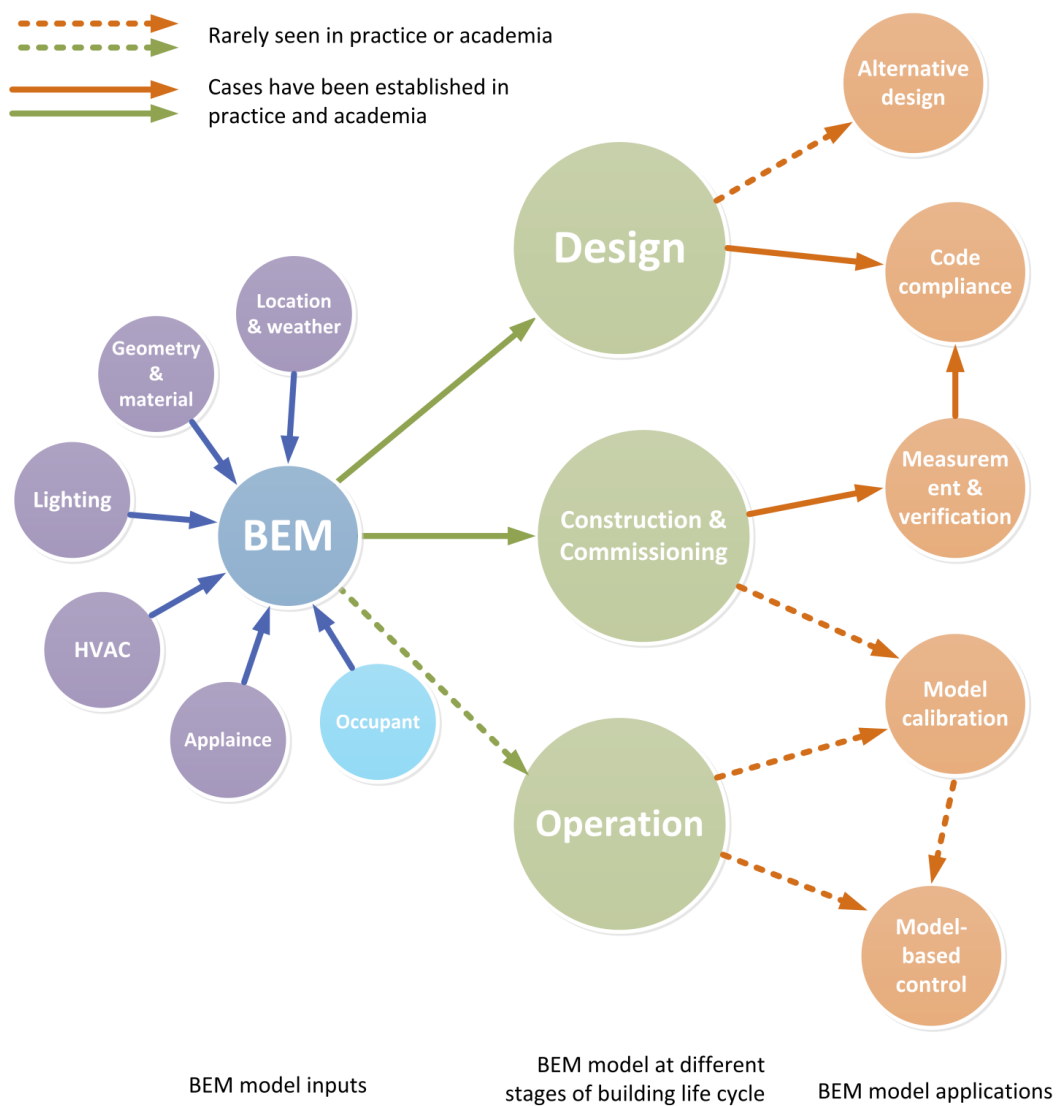


**Figure 1 the potential value of BEM in the building life-cycle.**

At the design stage, BEM can be used for design decision support, either for parametric design, or for code and standard compliance purpose. However, as seen in Figure 1, BEM is not often used for generating alternative design solutions in current practice. Literature review on building energy modeling for the purposes of design decision support and code and standard compliance is described in Section 1.2.2.

At the construction, commissioning, and early operation stages, BEM models are sometimes used for measurement and verification (M&V) for satisfying code and standard compliance in practice. For instance, LEED 2009 has three credit points for Measurement and Verification (M&V). During the M&V period, BEM models are calibrated during the one year post-construction occupancy period. Realizing the importance of M&V, LEED has made M&V a prerequisite to achieve any level of certification in its latest Version (LEED V4) (USGBC, 2013). Although M&V is effective to calculate energy savings by comparing the real measured data with baseline BEM models, the design stage BEM model calibration is necessary to make ensure the accuracy of modeling results. Here, “calibration” means comparing the measured data with the design case BEM model and updating the model parameters based on the comparison in order to make the BEM result as accurate as possible. Detailed literature review can be found in Section 1.2.3.

At the operation stage, the calibrated BEM model can be used for model-based building controls. Currently, there is a limited number of studies in this area. To the author’s knowledge, there is no direct industry application of using BEM model for building controls. Literature review with this aspect is discussed in Section 1.2.4.

## **1.2. Literature review**

In order to better understand the potential values of BEM in the building life-cycle, as shown in Figure 1, the previous studies are reviewed in four aspects following the BEM work flow in the building life-cycle. First, “Occupant behavior in buildings” provides an overview of various occupant behavior types that have energy impact on the buildings, which is often considered as a critical input for BEM models at the design stage and should be calibrated at the operation stage. Second, previous studies in both academia and industry are reviewed to summarize the current use of BEM models for design stage decision making and standard compliances. Third, “BEM model calibration” discusses various studies about BEM model calibration at the commissioning and operation stages and their similarities and differences. Fourth, “Building energy model-based predictive control” provides a comprehensive review on different types of model-based predictive controls and the pros and cons of these previous studies. At the end of each review section, a brief introduction of the dissertation’s intention is provided to address some of the gaps of the previous studies.

### ***1.2.1. Occupant behavior in buildings***

#### ***1.2.1.1. “Active” role of occupants***

The health, comfort, and productivity of the building occupants are considered key objectives for green building design and operation. Occupant behavior and feedback are necessary to achieve the desired total building performance (Hartkopf *et al.*, 1986). In other words, the occupants play an “active” role which is critical to the building operation. Numerous studies have developed

various control systems and modeling methods to better assist occupants in playing their “active” roles in buildings.

Table 1 shows a summary of reviewed literature of occupants’ “active” influence in buildings. 10 out of 15 studies demonstrate an energy impact of occupant behavior by using various individualized control systems and dashboards for building HVAC, lighting and plug load systems. Four studies about post occupancy evaluation and complaint handling show the occupant feedback can be useful for building diagnostics in existing buildings. Four studies show that providing occupants with individualized controls can influence their thermal comfort in existing buildings. Three studies show that providing occupants with individual controls can improve their subjective satisfaction towards their working environment in existing buildings.

**Table 1 Occupants’ “active” influence in buildings.**

Studies	Building diagnostics	Energy impact	Satisfaction impact	Comfort impact	Health impact
Availability of controls - opening windows and blinds (Raja <i>et al.</i> , 2001)			•		
Cost-effective Open-Plan Environments Survey (Veitch <i>et al.</i> , 2007)	•				
Individual comfort votes (Murakami <i>et al.</i> , 2007)		•	•		
National Environmental Assessment Toolkit (Loftness <i>et al.</i> , 2009)	•				
Bio-sensing adaptive HVAC control system (Choi, 2010)		•	•	•	•
Dashboard on office appliances (Lucid-Design, 2010)		•			
Dashboard on office appliances (Carrico and Riemer, 2011)		•			
Individual comfort votes (Daum, <i>et al.</i> 2011)		•		•	

**Table 1 Continue.**

Knowledge-based personal lighting control (Gu, 2011)		•	•		
Distributed comfort evaluation method (Klein <i>et al.</i> , 2012)		•		•	
Dashboard on office appliances (Yun, Lasternas, <i>et al.</i> , 2013)		•			
Post Occupancy Evaluation (Park, 2013)	•				
Enhanced complaint handling process (Goins and Moezzi, 2013)	•				
Agent-based approach to model active behaviors (Lee and Malkawi, 2014)		•		•	
Occupant action model (Bonte <i>et al.</i> , 2014)		•			

#### 1.2.1.2. “Passive” role of occupants

The studies above suggest that the occupant’s “active” behavior influences the indoor environment, as well as the energy consumptions of building HVAC, lighting, and plug load systems. But, the occupant’s “passive” role also impacts the building performance. Particularly, in assessing the building thermal and indoor air quality performance, heat and CO<sub>2</sub> generated by the occupants can influence the HVAC energy consumption to a great extent. Hence, the occupants are typically treated as “disturbances” in the HVAC control system design and operation. It is critical to study the occupant behavior at both individual and group levels to uncover this “passive” impact.

The following studies show that the occupants’ “passive” behavior has a significant impact on building energy consumptions. Hong and Lin (2012)’s simulation study showed that “for a typical single-occupancy office room, compared to the standard or reference work style, the

austerity work style consumes up to 50% less energy, while the wasteful work style consumes up to 90% more energy.” (Hong and Lin, 2012). Similarly, Glicksman and Taub (1997) conducted a simulation study on the occupant-controlled HVAC system in an open-plan office for the thermal and behavioral purposes. The study found that “when occupant sensors are used to reduce conditioning in unoccupied areas, energy consumption falls dramatically.” (Glicksman and Taub, 1997). Again, Masoso & Grobler’s energy audit study on six randomly selected commercial buildings in South Africa suggested that “more than 50% of energy is used during non-working hours than during the official working hours of 07:30–16:30 h”. 19%-28% of the building energy is consumed during the unoccupied hours of the weekends (Masoso and Grobler, 2010).

Numerous methods have been developed to study occupant behavior at both individual and group levels. The methods can be categorized as “direct approach” and “indirect approach” (Zhang *et al.*, 2012).

The direct approach is enabled by the development of information technology over the past few years, such as global positioning system (GPS), cellular data, wireless local area network (WLAN), infrared, radio frequency identification (RFID), ultrasound, Bluetooth, camera and LED (light-emitting diode) (Gu *et al.*, 2009; Hallberg *et al.*, 2003; Liu *et al.*, 2007; Swook *et al.*, 2010; Zandbergen, 2009). A few studies have applied some direct positioning technologies to learn occupant behavior and to assist in system controls in buildings. Table 2 shows a summary of these studies.

**Table 2 Direct approach of occupant behavior recognition and modeling studies in the building field.**

Studies	Direct approach
“Home gesture” to control lights, louvers, and blinds (Peters <i>et al.</i> , 2011)	WLAN triangulation
Lower complexity graphical occupancy model (Liao <i>et al.</i> , 2011)	Computer image processing
Fitbit® Zip™ occupant behavior modeling (Zhao <i>et al.</i> , 2013)	Bluetooth positioning
Smart phone application to control lighting systems (Bauereiss, 2013)	Ultrasonic positioning
Detect and track building occupants (Shih, 2014)	Computer image processing (image-based depth sensor and programmable pan-tilt-zoom camera)

Although direct positioning methods are effective in detecting various building occupant behaviors, privacy can be a major concern for deploying these technologies in the real world. Therefore, less intrusive “indirect” occupant positioning methods have been developed, which use environmental sensor data mining, energy consumption data mining, and other stochastic modeling approaches. These methods are simulated and tested in order to better control building HVAC systems while gathering little or no personal information about the occupants. Table 3 summarizes the studies that use indirect approach to model building occupant behavior.

**Table 3 Indirect approach of occupant behavior modeling studies in the building field.**

Studies	Indirect approach
“realistically reproduce key properties of occupant presence” (Page <i>et al.</i> , 2008)	stochastic modeling using Markov chain theory
Residential occupant behavior schedule to estimate cooling demand (Tanimoto <i>et al.</i> , 2008)	stochastic modeling methods
Controlling the building HVAC system with energy savings (Dong and Lam, 2011)	environmental sensor networks (CO <sub>2</sub> , acoustics, light, and motion sensor data and stochastic modeling methods
“produce the nonsynchronous change of occupancy in time and the uneven distribution of occupancy in space” (Wang <i>et al.</i> , 2011)	environmental sensor data and stochastic modeling methods
Stochastic agent-based occupancy model (Liao <i>et al.</i> , 2011)	stochastic modeling methods
A stochastic model that could learn the occupant behavioral patterns (Virote and Neves-Silva, 2012)	stochastic modeling methods
Occupancy patterns in an office building (Duarte <i>et al.</i> , 2013)	occupancy sensor data mining
A cluster analysis method was developed to identify the effects of occupant behavior on building energy consumption (Z. Yu <i>et al.</i> , 2013)	data mining framework
Probability of occupant long vacancy activities (greater than 1 week) and how they might influence building energy performance (Stoppel and Leite, 2014)	Probabilistic modeling methods
Generate realistic occupancy sequences for residential buildings (Aerts <i>et al.</i> , 2014)	Probabilistic modeling methods

The literature review above summarizes previous studies about the active and passive roles of occupants in buildings. Both roles are critical to the building energy consumption and occupant thermal comfort. This dissertation focuses on learning passive occupant behavior using indirect approach and developing a system that enables occupant to engage their active behavior in the control system.



### ***1.2.2. BEM for design decision making and standard compliance***

At the design stage, BEM can be used as a method to generate alternative design solutions to increase energy efficiency. For example, Karaguzel has developed and demonstrated a comprehensive method to perform “Simulation-Based Parametric Analysis of Building Systems Integrative Solar Photovoltaics” (Karaguzel, 2013). However, currently, practitioners typically do not use BEM models for the design decision making purposes. Instead, BEM models are built only after the design has been finalized and used to demonstrate compliance for codes and standards.

As an example, several software tools have capabilities to demonstrate the compliance of LEED NC 2009 EA section using BEM results. TRANE, an HVAC manufacture, claimed that one of its software “TRACE 700 can help document compliance with American Society of Heating, Refrigerating and Air Conditioning Engineers (ASHRAE) Standard 90.1 or validate the building’s eligibility for LEED certification” by filling the LEED EA Prerequisite 2 and Credit 1 templates (TRANE, 2013). Similarly, Bentley’s AECOSim Compliance Manager can “streamline the LEED certification process and maximize LEED credits” in the design stage (Bentley, 2013a). Its corresponding energy simulation tool - “AECOSim Energy Simulator” uses EnergyPlus (DOE, 2012) engine and can generate LEED reports of “peak loads, annual energy calculations, energy consumptions, carbon emissions, and fuel costs” (Bentley, 2013b). Another example, the COMNET Energy Modeling Portal for LEED Online was developed for eQUEST program to achieve the LEED EA Prerequisite 2 and Credit 1 (NBI, 2013). The eQUEST energy model file (SIM-format) can be uploaded onto this web-based tool. Then the COMNET XML

standard output file can be generated and uploaded to the LEED Online website fulfilling the submission templates.

Though these software tools provide practical compliance methods for users to evaluate building energy performance using BEM models in their proprietary formats, they have limited capability to perform the parametric design and support the decision making process at the design stage.

This dissertation aims to demonstrate how BEM models can be used to evaluate and compare building energy performance for various design alternatives.

### ***1.2.3. BEM model calibration***

One of the main reasons that BEM is undervalued in current practice is the inconsistency between BEM model simulation results and actual measured operation data. Most of the widely used building energy simulation tools, such as EnergyPlus, ESP-r, and TRNSYS, have been continuously validated since the 1980s (Candau and Piar, 1993; Jensen, 1995; Judkoff *et al.*, 2008; Lomas *et al.*, 1997). However, compared to the actual measured energy data, the results of BEM models created by these tools are inconsistent.

One study that evaluated this inconsistency is Frankel and Turner's comparison study (Frankel and Turner, 2008). The researchers compared BEM results with actual measured data for 90 LEED certified buildings. The results indicate that although the median value of the consistency between the simulated and measured data is over 80%, the variations among individual projects are substantial. The ratio of the measured energy use intensity (EUI) to design EUI ranges from less than 0.5 to more than 2.75 (Frankel and Turner, 2008), as shown in Figure 2.

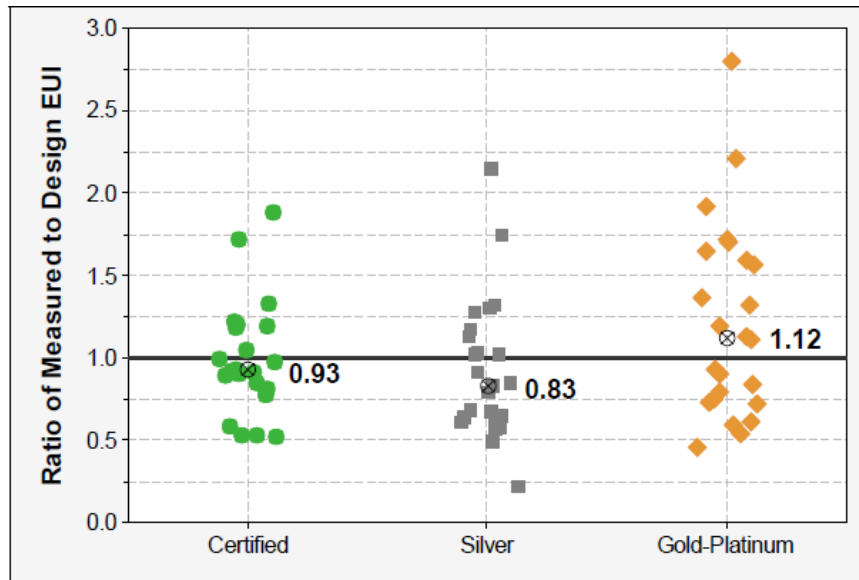


**Figure 2 Measured/Design EUI by LEED level, with medians (Frankel and Turner, 2008).**

Several studies have identified the reasons for the discrepancies between BEM results and metered energy usage. First, the weather data input can be a significant factor (Neto and Fiorelli, 2008). In some regions, weather varies greatly from year-to-year, so the typical weather file could be significantly different from the actual weather of the particular years of data collection. Second, plug load is also an important input factor, due to unpredictable computer usage and phantom loads (Perez, 1993). More importantly, occupant activity and their usage of the building may be the hardest variable to predict (Al-Homoud, 2001; Karlsson *et al.*, 2007; Lam and Hui, 1996; Neto and Fiorelli, 2008). Particularly, occupancy schedules and density can have considerable impact on HVAC loads and energy consumption (Dong and Lam, 2011; Lam and Hui, 1996; Zhao, Lasternas, *et al.*, 2014). These reasons could be the major causes of the inconsistent energy model results in current practice.

Occasionally, in LEED NC 2009, in order to get three points for Measurement and Verification (M&V) in the EA Credit 5 section, baseline BEM models are compared with real data during at least one year post-construction occupancy period, but not all LEED certified projects achieve this credit category. Realizing the importance of M&V, the newer version of LEED (V4) has made M&V a prerequisite that all LEED certified projects have to do (USGBC, 2013).

Several standards have defined the M&V methods. For example, International Performance Measurement and Verification Protocol (IPMVP) Option D provides a solution to demonstrate energy savings for new construction through whole building energy simulation (EVO, 2003). LEED 2009 also adopted this method as an option for M&V. Other relevant standards include “Federal Energy Management Program's M&V Guidelines: Measurement and Verification for Federal Energy Projects, Version 3.0” and “ASHRAE Guideline 14-2002, Measurement of Energy and Demand Savings” (ASHRAE, 2002; DOE, 2008). However, technically speaking, these standards are not designed for introducing step-by-step model calibration methods, but to standardize the calibration criteria to evaluate what is a calibrated BEM model. Therefore, to fulfill the established standards, developing a BEM model calibration method is essential to solve the problem of inconsistent modeling results.

Several studies have explored systematic and structuralized methods for empirical BEM model calibration. Raftery et al. developed a method to iteratively update an EnergyPlus model with empirical data. A “walk through audit”, such as human resources interviews, personnel counts, and multiple day/night occupancy surveys, was conducted to update the occupancy schedule in the design case BEM model (Raftery *et al.*, 2011). Kandil and Love proposed and demonstrated a method to calibrate an EnergyPlus model for a school building. Empirical data were collected

through a similar “walk through audit”, including interview and site visit, as well as long-term and spot measurement (Kandil and Love, 2013). Other studies also demonstrated the feasibility of various empirical BEM model calibration methods (Pan *et al.*, 2007; Pedrini *et al.*, 2002; Raftery, Keane, and O’Donnell, 2011). These studies are in consistent with what Reddy has noted in his calibration study that the empirical BEM model calibration methods are “manual, iterative, and pragmatic intervention” (Reddy, 2006).

Particularly, current empirical BEM model calibration methods often use the “walk through audit” approach to determine occupancy schedule. While this approach is necessary, it may not be scientifically accurate. One of the objectives of this dissertation is to develop a practical yet systematic and scientific method based on the established standards that will use empirical data to calibrate the design-stage BEM model.

#### ***1.2.4. Building energy model-based predictive control***

After a BEM model is calibrated, it can be useful in assisting the development of building control systems at the building operation stage in theory, as shown in Figure 1. Although numerous studies have focused on model-based (or simulation-based) building control theories and applications, BEM tools have not been widely used to create the building and system models in assisting building controls at the operation stage.

##### ***1.2.4.1. Early development of model-based building controls***

In the 1980s’, simplified HVAC and building models were used for “evaluating and optimizing building control strategies” (Kelly, 1988). In this study, two different types of simulation-based control systems were reviewed. In the first type, known as “static simulation-based control”,

simulation was performed during the control system design period to generate a set of scenarios for the control system to select in operation. The second type known as “real-time model-based control”, which used “real-time building system models, expert systems, or a combination of both” to assist control decisions in real-time. Similarly, Mahdavi systematically introduced the idea of model (simulation)-based control of building system operation. The two methods – “generate-and-test” and “bi-direction inference” – were proposed and tested for lighting controls in an actual office building case (Mahdavi, 2001). The feasibility of the model-based control systems have also been demonstrated by other studies in lighting, shading, and HVAC control areas (Clarke *et al.*, 2002; Jayada, 2003; Mahdavi and Pröglhöf, 2008; Mertz, 2003; Mo, 2003).

#### *1.2.4.2. Current model predictive control (MPC) studies in the building field*

One particular topic in the model-based control field is MPC (Garcia *et al.*, 1989). The majority of the models created for MPC can be categorized into two types - “forward (classical)” models and “data-driven (inverse)” models. The forward approach is “to predict the output variables of a specified model with known structure and known parameters when subject to specified input variables”, while the data-driven approach is “to determine a mathematical description of the system and to estimate system with known input and output variables.” (ASHRAE, 2009)

The forward modeling approach was adopted by the early studies focused on controlling the HVAC system at the component level. For instance, Wang and Jin (2000) developed an adaptive MPC controller for variable air volume (VAV) system using the simplified first principle-based single-zone building and VAV system component models (Wang and Jin, 2000). Several other MPC studies also used the forward modeling approach to control various building systems to

minimize energy consumption (or cost) and maintain indoor setpoint (Castilla *et al.*, 2011; Dong, 2010; Gyalistras, 2010; Henze *et al.*, 1997; Y. Yu *et al.*, 2013; Yuan and Ronald, 2006).

The data-driven modeling approach was utilized in other MPC studies to create models for control and optimization, such as (Freire *et al.*, 2008; Kolokotsa *et al.*, 2009; Paris *et al.*, 2010; Privara *et al.*, 2011). In these studies, the experimental and/or simulation input and output data were collected to create the data-driven models.

The studies mentioned above suggest that both forward and data-driven modeling methods are effective for MPC studies in the building field. However, from a practical point of view, there are still a few difficulties of directly using the forward and data-driven models in practice. First, the forward modeling approach is suitable for single zone and simple geometric buildings, but can be difficult to apply to the buildings with multiple zones and irregular geometric shapes. Second, the data-driven modeling approach often requires sensor data at the system component level and/or in the indoor/outdoor environment, which may not be available for some building projects due to cost, and other practical reasons in the building industry. Third, given the nature of the data-driven modeling algorithms, in some cases, full system dynamics may not be easily obtained from the available input data. In addition, developing forward and data-driven models typically requires high mathematical skills, which may decrease the likelihood of using MPC in daily operation by building industry practitioners, such as building operators and facility managers.

Instead of using the forward and data-driven models for MPC, an alternative solution is to use BEM tools to create building and system models. For instance, EnergyPlus is a well-developed, validated, and constantly updated whole building energy simulation program (Crawley *et al.*,

2001). In EnergyPlus, some modules of EnergyPlus are developed with the forward modeling approach, while others are created using the data-driven modeling approach. Therefore, EnergyPlus can be treated as a front-end platform that helps users to create the whole building and system models that different modeling approaches are employed in the back-end.

#### *1.2.4.3. Current difficulties and means of using BEM models in MPC*

However, it is not straightforward to use EnergyPlus in MPC studies.

The first issue of using EnergyPlus in MPC is the time synchronization problem between EnergyPlus and other control system development tools. Unlike Matlab and other control system design and performance simulation programs that provide users with simulation time management methods (Mathworks, 2012), EnergyPlus has its own internal run time mechanism that cannot be adjusted. Consequently, the synchronization may not be directly achieved. In order to solve this problem, Wetter recently developed a tool called Building Control Virtual Test Bed (BCVTB) (Wetter, 2011a), which provides a middleware platform for the time synchronization and co-simulation between EnergyPlus and Matlab, together with the EnergyPlus module of Energy Management Systems (EMS) for external co-simulation (DOE, 2013a).

The second difficulty of using EnergyPlus in MPC is the data interoperability. For example, as one of the model inputs, EnergyPlus simulation uses external weather file with sequential static time stamps. They may cause problems for optimization, which requires numerous repeated input information for each of the optimization iterations. Therefore, to solve this data interoperability problem, a new method to process the model input data (e.g., occupancy, lighting, and equipment schedules) is needed.



Another difficulty of using EnergyPlus in MPC is to solve the black-box optimization problem. The black-box optimization algorithms for MPC can be challenging to implement and execute in EnergyPlus due to its run time mechanism and the potential high temporal cost. To avoid this problem, several researchers have found some success in using simulation tools to develop the black-box building model for performance simulation, while using the simplified forward or data-driven system model for control optimization. For instance, Braun developed an optimal controller to optimize energy cost and peak electrical demand for the building thermal storage system. TRNSYS black-box zone model was used for the simulation while a forward model was developed for system optimization (Braun, 1990; TRNSYS, 2012). Similarly, Yahiaoui et al. proposed an MPC controller using ESP-r model as the black-box plant model while using Matlab/Simulink to develop simplified system models for control optimization (ESP-r, 2000; Yahiaoui *et al.*, 2006). Also, Bernal et al. introduced a control system that linked EnergyPlus black-box model with Matlab/Simulink via MLE+ as the plant model (Bernal *et al.*, 2012). Meanwhile, a forward system model was optimized in Matlab/Simulink environment and the control performance was simulated in the EnergyPlus model.

The studies above successfully demonstrated several solutions to avoid the difficulties of implementing the black-box optimization by simulating the black-box building models while optimizing simplified system models. Other studies have used some software tools to develop and optimize the entire black-box building model. For example, TRNSYS and GenOpt (Wetter, 2011b) were used for plant modeling and system optimization, respectively, to solve the black-box optimization problem in the studies of (Coffey *et al.*, 2010; Kummert *et al.*, 2011).

Two studies have addressed time synchronization, data interoperability, and black-box optimization problems all at once. May-Ostendorp et al. developed an MPC control system that was built in Matlab and connected to EnergyPlus by writing and reading text files. The control rules were generated by optimizing the window opening schedules to save energy (May-Ostendorp *et al.*, 2011). On the basis of the offline optimization framework above, Corbin et al. developed a real-time optimization framework for the MPC system by linking EnergyPlus, Matlab and a Building automation system (BAS). The test cases reported that the MPC system resulted in “54% energy savings with often improved occupant comfort” (Corbin *et al.*, 2012). This inspirational research provided a great solution to use EnergyPlus in MPC. However, a more complete MPC framework should be achieved and performance should be tested under different seasons with various building control strategies for both energy efficient and occupant thermal comfort purposes.

The primary goal of this dissertation is to utilize the calibrated BEM model to develop a model-based predictive control system that enables both active and passive HVAC system controls for heating, cooling and swing seasons, as well as to provide an individualized control system for occupants to regulate their own thermal comfort.

#### ***1.2.5. Summary of literature review***

In total, more than 340 directly related studies have been reviewed, 40 of which have direct contributions to this dissertation work. A summary for the 40 studies is listed in Table 4. Topics covered by studies are indicated by gray cells. Specific methods in each topic are indicated by black dots.

This dissertation will cover all the five major topics discussed in the literature review – “design decision support”, “indirect occupant behavior modeling”, “BEM model calibration”, “occupant-oriented control”, and “model predictive control”, as indicated in the head row of Table 4. The topics that were covered by a particular study are highlighted by grey cells.

Under each topic, several methods are reviewed and compared. The methods that were used in a particular study are highlighted by black dots.

**Table 4 Summary of the studies with direct contributions.**

Topic	Design decision support		Indirect occupant behavior modeling			BEM model calibration		Occupant-oriented control		Model predictive control			
Method	Design Alternatives	Standard Compliance	Sensor Networks	Stochastic Modeling	Electricity Data	Other Models	EnergyPlus	Others	Occupant Feedback	First Principle Models	Linear Identified Models	Other tool Models	EnergyPlus Models
Recent PhD Dissertation from Center for Building Performance and Diagnostics													
Dong (2010)			•			•				•			
Choi (2010)								•	•				
Srivastava (2010)								•		•			
Gu (2011)									•				
Yu (2012)						•				•	•		
Karaguzel (2013)	•					•							
Published studies and applications internationally													
Glicksman et al. (1997)			•				•	•					
Wang et al. (2000)										•			
Yuan et al. (2006)										•			
Yahiaoui et al. (2006)												•(ESPr)	
Murakami et al. (2007)									•				
Tanimoto et al. (2008)					•								
Page et al. (2008)				•									
Frankel et al. (2008)						•							
Freire et al. (2008)											•		
Kolokotsa et al. (2009)											•		
Paris et al. (2010)											•		
Agarwal et al. (2010)			•					•					
Salvalai et al. (2010)						•							

**Table 4 Continue.**

Fumo et al. (2010)			•		
Morosan et al. (2010)					•
Moon et al. (2010)					•
May-Ostendorp et al. (2011)					•
Privara et al. (2011)					•
Raftery et al. (2011)			•		
Hassan et al. (2011)			•		
Goldstein et al. (2011)		•			
Wang et al. (2011)		•			
Parys et al. (2011)		•			
Daum et al. (2011)				•	•
Castilla et al. (2011)					•
Coffey et al. (2011)					•(TRNSYS)
Hazyuk et al. (2012)					•
Strurzenegger et al. (2012)					•
Klein (2012)				• •	
Bernal (2012)					• •
Ryan (2012)			•		
COMNET (2012)	•				
TRACE 700 (2013)	•				
AECOSim (2013)	•				
Proposed Dissertation	•	•	•	•	•

### 1.3. Objectives and hypothesis

From the literature review above, BEM not only can be used to demonstrate the code and standard compliance, but also has potential to be used in all phases of the building life-cycle. This dissertation focuses on developing and demonstrating a set of methods to use BEM models during the entire building life-cycle. First, a BEM process is demonstrated for the purpose of design decision making at the design stage. Then a BEM model calibration method is introduced and tested at the commissioning and early operation stages. Finally, the calibrated BEM model is utilized in an occupant-oriented predictive control system at the operation stage to optimize energy and thermal comfort performance in the test-bed building. As a key step of the BEM process and important factor for the built environment, occupant behavior is also addressed in this dissertation from two different perspectives: (1) is to model the occupant behavior and schedule for the purpose of BEM model calibration; (2) is to actively engage occupants in the building control for the purpose of improving individual thermal comfort.

More specifically, this dissertation will test the following four hypotheses:

- Hypothesis 1: The design-stage BEM can be extended to the entire building life-cycle for a better building energy and thermal comfort performance.
- Hypothesis 2: An EnergyPlus BEM model can be calibrated using a systematic and scientific method with empirical data.
- Hypothesis 3: Model-based predictive control using EnergyPlus BEM model can reduce energy consumption and maintain occupant thermal comfort compared to conventional control algorithms.

- Hypothesis 4: Individual occupant comfort requirements can be met by engaging occupants for their comfort feedback through an online dashboard.

## **1.4. Dissertation chapter overview**

Chapter 2 introduces the overall concept of design-build-operate energy information modeling (DBO-EIM) infrastructure. Then, the case study of the first part of the DBO-EIM infrastructure – “energy modeling for design decision making” is also demonstrated.

Chapter 3 describes the development and test results of a method to calibrate the EnergyPlus model in a test-bed office building. First, “3.1. Overview” and “3.2. Test-bed building model creation and data collection” provide the research method overview and the background information of the case study building. Then, five major procedures and results of the calibration method are explained in detail, which are “3.3. Weather information for EnergyPlus input”, “3.4. Occupant behavior and schedule modeling”, “3.5. Daylight/Lighting and equipment operation calibration”, “3.6. Passive/Active HVAC system operation calibration”, and “3.7. Whole building energy model calibration result”.

Chapter 4 explains the development process and test results of the occupant-oriented mixed-mode EnergyPlus predictive control. First, in section 4.2, a baseline EnergyPlus model-based building control is developed and tested to establish the baseline performance of the building HVAC systems. Then, in section 4.3, an EnergyPlus predictive control (E<sup>+</sup>PC) system is developed and the performance is compared with the baseline control system. Next, in section 4.4, a mixed-mode passive/active E<sup>+</sup>PC (ME<sup>+</sup>PC) system is created and tested on the basis of the original E<sup>+</sup>PC to demonstrate the performance difference of using the passive HVAC system.

Lastly, in section 4.5, an occupant-oriented ME<sup>+</sup>PC (OME<sup>+</sup>PC) system is developed and tested using the real-time occupant feedback data to enable individual thermal environment control.

Chapter 5 summarizes the research findings, including the hypothesis testing results and other important research findings. Then the contribution is briefly presented (Full detail of the contribution can be accessed in Appendices). Finally, potential future work is discussed in the last part of the chapter.



# **Chapter 2. Design-build-operate energy information modeling (DBO-EIM) infrastructure and energy modeling at the design stage**

---

## **2.1. Overview**

This chapter introduces the concept of design-build-operate energy information modeling (DBO-EIM) infrastructure and illustrates the first part of that infrastructure: using a real building case study to demonstrate BEM for the purpose of design decision making. Figure 3 presents the DBO-EIM infrastructure showing the four stages of the building life-cycle.

At the design stage, in order to achieve an energy efficient building design, the baseline building energy model should be built according to the preliminary design and ASHRAE 90.1-2007 (or newer versions) and/or other building energy standards. Then the multidisciplinary design team should work together to propose alternative sustainable strategies, including design strategies for the building envelope, HVAC and daylight/lighting systems. Next, these alternative design strategies should be modeled with the same assumptions as the baseline building energy model, such as lighting schedules, equipment schedules, occupancy schedules, zone parameters, and other model inputs. Then the energy performance of these alternative design models can be compared and optimized to provide a more energy efficient design for the final proposed design case. At the end of the design stage, the proposed design case model can be updated based on the final design decision.

At the end of the construction stage, the building energy model should be updated based on the as-built drawings incorporating any changes between the construction drawings and the as-built drawings, in order to accurately reflect the actual completed building.

At the commissioning and early operation stages, the system parameters in the BEM model should be calibrated according to the testing and tuning results of HVAC, lighting and other building systems. The environmental aspects of the building energy model should be calibrated by using spot and long-term environmental and energy data measurements. In addition, the real-time weather information collected by the on-site weather station should be applied into the as-built building energy model to further calibrate the model.

At the operation stage, occupant, equipment, and lighting schedules should be adapted based on the post-occupancy condition, so the commissioning model becomes the “operation model”. This “operation model” is used for the model-based building control, which is the proposed “occupant-oriented mixed-mode EnergyPlus predictive control (OME<sup>+</sup>PC)”. OME<sup>+</sup>PC incorporates the real-time occupant thermal comfort feedback information along with other empirical data into the EnergyPlus model-based predictive control to optimize building HVAC energy consumption and occupant thermal comfort.

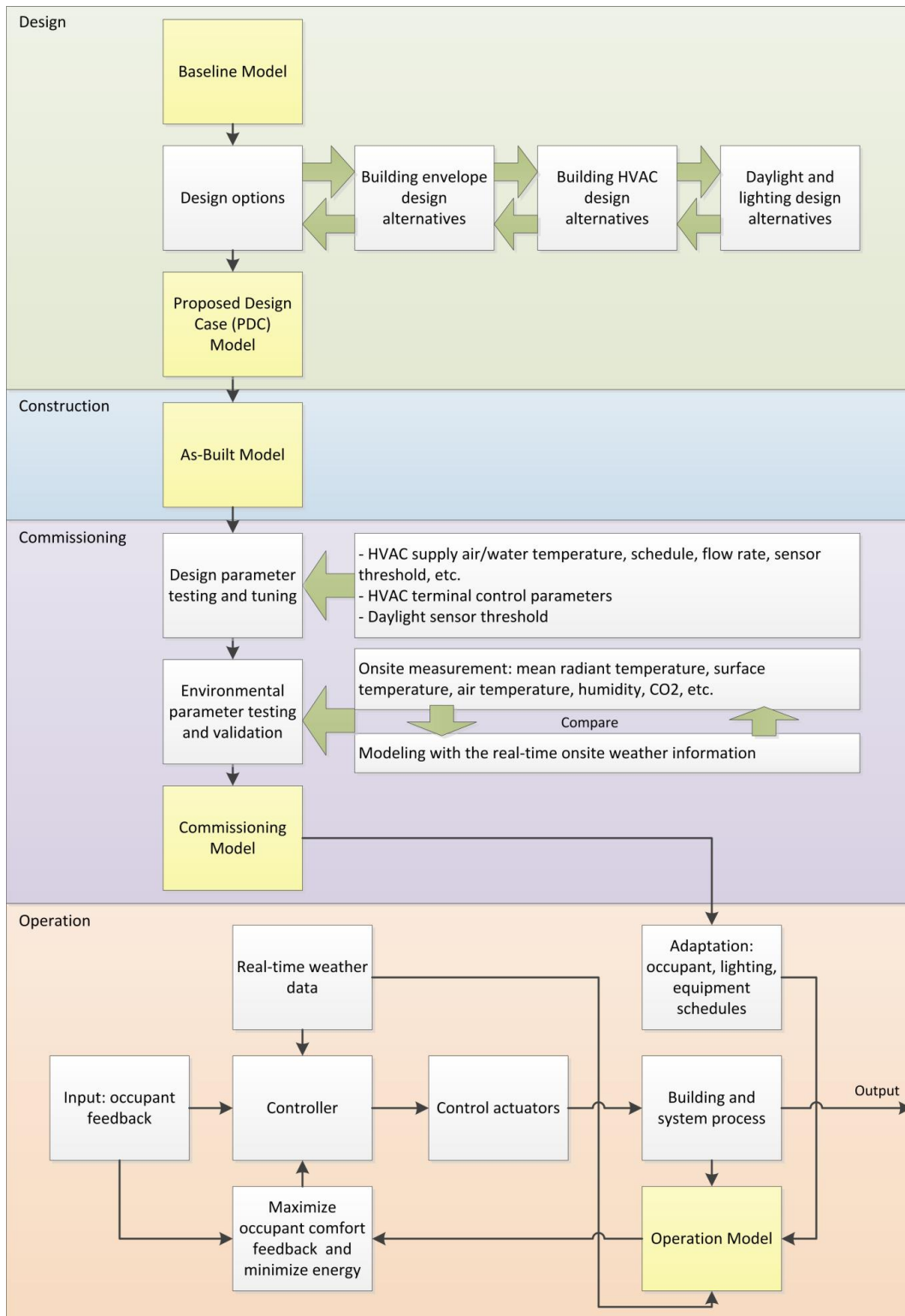


**Figure 3 DBO-EIM Infrastructure.**

## **2.2. Case study on BEM for design decision making**

In order to demonstrate the process of using BEM for the purpose of design decision making, a 2-story, 2,262m<sup>2</sup> office building is studied as a test-bed building. The building is Phipps Center for Sustainable Landscapes (CSL) (highlighted in orange in Figure 4), located on the campus of Phipps Conservatory and Botanical Gardens (highlighted in blue in Figure 4) in the suburban area of Pittsburgh, Pennsylvania, USA. Figure 5 shows the exterior and interior photos of the CSL building. More detailed description of the CSL building can be found in the reference of (Phipps, 2012).

There are two main reasons for choosing the CSL building as a case study for this dissertation. First, the timing of the CSL building's DBO process matches this dissertation's work plan. The building was designed in 2010. Its construction started in 2011 and completed in 2012 and was occupied in 2013. During those periods, the author not only had the opportunities to observe and contribute to the entire DBO process, but also achieved experimental and simulation studies for this dissertation. More importantly, the CSL building is a net zero energy building with numerous energy efficient design features and technologies compared to conventional office buildings. Using an efficient building as a case study makes more sense for the author to explore the state-of-the-art research methods to achieve better performance. For instance, the CSL building has achieved LEED Platinum (USGBC, 2011b) award in August 2013 and the Living Building Challenge Net Zero Energy Building Certification in February 2014 (ILFI, 2013).



**Figure 4** Satellite map of the CSL building (Source: Google Map

<https://www.google.com/maps/@40.4320873,-79.9487346,991a,35y,39.17t/data=!3m1!1e3>).



**Figure 5** Photos of the CSL building (left: exterior, right: interior).

The CSL building is equipped with a central Air Handler Unit (AHU) with ground source heat pump (GSHP) and energy recovery ventilator (ERV) as its cooling, heating, and ventilation systems. The under floor air distribution (UFAD) system is used for the open office, conference rooms and other regularly occupied spaces. The ceiling-based air distribution/exhaust system is used for several service spaces, such as restrooms, mechanical rooms, and storage rooms.

### ***2.2.1. Creation of energy models***

Detailed whole-building energy simulation models are developed by using DesignBuilder (DesignBuilder, 2012) and EnergyPlus programs. The results of different energy simulation alternatives are compared for the purpose of design decision making. At the design stage, all the models share the same assumptions of schedules and zone parameters based on the ASHRAE 90.1-2007 energy standard and design specifications. First, the baseline model and several design alternative (DA) models are created for the purpose of comparing load and energy consumptions. Then the proposed design case (PDC) model is created according to the construction drawings that are finalized based on the model comparison results and other practical factors.

The baseline and alternative design strategies used in all the different models are shown in Table 5 through Table 7. Figure 6 shows a screenshot of the baseline and the PDC model in the DesignBuilder program.

**Table 5 Baseline, design alternatives (DAs), and proposed design case (PDC) model assumptions.**

Model	Envelope	HVAC	Daylight/Lighting
Baseline	ASHRAE 90.1-2007 baseline envelope	ASHRAE 90.1-2007 system type 4	ASHRAE 90.1-2007 lighting assumptions
DA #1		HVAC design #1	
DA #2		HVAC design #2	
DA #3	Design case envelope	HVAC design #1	
DA #4		HVAC design #3	ASHRAE 90.1-2007 with daylight responsive controls
PDC			

**Table 6 ASHRAE 90.1-2007 baseline building energy model assumptions.**

Category	Strategies (U-value: W/m <sup>2</sup> -K)
Baseline envelope assumptions	External walls (0.071)
	Roof (0.176)
	Ground floor (0.177)
	External floor (0.072)
	Internal Floor (0.561)
	Double pane glazing (3.082) (SHGC: 0.368)
Baseline HVAC system type 4	Packaged rooftop heat pump, constant volume, direct expansion cooling
Baseline lighting assumptions	ASHRAE 90.1-2007 Section 9.

**Table 7 Alternative design building energy model assumptions.**

Category	Strategies
Design case envelope	Same opaque assemblies as ASHRAE 90.1-2007 baseline assumptions
	Low-E double and triple pane glazing with Krypton air gap (U-value: 0.781 – 1.444 W/m <sup>2</sup> -K) (SHGC: 0.466 – 0.597)
	External shading devices
HVAC design #1	Variable air volume (VAV) ceiling-based air distribution with terminal reheat system
HVAC design #2	VAV AHU + UFAD with terminal reheat for regularly occupied zones and ceiling-based air distribution with terminal reheat for other service zones
HVAC design #3	VAV AHU + ERV + GSHP + UFAD for regularly occupied zones and ceiling-based air distribution with terminal reheat for other service zones without terminal reheat
Daylight responsive lighting control	Based on the ASHRAE 90.1-2007 lighting design, regularly occupied zones are employed with daylight sensors to conduct daylight responsive controls

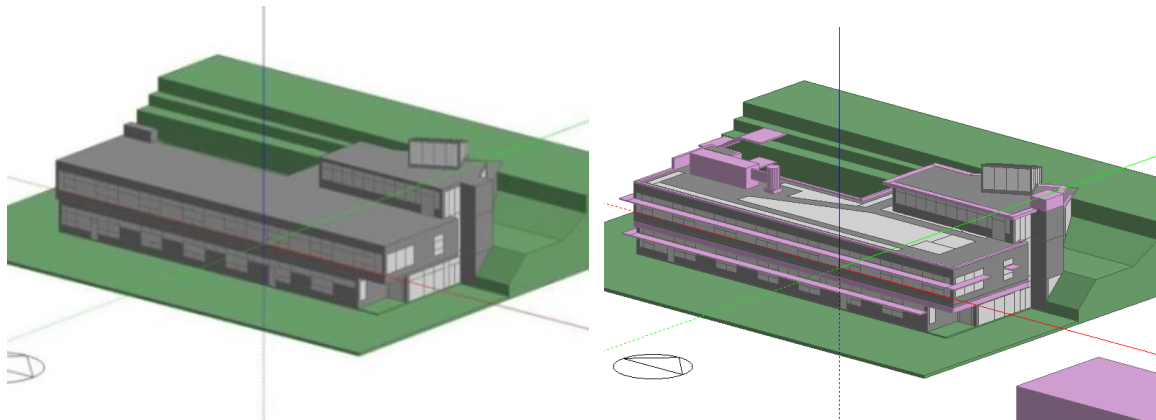


**Figure 6 Baseline (on the left) and PDC (on the right) models in the DesignBuilder program.**



### **2.2.2. Building load analysis**

In order to discover the impact of different design strategies on the building thermal load, the peak cooling and heating loads of the baseline and alternative designs are compared and analyzed, as shown in Figure 7. The loads are calculated by auto-sizing routines of EnergyPlus based on the Design Day (DOE, 2013b) data from TMY3 weather files (Seo *et al.*, 2009).

First, the Baseline is compared with DA #1. Given the same envelope design, the change of HVAC system does not influence cooling and heating design peak loads.

Second, DA #1 and DA #2, DA #3 and DA #4 are compared in pairs, respectively. It can be seen that DA #1 and DA #3 have higher cooling peak load and lower heating peak load, given the same envelope designs. However, the first finding (comparison between the Baseline and DA #1) suggests that HVAC system change does not influence building peak load. So the load change is caused by the differences of room air model set-up in the EnergyPlus program. DA #1 and DA #3 use the UFAD “Room Air Model” for the regularly occupied zones, which is a two-nodes room air model with floor plenum air supply (Buhl, 2007). The room air model of the other zones is a typical well-mixed one-node air model (Crawley *et al.*, 2001). The result of the higher cooling load is contradictory to the design expectation in practice. Generally, UFAD is considered to have higher cooling supply air temperature and lower supply air pressure, which implies lower cooling loads compared to ceiling-based air distribution systems. The reason is that in the EnergyPlus program, the design cooling load of a UFAD room includes the occupied zone, as well as contains its supply plenum and return plenum. So the “calculated cooling design load” is the overall cooling load of the three spaces. According to Schiavon *et al.*’s simplified UFAD cooling load calculation method, “UFAD has a peak cooling load 19% higher than an

overhead cooling load, and 22% of the total zone UFAD cooling load goes to the supply plenum in the perimeter.” (Schiavon *et al.*, 2010)

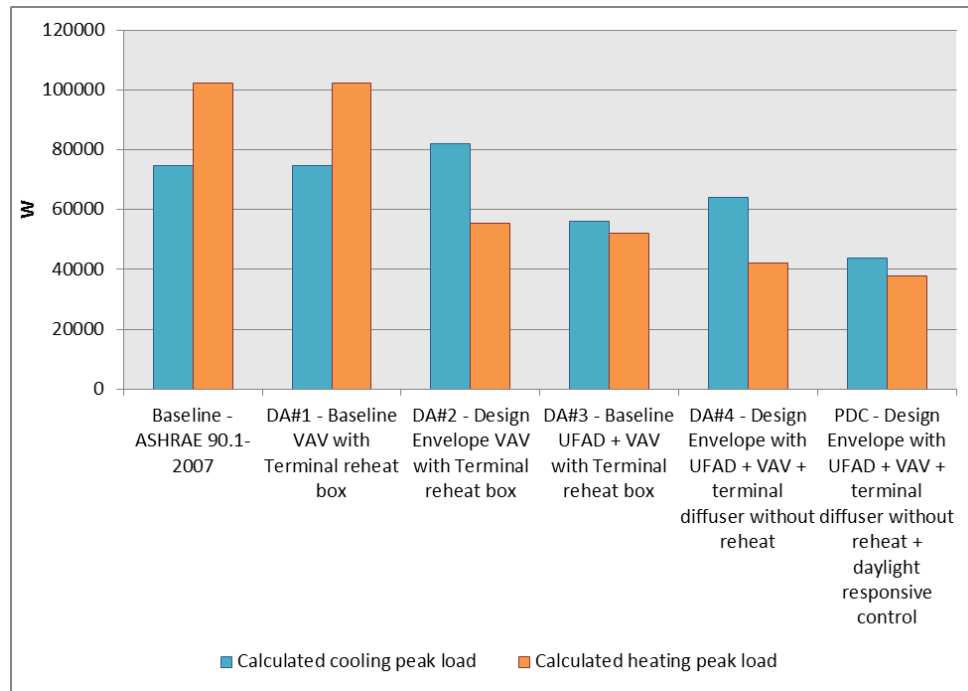


**Figure 7 Calculated building cooling and heating design loads of the six models.**

Third, the models with different envelope designs (DA #1 and DA #3) are compared. Given the same HVAC #1, the CSL PDC envelope can result in a 24.8% reduction in cooling design load and a 49.2% reduction in heating design load compared to the baseline envelope design.

Fourth, the load implication of daylight-responsive lighting control is analyzed by comparing DA #4 and PDC. In this model, given the same envelope and HVAC design, the daylight responsive lighting control can reduce the building cooling load by 31.5%.

### ***2.2.3. Building energy use intensity analysis***

After the load comparison, it is also necessary to compare the annual building energy use intensity (EUI) of the baseline and alternative design models. Figure 8 shows the annual EUI of all the design-stage BEM models. First, with the same baseline envelope design, the models with different conventional HVAC systems result in similar annual EUI ( $86.59 \text{ kWh/m}^2$ ,  $81.86 \text{ kWh/m}^2$ ,  $82.24 \text{ kWh/m}^2$  for the Baseline, DA #1, and DA #2, respectively). By comparing DA #1 and DA #3, with the same HVAC #1, the improvement of building envelope design shows a 28.3% reduction in HVAC (heating, cooling, fan, and pump) energy consumption and a 12% reduction in total energy consumption. By comparing DA #3 and DA #4, with the same PDC envelope, for HVAC #3, the annual HVAC energy consumption reduction is 25% and the annual total energy consumption reduction is 6.1%. By employing the daylight responsive lighting control system to PDC, and comparing it to the energy consumption result of DA #4, the outcome shows a reduction of 56.2% in lighting energy, 16.4% in HVAC energy, and 22.9% in the total energy consumption. Given the fact that glare is not considered, the daylight impact might be overestimated. In practice, when blinds are closed to solve glare issues, the electric lighting use and cooling energy use might be higher than this simulation result.

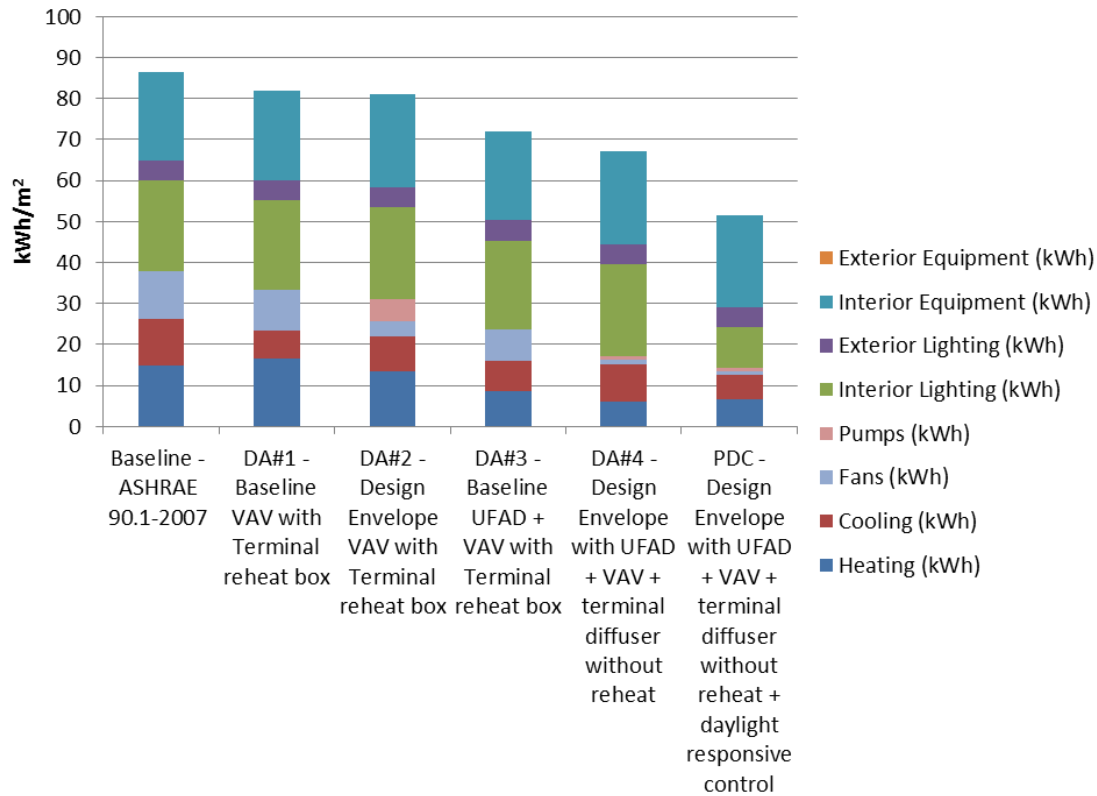


**Figure 8 Annul EUI of the design stage energy models.**

The EUI comparison of various benchmarks and the CSL PDC model is presented in Figure 9.

The U.S. 2003 CBECS (EIA, 2012) data, ASHRAE 90.1-2004, 2007, 2010, and 2013

Department of Energy (DOE) prototype medium office building (DOE, 2014b) energy model

data are used to benchmark the CSL PDC EnergyPlus model. Compared to the 2003 CBECS

national average EUI (revised in 2008) of medium office buildings ( $929 \text{ m}^2 - 2,323 \text{ m}^2$ ), the CSL

PDC model can save 75.39% of the annual energy consumption. Compared to the DOE

prototype medium office building models ( $4,982 \text{ m}^2$ ), with the same Pittsburgh TMY3 weather

file (ASHRAE Climate Zone 5A), the CSL PDC model can save 65.36%, 62.65%, 53.09%, and

49.75% for the year of 2004, 2007, 2010, and 2013, respectively.

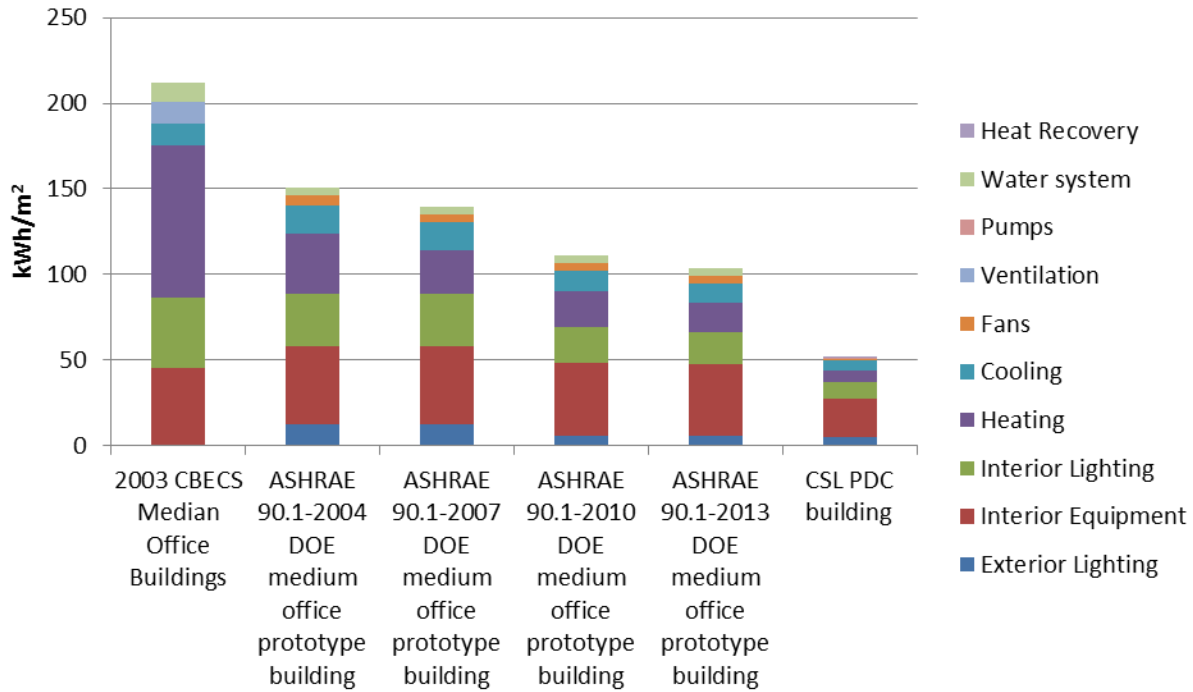


**Figure 9 Annual EUI of various benchmark and the CSL proposed design case models.**

#### **2.2.4. Indoor temperature analysis**

Dual temperature setpoints (with a band range of 23 °C and 24 °C and a tolerance of  $\pm 2.0$  °C on the boundaries) are used as the zone operation temperature. To ensure the models have “comfortable” indoor thermal conditions, “hour temperature setpoint not met” as an important thermal performance indicator has been analyzed. The highest number of “occupied hour temperature setpoint not met” of the PDC model is 122 hours, which meets the ASHRAE 90.1-2007 requirement of “not exceeding 300 hours.” (USGBC, 2011a).

### **2.3. Summary**

This chapter introduces the concept of DBO-EIM infrastructure and demonstrates the first part of the infrastructure – energy modeling for design decision making with a real building case study.

In the case study, the baseline, design alternative, and proposed design case EnergyPlus models are created and the simulation results are compared following the DBO-EIM infrastructure. The results show that the proposed design case building has better energy performance than the baseline, design alternative, and various benchmark building models. This energy comparison process would be of great help for the design team to make design choices to achieve better energy performance.

## Chapter 3. Design-stage EnergyPlus model calibration

---

### 3.1. Overview

BEM model calibration is the transition process between the design and operation stages in the DBO-EIM infrastructure to ensure the load and energy consumption and performance data between BEM model results and the real measured operation data are within the accepted criteria (ASHRAE, 2002). Therefore, it is critical to develop a practical and scientific method to conduct BEM model calibration for design-stage EnergyPlus models. There are typically six categories for BEM models, including location and weather, geometry and material, lighting system, plug load equipment system, HVAC system, and occupant behavior. Some of these input assumptions are generally constant when the design has been made, such as location, geometry, and material. However, some input assumptions, including weather, lighting system, equipment system, HVAC system, and occupant behavior, may have big variations between the design assumption and operation status. These inputs have to be calibrated based on real operation status to ensure the BEM accuracy. Among those inputs, occupant behavior can be especially difficult to measure or quantify directly in the building operation. Figure 10 shows the typical input assumptions and output results of a BEM model.

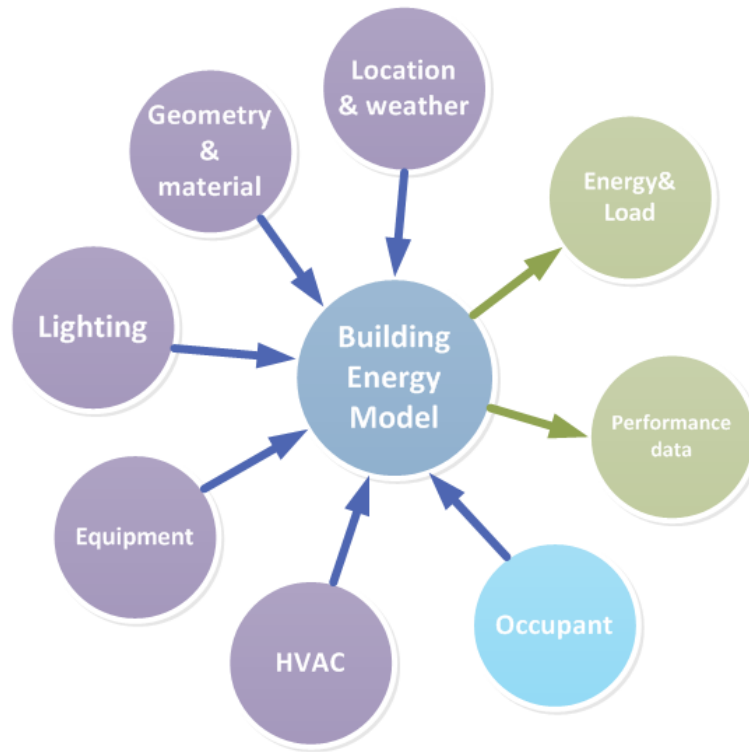


**Figure 10 Input assumptions and output results of the building energy model.**

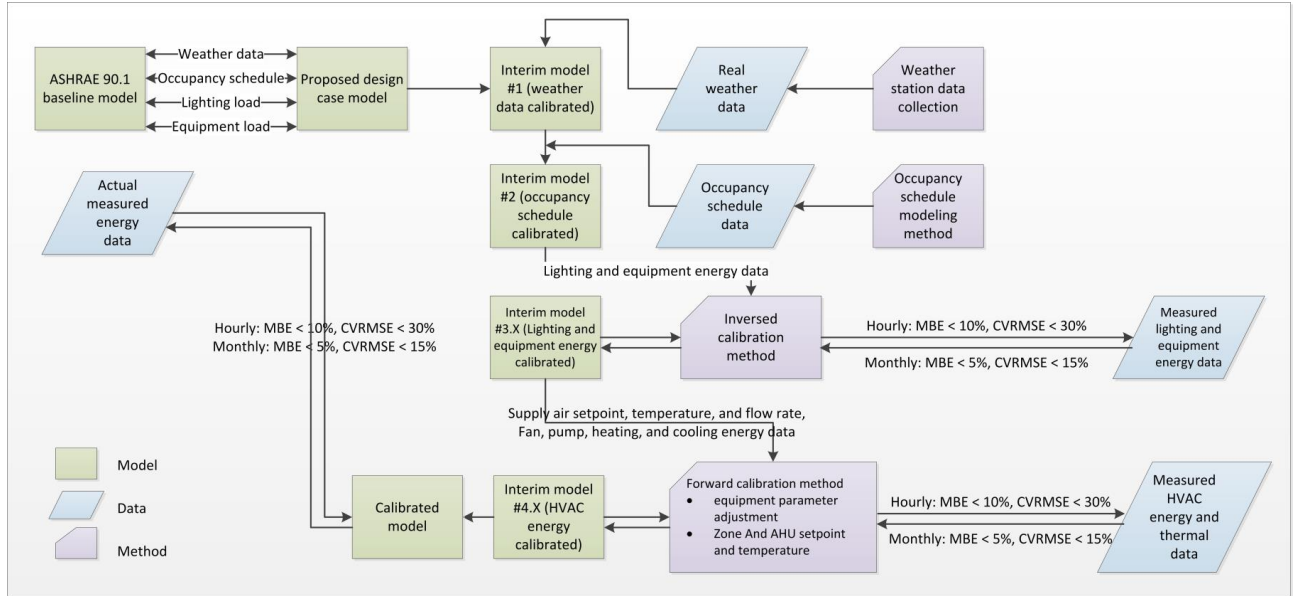
This chapter proposes and demonstrates a BEM calibration method using empirical data for the EnergyPlus model of the CSL building. In this method, occupancy schedules are learned by using data mining algorithms from office appliance energy consumption data. Monthly energy meter data and hourly building automation system (BAS) data are collected and used for the calibration. An inverse calibration procedure is developed for lighting and equipment schedule and power density calibration. HVAC system parameters and controls are calibrated with hourly zone temperature data and monthly energy data.

Figure 11 illustrates the procedures of the proposed EnergyPlus whole building energy model calibration method. The purpose of this calibration is to ensure that the energy model can generate energy consumption results close to the measured values using actual inputs, including weather, occupancy schedule, lighting and equipment schedules and densities, and the HVAC



system parameters and controls. The baseline model is created based on ASHRAE 90.1 Appendix G Building Performance Rating Method. The proposed design case model is created based on design drawings and specifications, with the same input assumptions as the baseline model for fair comparison purpose.

As shown in Figure 11, the first step of the calibration is to replace the TMY (typical meteorological year)-3 weather file with real weather information in accordance with the actual data collection period. The second step is to replace the assumed occupancy schedules with the “real (or learned)” occupancy schedules generated from the data mining study. The third step is to calibrate the interior lighting, interior equipment, exterior lighting, and exterior equipment power densities and schedules with monthly and hourly energy consumption data with a proposed “inversed calibration method”. The fourth and final step is to calibrate HVAC system parameters and controls. As most of these inputs will influence the HVAC system performance (as internal loads and “disturbances”), it is important that the HVAC system be calibrated after other input parameters and systems are calibrated. The calibration acceptance criterion for each calibration step are MBE (mean biased error)  $< 5\%$  and CVRMSE (coefficient of variation of the root mean squared error)  $< 15\%$  for monthly data calibration, and MBE  $< 10\%$  and CVRMSE  $< 30\%$  for hourly data calibration, respectively (ASHRAE, 2002). MBE and CVRMSE are defined by Equation (1 - 3).



**Figure 11 EnergyPlus whole building energy model calibration method.**

$$MBE = \frac{\sum_{i=1}^{N_s} (y_i - \hat{y}_i)}{\sum_{i=1}^{N_s} y_i} \quad (1)$$

$$\bar{Y}_S = \frac{\sum_{i=1}^{N_s} y_i}{N_s} \quad (2)$$

$$CVRMSE_{(S)} = \frac{\sqrt{\sum_{i=1}^{N_s} ((y_i - \hat{y}_i)^2 / N_s)}}{\bar{Y}_S} \quad (3)$$

where,  $y_i$  is the measured data;  $\hat{y}_i$  is the simulated data;  $N_s$  is the sample size; and  $\bar{Y}_S$  is the sample mean of measured data.

### 3.2. Test-bed building model creation and data collection

First, the calibration method is applied to the proposed design case CSL building EnergyPlus model (see Chapter 2 for detailed information). Then the EnergyPlus model is linked with Matlab/Simulink to simulate the actual control settings (Zhao, Lam, *et al.*, 2014). Since the CSL building construction was completed in December 2011 and was occupied in spring 2012, the author started to receive monthly energy consumption data from utility bills from January 2013 and the BAS data from August 2013. Hence, this study uses the data from the whole year of 2013 to calibrate the design case EnergyPlus model.

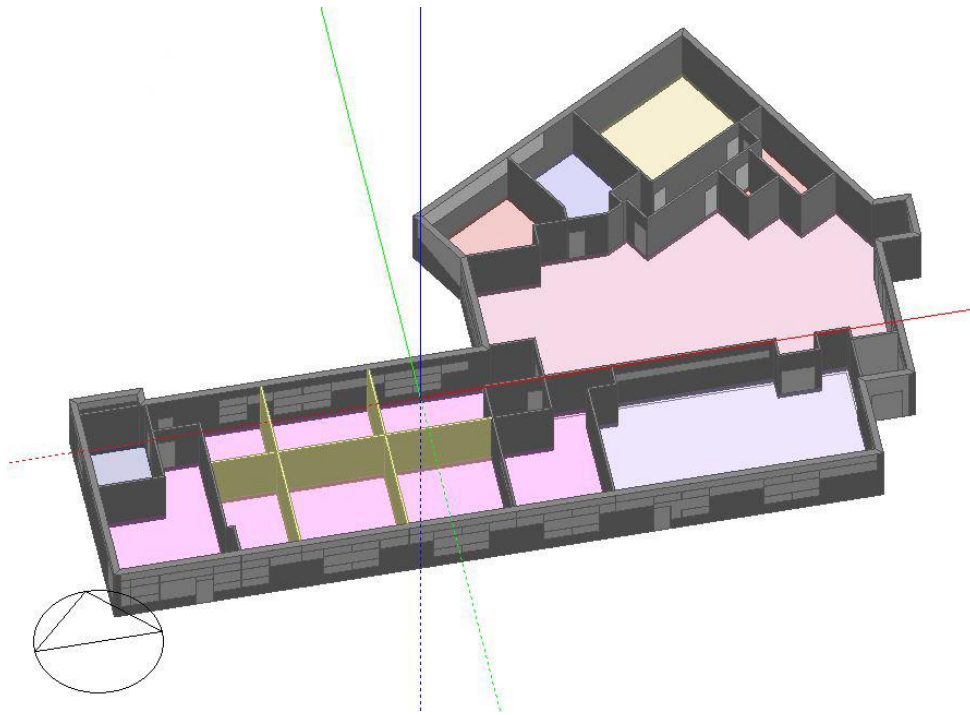


**Figure 12** Screen shot of the CSL building model in the DesignBuilder program.

### 3.3. Weather information for EnergyPlus input

Weather data is one of the key input variables (or disturbances) of BEM models. In most cases, for the purpose of standardization, TMY (typical meteorological year) weather files are used in BEM. However, there are substantial differences between the TMY weather data and the AMY (actual meteorological year) weather data, which is the actual measured data for a particular year. Figure 13 shows clear differences in dry bulb temperature value between the AMY 2013 weather data and the TMY weather data. Therefore, the AMY 2013 weather data (WBT, 2013) is used to replace the TMY weather data used in the design case EnergyPlus model, so that the weather input variables are consistent with the actual weather conditions in 2013.

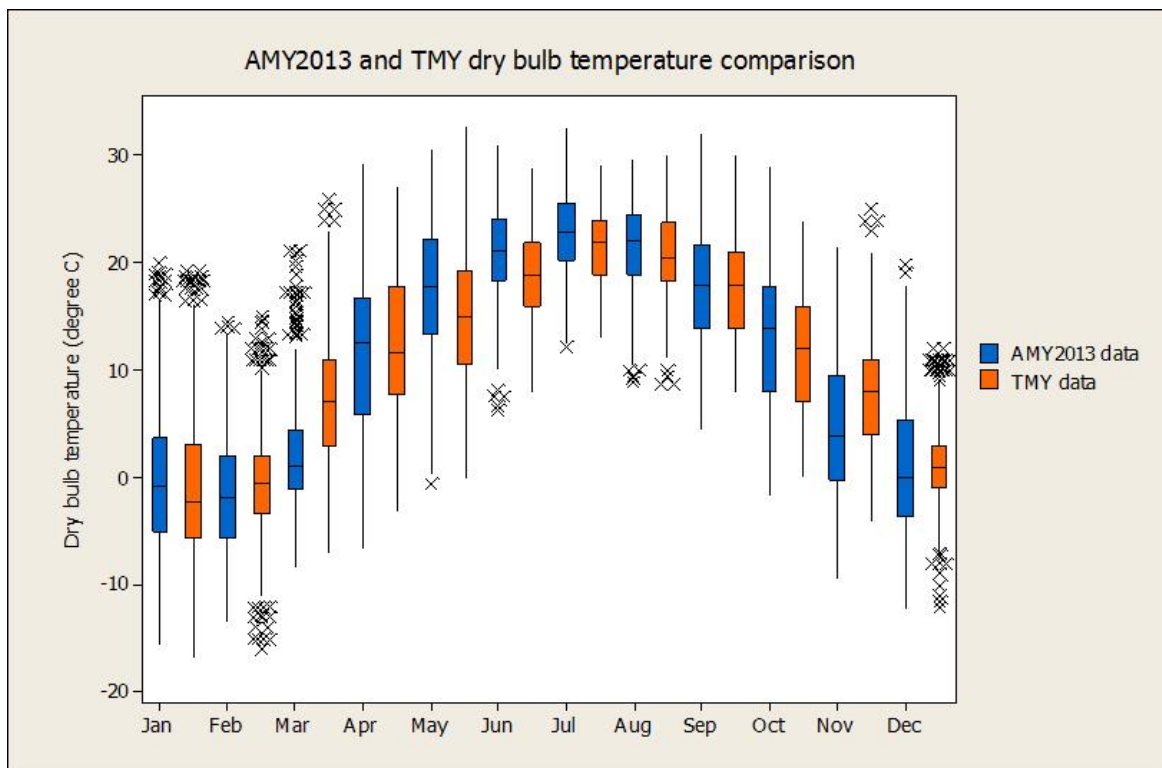


**Figure 13 Dry bulb temperature comparison between the AMY2013 and TMY weather data.**

### **3.4. Occupant behavior and schedule modeling**

From the literature review section of “1.2.1. Occupant behavior in buildings”, it is clear that occupants’ passive behavior has significant impact on building HVAC energy consumptions and that “indirect” occupant behavior learning approach is more practical for this case study. Hence, this section aims to develop a less intrusive “indirect” data mining approach to learn the occupants’ passive behavior. First, several methods and algorithms are explained in detail. Then using the most appropriate methods and algorithms, the dissertation presents a pilot study in a laboratory office and a real case study in the CSL building. Conclusions are drawn from the results of the two studies.

#### ***3.4.1. Experiment design***

The experiment aims to collect metered data of electricity consumptions of office appliances and occupant behavior “ground truth<sup>1</sup>” data concurrently in order to perform a data mining study using the two datasets.

Here, Plugwise<sup>®</sup> wireless smart meters (Plugwise, 2013) are used to collect individual office appliance electric power consumption data for each occupant with a 5-minute time interval. The electricity metered data of office appliances are used to build the occupant individual behavior models and group schedule models.

Ground truth data are used to train and validate the models. The ground truth data is collected with Fitbit<sup>®</sup> Zip<sup>™</sup> or Flex<sup>™</sup> pedometer (Fitbit, 2013a, 2013b) and a computer idle-time logging

---

<sup>1</sup> In machine learning, the term "ground truth" refers to the accuracy of the training set's classification for supervised learning techniques. This is used in statistical models to prove or disprove research hypotheses.

program installed in the occupant's computer. To reveal presence/absence information, participants are required to wear the pedometer when they are in the office for the period of the study. The pedometer contacts the Fitbit<sup>®</sup> Bluetooth Dongle every nine seconds when it is within a 20 feet (6.09 meter) range from the computer. In order to reveal whether the occupant is actively working with the computer, a Java script<sup>2</sup> has been developed and installed in all the participants' computers to record the time that neither keyboard nor mouse is used within five minutes.

By combining these two pieces of information, four behavioral scenarios can be recorded, as shown in Table 8. (1) "Occupied computer-based work" indicates the occupant is working with the computer actively at his/her office bay. (2) "Occupied non-computer-based work" indicates the occupant is at his/her bay, but is not using the computer actively. The possible activities include paper-based tasks, discussing with colleagues, having lunch, having phone calls and so on. (3) "Remote computer-based work" means the occupant is remotely accessing the computer to work from elsewhere, meaning that the computer is actively running but the occupant is not in the office. (4) "Unoccupied" means the occupant is not in his/her office bay and is not working with the computer. The first two scenarios indicate the occupant is in the office and the second two scenarios indicate the occupant is not in the office. By combining the information of individual presence and absence, with the 5-minute time interval, a group schedule can be generated and then can be used in BEM model calibration.

---

<sup>2</sup> Acknowledgement to Haopeng Wang for coding the script.

**Table 8 Occupant individual behavior ground truth.**

	Computer in active mode	Occupant in the bay
“Occupied computer-based work”	1	1
“Occupied non-computer-based work”	0	1
“Remote computer-based work”	1	0
“Unoccupied”	0	0

The data collection system architecture is shown in Figure 14. Both ground truth and electricity metered data are collected with Python (Python, 2012) programs developed by the research team<sup>3</sup> and stored in an online MySQL database (Oracle, 2014).

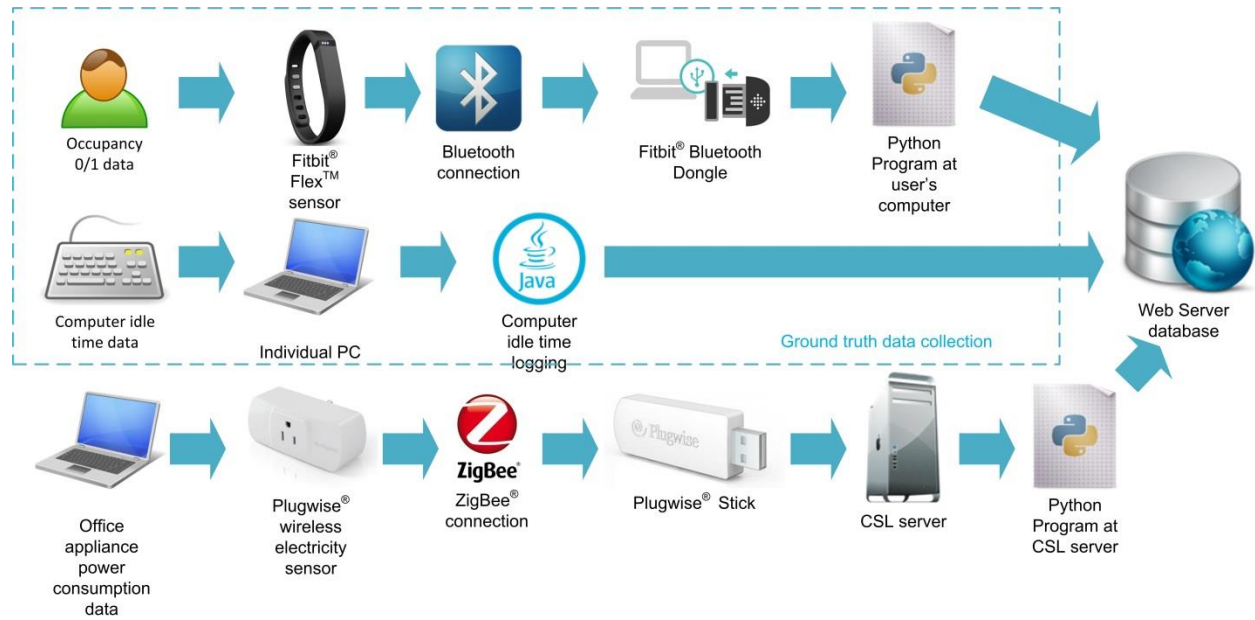


**Figure 14. Plug Load meter data and ground truth data collection architecture (The images of Fitbit®, Plugwise®, and ZigBee® are from (Fitbit, 2013a), (Plugwise, 2013), and (ZigBee, 2014)).**

<sup>3</sup> The research team consists of Jie Zhao, Ray Yun, and Haopeng Wang.

### 3.4.2. Nominal classification algorithms

Individual behavior data mining is a nominal classification problem. By definition, “in classification learning, the learning scheme is presented with a set of classified examples from which it is expected to learn a way of classifying unseen examples.” This method is a type of supervised learning that “the scheme operates under supervision by being provided with the actual outcome for each of the training examples.” (Witten *et al.*, 2011). For this study, the nominal class values are “Occupied computer-based work”, “Occupied non-computer-based work”, “Remote computer-based work”, and “Unoccupied”, as indicated in Table 8. The training dataset consists of power consumption data with 5-minute intervals over the data collection period. The attributes of each data instance are different office appliances. For privacy and generalization purposes, the appliances are categorized as computers, lights, and other appliances. Table 9 shows examples of instances in the training dataset with three attributes and three associated class values.

**Table 9 An example of the training dataset for the individual behavior learning.**

Instances	Attributes			Class value
	Computer (Watt)	Light (Watt)	Other (Watt)	
Instance #1	21	0	43	Occupied computer-based work
Instance #2	21	0	1	Remote computer-based work
Instance #3	14	0	1	Occupied non-computer-based work
Instance #4	0	0	1	Unoccupied

For this nominal classification problem, three algorithms are tested and compared, which are C4.5 decision tree (C4.5), locally weighted Naïve Bayes (LWNB), and support vector machine



(SVM). The model results are tested with ground truth data by 10-fold cross validation and compared across different algorithms with the 2-tailed paired T-test ( $p = 0.05$ ) (Witten *et al.*, 2011). Weka program is used to build, test, and compare the data mining model results (Weka, 2011).

#### 3.4.2.1. C4.5 decision tree algorithm

C4.5 decision tree algorithm is developed for classification learning based on the information gain theory. C4.5 aims to build the decision tree nodes (or leafs) recursively by maximizing the information gain of the attributes at each step (Quinlan, 1993). The information entropy and gain are calculated by Equations (4 – 6) (Moore, 2003).

Suppose an attribute dataset  $X$  has one of  $m$  values  $V_1, V_2, \dots, V_m$ .  $Y$  is the class value associated with the attribute dataset. The information entropy  $H(X)$  of the set is defined as,

$$H(X) = - \sum_{i=1}^m P(V_i) \log_2(P(V_i)) \quad (4)$$

where  $P(V_i)$  is the probability of getting the  $i^{\text{th}}$  class value when randomly selecting one from the dataset  $X$ . The conditional entropy  $H(Y|X)$  is defined as,

$$H(Y|X) = \sum_{i=1}^m P(X = V_i) H(Y|X = V_i) \quad (5)$$

where  $H(Y|X = V_i)$  is the entropy of  $Y$  among only those instances in which  $X$  has value  $V_i$ , named “specific conditional entropy”.  $P(X = V_i)$  is the probability of  $V_i$  in the dataset of  $X$ . The information gain  $IG(Y|X)$  is defined as,

$$IG(Y|X) = H(Y) - H(Y|X) \quad (6)$$

The pseudo-code for generating decision trees is defined by (Kotsiantis, 2007) as follows,

1. Check for base cases;
2. For each attribute  $a$ ;
3. Find the normalized information gain ratio from splitting on  $a$ ;
4. Let  $a\_best$  be the attribute with the highest normalized information gain;
5. Create a decision node that splits on  $a\_best$ ;
6. Recurse on the sublists obtained by splitting on  $a\_best$ , and add those nodes as children of node.

The decision tree algorithm has been used in the building realm to predict residential energy demand with over 90% accuracy (Yu *et al.*, 2010).

#### 3.4.2.2. Locally weighted Naïve Bayes (LWNB) algorithm

Locally weighted learning (LWL) is one type of “lazy learning” methods, which usually involve “storing the training data in memory, and finding relevant data in the database to answer a particular query.” LWL uses “locally weighted training to average, interpolate between, extrapolate from, or otherwise combine training data” (Atkeson *et al.*, 1999).

According to (Mitchell, 2010), naïve Bayes classifier is developed based on Bayes’ theory with the “naïve” conditional independence assumptions. Conditional independence is defined that “given random variables  $X$ ,  $Y$  and  $Z$ , we say  $X$  is conditionally independent of  $Y$  given  $Z$ , if and only if the probability distribution governing  $X$  is independent of the value of  $Y$  given  $Z$ ”, as shown in Equation (7),

$$(\forall i, j, k) P(X = x_i | Y = y_j, Z = z_k) = P(X = x_i | Z = z_k) \quad (7)$$

Assuming  $X$  contains  $n$  attributes which are conditionally independent of one another given  $Y$ , the Bayes rule of probability can be simply calculated by Equation (8).

$$P(X_1 \dots X_n | Y) = \prod_{i=1}^n P(X_i | Y) \quad (8)$$

The probability that  $Y$  will take on its  $k$ th possible value according to Bayes rule can be derived from Equation (9),

$$P(Y = y_k | X_1 \dots X_n) = \frac{P(Y=y_k)P(X_1 \dots X_n | Y=y_k)}{\sum_j P(Y=y_j)P(X_1 \dots X_n | Y=y_j)} = \frac{P(Y=y_k) \prod_i P(X_i | Y=y_k)}{\sum_j P(Y=y_j) \prod_i P(X_i | Y=y_j)} \quad (9)$$

where  $n$  is the total number of attributes.

The idea of LWNB classifier is to assign more weight to the training instances in the neighborhood and assign less weight to the instances that are further from the test instance (Frank *et al.*, 2002). With the local weighting mechanism, the right hand side of the Equation (9) can be estimated using Equation (10),

$$P(Y = y_k) = \frac{1 + \sum_{k=0}^m I(Y=y_k) \omega'_k}{p + \sum_{k=0}^m \omega'_k} \quad (10)$$

where  $m$  is the total number of instances,  $p$  is the total number of instances, and  $\omega'_k$  is the rescaled weight that considered the zero-frequency problem (Frank *et al.*, 2002).  $I(Y = y_k)$  is an indicator function, defined as,

$$I(Y = y_k) = \begin{cases} 1, & \text{if } (Y = y_k) \\ 0, & \text{otherwise} \end{cases} \quad (11)$$

The numeric attributes should also be considered differently from typical nominal attributes.

Details can be found in (Frank *et al.*, 2002).

#### ***3.4.2.3. Support vector machine (SVM) algorithm***

The concept of support vector machine is developed by Boser et al. and Cortes et al (Boser *et al.*, 1992; Cortes and Vapnik, 1995). The basic idea is that “input vectors are non-linearly mapped to a very high dimension feature space. In this feature space, a linear decision surface is constructed. Special properties of the decision surface ensure high generalization ability of the learning machine.” (Cortes and Vapnik, 1995)

SVM can solve both classification and regression (Support Vector Regression, SVR) problems (Drucker *et al.*, 1997). The algorithm has been successfully used in several studies in the building field to predict energy usage (Dong *et al.*, 2005; Li *et al.*, 2009; Solomon *et al.*, 2011), model heat pump systems (Esen *et al.*, 2008), and identifying key factors for Leadership in Energy and Environment Design (LEED) building markets (Zhao and Lam, 2012).

This study uses sequential minimal optimization (SMO) method to train the SVM classifier. The SVM theory and the SMO algorithm details can be found in (Dong *et al.*, 2005; Platt, 1998).

#### ***3.4.3. Numeric regression algorithms***

The occupant group schedule learning is a numeric regression problem. The goal of this learning is to predict the occupant group schedule pattern for typical workdays using the appliance energy data. Dissimilar to the individual behavior learning problem, all the appliances should be considered as attributes simultaneously, and the class value should be a number that varies from 0 to the total number of the valid participants N. Table 10 is an example of the training dataset for the group schedule learning.

3 algorithms are tested for this problem, which are linear regression (LR), locally weighted regression (LWR), and support vector regression (SVR). The model results are tested with ground truth data using 10-fold cross validation and compared across different algorithms using 2-tailed paired T-test ( $p = 0.05$ ). Weka program is used to build, test, and compare the data mining models.

**Table 10 An example of the training dataset for the group schedule learning.**

Instances	Attributes					Class value
	Computer-1 (W)	Light-1 (W)	...	Computer-N (W)	Light-N (W)	
Instance #1	21	0	...	23	8	N
Instance #2	21	0	...	21	0	N-1
Instance #3	14	0	...	10	0	N-5
Instance #4	0	0	...	0	0	0

#### 3.4.3.1. Linear regression (LR) algorithm

Linear regression is a commonly used algorithm for numeric prediction. The linear model can be expressed by Equation (12),

$$f(x) = \omega_0 + \omega_1 x_1 + \omega_2 x_2 + \cdots + \omega_k x_k \quad (12)$$

where  $f(x)$  is the class value;  $x_1, x_2, \dots, x_k$  are the attributes; and  $\omega_0, \omega_1, \dots, \omega_k$  are the weights.

The algorithm iteratively assigns weights to the model and computes the predicted class value and then tries to minimize the sum of squares of the differences between predicted class value and actual class value based on Equation (13) (Witten *et al.*, 2011),

$$J = \min \sum_{i=1}^n \left( f(x)^{(i)} - \sum_{j=0}^k \omega_j a_j^{(i)} \right)^2 \quad (13)$$

where  $n$  is the number of the total instances.

### 3.4.3.2. Locally weighted regression (LWR) algorithm

As part of the locally weighted learning algorithms, and similar to the idea of locally weighted Naïve Bayes, LWR is “a memory-based method that performs a regression around a point of interest using only training data that are “local” to that point.” (Cohn *et al.*, 1996)

Locally weighted scatterplot smooth (LOWESS) method is used to smooth data (Cleveland, 1979) for LWR. Irizarry et al. described the process of obtaining a LOWESS for a target covariate  $x_0$ . The local weight can be defined by Equations (14-18) (Irizarry, 2001),

$$\omega_i(x_0) = W\left(\frac{x_i - x_0}{h(x_0)}\right) \quad (14)$$

where  $W$  is defined by,

$$W(u) = \begin{cases} (1 - |u|^3)^3 & |u| \leq 1 \\ 0 & |u| > 1 \end{cases} \quad (15)$$

The span (or bandwidth)  $h(x_0)$  is defined by,

$$h(x_0) = |x_0 - x_i| \quad (16)$$

The smoothing window  $S(x_0)$  for  $x_0$  is then defined by,

$$S(x_0) = [x_0 - h(x_0), x_0 + h(x_0)] \quad (17)$$

Within the smoothing window,  $f(x)$  can be approximated. Assumed weights are defined by  $\omega = (\omega_0, \omega_1, \dots, \omega_k)'$ , which can be calculated by minimizing,

$$\hat{\omega} = \min_{\omega \in \mathbb{R}^k} \sum_{i=0}^n \omega_i(x_0) [Y_i - f(x)]^2 \quad (18)$$

where  $Y_i$  is the class value for each instance.

#### *3.4.3.3. Support Vector Regression (SVR) algorithm*

The SVR algorithm uses similar concept as the SVM algorithm and has been used by several studies in the building field as described in the section of “3.4.2.3. Support vector machine (SVM) algorithm”.

#### *3.4.4. Pilot study at the Intelligent Workplace*

This pilot study aims to demonstrate the feasibility of the proposed method with small scale participants in a laboratory office space.

##### *3.4.4.1. Experiment Setup and Data Processing*

The experiment is set up in the Intelligent Workplace (IW) on the Carnegie Mellon University (CMU) campus in Pittsburgh, Pennsylvania USA. It is designed to collect individual office appliance electricity consumption data and record occupant behavior ground truth data concurrently for two weeks. Six voluntary office workers (four males and two females) age from 24 to 28 years old participated in the experiment. The metered office appliances include desktop computers, computer monitors, task lights, speakers, laptop computers, hard drives and personal heaters.

#### 3.4.4.2. Individual behavior modeling results

Six datasets of 4332 instances with four to six attributes are trained and tested individually using 10-fold cross validation. C4.5 decision tree, locally weighted Naïve Bayes (LWNB), and support vector machine (SVM) algorithms are tested and compared. The results is compared with 2-tailed paired-T test ( $p = 0.05$ ).

The percentage of correctly classified instances and Kappa statistic (Carletta, 1996) values are compared using the modeling results.

Kappa statistic is used to measure the agreement of categorization by two or more raters (class values), taking into consideration of the agreement occurring by chance. Therefore, Kappa statistic value is believed to be more reliable than the simple percentage of correctly classified instances. It is defined by Equation (19) (Carletta, 1996),

$$\kappa = \frac{\text{Pr}(a) - \text{Pr}(e)}{1 - \text{Pr}(e)} \quad (19)$$

where,

$\text{Pr}(a)$  is the relative observed agreement among raters,

$\text{Pr}(e)$  is the hypothetical probability of chance agreement of all the raters.

If  $\kappa = 1$ , it means the model's classification result is in complete agreement with the ground truth. If  $\kappa = 0$ , it means the model's classification result is completely different from the ground truth.



The algorithm comparison results in Table 11 show that no statistically significant difference among the three algorithms is found. Therefore, from the practical point of view, C4.5 decision tree can be a suitable candidate. By comparing the six occupants, Occupant #1 and Occupant #6 have the highest percentage of correctly classified instances, but the kappa statistic value for Occupant #1 is the highest among all the subjects, while the kappa statistic value for Occupant #6 is the lowest among all. The possible explanation is that nominal value of Occupant #6 is highly skewed to “unoccupied”, which is 89.93% of the entire class value. While other subjects’ “unoccupied” class value percentages are 74.51%, 63.73%, 72.46%, 80.77%, and 72.25% from Occupant #1 to Occupant #5, respectively. Therefore, the percentage of correctly classified instances of Occupant #6 is not as trustworthy as Occupant #1.

Despite the diversity of the occupant behaviors, by using C4.5 algorithm, the average percentage of correctly classified instances is 92.39%, and the average kappa statistic is 0.68. The overall learning result is satisfactory.

**Table 11 Occupant behavior recognition result (percentage of correctly classified instances / kappa statistic).**

	Support vector machine	Locally weighted learning	C4.5 – decision tree
Occupant #1	95.96 / 0.87	96.00 / 0.87	96.02 / 0.87
Occupant #2	82.06 / 0.61	82.05 / 0.61	84.43 / 0.66
Occupant #3	94.92 / 0.85	94.94 / 0.85	94.95 / 0.85
Occupant #4	90.65 / 0.62	90.61 / 0.62	92.12 / 0.66
Occupant #5	89.26 / 0.71	88.85 / 0.70	89.56 / 0.71
Occupant #6	96.69 / 0.04	97.02 / 0.29	97.26 / 0.37

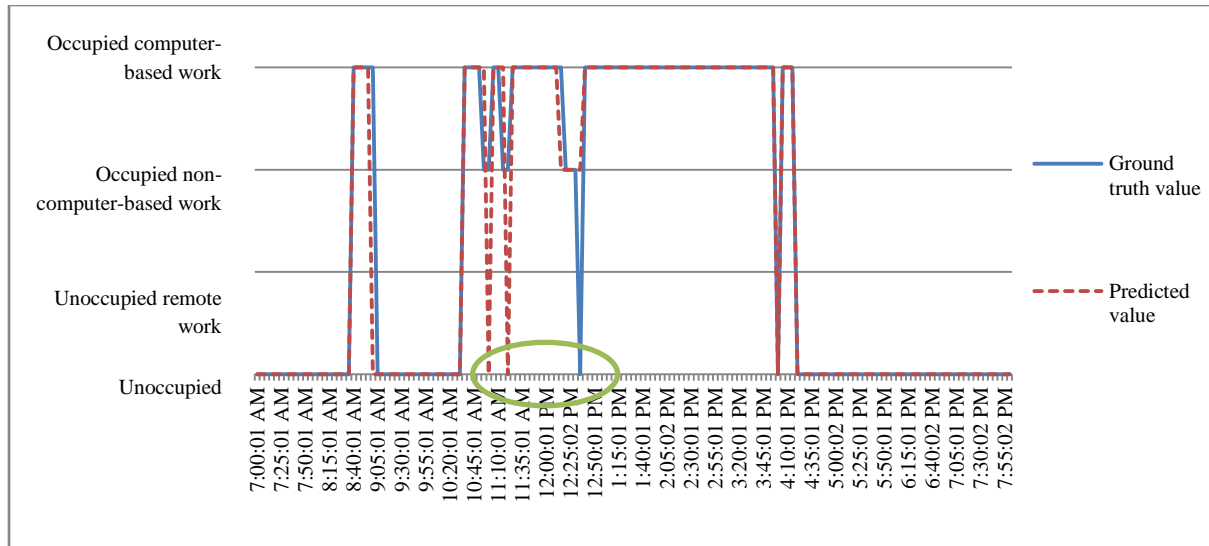


**Figure 15 True value and predicted value of Occupant #1 in a typical work day.**

Figure 15 illustrates the comparison between the ground truth value and predicted value of Occupant #1 in a typical work day. The model predicts fairly accurately for occupied computer-based work. However, the model fails to distinguish “occupied non-computer-based work” and “unoccupied” instances in two cases, as highlighted in Figure 15. First, from 11:00am to 11:20am, there are several “non-computer-based work” instances, but the model categorized the instances as “unoccupied”. When looking at the raw dataset of these incorrectly classified instances, the two computer monitors are off, due to the “sleep mode” setting of the computer. Given the fact that “computer” and “computer monitor” have high weights on the model, it is expectable the model may make mistakes in this situation. Second, at 12:35pm, the ground truth value is “unoccupied”, while the predicted value is “occupied non-computer-based work”. By comparing the raw data of electricity meters from 12:20pm to 12:35pm, no significant difference between the first three instances and the last one can be found. Thus the author believes that the ground truth value of 12:35pm may be a random error, which may occur when Fitbit® device

goes to the sleep mode. This error case can rarely happen during the experiment, because the occupant is required to wear it on the wrist to keep the acceleration sensor active during the experiment period.

#### 3.4.4.3. Group schedule modeling results

For economic and technical reasons, two datasets are compared for the occupant group schedule learning. One is a sub-metered raw dataset from individual appliances, which has 33 attributes. The other is the aggregated energy consumption data of all the appliances for each occupant, which has six attributes. The reason for comparing the two datasets is that the less data a method requires the more practical the method will be. In most office spaces, appliance-by-appliance sub-metering data may not be available but total plug load metering by occupant may be more likely.

**Table 12 Occupancy schedule prediction result (correlation coefficient / relative absolute error).**

	<b>Support vector regression</b>	<b>Locally weighted learning</b>	<b>Linear regression</b>
Dataset by appliances	0.93 / 0.27	0.85 / 0.48	0.93 / 0.28
Dataset by occupants	0.92 / 0.32	0.83 / 0.52	0.92 / 0.33

Two datasets are trained and tested by using support vector regression (SVR), locally weighted learning (LWL), and linear regression (LR) algorithms. Correlation coefficient and relative absolute error are used to evaluate the modeling performance of the three algorithms with the 10-fold cross validation. Correlation coefficient measures the statistical correlation between actual values and predicted values, which is defined by Equation (20). Relative absolute error is defined

as the total absolute error that normalized by the total deviation of actual values in the training dataset, as shown in Equation (21).

$$\text{Correlation coefficient} = \frac{S_{PA}}{\sqrt{S_P S_A}}, \quad (20)$$

$$\text{Relative absolute error} = \frac{|p_1 - a_1| + \dots + |p_n - a_n|}{|a_1 - \bar{a}| + \dots + |a_n - \bar{a}|} \quad (21)$$

where  $p_i$  is the predicted value;  $a_i$  is the actual value in the ground truth test dataset;  $\bar{a}$  is the mean value over the training data;  $S_{PA} = \frac{\sum_i (p_i - \bar{p})(a_i - \bar{a})}{n-1}$ ,  $S_P = \frac{\sum_i (p_i - \bar{p})^2}{n-1}$ ,  $S_A = \frac{\sum_i (a_i - \bar{a})^2}{n-1}$ ;  $\bar{a}$  is the mean value over the test data.

The model prediction results are shown in Table 12. No statistically significant difference is found among the three different algorithms and among the two datasets. Hence, for the purpose of predicting occupant group schedule, it is practical to use LR algorithm over the dataset by occupants. Figure 16 shows the comparison between the ground truth value and predicted value of occupant group schedule in a typical work day by using LR algorithm over the dataset by occupants.

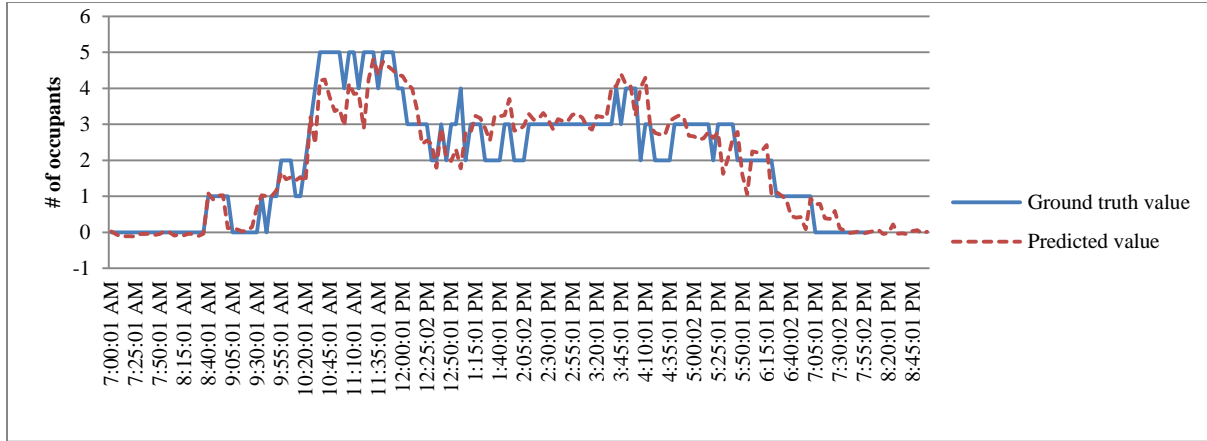


**Figure 16 True value and predicted value of occupancy schedule in a typical work day.**

### ***3.4.5. Case study at the Center for Sustainable Landscapes***

The pilot study has demonstrated the feasibility of the method in a small scale laboratory office space. This case study in the CSL building aims to implement the experiment in the real office space to further test the applicability of the method. 15 office workers in the open office spaces participated in the study voluntarily for three months from October to December 2013.

#### ***3.4.5.1. Experiment Setup and Data Processing***

The experiment data collection lasts for 84 days in the CSL open office spaces. 49 out of 84 days are valid weekdays that are included in the study. 27 days are weekends and holidays, which are excluded from the study, assuming there is no one working during the weekends and holidays.

The data instances of eight weekdays are also excluded from the study, because the datasets of those eight weekdays are not complete due to some technical issues (power shut down, internet connection issues, etc.) during the experiment. Figure 17 shows the statistics of weekdays and weekends (holidays) in the study.

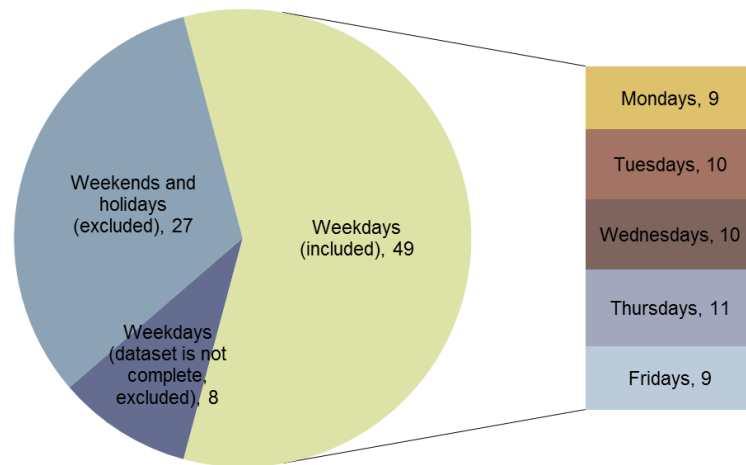


**Figure 17 The statistics of weekdays and weekends (holidays) in the study.**

The statistics of participants in the study are shown in Figure 18. The datasets of 5 out of 15 participants are invalid, i.e., the collected valid Fitbit<sup>®</sup> data or computer idle-time data instances are less than 30% of the total data instances. There are several possible reasons for the invalid data instances. For example, some participants did not charge their Fitbit<sup>®</sup> devices and some did not wear their devices on a regular basis. In other cases, some participants' work requires them to travel frequently with little time presence in the office. In total, 10 participants' datasets are included in the study.

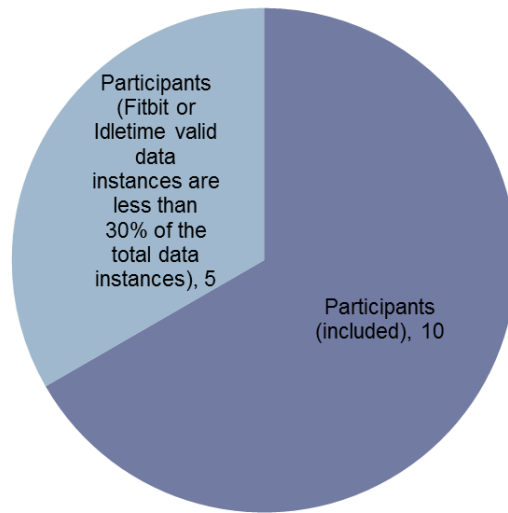


**Figure 18 The statistics of participants in the study (number of people is shown in the graph).**

14111 instances of the 5-minute power consumption data are collected for the 10 participants over the 49 days of the study. The total number of metered office appliances is 28. The types and numbers of the appliances are shown in Figure 19. 11 laptop computers, 10 task lights, three personal fans, two computer monitors, one charger, and one printer are metered for the study. However, the actual study has treated personal fans, computer monitors, the charger, and the printer as “others”, in order to eliminate the personal identifiable data to protect the participants’ privacy.

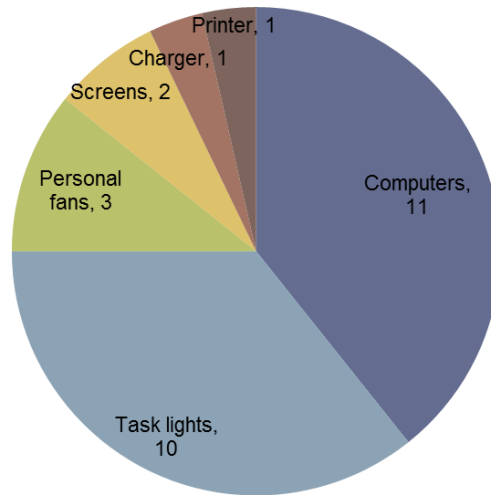


**Figure 19 The statistics of metered office appliances in the study.**

#### *3.4.5.2. Individual behavior modeling results*

First, C4.5 decision tree, locally weighted Naïve Bayes (LWNB), and support vector machine (SVM) algorithms are applied to each participant's training dataset. Then the results are cross validated and compared with 2-tailed paired test ( $p=0.05$ ). The percentage of correctly classified instances and Kappa statistic values are compared using the modeling results, as shown in Table 13.

For percentage of correctly classified instances, C4.5 has statistically significantly better accuracy in 9 out of 10 cases compared to LWL, and 8 out of 10 cases compared to SVM. Kappa value comparison shows a similar result that C4.5 has significant better performance for 7 out of 10 datasets.



**Table 13. Occupant individual behavior data mining result.**

	C4.5 decision tree		Locally weighted learning		Support vector machine	
	Correctly classified instances (%)	Kappa statistic	Correctly classified instances (%)	Kappa statistic	Correctly classified instances (%)	Kappa statistic
Occupant A	95.00	0.88	94.16*	0.88	95.00	0.87*
Occupant B	92.93	0.83	91.64*	0.81*	91.84*	0.8*
Occupant C	91.36	0.77	91.36	0.72*	88.64*	0.77
Occupant D	82.53	0.29	78.87*	0.03*	79.48*	0.01*
Occupant E	93.52	0.84	88.17*	0.82*	92.35*	0.7*
Occupant F	90.05	0.77	89.50*	0.76*	89.58*	0.76*
Occupant G	89.86	0.60	89.07*	0.53*	89.38*	0.51*
Occupant H	85.81	0.60	84.15*	0.57*	84.31*	0.57*
Occupant I	94.51	0.74	94.30*	0.74	94.32*	0.74
Occupant J	87.37	0.54	87.15*	0.56 <sup>#</sup>	87.19	0.56 <sup>#</sup>
Mean	90.29	0.69	91.36	0.64	91.10	0.63

\*statistically significant lower compared to C4.5 ( $p = 0.05$ ).

<sup>#</sup>statistically significant higher compared to C4.5 ( $p = 0.05$ ).

The average computation time of training and testing C4.5 models is 0.03 seconds. It has a clear advantage over the SVM's 0.06 seconds and LWL's 6.96 seconds. Therefore, C4.5 is selected to build the individual behavior model for all the occupants.

In order to reduce the possibility of over-fitting, the minimum instances per leaf of the C4.5 algorithm is set to be 10, suggesting that when testing the trained model, there should be at least 10 cases for each behavioral category.

The third column in Table 13 shows the Kappa statistic values of different datasets with C4.5 algorithm. The mean value of all the occupant behavior predictions is  $\bar{\kappa} = 0.69$ , the median value is  $\tilde{\kappa} = 0.77$ , the highest value is  $\kappa_{max} = 0.88$ , and the lowest value is  $\kappa_{min} = 0.29$ .

Occupant C and Occupant F have the same Kappa statistic value as the median value  $\tilde{\kappa} = 0.77$ , so detailed comparative analysis is presented for these two occupants. Figure 20 and Figure 21 show the parallel coordination plots of the attributes and class value of User C and User F in the Weka program, respectively. The x-axis represents the attributes and class values, which are coded by numeric values as 0, 1, 2, and 3. The y-axis presents the attribute values and codified behavior values. This plot provides readers a visual representation of the possible pattern between the attributes and the class value. Occupant C has a laptop computer and a desk lamp, which are both utilized rather frequently (with non-zero power consumptions); while Occupant F has a third (other) appliance besides the laptop computer and the lamp. In most cases, the lamp is not used (with zero power consumption), but the third appliance is in active mode (with non-zero power consumption). Clearly, the behavior patterns of the two occupants are very different, although the accuracy of the prediction results is similar.

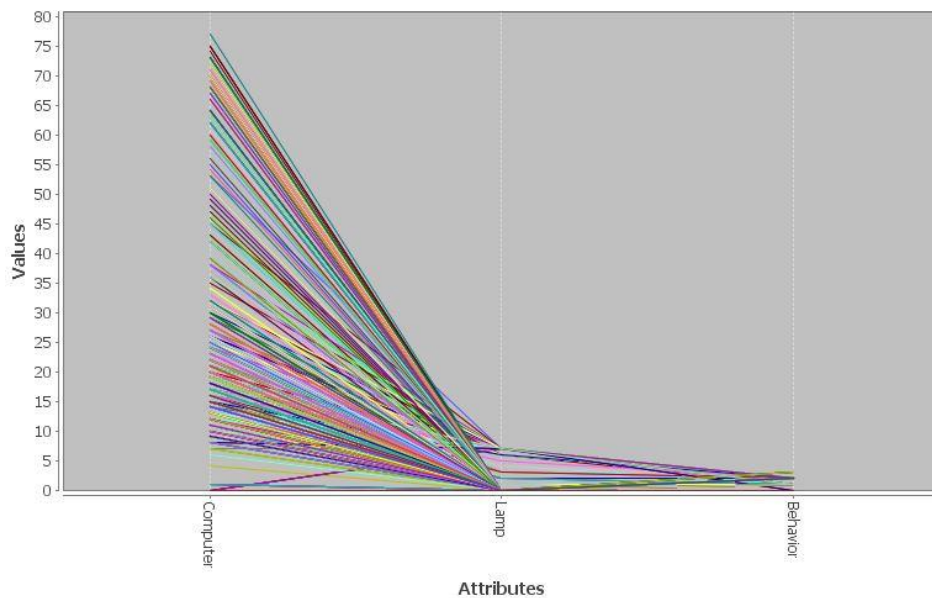


**Figure 20 Attributes and class value parallel coordination plots of occupant C (Value on the y-axis: power consumption data and types of behavior).**

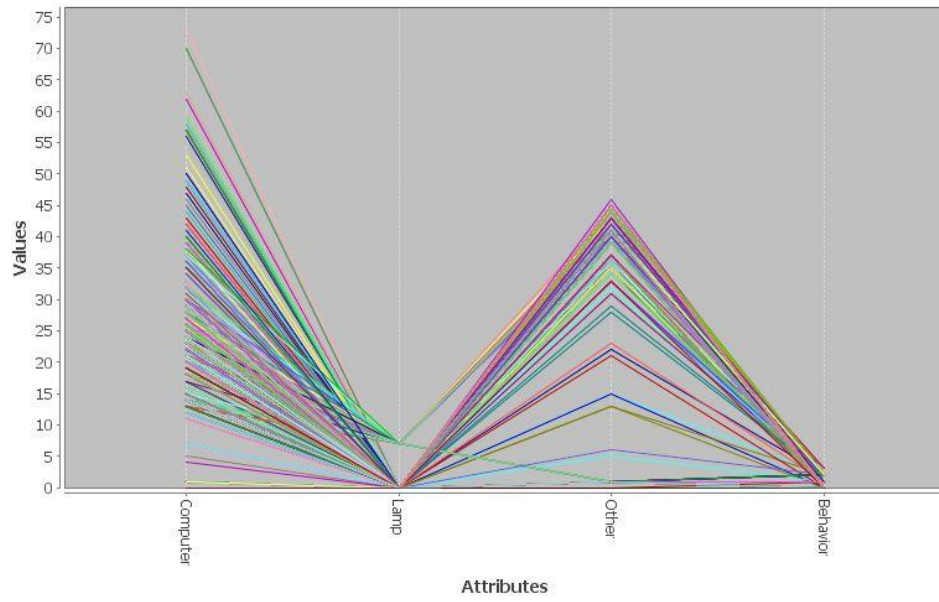


**Figure 21 Attributes and class value parallel coordination plots of occupant F (Value on the y-axis: power consumption data and types of behavior).**

The C4.5 decision tree models shown in Figure 22 and Figure 23 also suggest different use patterns for the two occupants. (Number A/Number B) in the “leaf” nodes in Figure 22 represents the ratio of the correctly classified instances to the incorrectly classified instances of the tree node. The fractional numbers at tree leafs mean there are missing attribute values in the dataset (Witten *et al.*, 2011). Occupant C has a very clear and consistent use pattern for his/her computer which can predict his/her working behavior fairly accurately. If the computer power is more than 12W, for more than 90% of the time, it is safe to draw the conclusion that the participant is actively working in the office. However, Occupant C’s model is not able to recognize the “non-computer-based work” behavior. Also the use of the lamp is not correlated to his/her behavior or occupancy status.

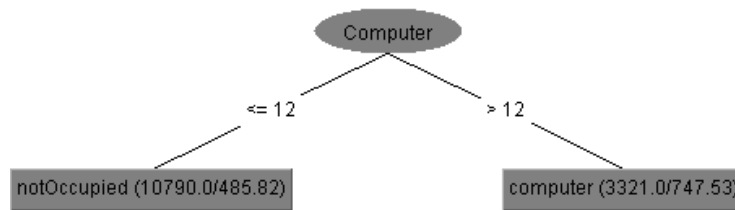


**Figure 22 C4.5 decision tree models of occupant C's behavior.**

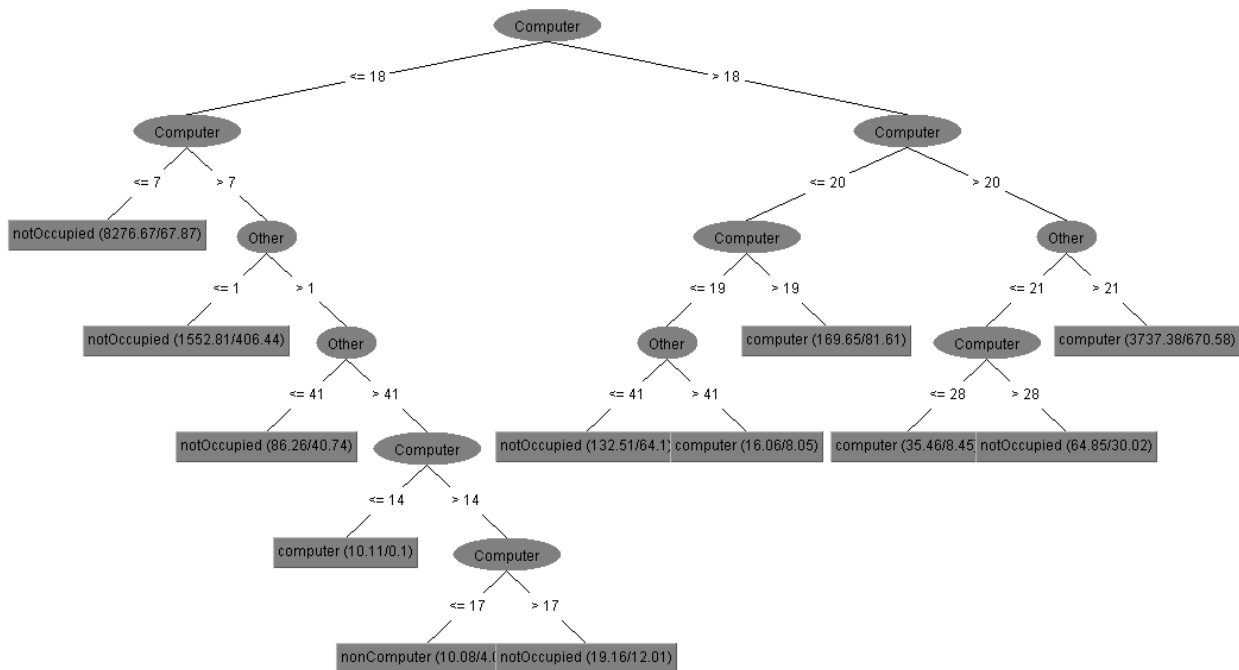


**Figure 23 C4.5 decision tree models of occupant F's behavior.**

Occupant F has a more complex use pattern that is not evident to classify based on the following two observations. First, the power consumption of the computer and the third appliance are the influential factors. Second, the task light does not play a role in the model. Figure 24 shows the ground truth value and the C4.5 predicted value of Occupant F's behavior in a typical weekday. There are two types of errors. (1) "Occupied non-computer-based work" is incorrectly

categorized as “computer-based work”, when the time duration of non-computer-based work is less than 10 minutes, which happened at 8:30h. This error may occur when the participant leaves office for a short period of time while leaving his/her computer on. (2) “Occupied non-computer-based work” is incorrectly categorized as “not occupied” when the time duration of non-computer-based work is longer than 30 minutes, which happened at 9:30h. This error suggests that the algorithm may not be able to accurately distinguish whether the computer is actually turned off or it is in the inactive (sleep) mode. Another noticeable pattern is that when status changes, there is usually a 5-minute time delay between the ground truth value and the predicted value. This is because the power consumption data is collected at the end of every five minutes. However, this delay has minimum impact on detecting individual behavior and group schedule in buildings.

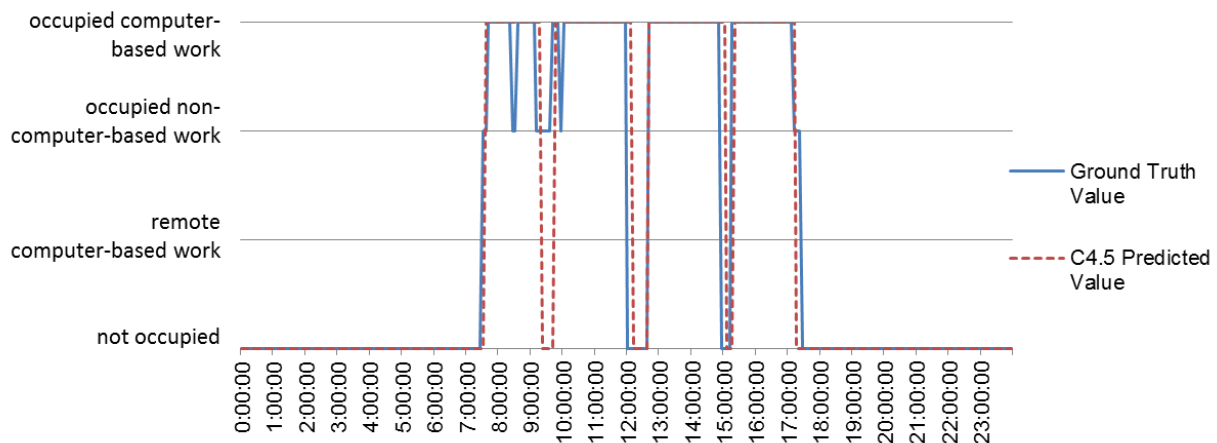


**Figure 24. Comparison of ground truth and model predicted value for occupant F.**

### 3.4.5.3. Group schedule modeling results

In order to better understanding the occupant group schedule in the studied office, weekday schedules are analyzed using Fitbit<sup>®</sup> and computer idle time logging datasets to establish the ground truth value. Figure 25 shows the average weekday schedule with 95% confidence interval, plotted in the Minitab program (Minitab, 2014). The biggest variation with 95% confidence interval is less than 10% during weekdays, and the highest occupancy rate as a group is lower than 80% over the study period. One reason of the lower occupancy rate could be that the office is mainly used for administration of a conservatory, so some of the participants have field obligations for events outside the office space. Another observation is that the lunch break pattern is fairly consistent as a group, starting from 11:45h to 13:00h. The lowest occupancy rate (41.43%) due to lunch break occurs at 12:50h, with the confident interval of [36.89%, 45.97%].

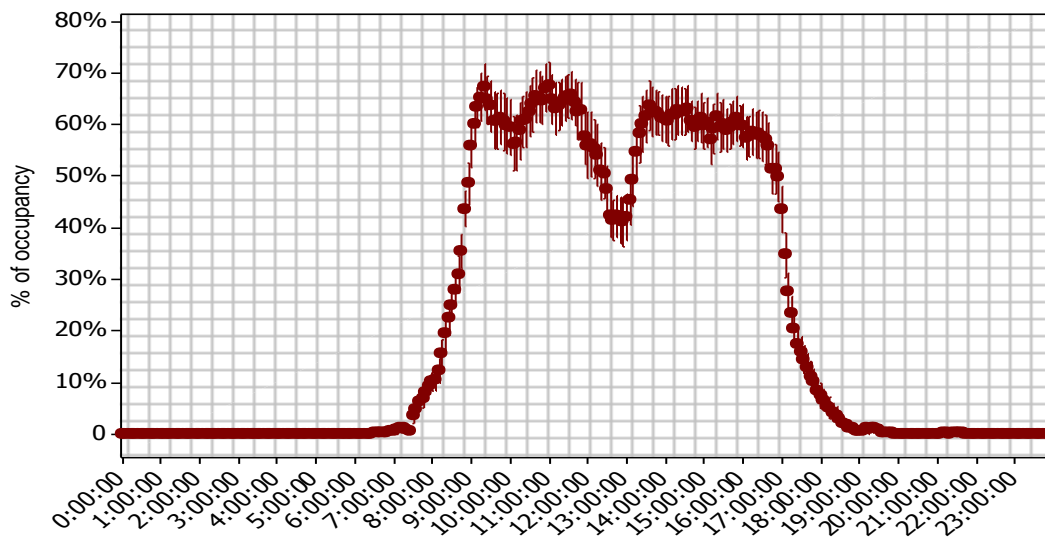


**Figure 25. Average weekday occupancy schedule with 95% confidence interval at the CSL building.**

Figure 26 shows the average group schedule comparison for different weekdays. There is a clear pattern that Tuesdays and Wednesdays have higher occupancy rates, Mondays and Thursdays have similar average occupancy rates, and Fridays have the lowest occupancy rates for the study period. There is a very consistent pattern for the time of arriving office, having lunch break, and leaving the office across different weekdays for the study group.

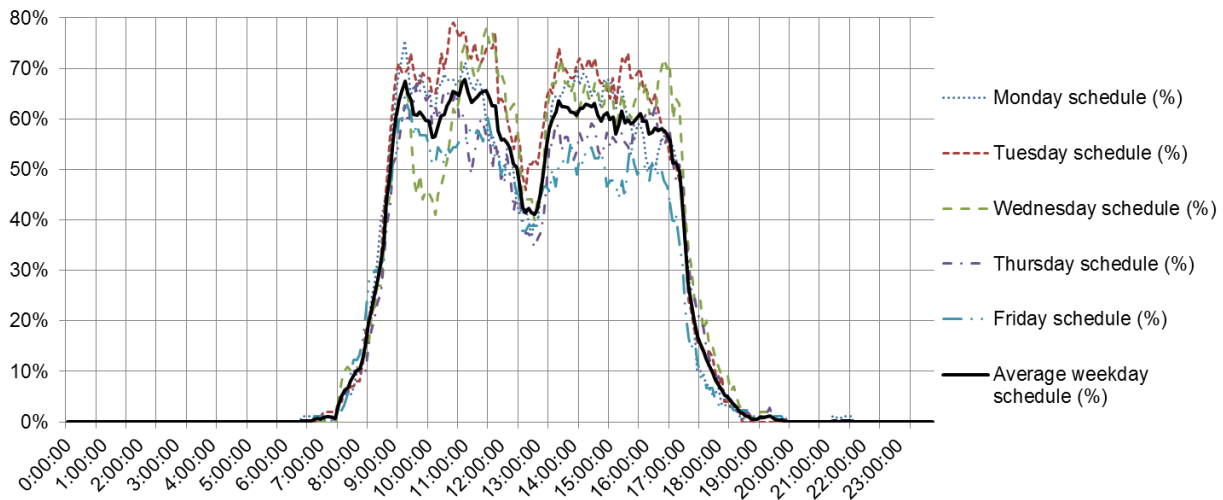


**Figure 26. Average occupancy schedule comparison for different weekdays at the CSL building.**

Linear regression (LR), locally weighted regression (LWR), and support vector regression (SVR) algorithms are tested for training the 5-minute power consumption data of all the 28 office appliances. Correlation coefficient and relative absolute error are used to evaluate the modeling performance of the three algorithms with the 10-fold cross validation. Table 14 shows the comparison of data mining results with different algorithms over the 28 appliances.

Table 14 also shows that that LWR has significant lower performance in both correlation coefficient and relative absolute error. LR and SVR have no significant difference in correlation coefficient and relative absolute error, but LR has significant advantage in “time to build the

model” (0.19s) compared to SVR (1706.85s). Therefore LR is chosen as the algorithm to learn the group schedule.

**Table 14. Group schedule data mining results with different algorithms over the 28 appliances.**

	Linear regression	Locally weighted regression	Support vector regression
Correlation coefficient	0.95	0.87*	0.95
Relative absolute error (%)	21.76	37.19*	20.13
Time to build the model (seconds)	0.19	0.01	1706.85

\*statistically significant lower compared to LR ( $p = 0.05$ ).

In order to reduce the number of the sensors to lower initial and maintenance cost so that the method may be more applicable for future studies or even real world applications, feature selection can be used to reduce the number of attributes in the data mining study. The first step of feature selection is to calculate the total attribute weights based on appliance types as shown in Figure 27. Compared to Figure 19, laptop computers are the dominant appliance type in terms of the quantity and weights. On the contrary, although there are more task lights than other appliances, the total weights of other appliances are heavier than the task lights’. Therefore, based on the two observations above, the 5-minute power consumption data of the 11 laptop computers are selected as key attributes to perform the second test using LR.



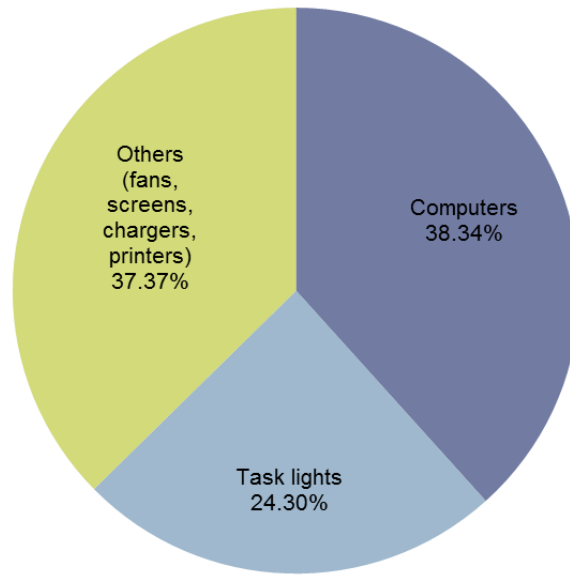


**Figure 27. Total attribute weights comparison by appliance type.**

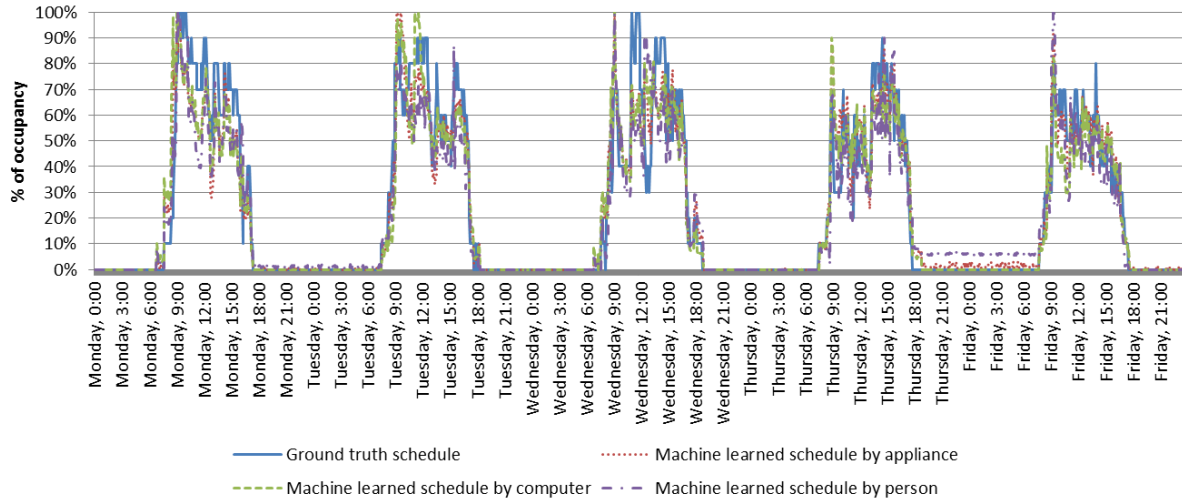
To further reduce the number of sensors, the author also considers using the total power consumption data per person as attribute. The argument is that, in future, researchers or practitioners can use a “smart power strip” (Sorensen, 2013) to monitor and record the total power consumption of plug loads without monitoring individual appliances with additional sensors. Therefore, the third test is performed with 5-minute total power consumption data per person as attributes.

Table 15 shows the group schedule data mining results of the three tests using the three different datasets. With 2-tailed paired T-test ( $p=0.05$ ), no statistically significant difference is found among the three tests. Therefore, the three datasets are all feasible to be used for similar future studies or applications. The actual use of the datasets should depend on the availability of sensor data.

**Table 15. Group schedule data mining results with different datasets.**

	Test #1: by appliance	Test #2: by laptop computer	Test #3: by person
Number of attributes	28	11	10
Number of instances	14111	14111	14111
Correlation coefficient	0.95	0.94	0.93
Relative absolute error (%)	21.76	22.01	31.07

Figure 28 and Figure 29 show the group schedule predicted value and the ground truth value in a typical working week and in a typical weekday, respectively. In general, the predictions for the three datasets follow the ground truth data fairly closely. However, in some cases, the “by laptop computer” dataset test tends to overestimate the value in both directions (bigger overshoots and undershoots). On the contrary, the “by person” dataset test tends to underestimate the value. It is also noticeable during Thursday night (19:00h) and early Friday morning (6:30h), the “by appliance” and “by person” tests have positive (but less than 10%) predictions, but the “by laptop computer” test has the correct zero prediction. This result suggests that during that time, either task lights or the appliances other than the laptop computer were in active mode, although the office was unoccupied. This observation can help the facility management team to make better policies of using appliances during the unoccupied time and influence the occupants to change their behavior towards energy efficiency (Yun, Scupelli, *et al.*, 2013).



**Figure 28. Group schedule predictions and the ground truth comparison in a typical week.**

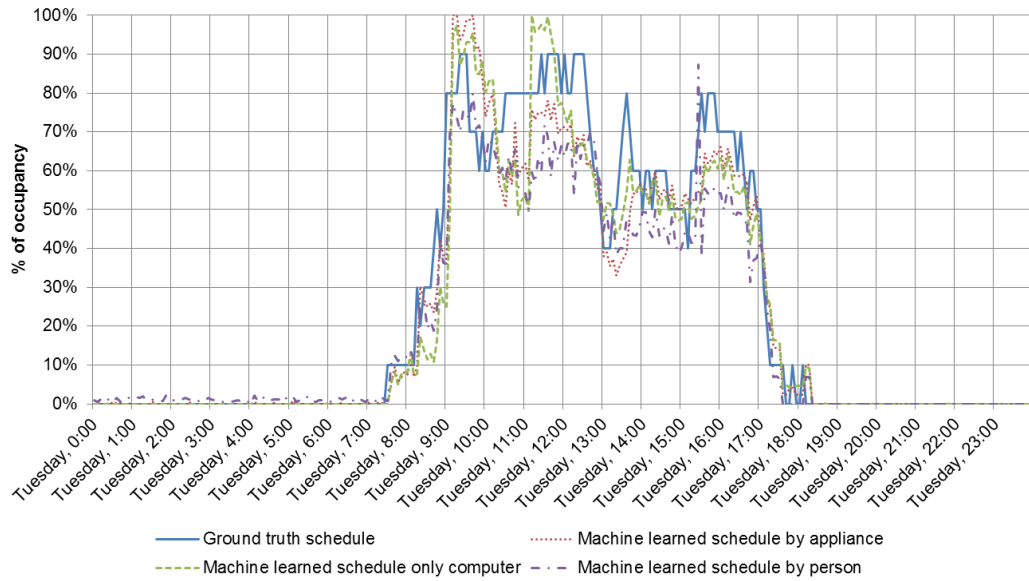


**Figure 29. Group schedule predictions and the group truth comparison in a typical weekday.**

#### *3.4.5.4. Limitations*

One limitation of the CSL case study is that the ground truth data collection experiment relies on the participants' behavioral consistency, which may contain missing and incorrect data. It has been mentioned before that 5 out of 15 participants' datasets are invalid to be used in the study. In addition, one type of error may occur when a participant uses his/her laptop at home while wearing the Fitbit®. The ground truth will treat this instance as “occupied computer-based work”. However, the real truth should be “unoccupied”, since the participant is not in the office but at home. Manual data cleaning process is necessary to correct this type of error before starting the data mining study.

Second limitation is that the test-bed office building is a high performance building. There is very limited number of appliances per person and all their appliances are new energy-efficient types. Less attributes and small range of attribute variations (low power consumptions) may simplify the prediction process and produce better-than-average results. A similar study can be conducted in a more high energy intensive office to compare the results.

### **3.5. Daylight/Lighting and equipment operation calibration**

An inverse calibration procedure is developed for lighting and equipment power density and schedule calibration. A Python script is written to automate part of the process (solid lines) in Figure 30.

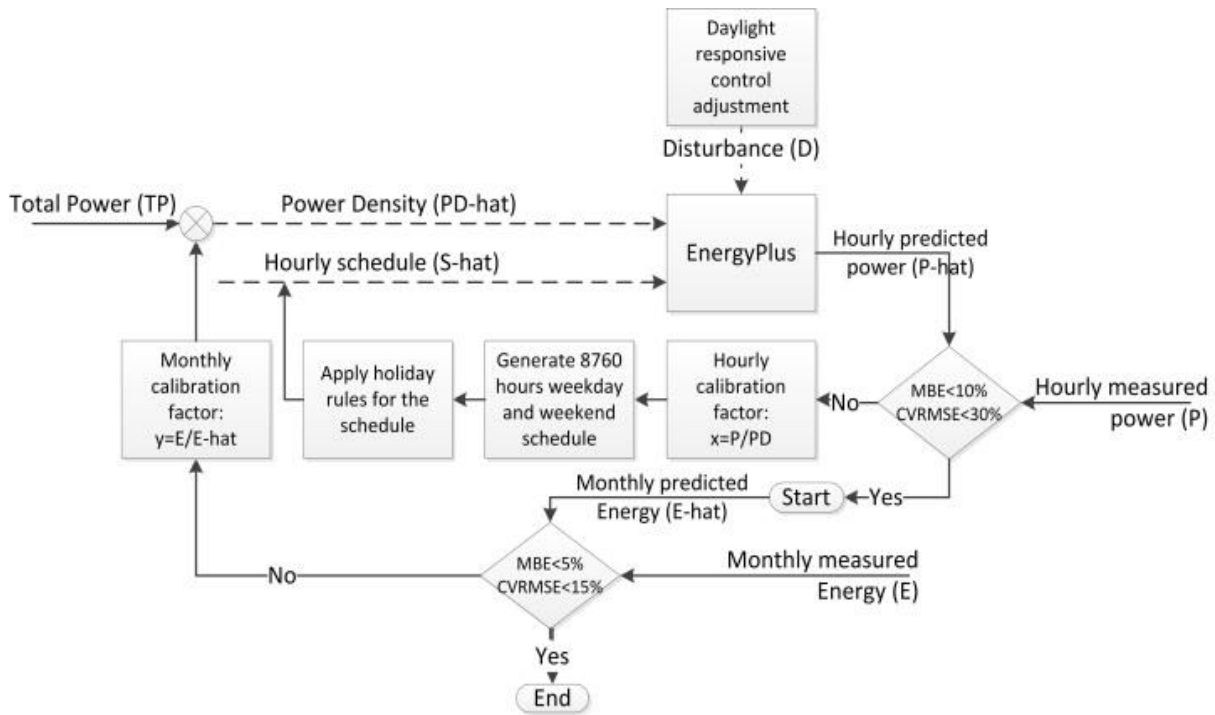


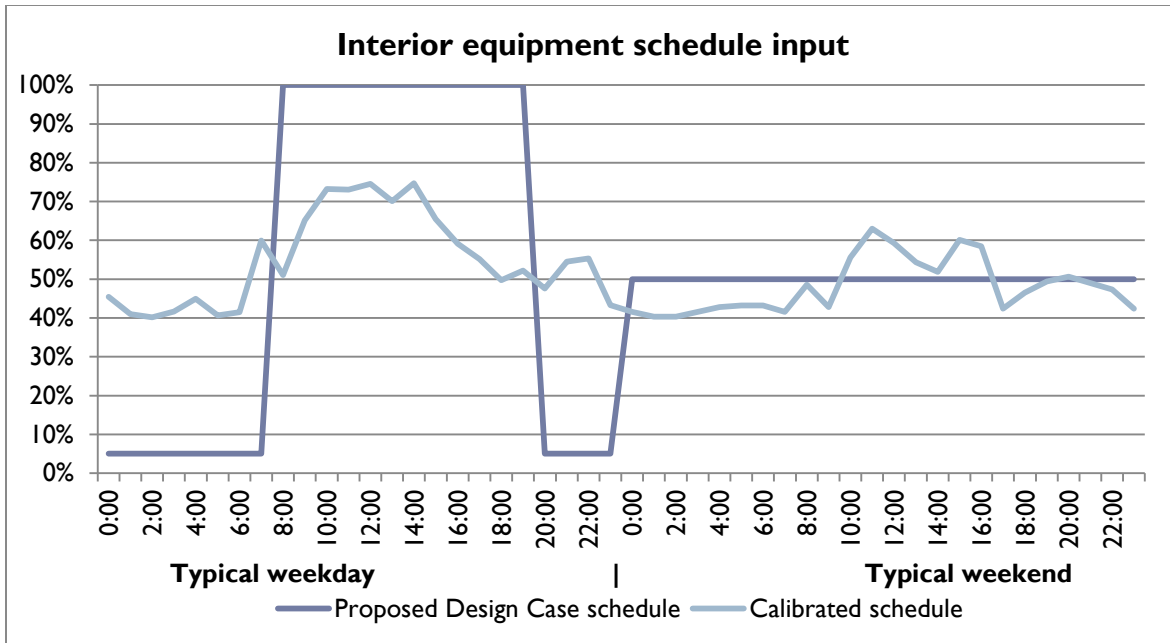
**Figure 30 The inverse calibration procedure.**

The method follows four steps. (1) Assumed power densities and hourly schedules are fed into the EnergyPlus model. (2) EnergyPlus hourly output power consumptions are compared with the actual measured data to test whether they meet the hourly mean biased error (MBE) and coefficient of variation of the root mean squared error (CVRMSE) criteria. (3) If the criteria are not met, an hourly inverse calibration factor, as calculated by taking the hourly measured power (PD), divided by the simulated power density (PD-hat), will be multiplied by the hourly schedule and generate an 8760-hours schedule including weekdays, weekends, and federal holidays to be directly used in the next iteration of EnergyPlus simulation. If the criteria are met, the program will check monthly MBE and CVRMSE criteria. (4) Monthly energy simulation data are compared with monthly metered data to calibrate the total lighting and equipment power. The

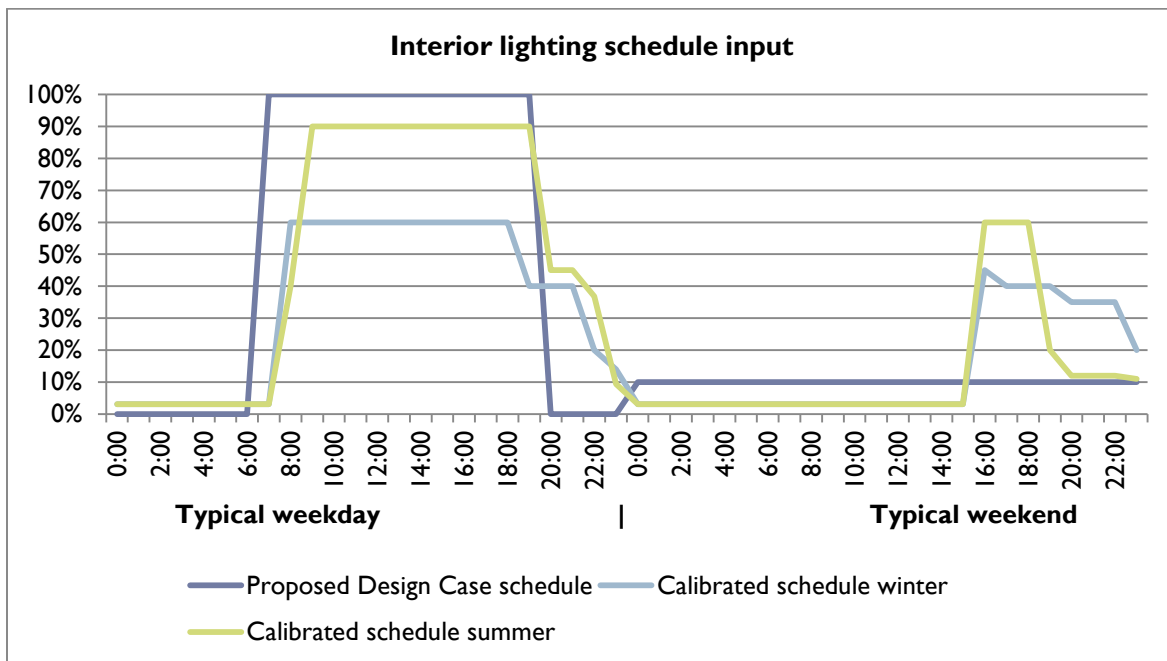
calibrated total power densities are calculated by multiplying the calibration factor  $E/\hat{E}$  by the assumed simulation lighting and equipment power densities.

Some manual effort is involved in the process, represented by the dash lines in Figure 30. Daylight responsive control is implemented in the CSL building, so during times when daylight can provide sufficient illuminance, the electrical lights are dimmed and lighting electricity consumption is reduced. Therefore, during these periods, the lighting electricity use and the EnergyPlus lighting schedule input (illuminance demand) are no longer correlated. Two steps are performed to solve this issue. (1) The daylight harvesting system is disabled in the EnergyPlus model to get the total power consumption value from electric lighting without daylight contribution; (2) the difference between the actual and the daylight-disabled power consumption is derived and used to adjust the actual schedule. Similarly, exterior lighting is also controlled by daylight sensor, so the monthly schedule is adjusted according to astronomical clock (the different number of daylight hours is taken into account).

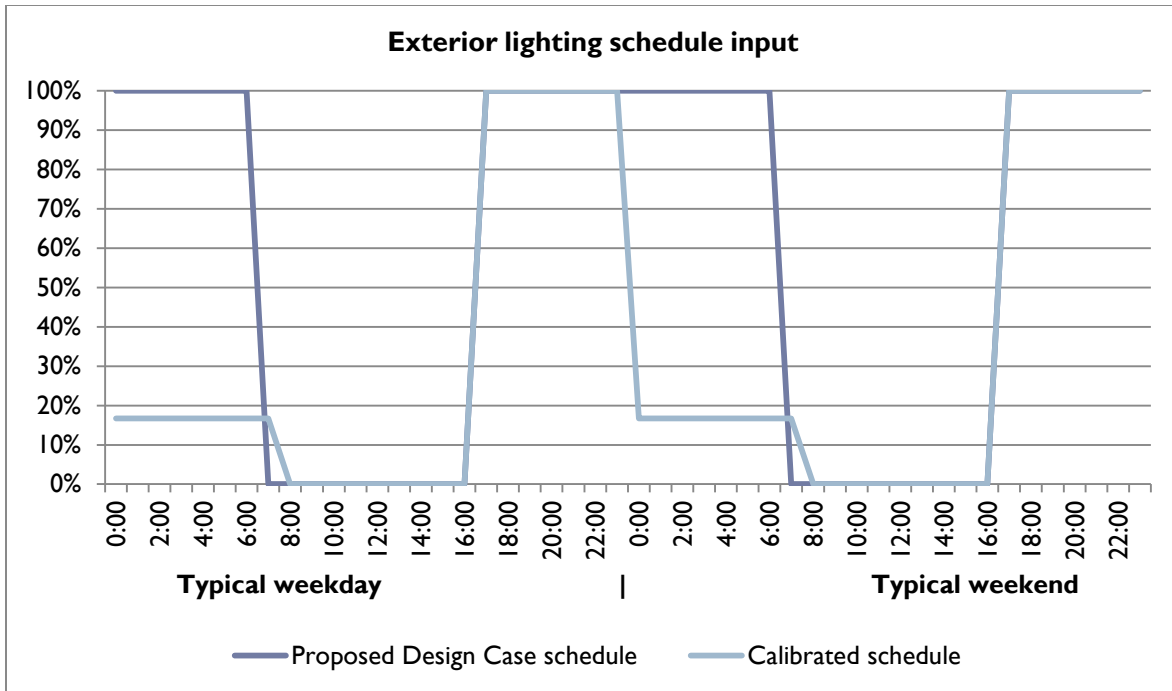
As the first part of this inverse calibration procedure, two typical weeks of hourly data in both August and December, 2013 are used to perform calibration. Figure 31 through Figure 34 compare the input schedules of the proposed design case and the calibrated model for interior equipment, interior lighting, exterior equipment, and exterior lighting, respectively. For interior equipment schedule, the difference of the calibrated schedules of the weekday and weekend are not as dramatic as the proposed design schedules. For interior lighting schedule, there is a clear difference between winter and summer conditions due to the use of the daylight responsive control. Exterior equipment and lighting follows fairly standard operation schedules.



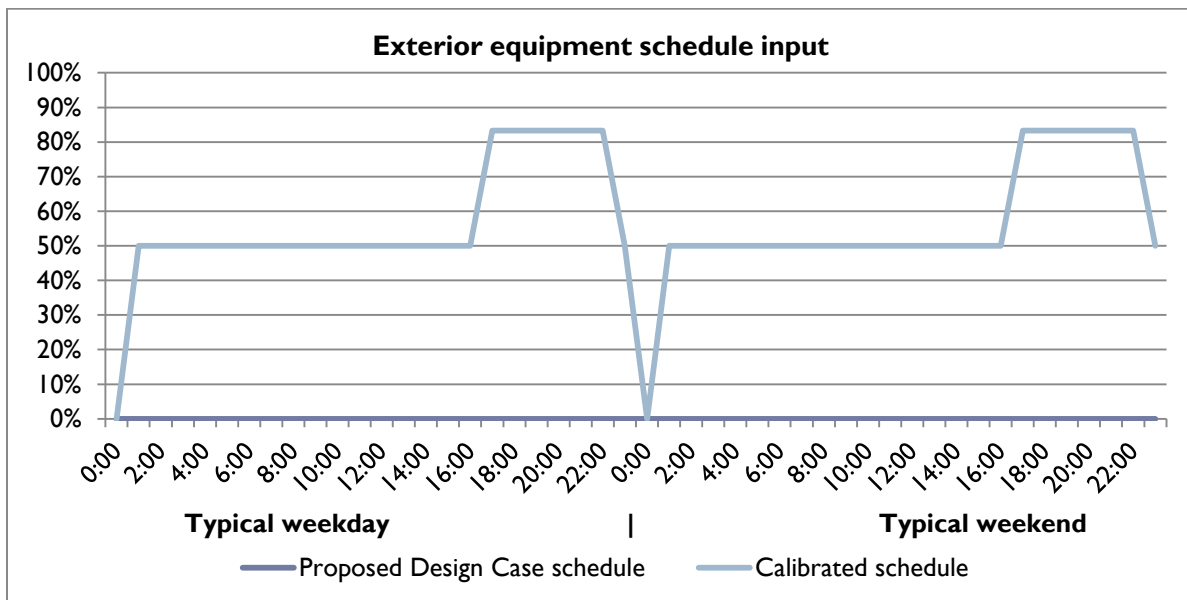
**Figure 31 Interior equipment hourly power input schedule (The calibrated interior equipment power density is  $29\text{W/m}^2$ ).**



**Figure 32 Interior lighting hourly power input schedule (The calibrated lighting power density is  $29\text{W/m}^2$ ).**



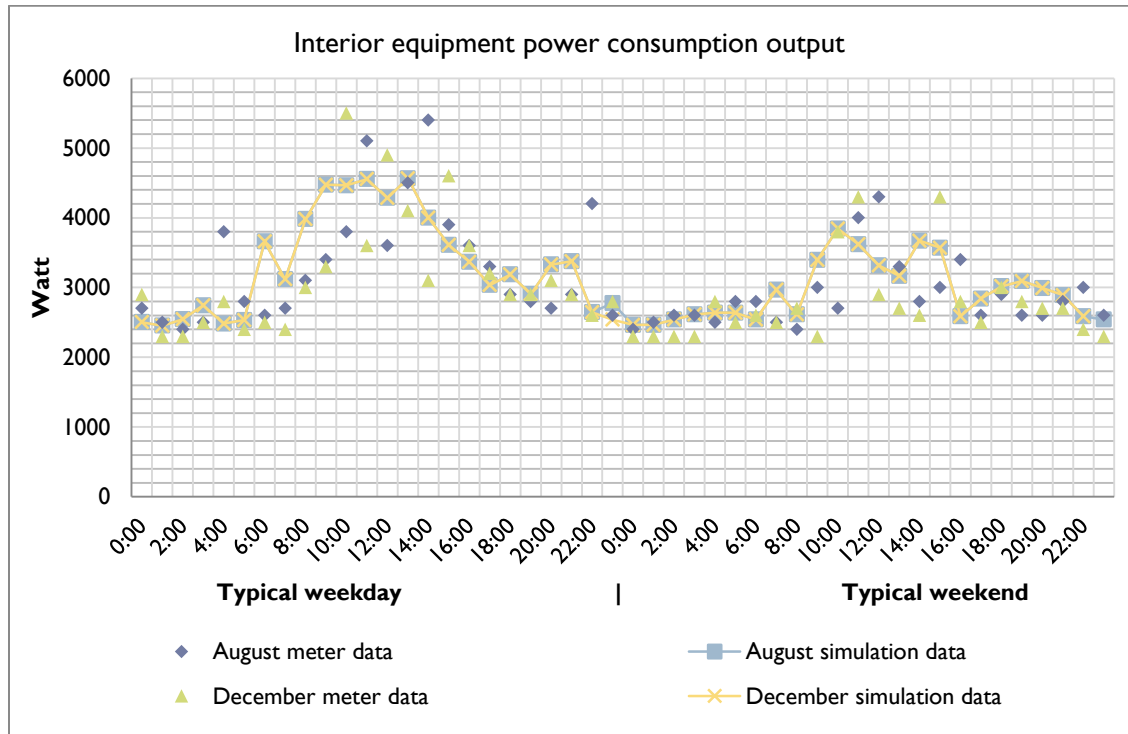
**Figure 33 Exterior lighting hourly power input schedule (The calibrated exterior total lighting power 600W).**



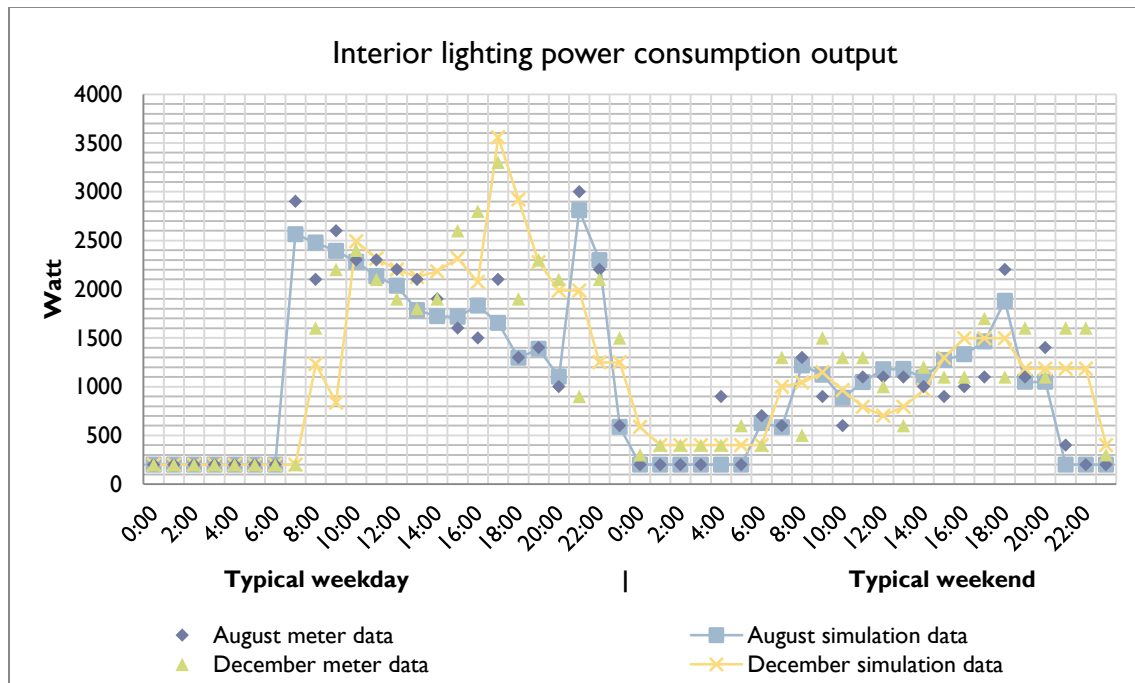
**Figure 34 Exterior equipment hourly power input schedule (The calibrated total exterior equipment power is 2560W).**



Figure 35 through Figure 38 show the hourly power consumptions of the interior equipment, interior lighting, exterior equipment, and exterior lighting, respectively. Interior equipment power consumption shows a very consistent profile between winter and summer for both weekdays and weekends. However, unlike interior equipment, interior and exterior lighting power consumptions between August and December are different mainly due to the use of the daylight-responsive control system. Exterior equipment power consumptions have relatively regular schedules, which have the same operation schedule for both weekdays and weekends in December and August (Only December data is shown in the figures).



**Figure 35 Interior equipment hourly power consumption output.**



**Figure 36 Interior lighting hourly power consumption output.**

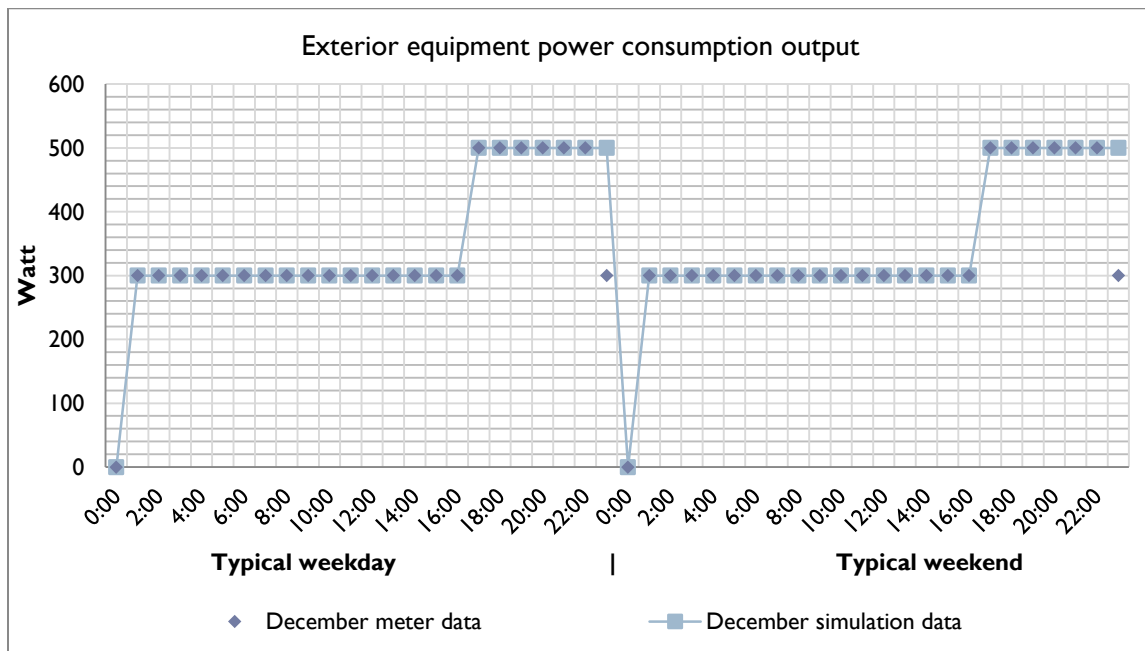


**Figure 37 Exterior equipment hourly power consumption output.**

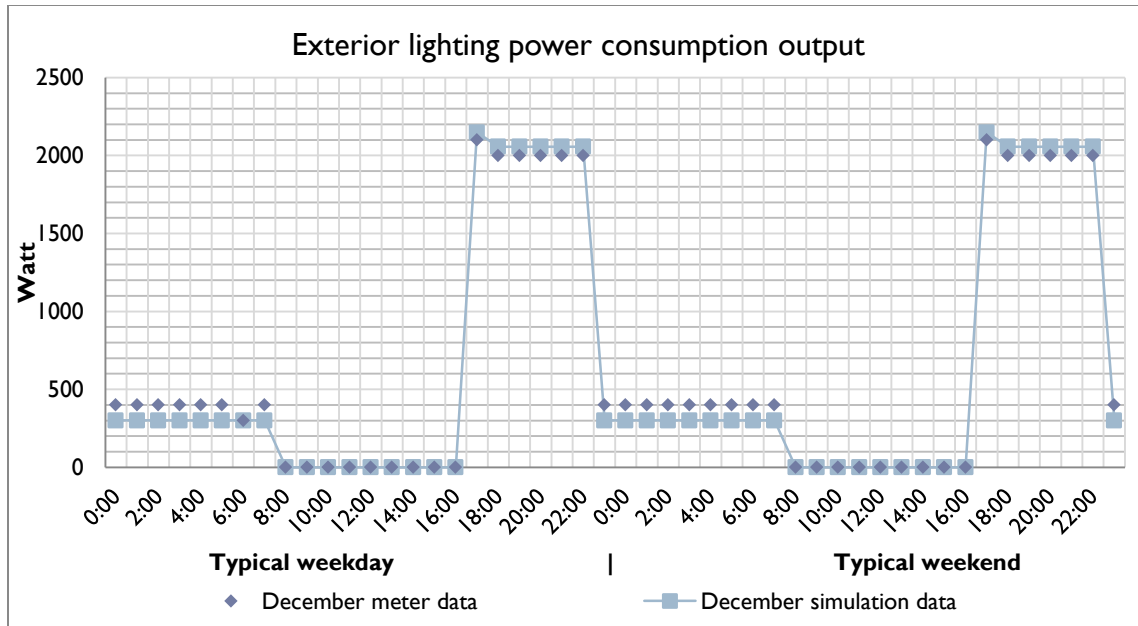


**Figure 38 Exterior lighting hourly power consumption output.**

As the result of the second part of the inverse calibration procedure, Figure 39 through Figure 42 show the comparison of the monthly energy consumption output of the ASHRAE 90.1-2007 baseline, proposed design case, calibrated model, and actual meter data of 2013 for interior equipment, interior lighting, exterior equipment, and exterior lighting, respectively. For interior equipment, interior lighting, and exterior lighting, the ASHRAE 90.1-2007 baseline and the proposed design case models all have much higher monthly energy consumptions than the actual metered data in 2013. The reason is that according to the requirement of Appendix G of ASHRAE 90.1-2007, the proposed design case power densities are kept consistent with the baseline assumptions for the purpose of fair comparison,. Exterior equipment is not simulated in the baseline or the proposed design case model. Compared to the actual metered data in 2013, all the calibrated monthly energy consumptions of the four equipment and lighting types have minimum variations.

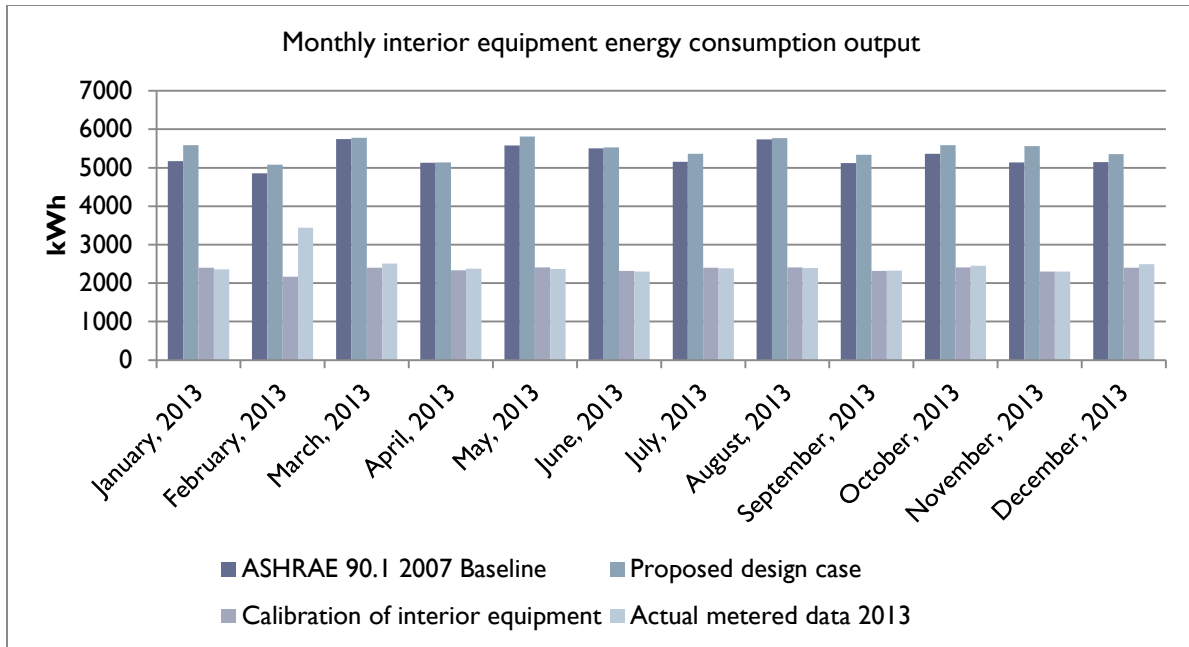


**Figure 39 Interior equipment monthly energy consumption output.**

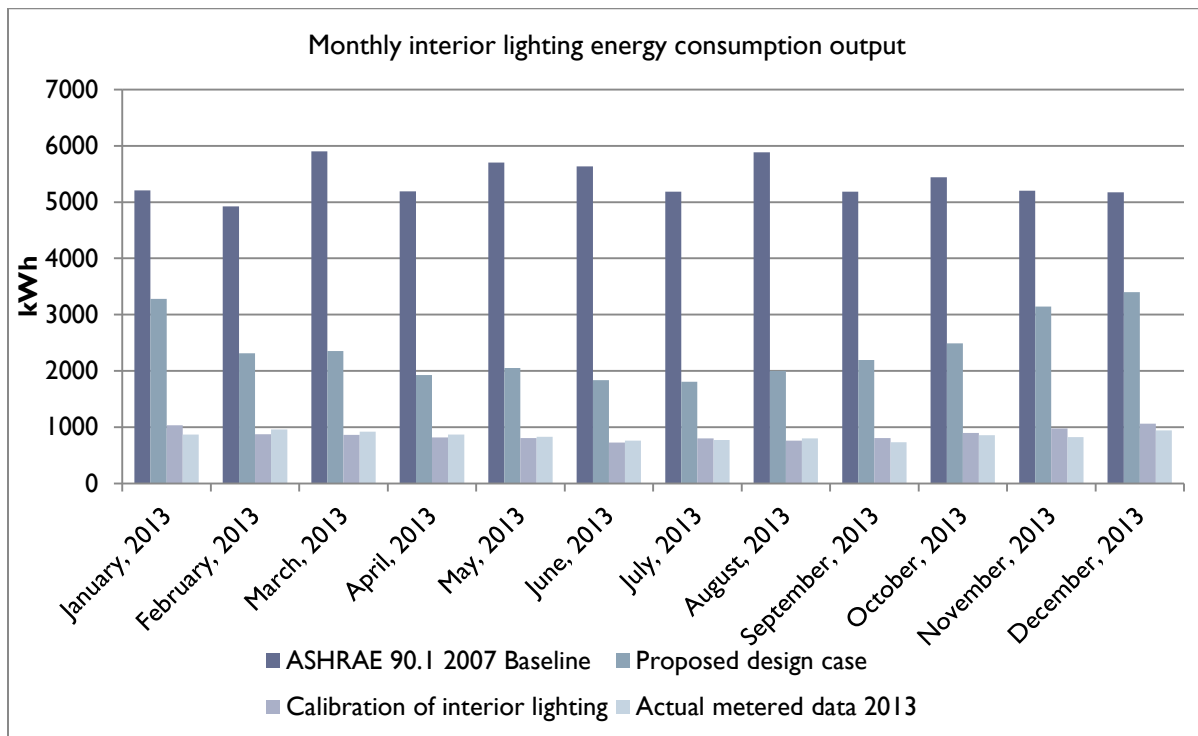


**Figure 40 Interior lighting monthly energy consumption output.**

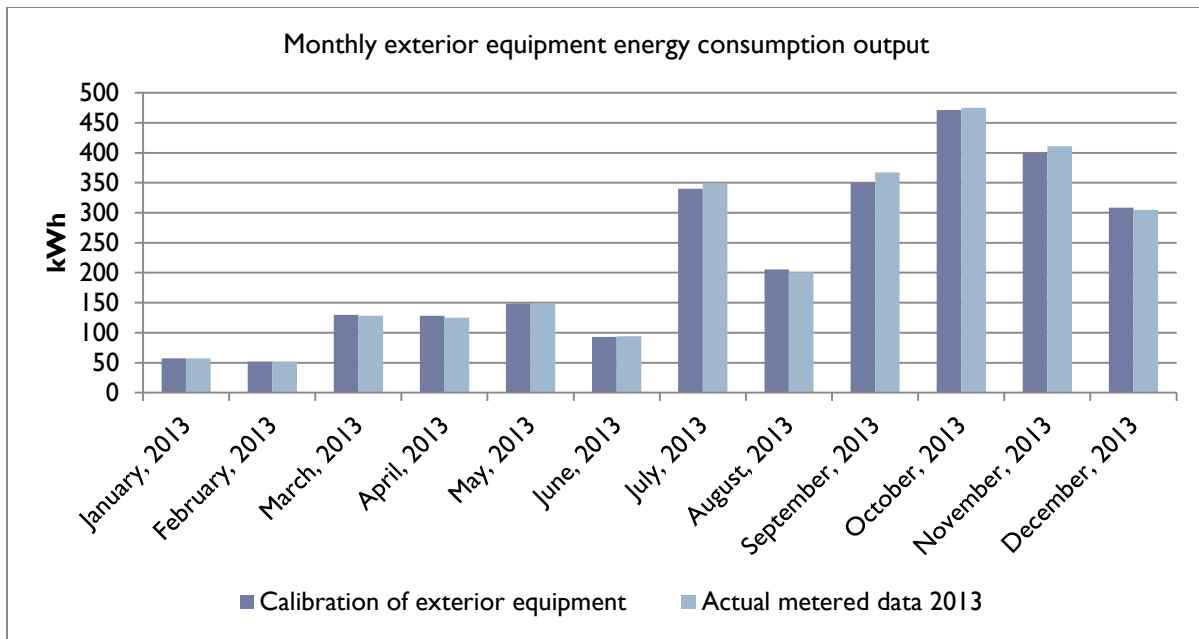


**Figure 41 Exterior equipment monthly energy consumption output.**

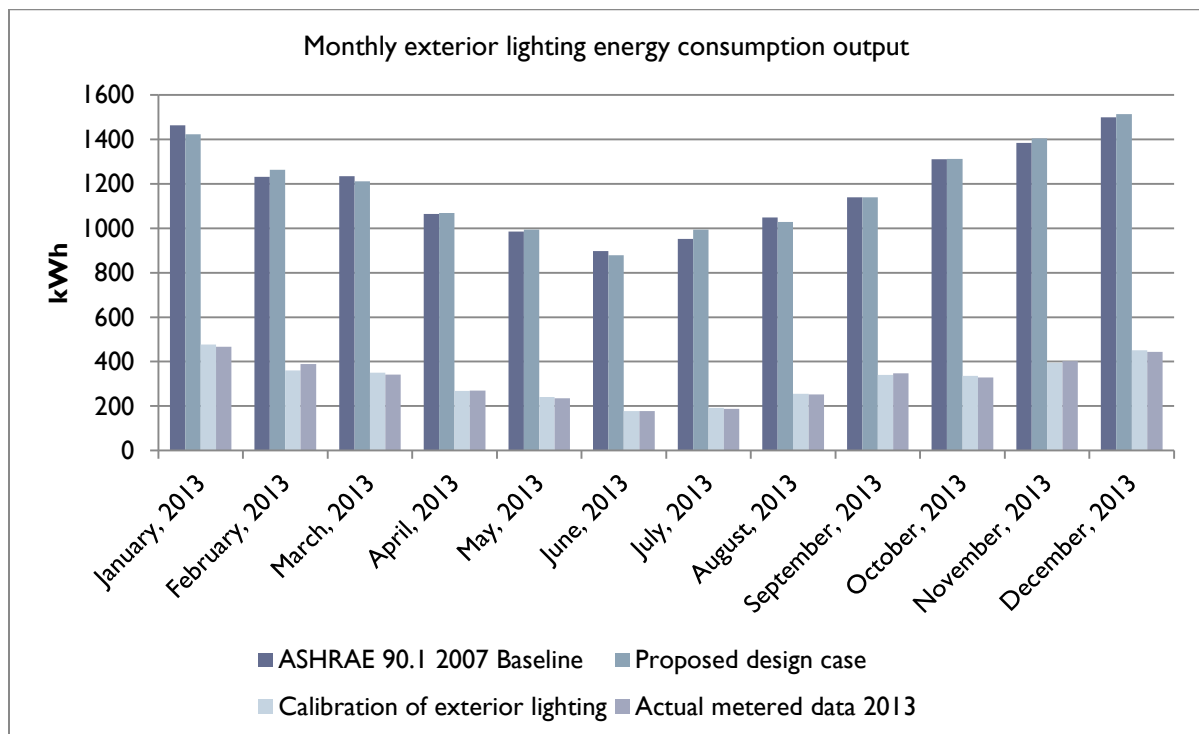


**Figure 42 Exterior lighting monthly energy consumption output.**

In summary, Table 16 shows the mean biased errors (MBEs) and coefficient of variation the root mean squared errors (CVRMSEs) results of the hourly power consumption and monthly energy consumption for the interior equipment, interior lighting, exterior equipment, and exterior lighting. The results meet the ASHRAE Guideline 14-2002 thresholds, which are 10% of MBE and 30% of CVRMSE for hourly calibration and 5% of MBE and 15% of CVRMSE for monthly calibration.

**Table 16 Lighting and equipment energy calibration statistical results.**

	Interior equipment	Interior lighting	Exterior lighting	Exterior equipment
MBE (hourly - weekdays)	-0.55%	1.94%	-2.62%	0.51%
MBE (hourly – weekends/holidays)	-0.55%	-0.23%	-2.62%	0.51%
MBE (monthly)	4.84%	-0.03%	0.01%	1.06%
CVRMSE (hourly - weekdays)	21.49%	29.32%	11.53%	22.08%
CVRMSE (hourly – weekends/holidays)	14.68%	29.53%	11.53%	22.08%
CVRMSE (monthly)	14.97%	10.29%	3.13%	2.99%

### **3.6. Passive/Active HVAC system operation calibration**

#### ***3.6.1. Active HVAC system model calibration***

A central AHU with a geothermal heat pump system is used to heat, cool, and ventilate the CSL building. First, the parameters of key HVAC equipment are verified based on installed manufacturer datasheet and testing data. Table 17 illustrates the verified EnergyPlus model HVAC input parameters.

**Table 17 HVAC equipment parameter calibration.**

	<b>EnergyPlus model input</b>
AHU supply fan	Maximum Flow Rate: 5.85 (m <sup>3</sup> /s)
	Total Pressure Rise: 1740.595 (Pa)
	Motor Efficiency: 0.813
Geothermal heat pump	Rated Cooling Capacity: 123320.8 (W)
	Rated Heating Capacity: 104450.5 (W)
Geothermal Heat Exchanger	Bore Hole Radius: 0.073 (m)
	Bore Hole Length: 155.45 (m)
	Ground Thermal Heat Capacity: 2250000 (J/m <sup>3</sup> -K)
	Ground Thermal Conductivity: 2.86 (W/m-K)

The total pressure rise of the supply fan (shown in the third row of Table 17) is calculated by Equation (22-25).

$$P_T = P_S + P_V \quad (22)$$

$$P_V = \frac{1}{2} \rho V^2 \quad (23)$$

$$\rho = \frac{P_{abs}}{R_{specific} T} \quad (24)$$

$$V = \frac{\dot{V}}{A} = \frac{\dot{M}}{\rho A} \quad (25)$$

where,

$P_T$  is the fan total pressure rise (Pa);

$P_S$  is the fan static pressure (Pa), equals to 6.68 (inches of water) = 249.14 (Pa);

$P_V$  is the fan velocity pressure rise (Pa);

$\rho$  is the supply air density (kg/m<sup>3</sup>);

$V$  is the supply air velocity (m/s);

$P_{abs}$  is the supply side absolute air pressure at AHU outlet (Pa);

$R_{specific}$  is the specific gas constant for dry air, equals to 287.058 (J/(kgK));

$T$  is the absolute supply air temperature (K);

$\dot{V}$  is the supply air volume flow rate ( $1\text{m}^3/\text{s} = 2118.88$  cubic feet per minute (CFM));

$A$  is the section area of supply air outlet, equals to  $0.5194\text{ (m}^2\text{)}$ ;

$\dot{M}$  is the supply air mass flow rate (kg/s).

After the AHU equipment parameters are verified, zone control setpoints are calibrated based on the measured hourly data for all the heating, cooling, and swing seasons. The last step is to compare simulated monthly HVAC energy consumption by end use with metered monthly data and make changes when necessary.

### ***3.6.2. Passive HVAC system model calibration***

The CSL building is equipped with motorized windows for the purpose of natural ventilation. If the windows are open, the active HVAC system will be turned off. The control logics of the window open conditions are shown in Table 18. Type #4 logic is used for regularly occupied open office spaces.

In the EnergyPlus model, an “AvailabilityManager:HybridVentilation” object is enabled to simulate the natural ventilation control for the CSL building. This object serves two purposes: “1) prevents simultaneous natural ventilation and HVAC system operation, and 2) allows users to examine various ventilation strategies to maximize natural ventilation in order to reduce heating/cooling loads.” (DOE, 2010). Outdoor wind speed, outdoor temperature, indoor/outdoor



enthalpy, and schedules are defined to simulate the actual Type #4 control logic. However, the outdoor temperature range is defined as 15 – 25 °C, instead of 17 – 32 °C based on the calibration results of the measured indoor temperature data. See the following section for details.

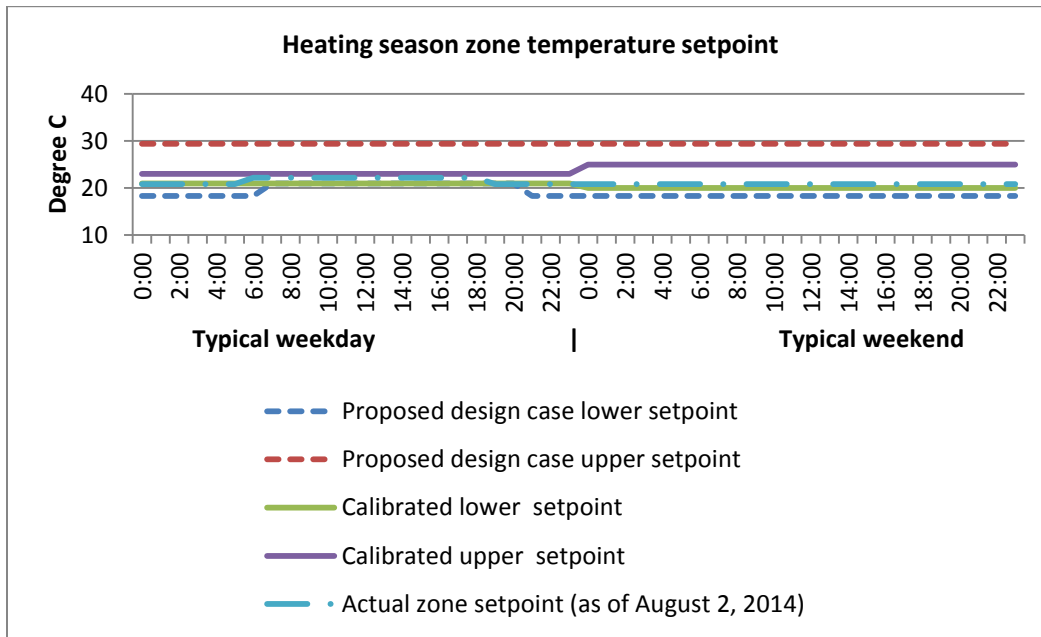
**Table 18 Summary of window open conditions (Source: ALC WebCtrl Logic as of July 30, 2014).**

Logic	Location	Zone temperature	Wind speed (mph)	Outdoor temperature (°C)	Precipitation (Yes/No)	Enthalpy
Type #1	1 <sup>st</sup> floor atrium & Room 111	zone temperature > zone setpoint	< 20 mph	18-32	-	-
Type #2	2 <sup>nd</sup> and 3 <sup>rd</sup> floor atrium	zone temperature > zone setpoint	< 20 mph	18-35	-	-
Type #3	3 <sup>rd</sup> Floor Atrium Roof Vent	zone temperature > zone setpoint	< 20 mph	18-35	No	-
Type #4	1 <sup>st</sup> Floor Room 102-104-107-110-108 & 2 <sup>nd</sup> Floor Room 201-202-204-205	zone temperature > zone setpoint	< 20 mph	17-32	No	zone enthalpy > outdoor enthalpy – 0.5

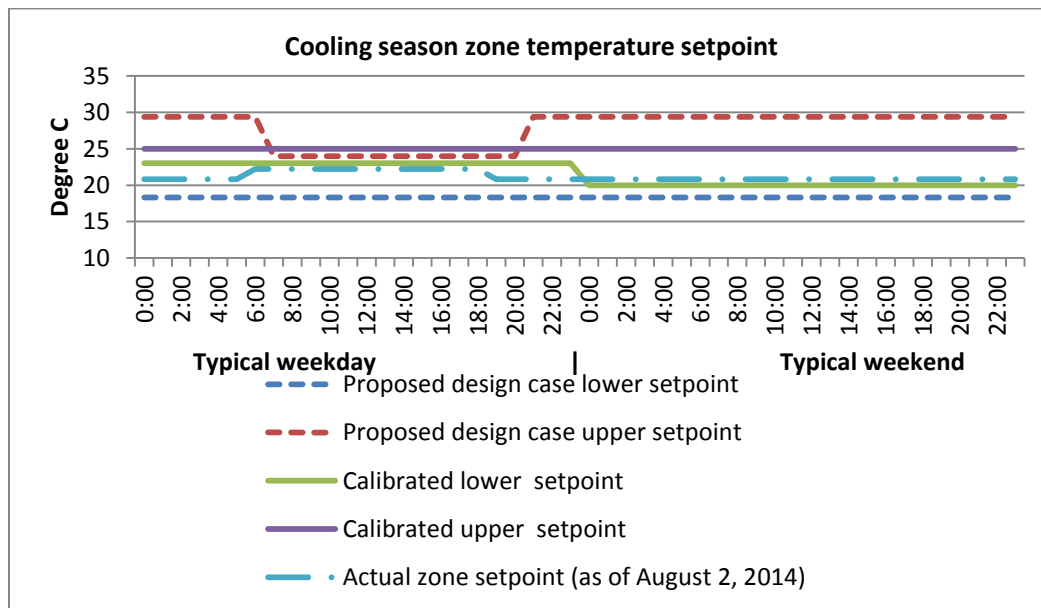
### ***3.6.3. Passive/Active HVAC system calibration result***

The first set of HVAC system calibration results includes HVAC zone air setpoint and measured temperatures in heating, cooling, and swing seasons. Figure 43 through Figure 45 show the setpoint comparisons among the proposed design case setpoints, the calibrated setpoints, and the actual zone setpoints in the BAS for heating season, cooling season, and swing season, respectively. It can be noted that the actual zone setpoint remains the same for all seasons. Looking at the actual operation temperature of the zone, the setpoint is not met for most of the operating hours, especially during unoccupied periods. Therefore, in order to rationalize the calibrated model, the calibrated setpoints are derived from the actual measured data. Compared

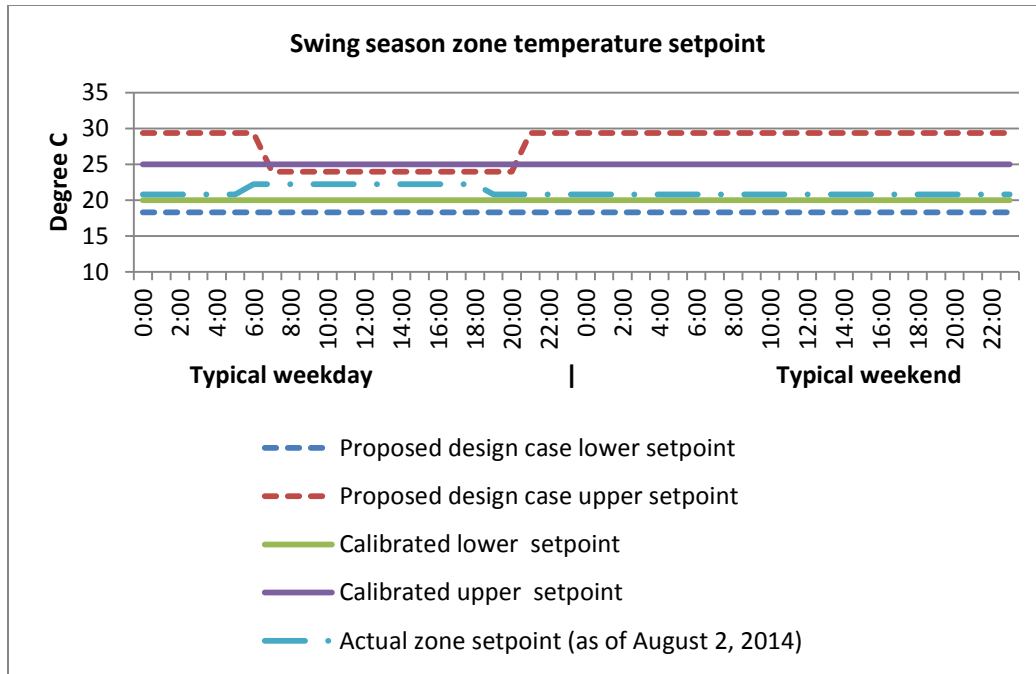
to the proposed design case assumptions, the calibrated setpoint band is much narrower, results in relatively higher energy consumption.



**Figure 43 Heating season zone air temperature setpoints comparison.**



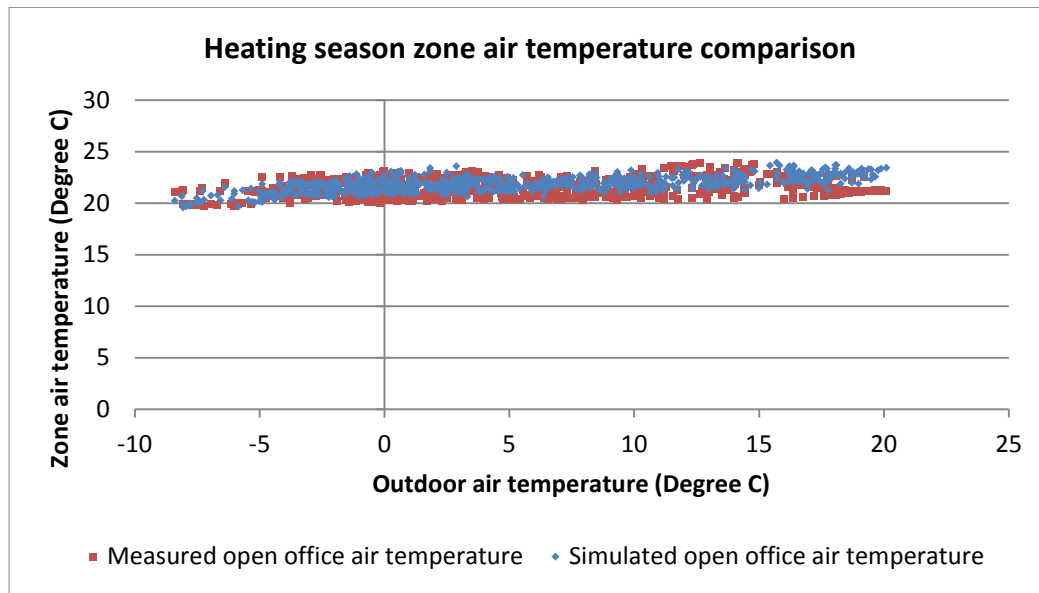
**Figure 44 Cooling season zone air temperature setpoints comparison.**



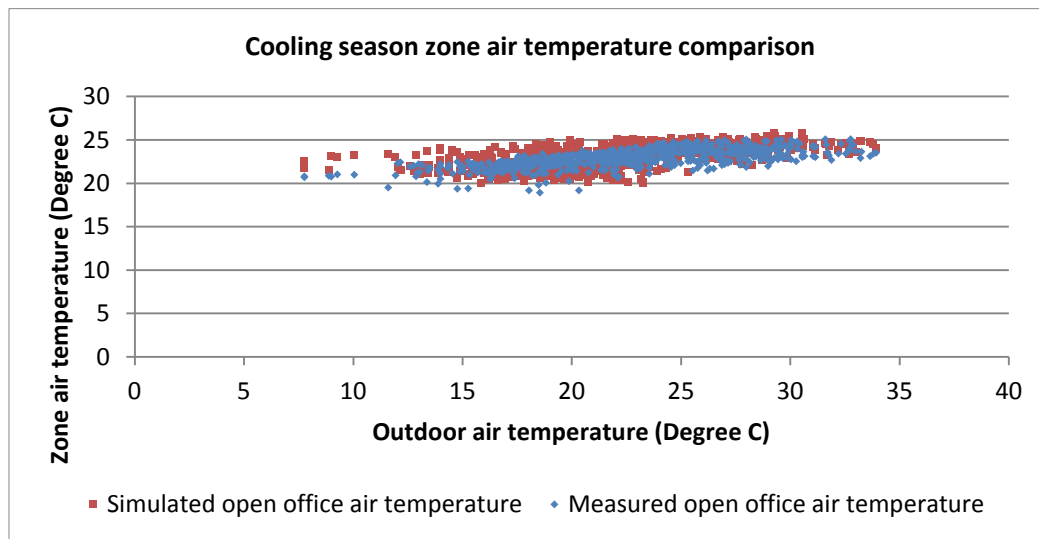
**Figure 45 Swing season zone air temperature setpoints comparison.**

Figure 46 through Figure 48 show the measured and calibrated hourly air temperature data corresponding to the measured outdoor temperature in the first floor open office of the CSL building for heating, cooling, and swing seasons, respectively. The scattered plots suggest a generally consistent match between the measured data and the calibrated model simulation result during the entire month of different seasons. Table 19 summarizes the hourly zone temperature calibration errors in different seasons, respectively. All the mean biased error (MBE) and coefficient of variation the root mean squared error (CVRMSE) results meet the requirements of ASHRAE 14-2002 Guideline. However, the calibration of the swing season has relatively higher error rate. A possible reason for the discrepancy is the difference between the real mixed-mode HVAC system setting and the EnergyPlus model configuration. As mentioned in section “3.6.2. Passive HVAC system model calibration”, the temperature boundary for natural ventilation is set to be (20 – 25 °C) in the calibrated EnergyPlus model, while the actual temperature boundary is

(17 - 32 °C) in the BAS system. During the calibration process, the author has tried to implement the actual temperature boundary setting in the EnergyPlus model. However, the simulated zone air temperature could not meet the calibrated zone air temperature setpoints. Therefore, the setting was adjusted based on the calibrated zone air temperature setpoints.



**Figure 46 Heating season zone air temperature comparison.**



**Figure 47 Cooling season zone air temperature comparison.**

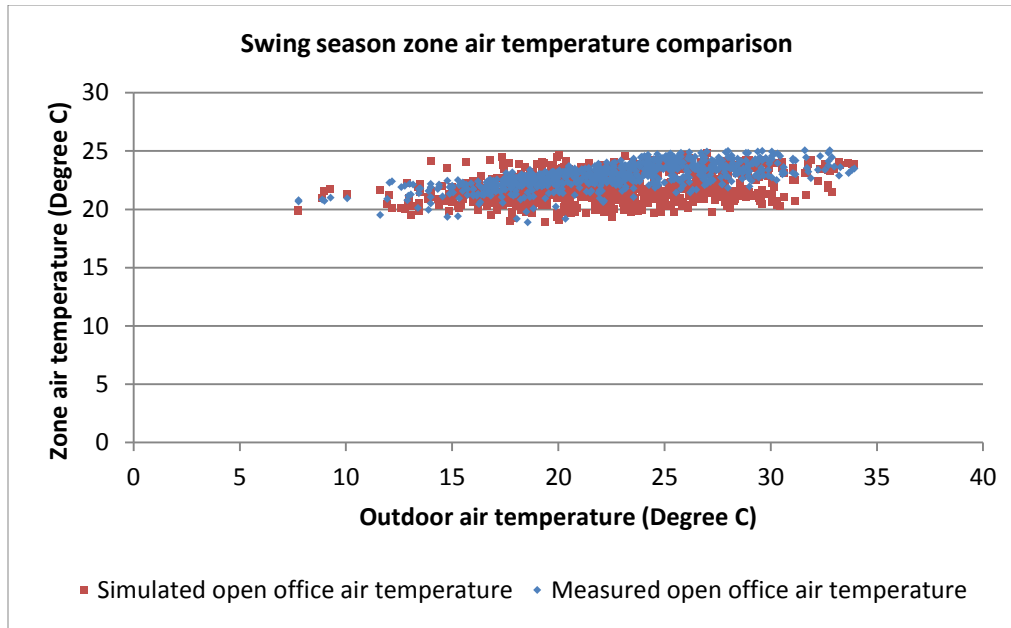


**Figure 48 Swing season zone air temperature comparison.**

**Table 19 Summary of calibration errors in different seasons.**

	mean biased error (MBE)	coefficient of variations the root mean squared error (CVRMSE)
Heating season (hourly temperature)	-1.83%	4.42%
Cooling season (hourly temperature)	-1.12%	6.29%
Swing season (hourly temperature)	4.15%	8.02%

The second part of the HVAC calibration outcome is the monthly HVAC energy consumption calibration results as shown in Figure 49. In the first three months of the study period, AHU energy consumption was metered as a total due to the metering limitation. Then after March of 2013, separate meters were installed for the energy consumptions of fan, pump, heating, and cooling systems, respectively. Therefore, the detailed comparisons can be made for the nine

months of the study period. In summary, over the 12 months, the mean biased error (MBE) of the monthly HVAC energy between the calibrated model and the actual meter data is 0.1%, and the coefficient of variation the root mean squared error (CVRMSE) is 15%.

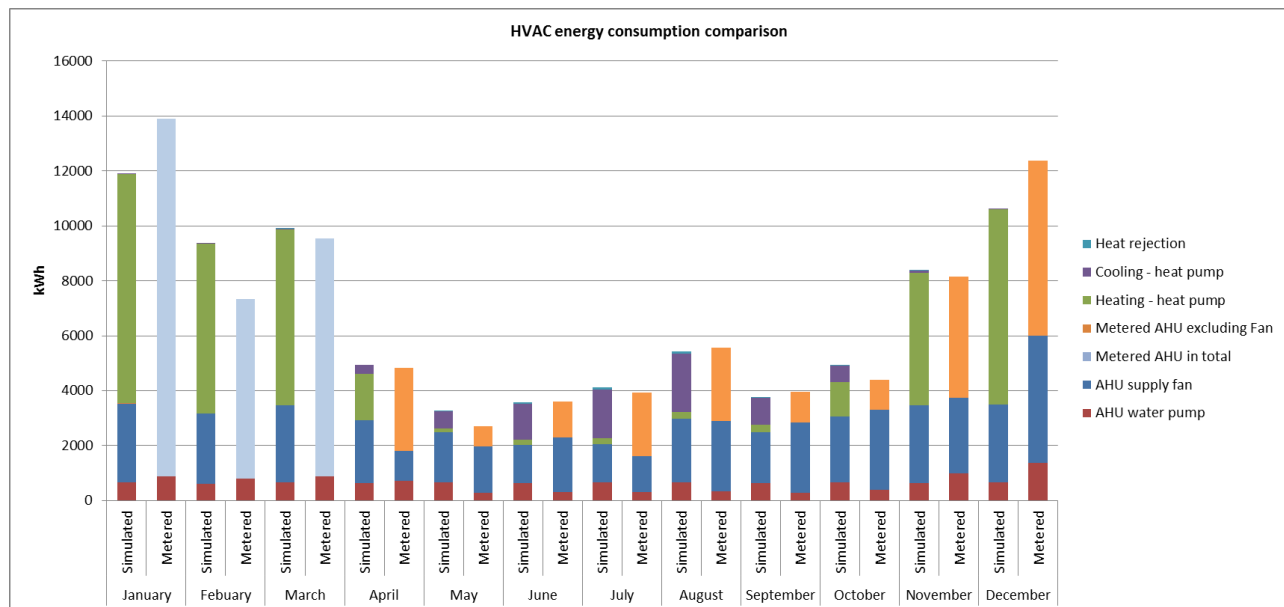


**Figure 49 Monthly HVAC energy consumption calibration result.**

### 3.7. Whole building energy model calibration result

Figure 50 shows the total annual EUI comparison among the AHSRAE 90.1-2007 baseline model, proposed design case model, calibrated model, and actual metered data of the CSL building. The horizontal line shows the metered energy generation intensity ( $59\text{kWh/m}^2$ ) of the 125kW photovoltaic system on the Phipps campus. The CSL building achieved net zero site energy for the year of 2013 based on the definition of (Torcellini *et al.*, 2006). Table 20 shows the mean biased error (MBE) and the coefficient of variations the root mean squared error

(CVRMSE) of the three models compared to the actual metered data for the year of 2013. The final calibrated model has an MBE of 1.27% and a CVRMSE of 6.01%. The model can be considered well calibrated.

It should also be noted that there are significant variations between the design case assumptions and the actual building operations. First, the design case model uses the same lighting and equipment power densities and schedules as in the ASHRAE baseline model for the purpose of fair comparisons, while the actual building lighting and equipment power density is much less than the baseline assumptions. Second, the HVAC energy consumption of the design case model uses night setback strategies and varies for different seasons to save energy. On the contrary, in the actual building operation, setpoint schedule is more stringent and more consistent through different seasons. This control strategy difference causes a considerable variation in HVAC energy consumption between the design case energy model and the actual building operation. The resulting effect is that the MBE of the total energy use intensity of the design case model compared to the measured data is -7.29%, and the CVRMSE is 93.40%.

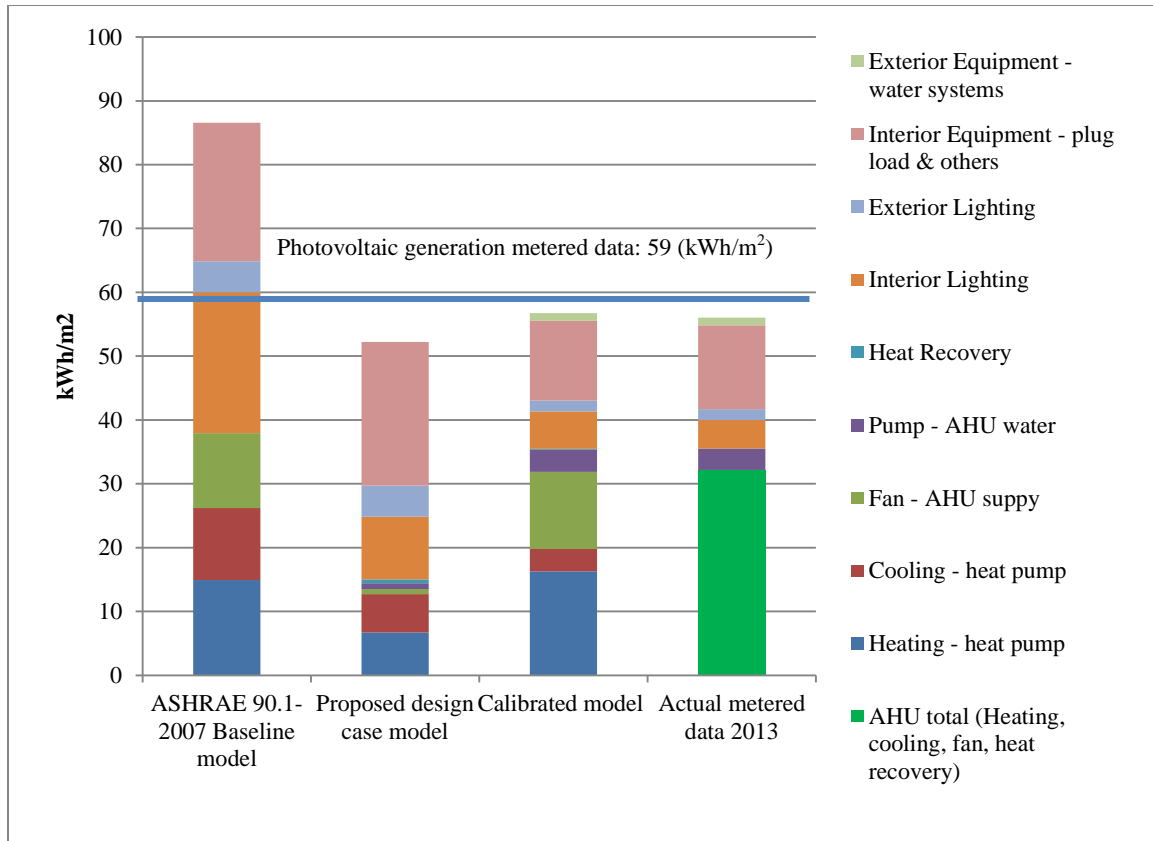


**Figure 50 Total annual EUI comparison for the CSL building.**

**Table 20 Errors of total annual EUI compared with measured data for the three models.**

	Baseline	Design	Calibrated
Mean biased error (MBE)	35.30%	-7.29%	1.27%
Coefficient of variations the root mean squared error (CVRMSE)	79.88%	93.40%	6.01%



### 3.8. Summary

This chapter demonstrates an EnergyPlus model calibration method using empirical data in the CSL building. The occupancy schedule data mining procedure is tested in two office building spaces and the results are satisfactory. The daylight/lighting and equipment inverse calibration procedure and the active/passive HVAC system calibration procedure are also demonstrated in the test-bed building. The final calibrated model has a mean biased error (MBE) of 1.27% and a coefficient of variation the root mean squared error (CVRMSE) of 6.01%. The model can be considered well calibrated. The overall method provides a scientific and systematic framework to conduct high accuracy EnergyPlus model calibration. The calibrated EnergyPlus model will be used for the control system design and simulation in Chapter 4.

The most important part of this calibration study is the development of an occupant behavior and schedule modeling method, which is tested in two office spaces. Office appliance power consumption data are collected and trained by using C4.5 decision tree, locally weighted naïve Bayes, support vector machine, linear regression, locally weighted regression, and support vector regression algorithms. The comparative data mining studies show that C4.5 decision tree is a suitable algorithm for learning the occupant individual behavior and linear regression is a suitable algorithm for learning the group schedule. Both studies show that the percentage of correctly classified individual behavior instances is above 90%. The correlation coefficient of the predicted group schedules versus the ground truth schedules is also above 0.90. The modeling method is robust and the accuracy is adequate.

The occupant behavior data mining results also show diversified behaviors in using office appliances on the individual level yet fairly consistent schedules as a group. The findings directly

support the following two suggestions, (1) it is important to develop a system that will persuade occupants to change their appliance use behavior thereby reducing energy consumption. (2) It is necessary and effective to learn the “real” group schedule during operation to better control the HVAC system and reduce its energy consumption.

# Chapter 4. Occupant-oriented mixed-mode

## EnergyPlus predictive control (OME<sup>+</sup>PC)

---

### 4.1. Overview

This chapter focuses on the design and performance simulation of a model-based predictive control system at the operation stage using the proposed design case and calibrated EnergyPlus models with simulated and measured data. In section 4.2, a baseline EnergyPlus model-based building control system is developed to demonstrate the feasibility of using a co-simulation framework with Matlab/Simulink and EnergyPlus to perform multi-zone rule-based control and obtain its energy and thermal comfort performance as a base case. In section 4.3, an EnergyPlus Predictive Control (E<sup>+</sup>PC) system is developed to maintain the same comfort criteria as the baseline control but to minimize the active HVAC system energy consumption using the model-based predictive control theory. In section 4.4, a mixed-mode passive/active EnergyPlus Predictive Control (ME<sup>+</sup>PC) system is developed based on E<sup>+</sup>PC, in order to control both the active and passive (window opening) HVAC systems in the CSL building. The energy and comfort performance is compared between E<sup>+</sup>PC and ME<sup>+</sup>PC. In section 4.5, an occupant-oriented mixed-mode passive/active EnergyPlus Predictive Control (OME<sup>+</sup>PC) system is developed based on ME<sup>+</sup>PC. The real-time occupant thermal comfort feedback data are introduced into OME<sup>+</sup>PC to meet different individual thermal comfort requirements. The comfort and energy performance is compared between ME<sup>+</sup>PC and OME<sup>+</sup>PC.

## 4.2. Baseline EnergyPlus model-based building control

The goal of the baseline control is to set up a co-simulation framework using Matlab/Simulink and EnergyPlus to perform multi-zone rule-based control and obtain its energy and thermal comfort performance as a benchmark. For the six open office zones, Predicted Mean Vote (PMV) is used as a thermal comfort control criterion, which may better represent occupant comfort than merely using air temperature as suggested in previous studies (Daum *et al.*, 2011; Murakami *et al.*, 2007; Yang and Su, 1997; Y. Yu *et al.*, 2013). Three out of six variables in the PMV calculation matrix are pre-defined in Table 21 in this baseline control, which are metabolic rate, air speed, and clothing insulation. The air temperature, mean radiant temperature and relative humidity values are calculated in EnergyPlus at each simulation iteration. Other thermal zones, such as storage rooms and restrooms, are controlled by the conventional temperature dual-setpoint method in EnergyPlus. Table 21 lists the input assumptions of setpoint, comfort, weather and schedule.

**Table 21 Assumptions for the baseline and E<sup>+</sup>PC controls.**

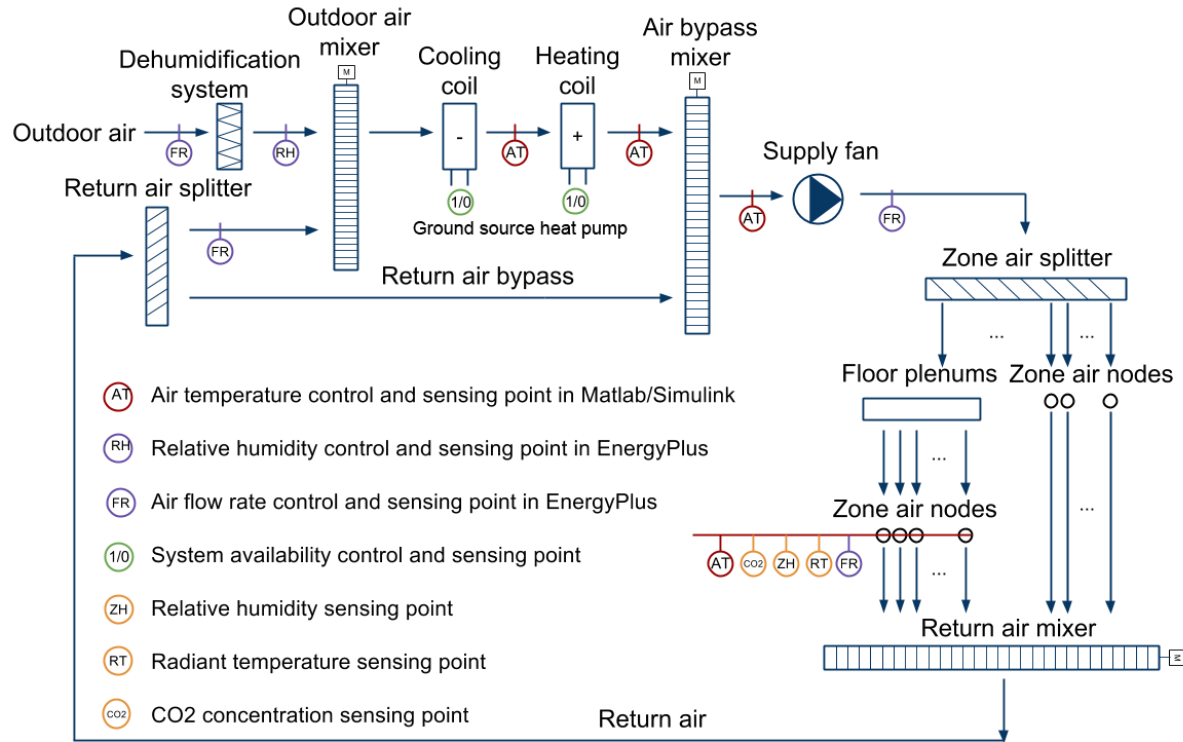
		Baseline	E <sup>+</sup> PC
Zone control	Weekdays 7:00-20:00	PMV control: [-0.5, 0.5], Temperature control: [22, 24] °C for other conventional controlled zones	
	Weekends & weekdays 20:00-7:00	PMV control: [-2, 2], Temperature control: [18, 28] °C for other conventional controlled zones	
Comfort assumptions		met = 1.0, air speed = 0.137 m/s cooling season clo = 0.7, heating season clo = 1.0	
Weather and schedules		TMY3 – Pittsburgh International Airport, design case occupancy, lighting, and equipment schedules	.csv files with the same information as the Baseline's

Figure 51 shows the HVAC diagram of the EnergyPlus model, as well as the control and sensing points in the HVAC's air loop system. Four types of control and sensing points are shown on the diagram using four different colors: red represents control and sensing points in Matlab/Simulink, purple represents control and sensing points in EnergyPlus, green represents availability control points in Matlab/Simulink, and yellow represents sensing points in EnergyPlus. Specifically, "AT" represents the air temperature control points with the control logic implemented in Matlab/Simulink. "RH" represents the relative humidity setpoint control of the desiccant dehumidification system in EnergyPlus, which is  $< 50\%$  for occupied hours. "FR" represents the air flow rate of the outdoor air, return air (and its bypass), and supply air, which are controlled in EnergyPlus based on the temperature setpoints "AT". "1/0" represents the binary control signal for the availability of the cooling and heating coils. "RH", "RT", and "CO<sub>2</sub>" represent the relative humidity, radiant temperature, and CO<sub>2</sub> concentration measurements, respectively, in each different open office zone. All the points shown on the diagram are measured in EnergyPlus using the "System Node Output" function (Pang *et al.*, 2011).

One should note that the coil system modeled in EnergyPlus is different from the actual installed proprietary Tricoil<sup>®</sup> system manufactured by Berner International Corp<sup>4</sup>. The pre-cooling and free-reheat coils, which directly utilize the water from geothermal system, are not modeled due to the information availability and the limitation of EnergyPlus. The main heating and cooling coil that connects to the ground source heat pump is modeled in EnergyPlus for heating and cooling purposes, as shown in Figure 51.

---

<sup>4</sup> See reference at [http://www.bernerenergy.com/\\_energy/html/products\\_tricoil\\_system.html](http://www.bernerenergy.com/_energy/html/products_tricoil_system.html).



**Figure 51 Air loop HVAC diagram and control/sensing points.**

MLE+ (version 1) together with Building Control Virtual Test Bed (BCVTB) is used as the co-simulation platform for Matlab/Simulink and EnergyPlus. “MLE+ is a Matlab toolbox for co-simulation with the whole-building energy simulator EnergyPlus”. It “provides a set of Matlab functions and classes, as well as a Simulink library, for performing co-simulation with EnergyPlus.” (Nghiem, 2012). MLE+ enables users to directly develop algorithms and use functions in Matlab/Simulink. Although MLE+ adopts the same data exchange mechanism as BCVTB, users do not need to do the data transfer through Ptolemy (Buck *et al.*, 1994) interface of the BCVTB. Figure 52 shows the baseline control implementation schema. A two-loop cascade control is implemented in the co-simulation environment. At the central level, the air handler unit (AHU) setpoint is controlled by rule-based control law using both outdoor air

temperature and average zone PMV feedback. At the zone level, air flow rate is controlled by adjusting floor-based diffuser's damper position in EnergyPlus according to the temperature setpoint calculated in Matlab/Simulink. Each zone can have different temperature setpoints based on its PMV value, which is calculated at each simulation iteration.

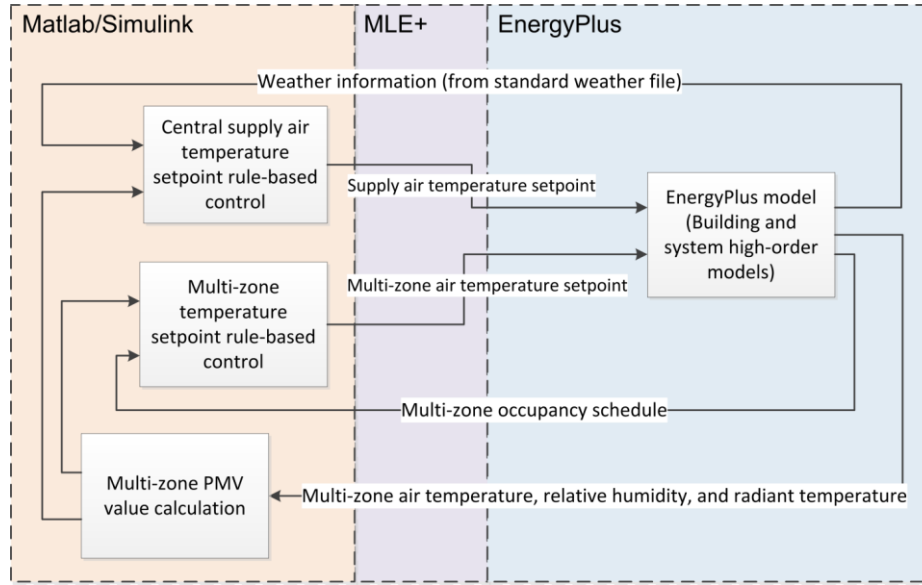


**Figure 52 Baseline control implementation schema.**

### 4.3. EnergyPlus Predictive Control ( $E^+PC$ )

#### 4.3.1. $E^+PC$ problem description

The objective of  $E^+PC$  is to maintain the same PMV comfort criteria as the baseline control but to minimize the active HVAC power consumption by optimizing the AHU supply air temperature. The objective function can be described as,

$$J(x, t) = \min(Q_c(x, t) + Q_h(x, t) + Q_f(x, t) + Q_p(x, t)) \quad (26)$$

subject to,

$$|PMV| = \begin{cases} \leq 0.5, & f_{occ}(t) \neq 0 \\ \leq 2, & \text{otherwise} \end{cases} \quad (27)$$

$$T_C(x, t) \in (14, 18) \quad (28)$$

$$T_H(x, t) \in (24, 32) \quad (29)$$

$$A_H * A_C = 0 \quad (30)$$

$$T_S(x, t) \in \begin{cases} (14, 20), & A_C=1 \\ (24, 32), & A_C=0 \end{cases} \quad (31)$$

where,

$t$ , time (s);

$x$ , the optimized supply air temperature setpoint, (°C);

$J(x, t)$ , total HVAC system power at time  $t$ , (kW)

$Q_c(x, t)$ , cooling system power at time  $t$ , (kW);

$Q_h(x, t)$ , heating system power at time  $t$ , (kW);

$Q_f(x, t)$ , supply air fan power at time  $t$ , (kW);

$Q_p(x, t)$ , water pumps power at time  $t$ , (kW);

$f_{occ}(t)$ , occupancy status at time  $t$ , (0, 1);

$T_C(x, t)$ , cooling coil air outlet temperature setpoint at time  $t$ , (°C);

$T_H(x, t)$ , heating coil air outlet temperature setpoint at time  $t$ , (°C);

$A_H$ , availability of heating coil, (0, 1);

$A_c$ , availability of cooling coil, (0, 1);



$T_s(x, t)$ , supply air temperature at time  $t$ , (°C).

The exhaustive search algorithm (or Brute-force algorithm) is chosen to solve the problem for the following reasons. First it is a “test-and-generate” algorithm, which is a type of algorithm that can be used for “black-box” simulation-based optimization (Kolda *et al.*, 2003). Second, the algorithm is suitable for the problem that has “reasonable” computation time and discrete variables (Sinha, 2008). The E<sup>+</sup>PC optimization problem has multiple constraints which results in a small search space. For example, in the cooling mode, the search space for the cooling coil is from 14 to 18 °C and for practical reasons, 0.5 °C difference is a reasonable discrete interval, resulting in nine iterations per planning horizon. The total optimization time for each planning horizon is about five minutes for E<sup>+</sup>PC, which is feasible for real-time simulation for one-hour execution horizon. Although the planning horizon is one hour, the total optimization simulation period is 24 hours in accordance with the EnergyPlus run time.

Equations (28-31) indicate that the optimization problem has binary parameters, which needs to be separated into two different optimization spaces: cooling mode and heating mode. The optimization is conducted in these two modes separately using the outdoor temperature as the separator for the two spaces in accordance with the real system operation.

$$\begin{cases} J = \min(f_{\text{power}}(x, t)), & \text{if Eq.(27) is satisfied} \\ J = \min(|f_{\text{PMV}}(x, t)|), & \text{otherwise} \end{cases} \quad (32)$$

When the comfort constraints are not met, they are handled by Equation (32) to guarantee that the thermal comfort performance is prioritized. If the comfort constraints defined in equation (27) is met, the algorithm minimizes the power consumption; otherwise, the algorithm ignores the power consumption, but find the value that is the closest to the boundary defined in Equation (27)

from the past optimization iteration results. This penalty function is evaluated at each simulation iteration. The constraint choices in Equation (32) between the PMV boundary and power boundary can switch during the same planning horizon.

#### 4.3.2. $E^+PC$ implementation

Figure 53 shows the  $E^+PC$  implementation schema. Compared to the baseline rule-based control implementation schema,  $E^+PC$  introduces a “Data input layer”. In “Data input layer”, weather, occupancy, lighting, and equipment information is contained in independent text files (CSV, Comma Separated Values). It is essential and beneficial to override the EnergyPlus internal weather and schedule data by using the “Data input layer” and “Receding horizon” module in the “Control layer”. The “External Interface - Actuator” function in the EnergyPlus model is used for the data override (Pang, et al. 2011). The “Data input layer” is implemented to solve the critical data interoperability issue in the following two aspects.

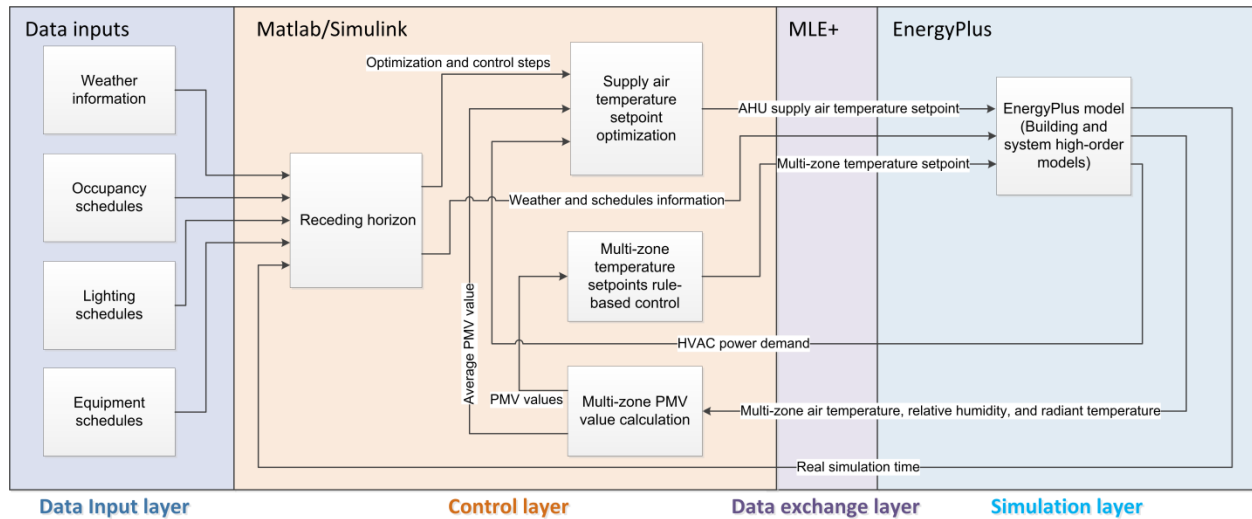


**Figure 53  $E^+PC$  implementation schema.**

First, E<sup>+</sup>PC needs to perform optimization in EnergyPlus, which uses the same day weather and schedule information multiple times for one execution horizon. Some of the rules in EnergyPlus require that at least 24-hour simulation should be performed for each of the optimization iteration. For instance, EnergyPlus only permits solar radiation data input from 5am to 8pm in accordance with sun position and building site location. The rule requires each of the optimization iteration to be at least 24 hours no matter how long the actual planning horizon is. In E<sup>+</sup>PC, the planning horizon and execution horizon are both one hour. Figure 54 illustrates the concept of “Receding horizon” for E<sup>+</sup>PC. Axis (a) represents real days for the control system. Axis (b) represents the one-hour execution horizon of the control system. Axis (c) represents the optimization iterations. For each one-hour execution horizon, n (n depends on the size of optimization search space, in this case, n equals to nine) optimization iterations are required, as indicated by orange arrows in Figure 54. Axis (d) represents real simulation time steps in EnergyPlus. For each optimization iteration, 24 hours of simulation time steps in EnergyPlus are needed as explained above. Axis (e) represents the time steps of the various EnergyPlus input files, including weather file, occupancy schedule, equipment schedule, and lighting schedule. For each of the optimization iteration of the same execution horizon, the same day model input data should be used n times, as indicated by the purple arrows pointing to Axis (d).

The second reason to use separate data inputs to override the weather and schedule information is that this method can facilitate the development of potential real-time control in the real building operation in future. The “Data input layer” in fact provides an interface for potential real operation data input. The data files in “CSV” or other machine readable format can be easily updated with the real-time information by linking with the indoor sensors network and on-site weather station via BAS. See the section of “4.5. Occupant-oriented ME+PC (OME+PC)” for



“Multi-zone temperature setpoint rule-based control” and “Multi-zone PMV value calculation” modules are the same as the ones in the baseline control.

“Data exchange layer” is used for data communication and time synchronization functions, technical details can be found in (Nghiem, 2012). In “Simulation layer”, the inputs of the EnergyPlus model are “AHU supply air temperature setpoint”, “Weather and schedules information”, and “Multi-zone temperature setpoint”. The outputs are “HVAC power demand”, “Multi-zone air temperature, relative humidity, and radiant temperature”, and “Real simulation time”, which is used for time synchronization between Matlab/Simulink and EnergyPlus.

### ***4.3.3. Result comparison between baseline and E<sup>+</sup>PC***

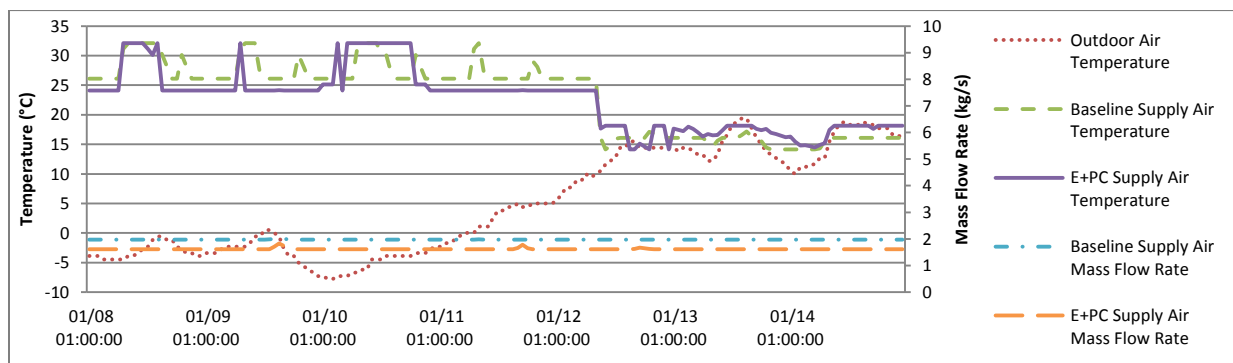
#### ***4.3.3.1. Heating season results***

The baseline control and E<sup>+</sup>PC are simulated for one typical design week in the heating season (January 8<sup>th</sup> – January 14<sup>th</sup>) using TMY (typical meteorological year)-3 weather information in Pittsburgh, Pennsylvania, US (Pittsburgh Intl AP 725200). The same initial warm-up condition is set to be January 8<sup>th</sup> for both the baseline model and E<sup>+</sup>PC. Figure 55 shows the supply air temperature, outdoor air temperature, and supply air mass flow rate of the baseline and E<sup>+</sup>PC. E<sup>+</sup>PC can maintain an average lower supply air temperature and supply air mass flow rate than the baseline in the heating mode before 9am January 12<sup>th</sup>. From 9am January 12<sup>th</sup> to 12am January 14<sup>th</sup>, the system changes from heating mode to cooling mode, mainly due to the rise of the outdoor temperature. E<sup>+</sup>PC generally has a higher supply air temperature during this period for the energy saving purpose. It is common that in the heating season, due to the heat gain from occupants, equipment, and other internal loads, the office building’s cooling load may exceed its

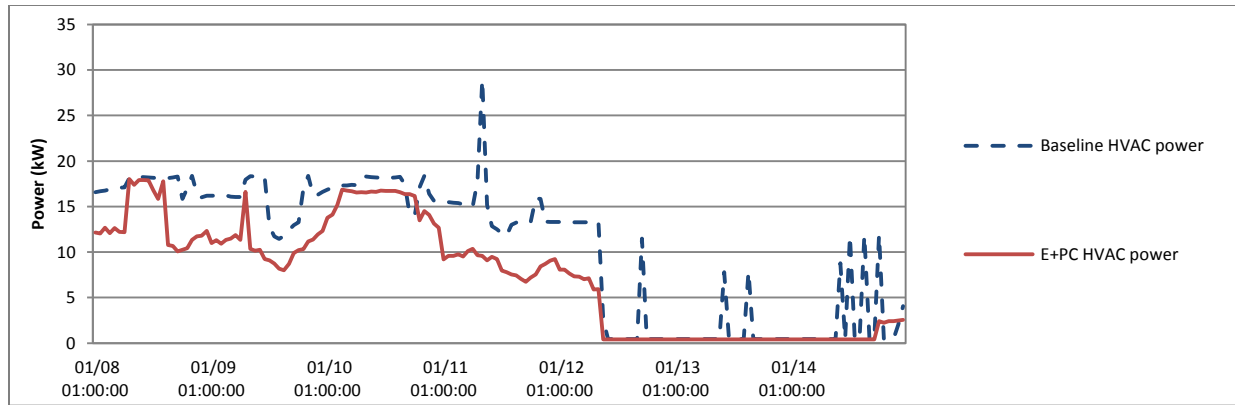
heating load when the outdoor temperature rises. Another observation is that E<sup>+</sup>PC can reduce PMV spikes found in the baseline rule-based control. In the baseline model, the dual-setpoint PMV control only makes changes once the PMV has violated the setpoint boundaries, and this delayed response may result in overshoots and undershoots. E<sup>+</sup>PC is able to look ahead the future possible situations and make an optimal decision for the control setpoint at each execution horizon to reduce the total instances of overshoots and undershoots.

Figure 56 illustrates the HVAC power comparison between the baseline control and E<sup>+</sup>PC. Due to a lower heating supply air temperature as shown from January 8<sup>th</sup> to January 12<sup>th</sup> in Figure 55, a higher cooling supply air temperature as shown from January 12<sup>th</sup> to January 14<sup>th</sup> in Figure 55, and lower fan speed, the energy consumption reduction is found to be 28.9% during the one-week heating season simulation period, as shown in Table 22

Figure 57 shows the average zone PMV comparison between the two systems. E<sup>+</sup>PC pushes the PMV value to the boundaries to minimize energy. For example, in the first three days in the heating mode, the PMV value is closer to the lower constraint boundary, and in the last two days in the cooling mode, the PMV value is closer to the upper constraint boundary.



**Figure 55 Outdoor temperature and control variables of the baseline and E<sup>+</sup>PC in the heating season.**



**Figure 56 Energy performance of the baseline and E<sup>+</sup>PC in the heating season.**

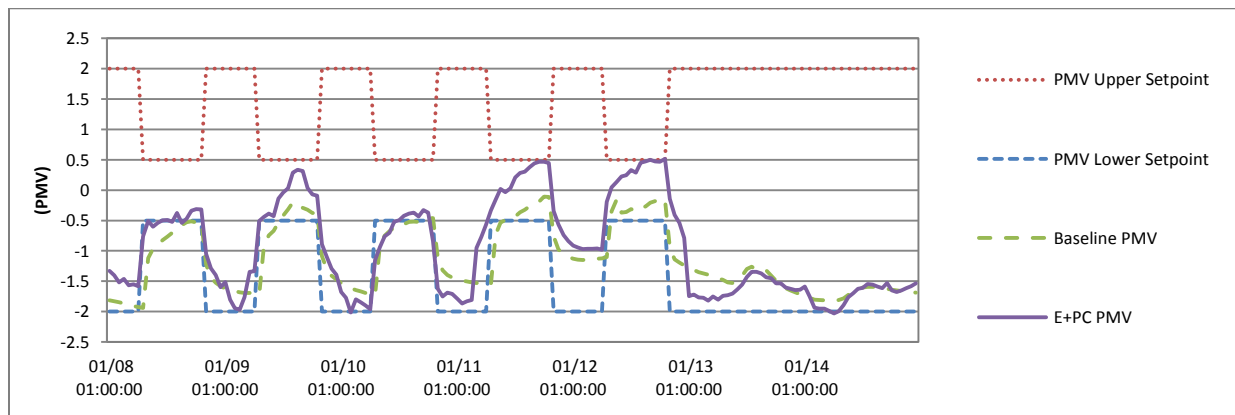


**Figure 57 Thermal comfort performance of the baseline and E<sup>+</sup>PC in the heating season.**

**Table 22 One week HVAC energy consumption comparison for the CSL building.**

	Baseline energy (kWh)	E <sup>+</sup> PC energy (kWh)	Energy savings (%)
one week heating season simulation	1784.8	1268.7	28.9%
one week cooling season simulation	1154.8	1123.8	2.7%
Total	2949.6	2391.5	18.9%

In Figure 58, the heating season median PMV in the unoccupied hours is -1.60 (with a lower quartile of -1.76 and an upper quartile of -1.35) for E<sup>+</sup>PC, and -1.54 (with a lower quartile of -1.68 and an upper quartile of -1.32) for the baseline, respectively. E<sup>+</sup>PC makes majority of the PMV values in the unoccupied hours to be lower than the baseline but still within the constraint boundary. However, in the morning of January 10<sup>th</sup>, there are instances that PMV is out of the constraint boundary. One reason could be that only 6 out of 30 thermal zones of the whole building are controlled by E<sup>+</sup>PC using the PMV criterion. Other zones are controlled by conventional temperature dual setpoint in EnergyPlus. With only one central AHU supplying for all the thermal zones, the impact of the AHU supply air temperature and flow rate change may not be sensitive enough. In other words, the thermal conditions of the other 24 zones may influence the six PMV-controlled zones. It is a limitation of E<sup>+</sup>PC. However, from the practical standpoint, it is reasonable and economical to only consider controlling the six highly occupied open office zones with more advanced control strategies without considering other rarely occupied service zones, such as restrooms and mechanical rooms. The other possible reason is that the planning horizon of E<sup>+</sup>PC is one hour, which is ideal if considering the building thermal mass effect. The optimizer is only able to see what will happen in the next hour, but cannot take into consideration of a longer period. It is another limitation of the study.

In Figure 59, the heating season median PMV in occupied hours is -0.15 (with a lower quartile of -0.48 and an upper quartile of 0.29) for E<sup>+</sup>PC, and -0.54 (with a lower quartile of -0.69 and an upper quartile of -0.32) for the baseline, respectively. The PMV of E<sup>+</sup>PC has fewer low value outliers, which implies E<sup>+</sup>PC has better ability to maintain the PMV constraints in the heating season occupied hours.



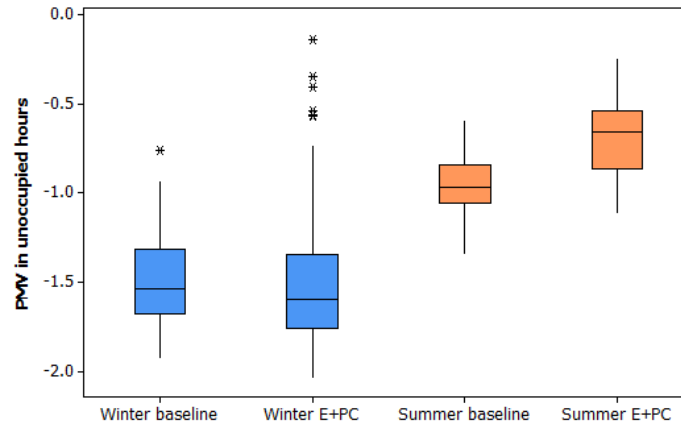


**Figure 58 PMV distribution in unoccupied hours.**

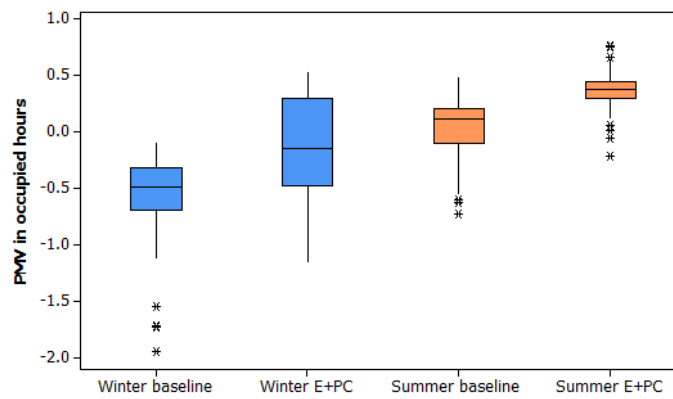


**Figure 59 PMV distribution in occupied hours.**

#### 4.3.3.2. Cooling season results

The baseline control and E<sup>+</sup>PC are simulated for one typical design week in the cooling season (July 8<sup>th</sup> – July 14<sup>th</sup>) using the TMY (typical meteorological year)-3 weather information in Pittsburgh, Pennsylvania, US (Pittsburgh Intl AP 725200). The same initial warm-up condition is set to be July 8<sup>th</sup> for both the baseline and E<sup>+</sup>PC. The supply air temperature, outdoor air temperature, and supply air mass flow rate of the baseline and E<sup>+</sup>PC are shown in Figure 60.

Unlike the baseline, E<sup>+</sup>PC varies the supply air temperature setpoint more often. During the highly occupied afternoon hours, the supply air temperature is clearly lower than that in the baseline control, which indicates more cooling energy consumption. However, in less or non-occupied hours, the supply air temperature tends to increase up to 20 °C, which indicates less cooling energy consumption. In general, the supply air flow rate of E<sup>+</sup>PC is lower than that of the baseline, which implies the supply fan power consumption decreases over the simulation period.

Figure 61 and Figure 62 show the hourly power consumption profiles for one week and one day, respectively. Although it is difficult to see a general pattern of energy savings from the figures, the cumulative energy savings during one cooling week is 2.7% as shown in Table 22.

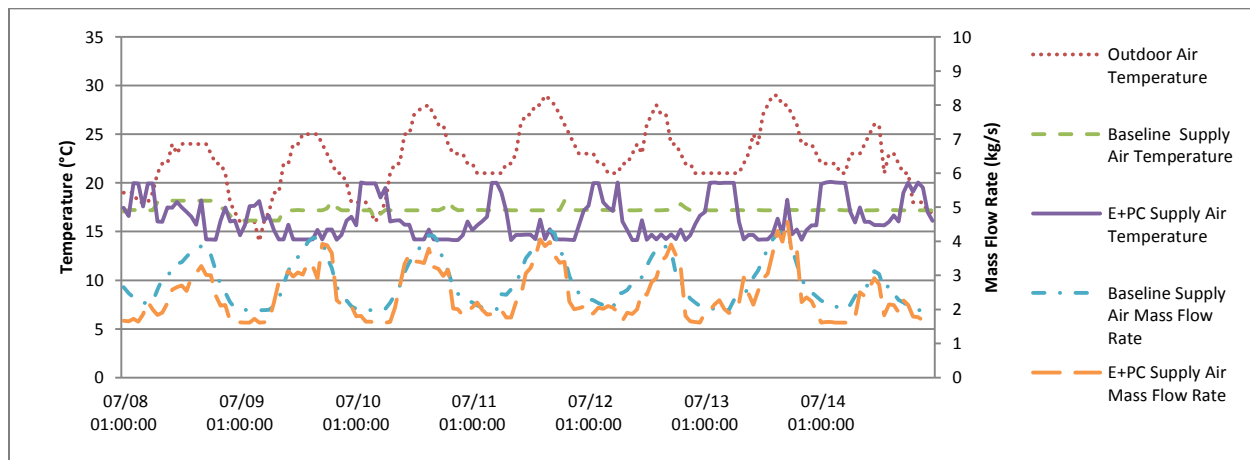


**Figure 60 Outdoor temperature and control variables of the baseline and E<sup>+</sup>PC in the cooling season.**

The PMV value of the two systems is shown in Figure 63. Similar to the heating season results, the PMV value is pushed towards the upper boundary during both the occupied and unoccupied hours. On July 10<sup>th</sup>, 11<sup>th</sup>, and 12<sup>th</sup>, there are a few times around noon when the PMV value

exceeds the upper constraint boundary. The reasons for this violation should be similar to the ones which have been discussed in “4.3.3.1. Heating season results”.

Figure 58 and Figure 59 provide a clearer picture on the PMV distribution. E<sup>+</sup>PC has higher average PMV within the constraint boundary for energy saving purpose compared to the baseline rule-based control. In the unoccupied hours, E<sup>+</sup>PC median PMV is -0.66 (with a lower quartile of -0.87 and an upper quartile of -0.54); the baseline median PMV is -0.97 (with a lower quartile of -1.05 and an upper quartile of -0.84). Similarly, in the occupied hours, E<sup>+</sup>PC median PMV is 0.37 (with a lower quartile of 0.30 and an upper quartile of 0.44); the baseline median PMV is 0.11 (with a lower quartile of -0.10 and an upper quartile of 0.20).

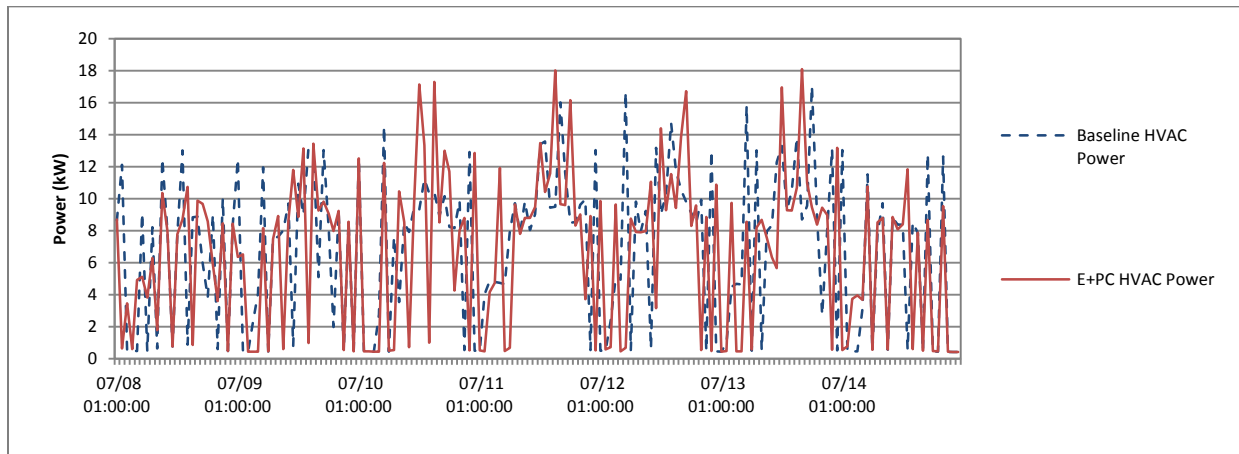


**Figure 61 One week plot of energy performance of the baseline and E<sup>+</sup>PC in the cooling season.**

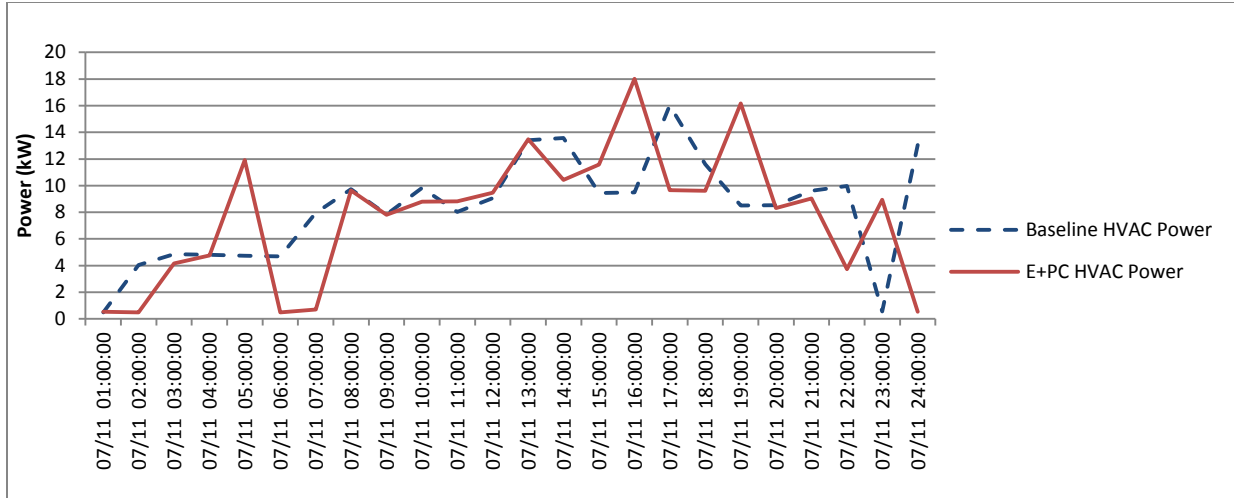


**Figure 62 One day plot of energy performance of the baseline and E<sup>+</sup>PC in the cooling season.**

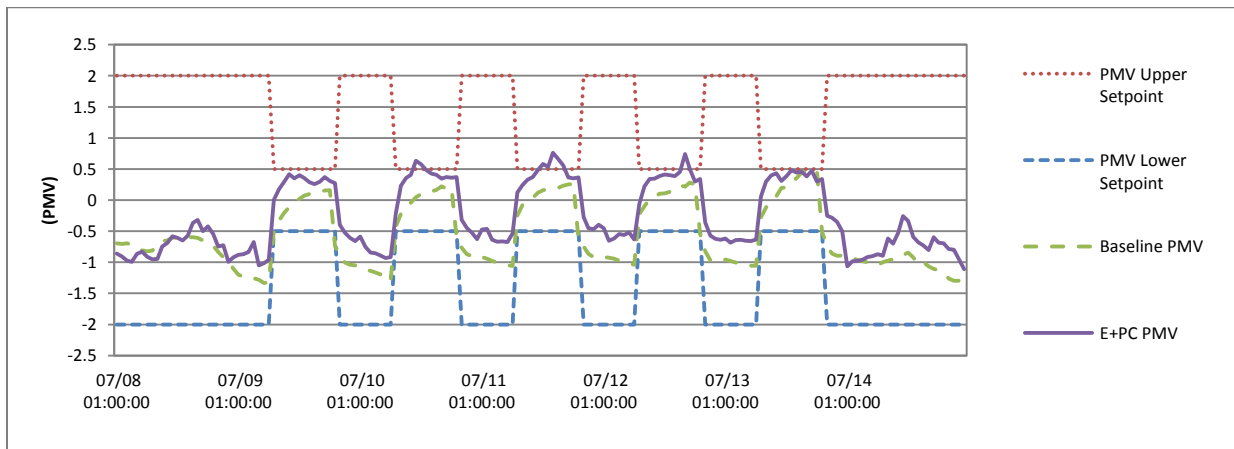


**Figure 63 Thermal comfort performance of the baseline and E<sup>+</sup>PC in the cooling season.**

#### 4.4. Mixed-mode passive/active E<sup>+</sup>PC (ME<sup>+</sup>PC)

E<sup>+</sup>PC has successfully demonstrated the use of the EnergyPlus model in the predictive control simulation and the results have shown better energy performance while maintaining thermal

comfort criteria. However, only the active heating and cooling system is simulated and controlled in E<sup>+</sup>PC. This section will introduce a mixed-mode passive/active E<sup>+</sup>PC (ME<sup>+</sup>PC) to achieve the following two objectives. The first objective is to add an air quality (CO<sub>2</sub> concentration) constraint to the E<sup>+</sup>PC objective functions, so that the advanced mixed-mode HVAC system control not only can meet the thermal comfort criteria, but also can meet the minimum ventilation requirement of CO<sub>2</sub> concentration in office spaces. The second objective is to incorporate the passive cooling strategy into E<sup>+</sup>PC, so that the control system can handle both active mechanical HVAC system and passive motorized window opening system to further reduce the HVAC energy consumption.

#### ***4.4.1. CO<sub>2</sub> concentration as a constraint***

According to ASHRAE 62.1-2010 Ventilation for Acceptable Indoor Air Quality, the maximum value of indoor CO<sub>2</sub> concentration is 700ppm above outdoor CO<sub>2</sub> level (ASHRAE, 2010). The indoor CO<sub>2</sub> constraint is defined for the objective function in Equation (26),

$$C02_{max}(t) < C02_{outdoor}(t) + 700 \quad (33)$$

where,

$t$ , time (s);

$C02_{max}(t)$ , the highest CO<sub>2</sub> concentration level of the controlled zones (ppm);

$C02_{outdoor}(t)$ , CO<sub>2</sub> concentration level of the outdoor air condition (ppm).

A new penalty function is introduced in the objective function to make sure ME<sup>+</sup>PC optimizes power consumptions when the CO<sub>2</sub> constraint is met, and maximizes the supply air flow rate ( $f_{\text{flow}}(x, t)$ ) when the CO<sub>2</sub> constraint is not met.

$$\begin{cases} J = \min(f_{\text{power}}(x, t)), & \text{if Eq.(33) is satisfied} \\ J = \max(f_{\text{flow}}(x, t)), & \text{otherwise} \end{cases} \quad (34)$$

Figure 64 shows the implementation schema of ME<sup>+</sup>PC. The “Weather information” block (highlighted in green) in the “Data input layer” is updated to include the outdoor CO<sub>2</sub> concentration level. The outdoor CO<sub>2</sub> concentration data is from the weather station located 0.9 miles away from the CSL building. The “Receding horizon” block (highlighted in green) in the “Control layer” is updated to handle the time synchronization issue of the outdoor CO<sub>2</sub> concentration data input in the same way that other weather data are manipulated. The “Multi-zone PMV value calculation” block (highlighted in green) in the “Control layer” is updated to take in the zone CO<sub>2</sub> concentration level data and compares it with the outdoor CO<sub>2</sub> concentration data using Equation (33). The comparison results feed into the “Supply air temperature setpoint optimization” block (highlighted in green) to determine whether to optimize the supply air temperature or to simply maximize the supply air flow rate to guarantee the indoor air quality satisfies the ASHRAE 62.1-2010 standard requirements. The zone CO<sub>2</sub> concentration level is simulated in EnergyPlus in the “ZoneAirContaminantBalance” section using the measured outdoor CO<sub>2</sub> data.

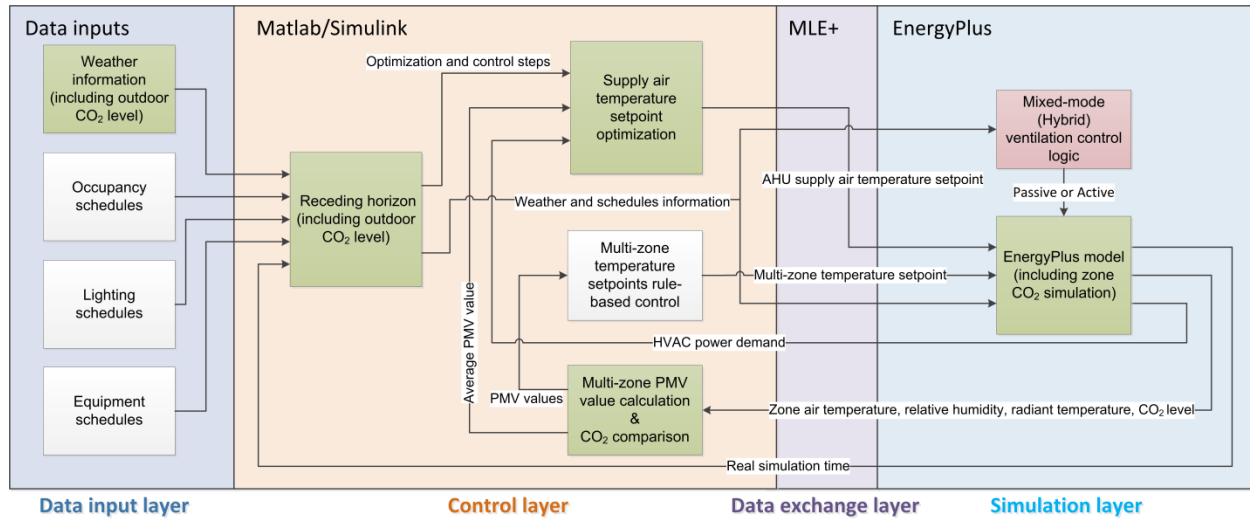


**Figure 64 ME<sup>+</sup>PC implementation schema.**

#### **4.4.2. ME<sup>+</sup>PC design and implementation**

The CSL building is equipped with motorized windows for the office spaces. ME<sup>+</sup>PC utilizes the window opening strategy to further reduce the active HVAC system energy consumptions.

The window opening control logic is shown in Figure 65. The logic is implemented in “AvailabilityManager:HybridVentilation” in EnergyPlus as discussed in “3.6.3. Passive/Active HVAC system calibration result”.

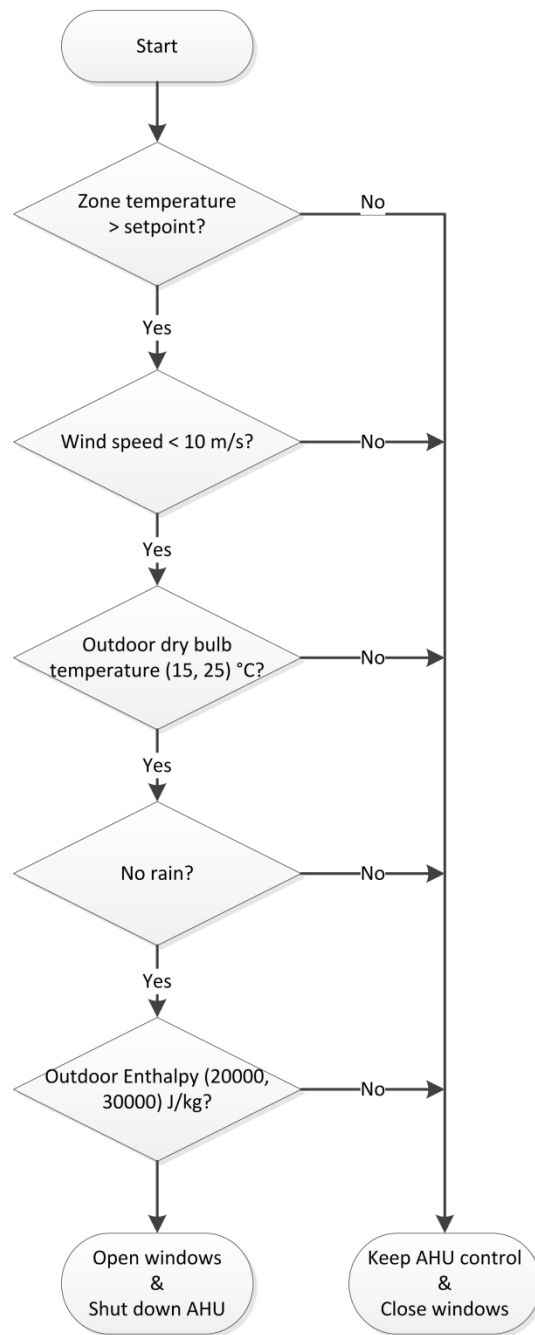


**Figure 65 Window opening control logic.**

As highlighted in red in Figure 64, the window opening logic is implemented in the EnergyPlus model. The logic takes in the the weather information and decides whether to continue with the



established predictive control optimization (active mode) algorithm or switch to the passive mode (opening windows) and shut down the AHU to reduce its energy consumption.

#### ***4.4.3. Result comparison between E<sup>+</sup>PC and ME<sup>+</sup>PC***

E<sup>+</sup>PC and ME<sup>+</sup>PC are simulated for one typical design week in the swing season (October 1<sup>st</sup> – October 7<sup>th</sup>) using 2013 AMY weather information in Pittsburgh, Pennsylvania, USA. The same initial warm-up condition is set to be October 1<sup>st</sup> for both E<sup>+</sup>PC and ME<sup>+</sup>PC.

Figure 66 shows the supply air temperature, outdoor air temperature, and supply air mass flow rate of E<sup>+</sup>PC and ME<sup>+</sup>PC. The outdoor air temperature fluctuates from 10 °C up to 28 °C during the seven simulation days, which represents a typical swing season temperature range in Pittsburgh, PA. E<sup>+</sup>PC uses full air conditioning maintains the supply air temperature between 15 °C and 18 °C and mass flow rate fairly constant (less than 2 kg/s) for both occupied and unoccupied periods, thanks to the optimization. During unoccupied night time, ME<sup>+</sup>PC's passive mode is active and the AHU supply air flow rate is zero. During occupied daytime, ME<sup>+</sup>PC has slightly lower or similar supply air temperature and higher flow rate for most times with spikes when outdoor temperature rises above 25 °C (e.g., on the afternoon of 10/02 and the morning of 10/06). The results suggest that ME<sup>+</sup>PC can reduce fan power and cooling power consumptions greatly by taking advantage of night time passive cooling, but it may create spikes at times when the outdoor conditions are close to the upper setpoint boundary (25 °C). In future work, window opening logic setpoints could be optimized to identify the optimal balance point between the night time cooling and daytime AHU operation.

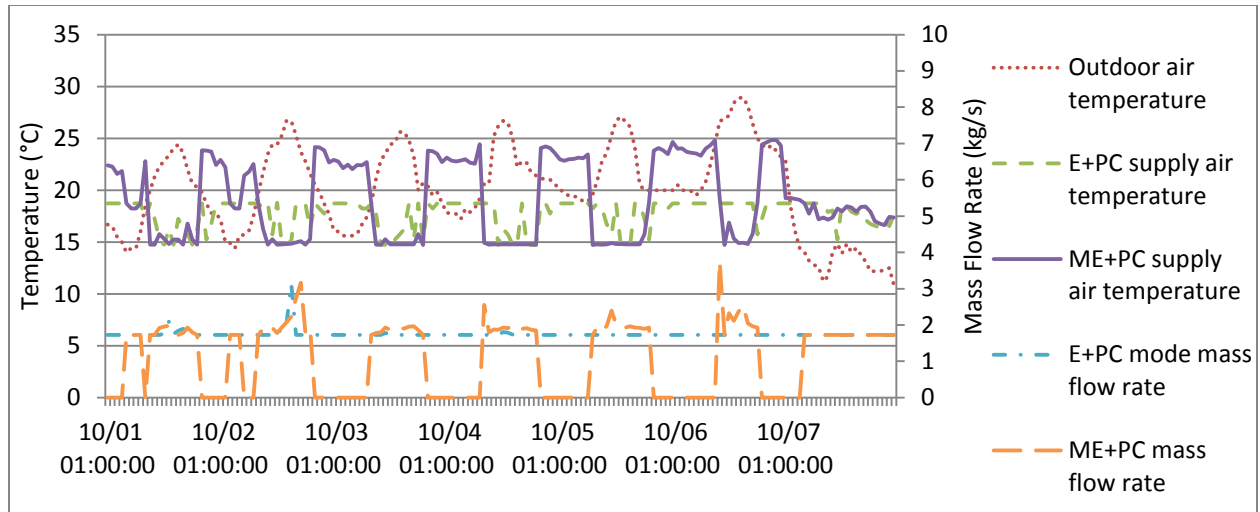
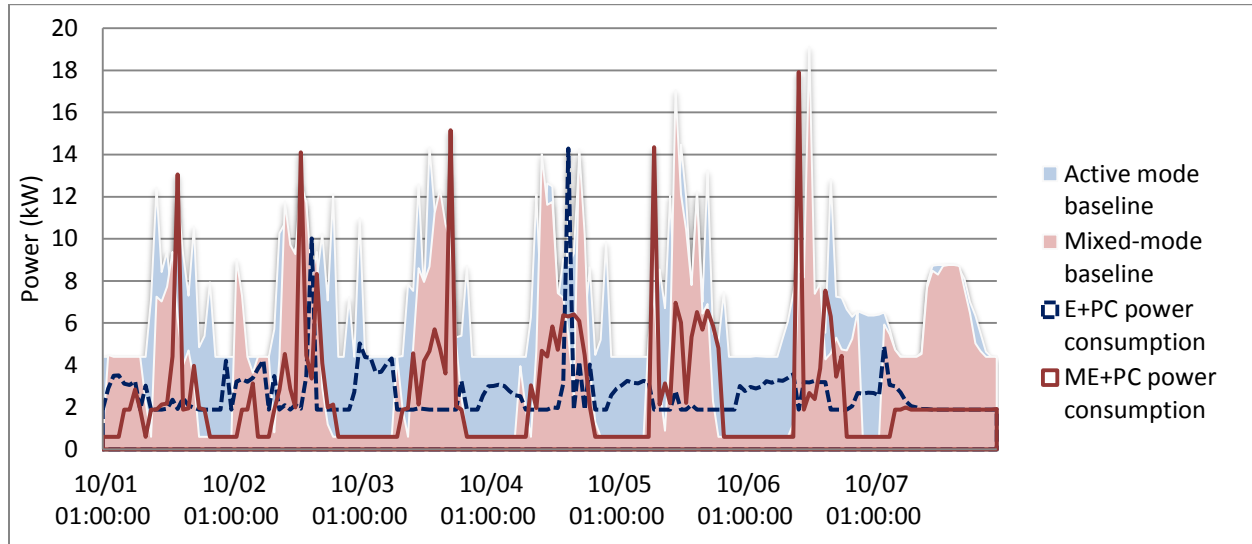


**Figure 66 Outdoor temperature and control variables of E<sup>+</sup>PC and ME<sup>+</sup>PC in the swing season.**

In order to distinguish whether the energy savings are from the passive strategy or from the optimization algorithm, the HVAC power demand are compared among the four control models: active mode baseline control, mixed-mode baseline control, E<sup>+</sup>PC and ME<sup>+</sup>PC, as shown in Figure 67. The setting of the active mode baseline control is consistent with the one in Section 4.2., which uses typical rule-based control algorithm with the same model inputs as E<sup>+</sup>PC. The mixed-mode baseline control is created based on the active mode baseline control and uses the same window opening logic as ME<sup>+</sup>PC.

The first observation is that the mixed-mode baseline control and ME<sup>+</sup>PC can reduce energy significantly during most of the unoccupied night time, due to the shutdown of AHU while opening windows. Another important observation is that ME<sup>+</sup>PC has more power spikes during daytime, compared to E<sup>+</sup>PC, especially when transiting from the passive mode to the active mode. The reason can be that the E<sup>+</sup>PC's optimization algorithm shifts the energy consumptions earlier in the morning and maintains the zone air temperature at a lower level, so that during the warmer daytime, AHU does not need to consume high power to deliver super cooled air at a high

air flow rate. However, ME<sup>+</sup>PC cannot do this because the passive strategy often takes over the control during unoccupied night time hours as long as the criteria are met.



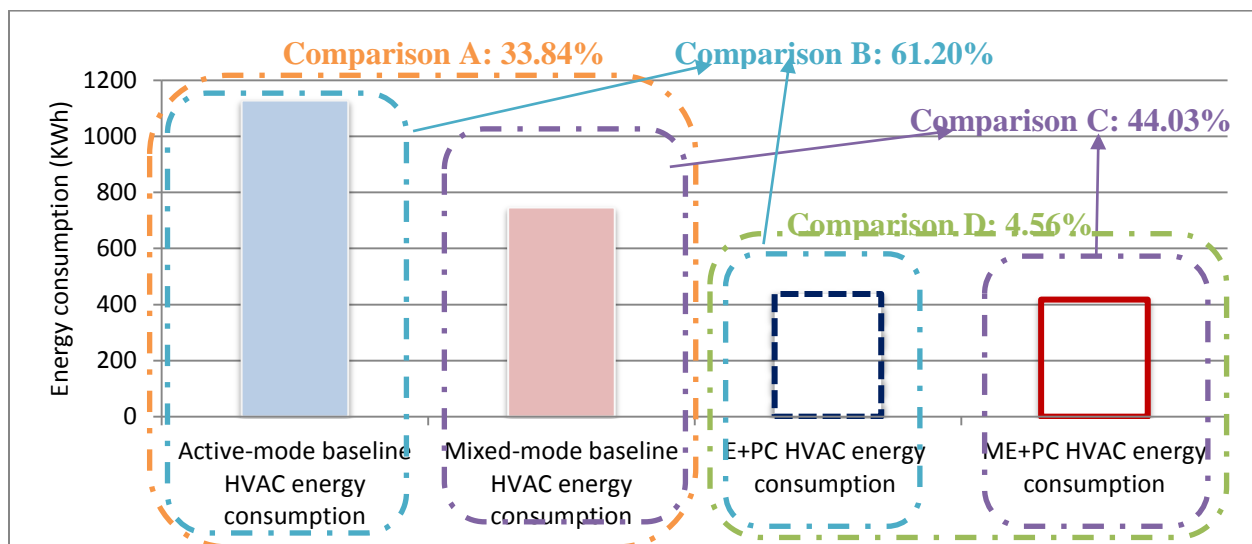
**Figure 67 One week plot of the power consumptions of the active mode baseline, mixed-mode baseline, E<sup>+</sup>PC, and ME<sup>+</sup>PC in the swing season.**

Figure 68 shows the total HVAC energy consumption of the active mode baseline control, mixed-mode baseline control, E<sup>+</sup>PC, and ME<sup>+</sup>PC during the simulation period. There are four pairs of comparisons in the figure.

Comparison A shows that merely using the passive window opening strategy on a baseline rule-based control system without any predictive control algorithm results in a 33.84% energy saving during the simulation period. Comparison B suggests that only optimizing the active HVAC control system can save 61.20% energy during the simulation period. Comparison C shows that compared to the rule-based mixed-mode control system, ME<sup>+</sup>PC can save 44.03% energy during the simulation period, thanks to the predictive control algorithm. Comparison D indicates a 4.56% energy savings between ME<sup>+</sup>PC and E<sup>+</sup>PC, which suggests that passive strategy can be used

along with the predictive control algorithm to further reduce the energy consumption. In summary, the four comparisons suggest that both passive window opening strategy and the model-based predictive control algorithm are very effective to reduce the active HVAC energy consumption.

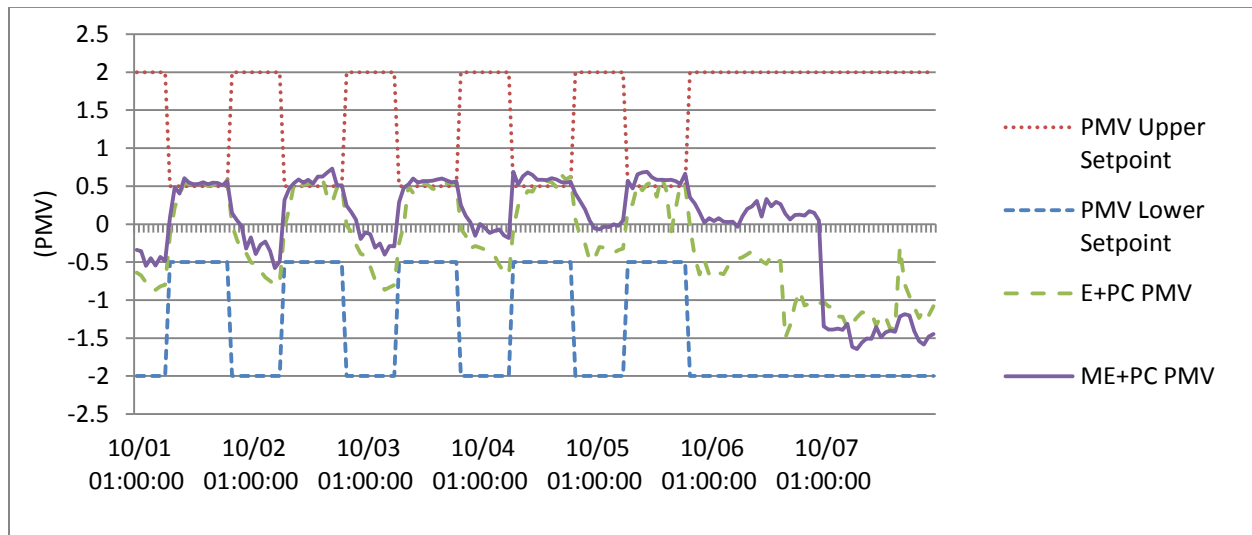
However, improvements could be made to further investigate and optimize the passive control strategies in order to make the mixed-mode predictive control works better.



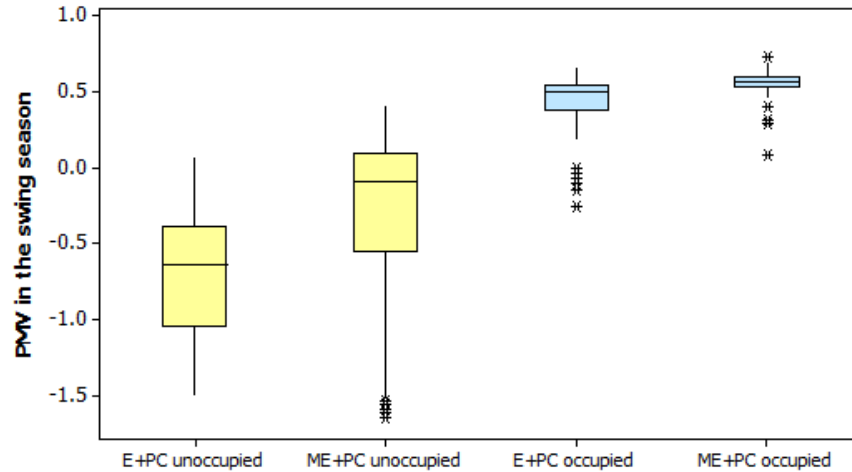
**Figure 68 One week total HVAC energy consumption of the active mode baseline, mixed-mode baseline, E<sup>+</sup>PC, and ME<sup>+</sup>PC in the swing season.**

Figure 69 shows the average zone PMV comparison between E<sup>+</sup>PC and ME<sup>+</sup>PC. In general, E<sup>+</sup>PC has better capability to maintain the PMV value under 0.5 during the occupied hours. E<sup>+</sup>PC keeps a lower PMV value during unoccupied night hours to “prepare” for the daytime temperature rise. In contrast, ME<sup>+</sup>PC has a few minor violations during warmer hours during the daytime. The comfort criterion is loosen during weekends for October 6<sup>th</sup> and 7<sup>th</sup>.

Figure 70 shows the distribution of the PMV value in the unoccupied and occupied hours of the simulation period. Clearly, ME<sup>+</sup>PC results in higher PMV values for both unoccupied and occupied hours. In the unoccupied hours, the median PMV is -0.64 (with a lower quartile of -1.05 and an upper quartile of -0.64) for E<sup>+</sup>PC, and -0.09 (with a lower quartile of -0.55 and an upper quartile of -0.10) for ME<sup>+</sup>PC, respectively. In the occupied hours, the median PMV is 0.51 (with a lower quartile of 0.38 and an upper quartile of 0.54) for E<sup>+</sup>PC, and 0.57 (with a lower quartile of 0.53 and an upper quartile of 0.60) for ME<sup>+</sup>PC, respectively. All the values are typically considered as thermally comfortable.



**Figure 69 Thermal comfort performance of E<sup>+</sup>PC and ME<sup>+</sup>PC in the swing season.**



**Figure 70 PMV distribution in unoccupied and occupied hours in the swing season.**

#### **4.5. Occupant-oriented ME<sup>+</sup>PC (OME<sup>+</sup>PC)**

E<sup>+</sup>PC has demonstrated the feasibility of using the EnergyPlus model with the model-based predictive control algorithm to optimize the building active HVAC system operation. ME<sup>+</sup>PC has demonstrated the feasibility of using the EnergyPlus model to implement the mixed-mode model-based predictive control algorithm to control both passive and active HVAC systems. The simulation results of E<sup>+</sup>PC and ME<sup>+</sup>PC have shown significant energy saving potentials while maintaining the averaged “group” occupant thermal comfort. However, individual thermal comfort preference has not yet been considered in either E<sup>+</sup>PC or ME<sup>+</sup>PC.

Therefore, the first objective of developing OME<sup>+</sup>PC is to demonstrate the feasibility of a system that allows each occupant to control his/her own thermal comfort using internet-based technologies. The second objective of developing OME<sup>+</sup>PC is to link the Matlab/Simulink and EnergyPlus co-simulation control model to the internet-based real-time database, so that OME<sup>+</sup>PC can potentially be used in the real-time BAS control in future studies.

#### ***4.5.1. Occupant subjective feedback data collection***

In order to achieve the objectives of OME<sup>+</sup>PC, it is worthwhile to investigate the actual individual occupant subjective feedback, and aim to find some patterns that can potentially be implemented in OME<sup>+</sup>PC. An internet-based data collection system is developed for the occupants in the CSL case study, as shown in Figure 71. A dashboard interface is designed using HTML and PHP to collect occupants' individual thermal comfort with the question of "How are you feeling (thermally)?" and clothing insulation factor with the question of "What are you wearing?" The thermal comfort band ranges from -2 to 2 based on the PMV definition. The clothing insulation band ranges from 0.4 to 1.9, representing from "shorts & T-shirts" to "jacket and overcoat". The occupants are required to provide the two pieces of information concurrently when they are not feeling thermally comfortable. All the data are stored in an internet-based MySQL database with timestamps.

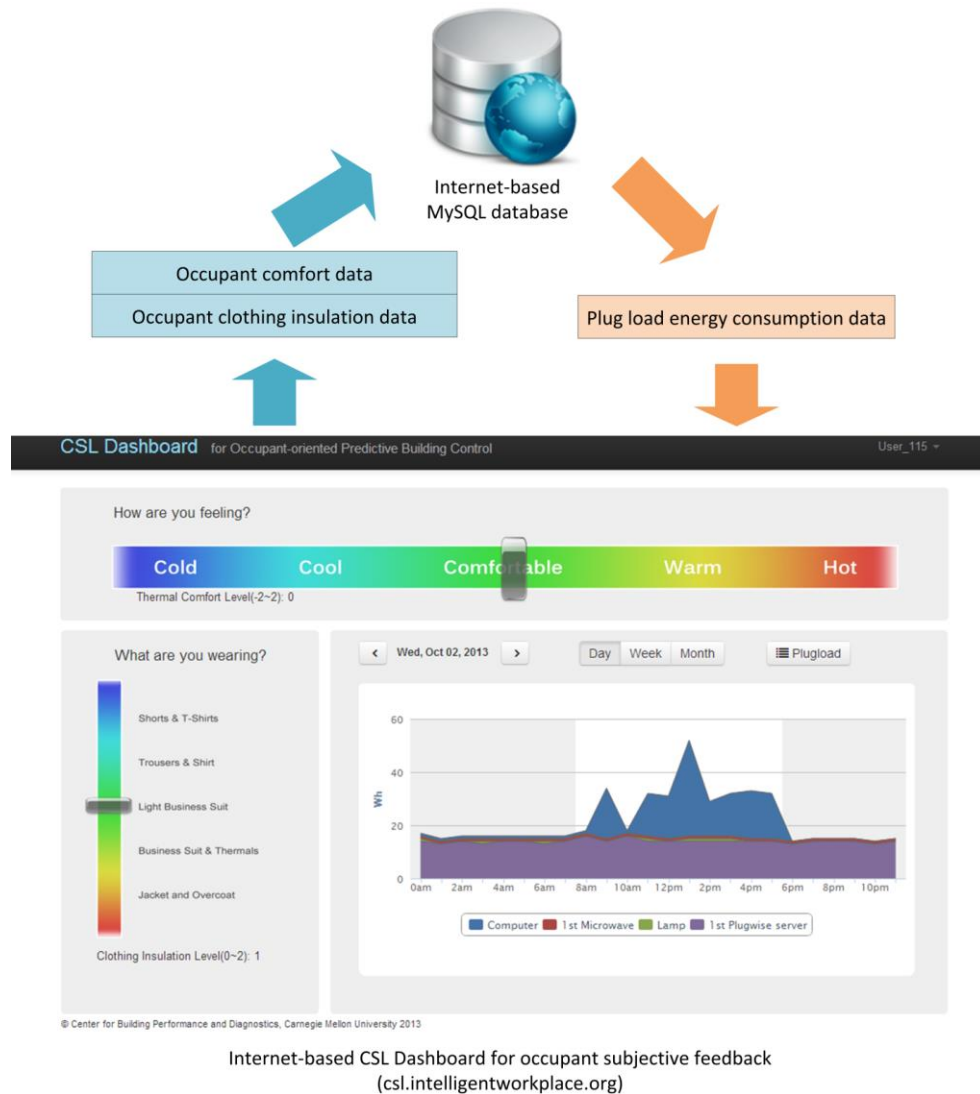


**Figure 71 Internet-based occupant subjective feedback data collection system.<sup>5</sup>**

The other part of the dashboard displays the plug load energy consumption information for the purpose of learning passive occupant behavior, which is not relevant to this particular experiment. Details about the plug load energy consumption information have been discussed in section “3.4. Occupant behavior and schedule modeling”.

<sup>5</sup> Acknowledgements to Ray Yun, Haopeng Wang, and Bertrand Lasternas for helping implement the dashboard.



#### ***4.5.2. Real-time BAS data collection***

In order to demonstrate OME<sup>+</sup>PC can potentially be used with BAS in practice, a real-time data collection system – The OSIsoft PI System (OSIsoft, 2014c) is installed in the CSL building and linked to OME<sup>+</sup>PC.

The data sources of the CSL building include on-site weather station from Campbell Scientific (Campbell, 2014), lighting and HVAC system operation data from Lutron (Lutron, 2014) and Automated Logics (AutomatedLogic, 2012), respectively, air quality data from Aircuity system (Aircuity, 2013), and energy generation and consumption metering data from E-mon system (E-Mon, 2010). All the systems above have been integrated into the Automated Logic's WebCtrl BAS system via BACnet protocol, as shown in Figure 72.

The PI system interface node (software program) is installed in the CSL building's Automated Logic's BAS server. The PI interface node links Automated Logic's WebCtrl BAS interface via BACnet protocol (ASHRAE, 2014) to access all the data points. The PI interface node then transfers the collected data to a PI server (hardware) through internet at the time step defined by the researchers. The PI server is physically located at the Intelligent Workplace of CMU. The PI server manages all the data on the internet, so that users can access the data using PI client applications through internet in any location at any time.

The arrows in Figure 72 represent the possible directions of data flow. WebCtrl BAS can access all the data from different building systems but can only send commands to the HVAC system for control purposes. The OSIsoft PI system only reads data from the BAS system and stores them in the PI server. The data collection system does not interfere with the BAS's normal control operation.

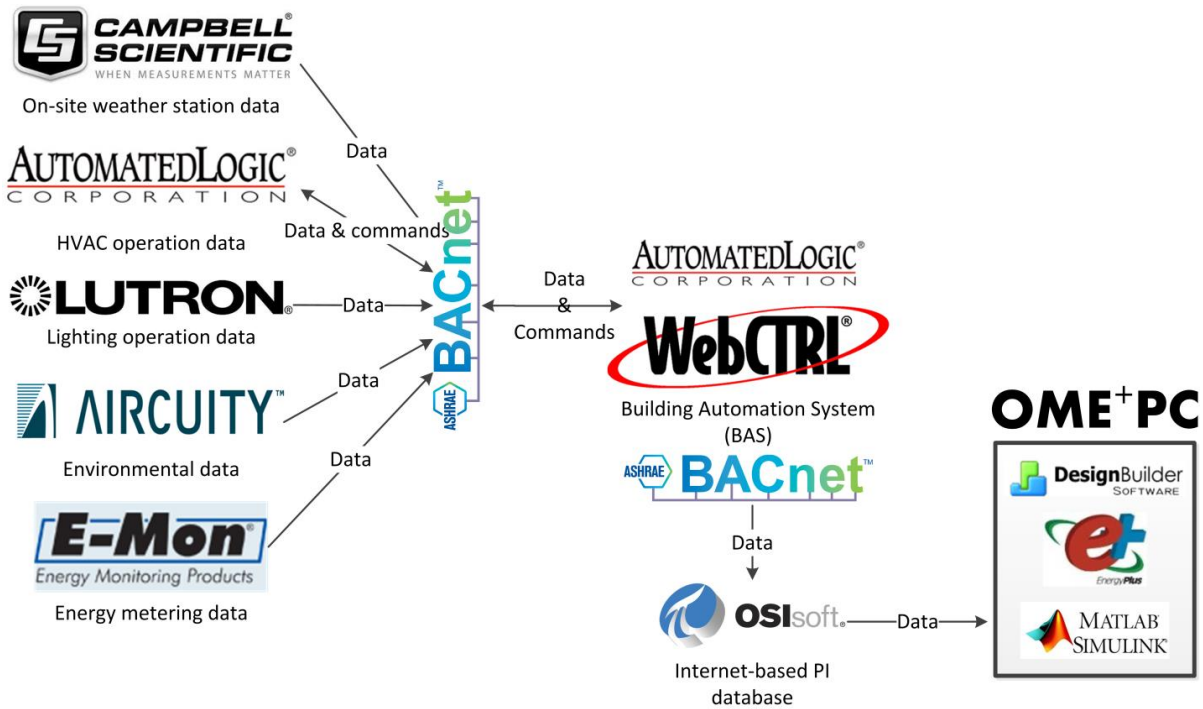


**Figure 72 PI system data collection system architecture for the CSL building.<sup>6,7</sup>**

#### ***4.5.3. Occupant subjective feedback and thermal environment data analysis***

In order to find useful patterns of occupant thermal preference, the subjective thermal comfort votes from the internet-based database and the objective thermal environment measurement data from the PI server are mapped based on spatial and temporal information. In the CSL case study, a total of 15 volunteers have participated and provided their subjective feedback on thermal comfort and clothing insulation information from October to December 2013. Among the 15 volunteers, only three occupants (20%) have more than 30 effective voted instances on both thermal comfort and clothing insulation concurrently, as shown in Figure 73. Eight (53%)

<sup>6</sup> The logo images in the figure are from the official websites of Campbell Scientific, Automated Logic, Lutron, Aircuity, E-Mon, BACnet, OSIsoft, DesignBuilder, EnergyPlus, and Matlab.

<sup>7</sup> Acknowledgements to Bertrand Lasternas, Mike Mihuc, Jason Wirick, and Craig Power for implementing the PI server in the CSL building.

occupants have less than 30 effective voted instances and four occupants (27%) have no effective voted instance over the experiment period. From the statistical point of view, three datasets with more than 30 effective voted instances are mapped with their corresponding thermal zone air temperature and relative humidity measured data, respectively.

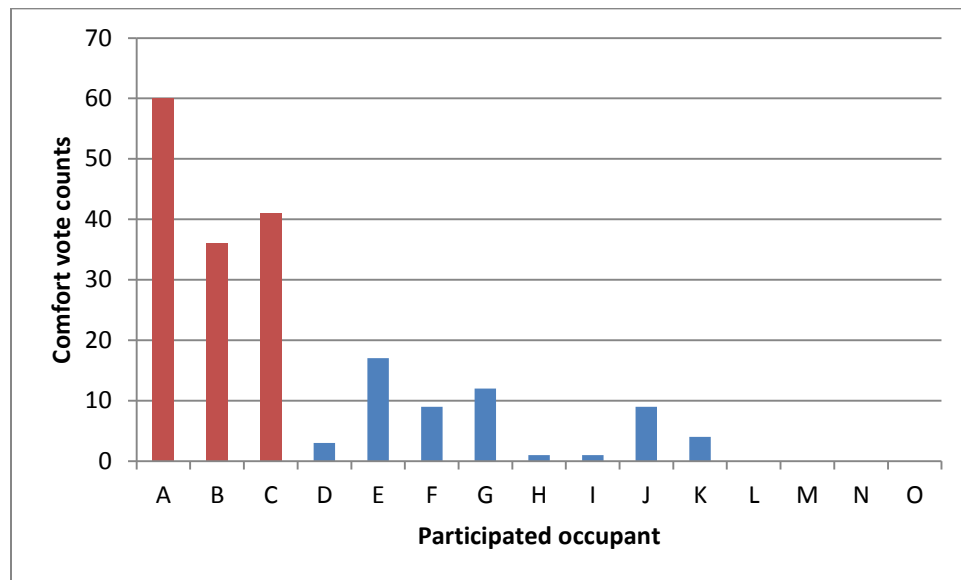


**Figure 73 Statistics of occupants’ effective voted instances during the experiment period.**

Figure 74 - Figure 76 illustrate Subject A’s marginal plots of air temperature, relative humidity, and clothing insulation (y-axis) versus the thermal comfort vote (x-axis), respectively. The histograms (N = 60) of the variables are shown on the top and right sides of the plot areas. In general, Subject A feels cold for the majority of votes regardless of actual air temperature (20 - 25 °C) and relative humidity (20 - 60%) measurements. One noticeable pattern is that all the “very cold” votes are the times when the air temperature drops below 21 °C. Figure 76 shows that most of the “feeling cold” votes are correlated with clothing insulation factor above 1.5, which suggests that although Subject A has adapted his/her clothes based on the thermal comfort feeling, he/she was still feeling cold during the study period.

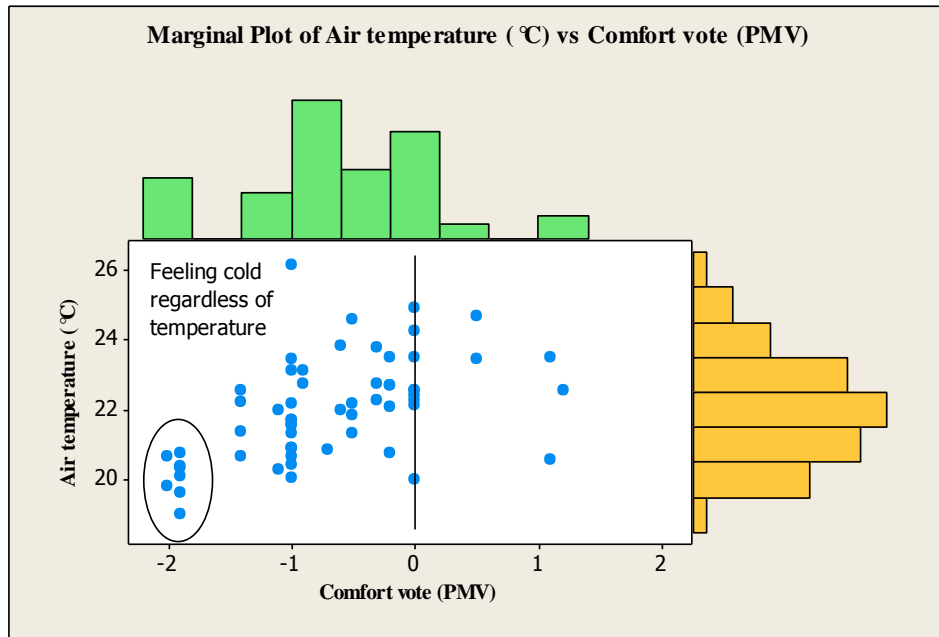


**Figure 74 Marginal plot of air temperature vs. comfort vote of Subject A.**

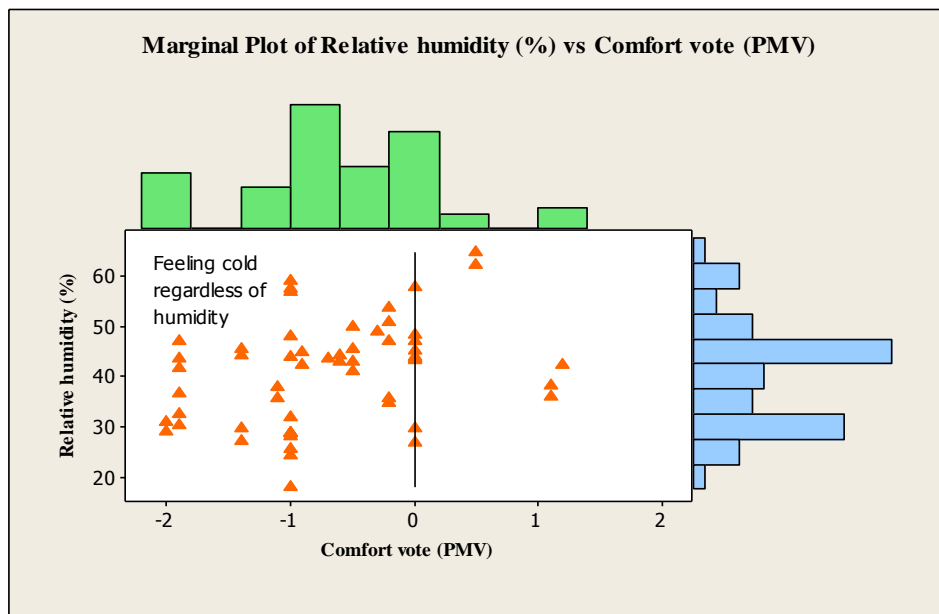


**Figure 75 Marginal plot of relative humidity vs. comfort vote of Subject A.**

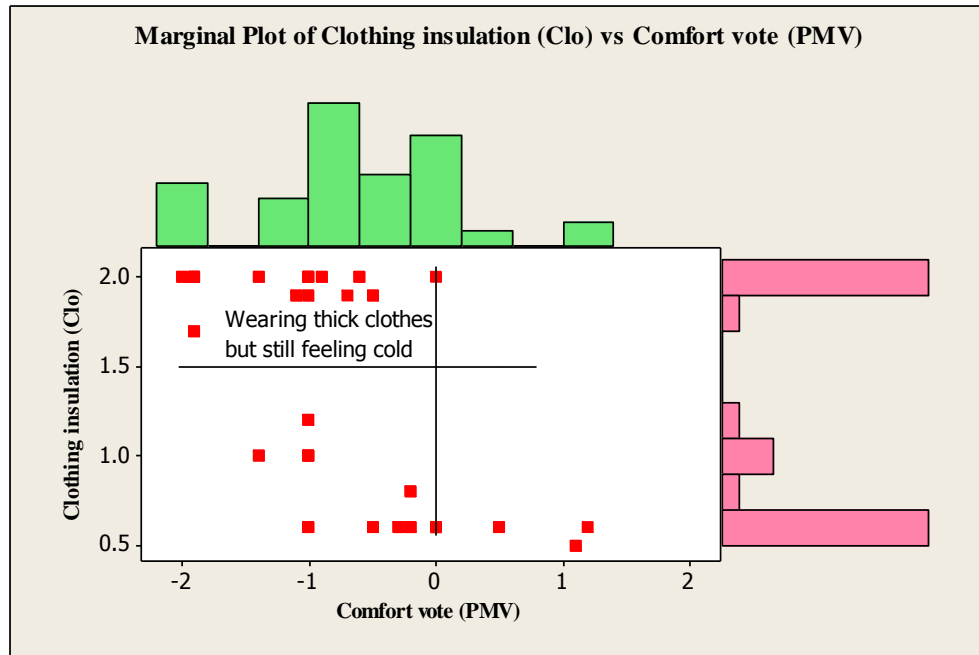


**Figure 76 Marginal plot of clothing insulation vs. comfort vote of Subject A.**

Figure 77 - Figure 79 show Subject B's marginal plots of air temperature, relative humidity, and clothing insulation (y-axis) versus the comfort vote (x-axis), respectively. The histograms (N = 36) of the variables are shown on the top and right sides of the plot areas. In general, Subject B feels cold for the majority of votes regardless of actual air temperature (20 - 25 °C) and relative humidity (20 - 60%) measurements. Figure 79 shows that almost all the "feeling cold" votes (except for one vote) are correlated with clothing insulation factor around 0.5, which suggests that Subject B has relatively thin clothes in the office compared to the typical business dress. Arguably, Subject B could have improved his/her thermal comfort level easily by adding a jacket or another layer of clothes. This result is very different from the data of Subject A, who has already had thick clothes but still feels cold.

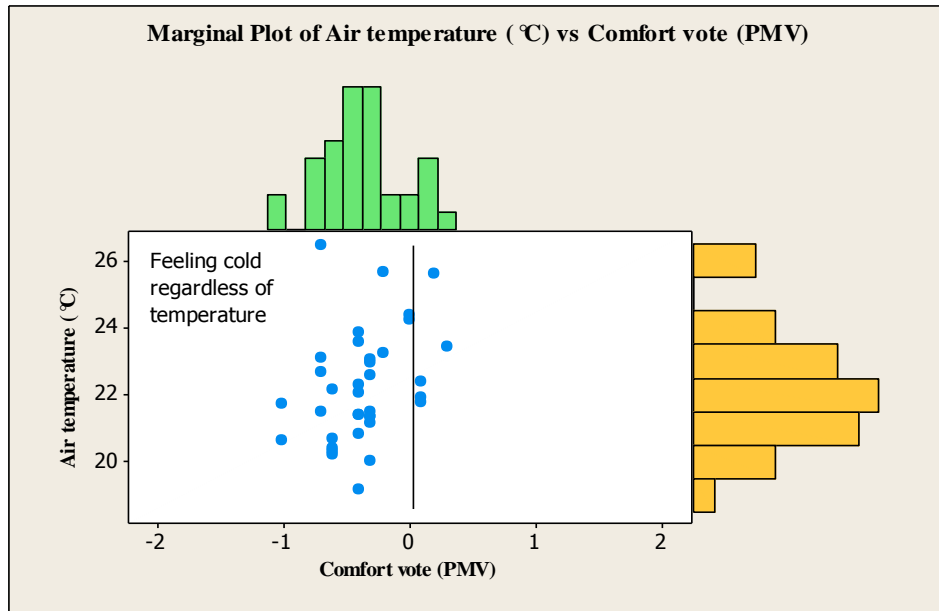


**Figure 77 Marginal plot of air temperature vs. comfort vote of Subject B.**

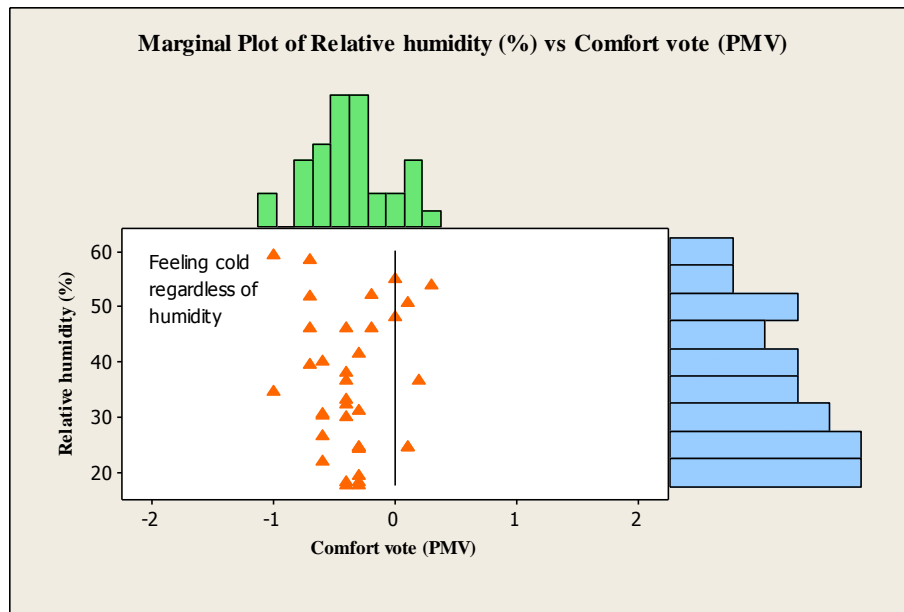


**Figure 78 Marginal plot of relative humidity vs. comfort vote of Subject B.**

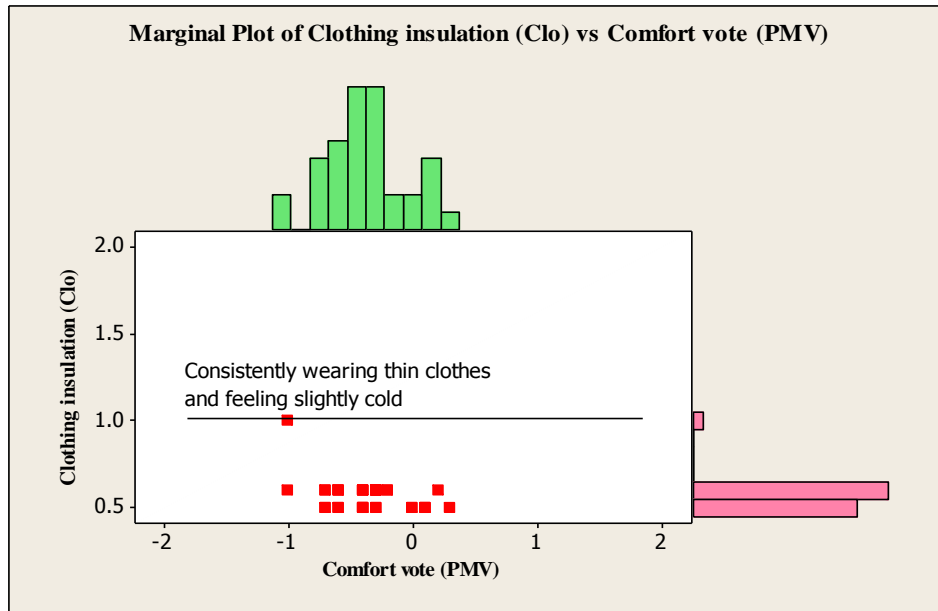


**Figure 79 Marginal plot of clothing insulation vs. comfort vote of Subject B.**

Figure 80 - Figure 82 show Subject C's marginal plots of air temperature, relative humidity, and clothing insulation (y-axis) versus the comfort vote (x-axis), respectively. The histograms (N = 41) of the variables are shown on the top and right sides of the plot areas. In general, Subject C feels warm, especially when the air temperature is above 22 °C and relative humidity is above 45%. Figure 79 shows the clothing insulation factor is mostly below 1.0, which suggests that Subject C has relatively thin clothes in the office compared to typical business dress, but the subject still feels warm in general. This is clearly different from the other two subjects' profiles.

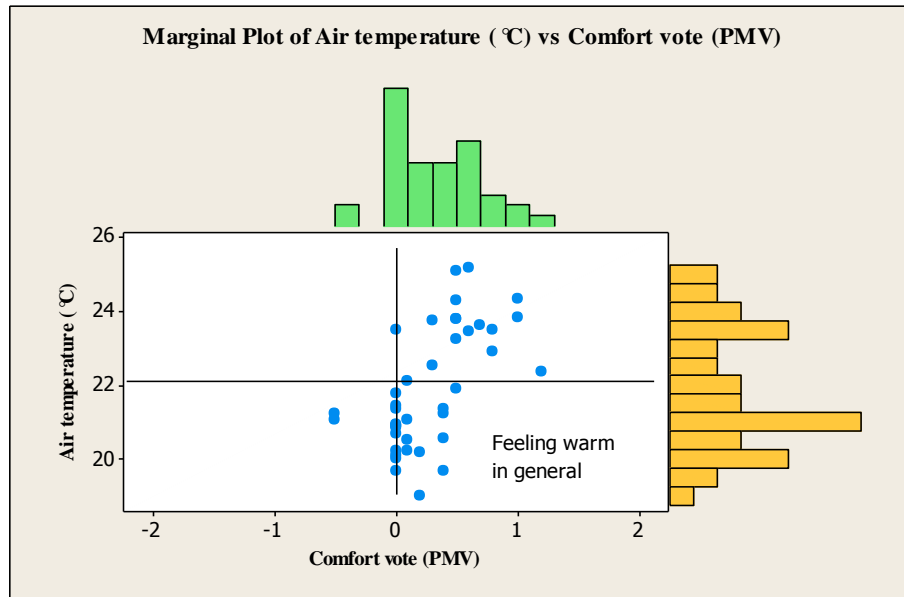


**Figure 80 Marginal plot of air temperature vs. comfort vote of Subject C.**

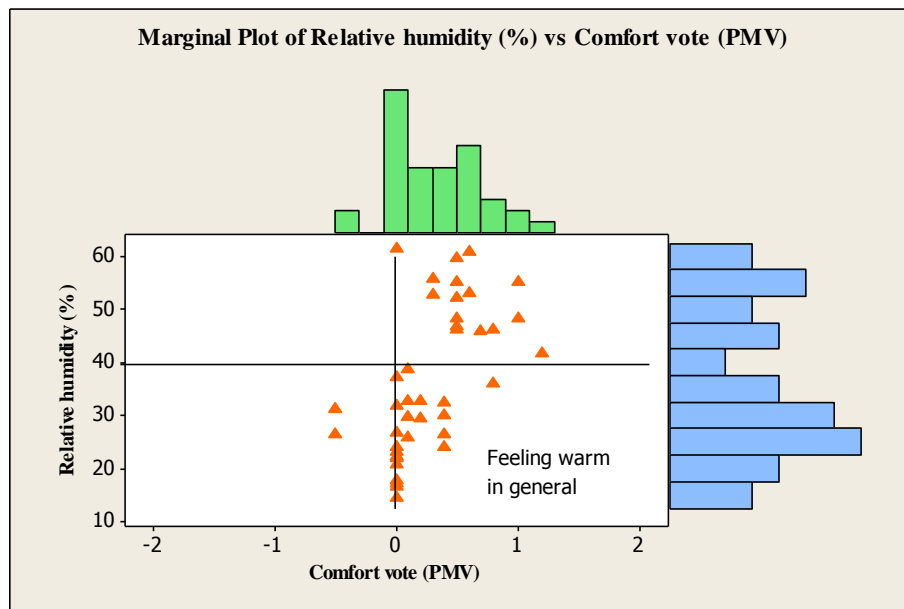


**Figure 81 Marginal plot of relative humidity vs. comfort vote of Subject C.**



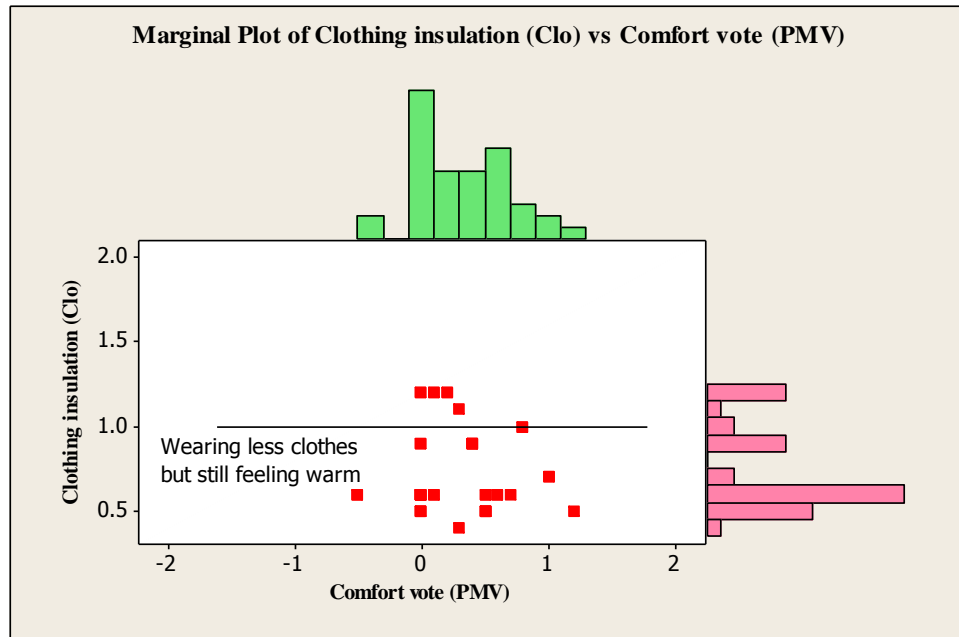


**Figure 82 Marginal plot of clothing insulation vs. comfort vote of Subject C.**

By comparing the three subjects' data and taking into consideration of the overall voting statistics, the following conclusions can be drawn. 11 out of 15 volunteers express their opinions on their thermal comforts when they do not feel comfortable, which indicates thermal comfort is something important for the test group to consider at workplaces. However, people have very different sensitivities and tolerances to thermal comfort. Three subjects voted over 30 times during the three months experiment periods, but most people voted less than 30 times. In addition, among the three subjects, the data shows very different comfort preferences and clothing choices. However, the thermal comfort preference and clothing choice of each individual are mostly consistent for the majority of time during the entire experiment period. Therefore, it is necessary to develop a control system that can accommodate individual occupant thermal comfort preference, and based on the individual preference, the control system could make consistent adjustment to meet individual needs.

#### 4.5.4. OME<sup>+</sup>PC design and implementation

The design of OME<sup>+</sup>PC aims to take in the real-time individual occupant subjective feedback information and 24-hour weather forecast data from the internet-based databases, and customize each zone setpoint based on this feedback information.

Figure 83 shows the implementation schema of OME<sup>+</sup>PC. Compared to the ME<sup>+</sup>PC schema, new modules are introduced and some modules are updated to achieve the objectives.

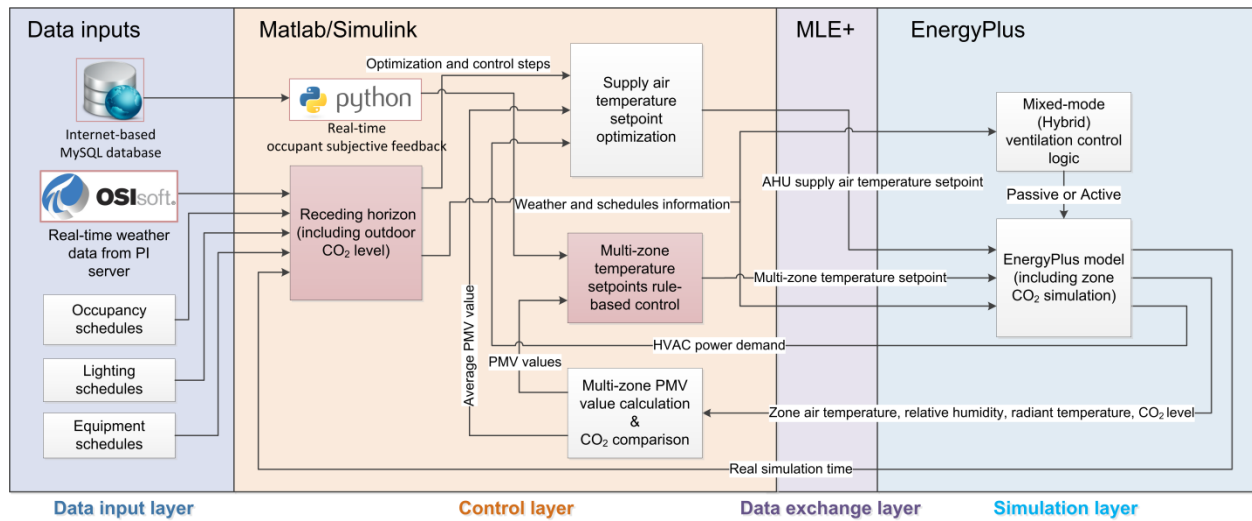


**Figure 83 OME<sup>+</sup>PC implementation schema.<sup>8</sup>**

First, in the “Data input layer”, an internet-based MySQL database, which stores the real-time occupant subjective feedback data, is connected to control system. Two Python scripts (getComfortAdjustmentValue.py and getCloAdjustmentValue.py) are written to query the latest thermal comfort and clothing insulation feedback data from the internet-based MySQL database, respectively. The Python scripts compare the date and time of the two pieces of feedback

<sup>8</sup> The logo images in the figure are from the official websites of OSIssoft and Python.org.

information to ensure they are collected at the same time (within the same hour). If the occupant somehow does not provide both data points at the same time, the Python script assumes the missing data as default value (PMV=0 and clo=1). A Matlab script (python.m) is written to execute the Python scripts in the Matlab/Simulink environment. In the “Control layer”, the “Multi-zone temperature setpoints rule-based control” module takes in the occupant subjective feedback information and computes the adjusted PMV setpoints for the zone that is occupied by the voter. This module enables occupants to adjust their own individual thermal comfort setpoints by easily voting on an internet-based dashboard in real time.

Second, the PI server is used to acquire real-time and forecasted weather data to replace the CSV-format static historic weather data. The data acquisition schema is shown in Figure 84. The weather forecast data, including temperature, relative humidity, wind speed, wind direction, and sky cover are forecasted using the Weather Underground’s BestForecast<sup>TM</sup> model, which has higher accuracy than the widely used National Weather Service’s National Digital Forecast Database (NDFD), according to (Weather-Underground, 2014a). A Python script (#1) is created to use the Weather Underground API (application programming interface) (Weather-Underground, 2014b) to automatically upload the forecasting data to the PI server using the PI Universal File Load (UFL) Interface (OSIsoft, 2014b).

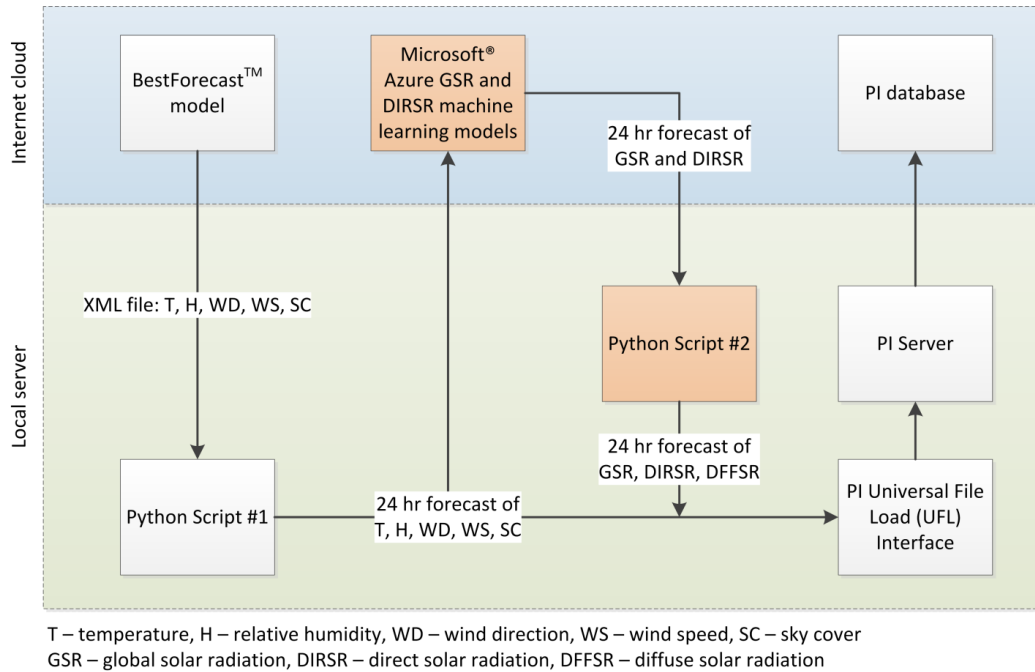


**Figure 84 Weather forecast data acquisition schema.<sup>9</sup>**

However, two pieces of weather data that are required by EnergyPlus simulation – direct solar radiation and diffuse solar radiation – are not directly forecasted by Weather Underground. Hourly global and direct solar radiation measured data are collected with the Hobo weather station (Onset, 2014) on the roof of Intelligent Workplace of CMU. Two machine learning models are created by using Microsoft® Azure cloud-based machine learning tool (Microsoft, 2014) to predict global and direct solar radiation, respectively. The Boosted Decision Tree Regression algorithm (Dietterich, 2000; Elith *et al.*, 2008) is used in the two models. The shared input parameters of the global and direct solar radiation prediction models are the 24-hour forecast data of month, day, hour, temperature, relative humidity, wind speed, wind direction,

<sup>9</sup> This is a collaborative work accomplished by Bertrand Lasternas, Yogi Venkata Gopalan and Jie Zhao at CMU. This dissertation contributes to the development of the orange-color modules.

and sky cover. Global solar radiation is also used as an input parameter for direct solar radiation prediction.

Table 23 and Figure 85 show the machine learning results of global and direct solar radiations. It is clear that the prediction accuracy of the global solar radiation is much better than that of the direct solar radiation. The most obvious reason is that direct solar radiation in nature has very high and sometimes random variations from time to time due to its sensitivity to cloud movement. The other possible reason is that there is less number of data instances in the direct solar radiation dataset than in the global solar radiation dataset, and theoretically it is more difficult to predict accurately with less data instances. A Python script (#2) is written to use the Azure API to push data to Azure and receive solar radiation prediction results from Azure.

**Table 23 Result comparison of the global and direct solar radiation machine learning models.**

	# of instances of the training model	# of parameters of the training model	Correlation coefficient of the training results	Relative absolute error of the training results
Global solar radiation	4379	8	0.99	7.00%
Direct solar radiation	2032	9	0.67	40.48%

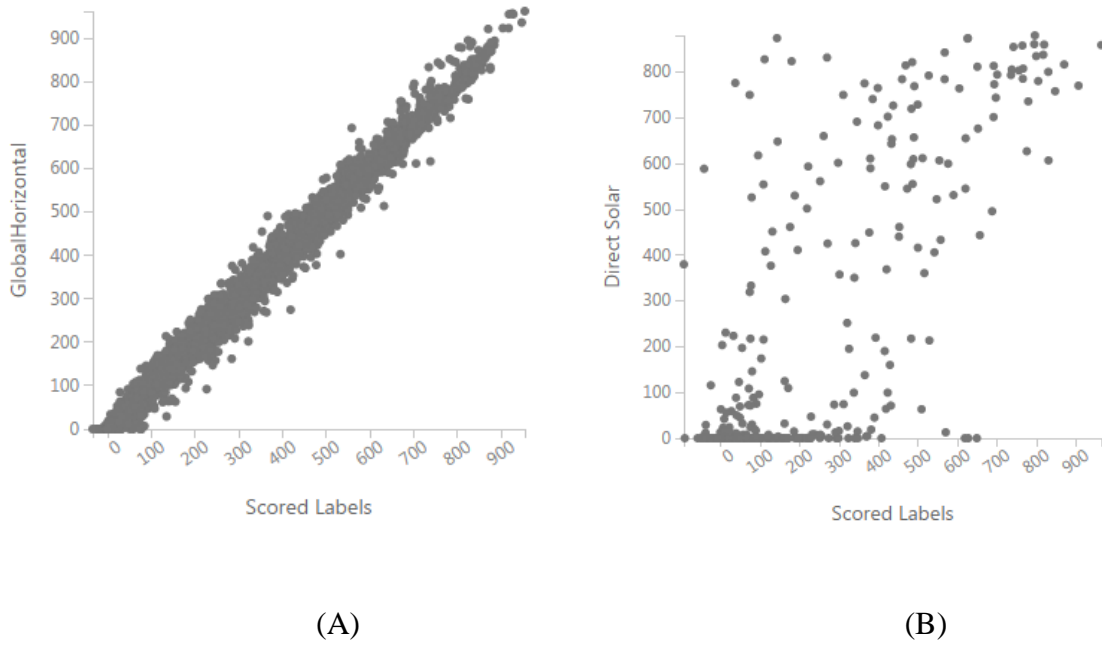


**Figure 85 Scatter plot of the measured data versus predicted value (A – global solar radiation, B – direct solar radiation).**

Hourly diffuse solar radiation is calculated from global solar radiation in Python script (#2) based on the following equations derived from (Erbs *et al.*, 1982; UO-SRML, 2012).

$$I_{dif} = \begin{cases} (1.0 - 0.09k_T) \times I, & \text{for } k_T \leq 0.22 \\ \left( \begin{array}{l} 0.9511 - 0.1604k_T \\ +4.388k_T^2 - 16.638k_T^3 \\ +12.336k_T^4 \end{array} \right) \times I, & \text{for } 0.22 < k_T \leq 0.80 \\ 0.165, & \text{for } k_T > 0.80 \end{cases} \quad (35)$$

$$k_T = \frac{I}{I_0} \quad (36)$$

$$I_0 = 1367 \times (R_{av}/R)^2 \quad (37)$$

$$\left( \frac{R_{av}}{R} \right)^2 = 1.00011 + 0.034221 \cos(\beta)$$

$$\begin{aligned}
&+0.001280 \sin(\beta) + 0.000719 \cos(2\beta) \\
&+0.000077\sin(2\beta)
\end{aligned} \tag{38}$$

$$\beta = 2\pi n/365 \tag{39}$$

where,

$I_{dif}$  is the hourly diffuse solar radiation incident on a horizontal surface ( $\text{W/m}^2$ );

$I$  is the hourly global solar radiation incident on a horizontal surface ( $\text{W/m}^2$ );

$k_T$  is the hourly clearness index;

$I_0$  is the hourly extraterrestrial solar radiation incident on a horizontal surface ( $\text{W/m}^2$ );

$R_{av}$  is the mean sun-earth distance (m);

$R$  is the actual sun-earth distance depending on the day of the year (m);

$\beta$  is the angle of the day of the year (radian);

$n$  is the number of the day of the year.

In total, eight pieces of 24-hour hourly weather forecast data are streamed to the internet cloud-based PI database at each hour: temperature, relative humidity, wind speed, wind direction, sky cover, global solar radiation, direct solar radiation, and diffuse solar radiation. As shown in the “Control layer” of Figure 83, the receding horizon function module takes in the real-time weather forecast data and match to the timestamp of the planning and execution horizons of the

control schema. In Matlab, PIOLEDB toolbox developed for connecting the PI server by (OSIsoft, 2014a), is used to read the weather forecast data in the PI database.

#### ***4.5.5. Result comparison between ME<sup>+</sup>PC and OME<sup>+</sup>PC***

OME<sup>+</sup>PC is simulated using the same occupancy, equipment, and lighting schedule inputs as the ones used in ME<sup>+</sup>PC. Although OME<sup>+</sup>PC is linked to the PI server database for the real-time weather forecast data, in order to do fair comparisons, the same weather information (October 1<sup>st</sup> to 7<sup>th</sup>, 2013) is used for the result simulation. The only different input between OME<sup>+</sup>PC and ME<sup>+</sup>PC is the occupant thermal comfort preference range. As shown in Table 24, ME<sup>+</sup>PC uses the default value (PMV = 0) for all the occupants in the six open office zones, while in OME<sup>+</sup>PC, the three occupant preferences are simulated in the three open office zones, respectively, based on the data analysis results in section “4.5.3. Occupant subjective feedback and thermal environment data analysis”. The default value is implemented in the other three zones.

**Table 24 Thermal comfort and clothing insulation preferences in OME<sup>+</sup>PC.**

	Thermal comfort preference range in occupied hours (PMV)	Clothing insulation preference (Clo)
Default value	(-0.5, 0.5)	1.00
Occupant A	(0.19, 1.19)	1.25
Occupant B	(-0.14, 0.86)	0.57
Occupant C	(-0.78, 0.22)	0.74

Figure 86 shows the simulation result comparison of the PMV values of different zones in OME<sup>+</sup>PC. It is clear that the default PMV performance obeys the original (-0.5, 0.5) range in occupied hours, but the three adjusted thermal zone PMV values are shifted either up or down to meet the individual comfort preference. Therefore, this result demonstrates that OME<sup>+</sup>PC is



capable of providing individualized thermal environment based on occupants' comfort preferences.

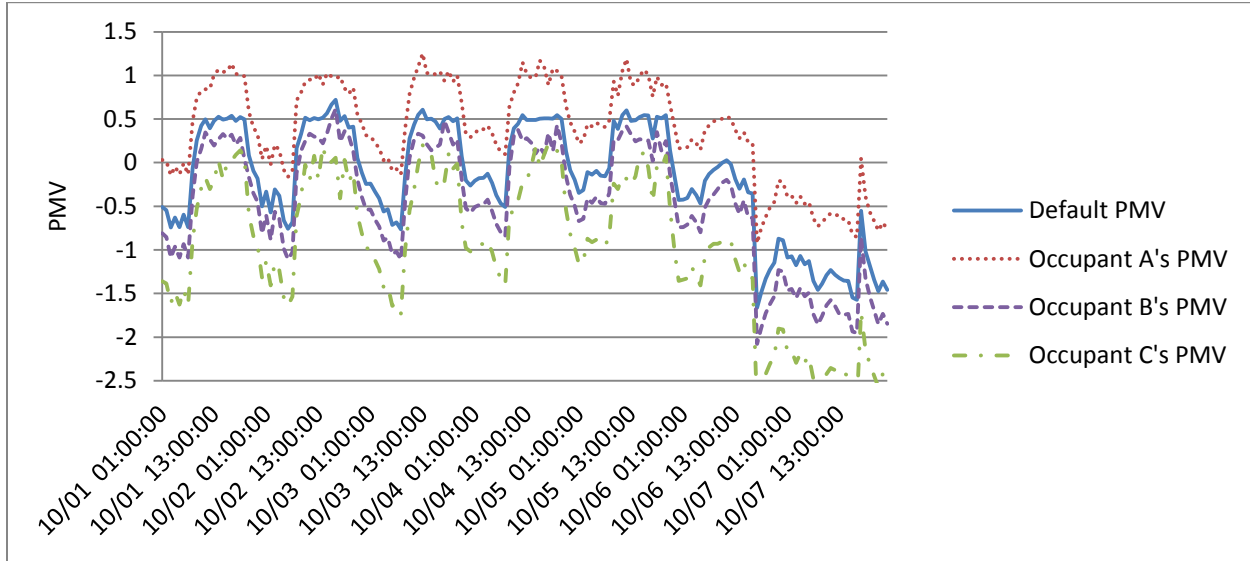


**Figure 86 Thermal comfort performance of different zones in OME<sup>+</sup>PC in the swing season.**

In order to further investigate the energy implications of allowing occupants to choose their own thermal comfort preferences, the OME<sup>+</sup>PC's AHU supply air temperature, flow rate, and power consumption data are compared with ME<sup>+</sup>PC's. As shown in Figure 87, OME<sup>+</sup>PC has generally higher supply air temperature and lower mass flow rate during occupied daytime for cooling. In addition, OME<sup>+</sup>PC has fewer occupied cooling hours during the first four weekdays. In accordance with the performance of control variables, the power consumption of OME<sup>+</sup>PC is lower than ME<sup>+</sup>PC, as illustrated in Figure 88. During the one week simulation period in the swing season, OME<sup>+</sup>PC has a 37.37% energy reduction compared to ME<sup>+</sup>PC.

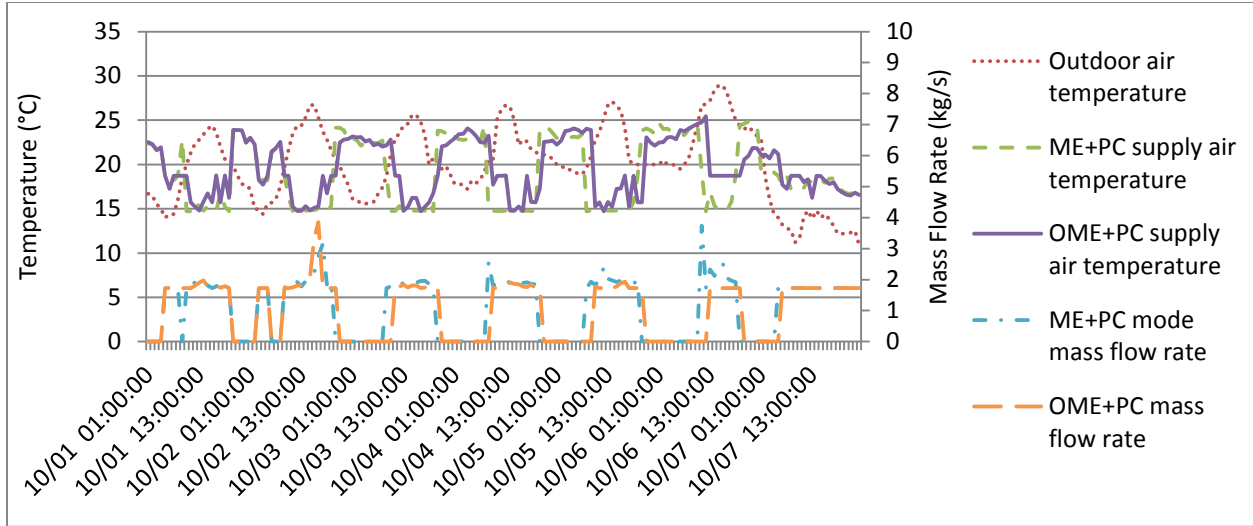


**Figure 87 Outdoor temperature and control variables of ME<sup>+</sup>PC and OME<sup>+</sup>PC in the swing season.**

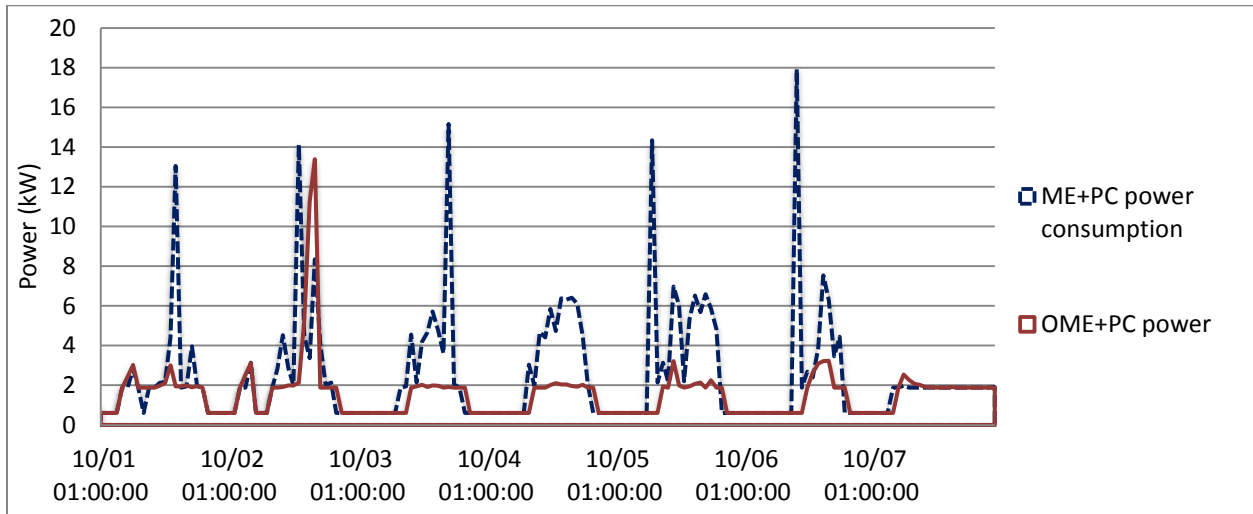


**Figure 88 One week plot of the power consumptions of ME<sup>+</sup>PC and OME<sup>+</sup>PC in the swing season.**

However, the energy reduction is mainly caused by the “warmer” thermal preference of Subject A and B, so the setpoints of zone temperatures are higher than the default value. The occupant preference can vary significantly based on season, location, physical and psychological changes. For instance, even with the same group of occupants given the same setting of OME<sup>+</sup>PC, the

energy consumption could be increased during heating seasons, since the occupants demand warmer environment than the default mode. Therefore, the conclusion of OME<sup>+</sup>PC simulation study is that introducing the individual occupant thermal comfort preference in the control system can have significant energy impact while providing customized thermal environment to individuals. More in-depth investigation could be conducted in the future.

## **4.6. Summary**

This chapter describes the development and simulation results of four model-based control schemes: the baseline, E<sup>+</sup>PC, ME<sup>+</sup>PC, and OME<sup>+</sup>PC. Figure 89 shows the development processes, methods, and outcomes of the four control schemes. The first set of outcomes is that a co-simulation platform is created for EnergyPlus and Matlab/Simulink via MLE+. The co-simulation platform is tested numerous times during the development process and it can be systematically updated with minimum effort. The second set of outcomes is that during the simulation periods (heating, cooling, and swing seasons), E<sup>+</sup>PC, ME<sup>+</sup>PC, and OME<sup>+</sup>PC can all reduce HVAC energy consumptions and maintain occupant thermal comfort with the model-based predictive control algorithm. The third set of outcomes is that using the mixed-mode active/passive control algorithm, more energy savings can be achieved and the occupant thermal comfort can be maintained. Last but not least, the final outcome of implementing the real-time thermal comfort feedback system, OME<sup>+</sup>PC can provide individualized thermal environment for occupants and can also influence the HVAC energy consumption. Given the Pittsburgh weather

context and the current operation assumptions, implementing OME<sup>+</sup>PC in the test-bed building is expected to save HVAC energy consumption by 29.37% on an annual basis.<sup>10</sup>

During the development process, there are other interesting findings. First, in current industry practice, integrating all types of building systems and performing real-time BAS data collection and control is complicated and may be costly. It took a lot of effort for the test-bed building project team to integrate all the systems into the BAS. Even if the systems are integrated, it may not always be convenient for building operators to retrieve and compare various types of data across systems. To solve these problems, the research team installed a PI system in the test-bed building, which provides a uniform and consistent platform for different stakeholders to better utilize the building environmental, system operation, energy/water consumption, and other pertinent data.

Second, during the development process of ME<sup>+</sup>PC, the author has found that using the simple rule-based passive cooling control algorithm (i.e. opening window and shutting down the mechanical system when the outdoor and indoor conditions meet the predefined criteria) can save 33.84% of the HVAC energy consumption during the swing season based on the simulation results. This finding emphasizes the importance and effectiveness of using mixed-mode HVAC systems to save energy for office buildings in swing seasons.

Third, the data analysis of occupant thermal comfort feedback experiment suggests that thermal comfort as an important factor that occupants are aware of in their workplaces. Beyond this

---

<sup>10</sup>

<sup>1</sup>Annual HVAC energy saving = baseline energy – (one week heating \* 22 weeks + one week cooling \* 13 weeks + one week swing \* 17 weeks).

awareness, it is evident that individuals in the test group have very different sensitivities and tolerances to thermal comfort, and among the most sensitive individuals, there are different comfort preferences and clothing choices. However, for each individual, thermal comfort preference and clothing choice remain consistent for the majority of time during the experiment period. These findings strongly support the need for providing individualized thermal comfort control systems for office workers.

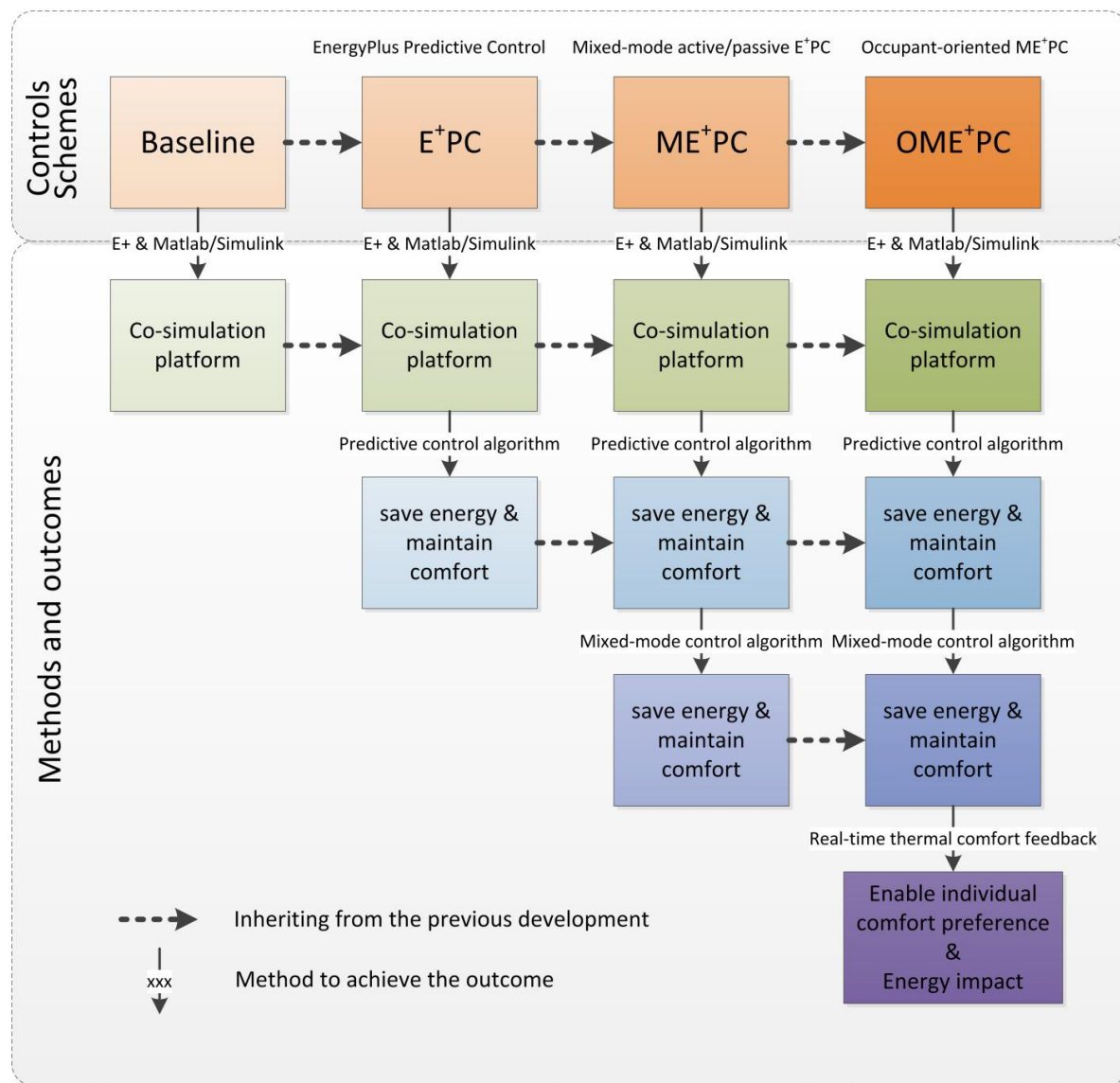


**Figure 89** Different control schemes, as well as their methods and outcomes.

# Chapter 5. Conclusions

---

## 5.1. Summary of findings

First, this dissertation has demonstrated a modeling method in which BEM models are used to assist building design decision making process at the design stage. Then at the commissioning and early operation stages, an empirical BEM model calibration method has been tested to calibrate the design stage BEM model. Finally, a real-time occupant-oriented mixed-mode EnergyPlus predictive control system has been developed and simulated at the operation stage.

The dissertation has presented several simulation and experimental studies using the test-bed office building. The findings of these studies are summarized into two categories. The first part is the hypothesis testing results that are the primary objectives of this dissertation. The other category consists of the research findings that do not directly contribute to the hypotheses, but are equally important to present to the audience in the building science research realm and could benefit future studies.

### 5.1.1. *Hypothesis testing results*

- Hypothesis 1: The design-stage BEM can be extended to the entire building life-cycle for a better building energy and thermal comfort performance.
- Hypothesis 2: An EnergyPlus BEM model can be calibrated using a systematic and scientific method with empirical data.

- Hypothesis 3: Model-based predictive control using EnergyPlus BEM model can reduce energy consumption and maintain occupant thermal comfort compared to conventional control algorithms.
- Hypothesis 4: Individual occupant comfort requirements can be met by engaging occupants for their comfort feedback through an online dashboard.

The four hypotheses have been tested with the studies following the concept of DBO-EIM infrastructure throughout the different stages of the test-bed building.

Chapter 2 presented the concept of DBO-EIM infrastructure and demonstrated the method of using BEM process for design decision making with the test-bed building. By using this method, the case study results have shown that the proposed design case building model has better energy performance than the baseline, design alternatives, and various benchmark buildings.

Chapter 3 demonstrated an EnergyPlus model calibration method with occupancy schedule data mining and empirical data using the design-stage BEM model. The final calibrated model has a mean biased error of 1.27% and a coefficient of variation of the root mean squared error of 6.01%. In light of the results, the model can be considered well calibrated. This overall calibration method provides a scientific and systematic framework to conduct high accuracy EnergyPlus model calibration.

Chapter 4 presented the development process and simulation results of the occupant-oriented mixed-mode EnergyPlus predictive control (OME<sup>+</sup>PC) system on the basis of the calibrated BEM model. Given the Pittsburgh weather context and the current operation assumptions, the simulation results of OME<sup>+</sup>PC have suggested a 29.37% reduction in annual HVAC energy consumption and enabled the individual thermal comfort-based control for the building

occupants. OME<sup>+</sup>PC can also link real-time weather forecast data through an internet-based database, which enables future studies to test the control system in actual building operations.

In summary, the entire dissertation has demonstrated that the original design stage EnergyPlus model can be updated and utilized through the entire DBO-EIM process. Compared to typical building operation, implementing this process can achieve better energy and thermal comfort performance.

### ***5.1.2. Other research findings***

During the process of developing and testing the Design-build-operate Energy Information Modeling (DBO-EIM) infrastructure, the author has discovered several research findings that do not directly contribute to the hypothesis testing results, but are equally important to present to the general audience in the building science research field for future studies.

First, using data mining algorithms, the dissertation has developed a practical occupant behavior and schedule modeling method. This method constitutes a critical step in performing BEM model calibration, which has been tested in two office buildings. The results have shown that the average percentage of correctly classified individual behavior instances for the two case studies is above 90%. Similarly, the correlation coefficient of the predicted group schedules versus the ground truth schedules is above 0.90. The modeling method is robust and the accuracy is adequate. In addition, the experiment results have shown diversified behaviors in using office appliances on the individual level yet a fairly consistent schedule as a group. The findings directly support the following two suggestions, (1) it is important to develop a system that could persuade occupants to change their appliance use behavior thereby reducing energy consumption.



(2) It is necessary and effective to learn the “real” group schedule during operation to better control the HVAC system and reduce its energy consumption.

Second, during the development process of OME<sup>+</sup>PC, the author has discovered that, in current industry practice, integrating all types of building systems and performing real-time BAS data collection and control is a complicated process. It took a lot of effort for the test-bed building project team to integrate all the systems into the building automation system (BAS). Even if the systems are integrated, it may not always be convenient for building operators to retrieve and compare various types of data across systems. To solve these problems, the research team has installed a PI system in the test-bed building, which provides a uniform and consistent platform for different stakeholders to better utilize the building environmental, system operation, energy/water consumption, and other pertinent data.

Third, during the development process of ME<sup>+</sup>PC, the author has found that simple rule-based passive cooling control (i.e. opening window and shutting down the mechanical system when the outdoor and indoor conditions meet the predefined criteria) can save 33.84% of the HVAC energy consumption during the swing season based on the simulation results. This finding emphasizes the importance and effectiveness of using mixed-mode HVAC systems to save energy for office buildings in swing seasons.

Last but not least, the data analysis of the occupant thermal comfort feedback experiment suggests that thermal comfort as an important factor that occupants are aware of in their workplaces. Beyond this awareness, it is evident that individuals in the test group have very different sensitivities and tolerances to thermal comfort, and among the most sensitive individuals, there are different comfort preferences and clothing choices. However, for each

individual, thermal comfort preference and clothing choice remain consistent for the majority of time during the experiment period. These findings strongly support the need for providing an individualized thermal comfort control system to office workers.

## **5.2. Contributions**

The completed Design-build-operate Energy Information Modeling (DBO-EIM) infrastructure is the most important contribution of this dissertation to the building science research field and potentially to the building industry. The dissertation has demonstrated this infrastructure with the test-bed office building over the design, commissioning and operation periods, and presented all the research findings. The test-bed building provides numerous real-time data and experiment opportunities for this dissertation. However, the building is a special case, in that it is a net-zero energy building with very advanced “deep green” building design concepts and technologies as such. Many of design solutions and operation technologies are not common among “typical” office buildings. Therefore, a question may be raised, “can the DBO-EIM infrastructure be used in normal office buildings to improve their energy efficiency and occupant thermal comfort?”

In order to answer this question, the DBO-EIM infrastructure should be generalized so that it can be used for future studies and potential industry applications in a wider range of office buildings. Hence, in the Appendices, the author has demonstrated how to implement the entire DBO-EIM infrastructure in a generic DOE prototype medium office building EnergyPlus model under the Pittsburgh climate (DOE, 2014a), where the step-by-step development process and the computation time of the critical steps are presented as references for future studies and potential applications.

### 5.3. Future work

This dissertation has presented the concept of Design-build-operate Energy Information Modeling (DBO-EIM) infrastructure and demonstrated it with a real office building. The results of these studies have shown the feasibility and effectiveness of the infrastructure. However, in future, this infrastructure could be improved in several aspects to further streamline the entire process and make it more applicable to both researchers and practitioners.

First, the EnergyPlus model calibration method could be further automated and adapted with advanced information technology. The current method has several automated procedures, but involves several manual steps, such as lighting energy consumption calibration with daylight-responsive controls. Future studies could use data mining technologies to integrate these steps into the overall calibration method. In addition, with the real-time building automation system (BAS) data provided by the internet-based PI system, the model can be calibrated more often and even in real time, so that the model can evolve and adapt to any changes automatically and always reflect the latest status of the building operation. Advanced adaptive control theories could play a significant role in the process.

Second, various MPC optimization algorithms could be implemented based on the choices of building systems to demonstrate the feasibility of the DBO-EIM infrastructure. For instance, if a multi-zone variable air volume (MZVAV) system is used in the building, the control variables of both AHU and multiple terminal reheat boxes should be considered for optimization. Therefore, future researchers could consider using the distributed MPC algorithm for the MZVAV system.

The third aspect of future work could focus on developing optimized control algorithms for the mixed-mode cooling system. In this dissertation, a rule-based passive cooling control algorithm is implemented together with the active MPC system control algorithm. The control system worked well in terms of saving energy and maintaining occupant thermal comfort in general, but there are times when thermal comfort is compromised and there are other times when the active system has to push its operation to extremes in order to meet the setpoint. In future, researchers could first focus on improving the passive cooling control algorithm with physical experiments or simulations to identify a proper algorithm for a specific building in a specific location. Then based on the optimized passive algorithm, further improvement of the mixed-mode control algorithm can be made.

Furthermore, future studies could focus on continuing the occupant subjective thermal feedback study with a larger sample size under different seasons and locations. The study in this dissertation has already found very interesting patterns, despite the small sample size (15 people) and the experiment duration is relatively short (three months). One could imagine that if future studies could incorporate more individuals under different seasons and locations, the findings would be very valuable for understanding occupant thermal comfort and behavior in general, and for developing more appropriate occupant-oriented control systems.

# References

---

- Aerts, D., Minnen, J., Glorieux, I., Wouters, I., and Descamps, F. (2014). A method for the identification and modelling of realistic domestic occupancy sequences for building energy demand simulations and peer comparison. *Building and Environment*, 75, 67-78.
- Aircuity. (2013). Aircuity. 2013, from <http://www.aircuity.com/>
- Al-Homoud, M. S. (2001). Computer-aided building energy analysis techniques. *Building and Environment*, 36(4), 421-433.
- ASHRAE. (2002). ASHRAE Guideline 14-2002, Measurement of Energy and Demand Savings: ASHRAE.
- ASHRAE. (2009). *2009 ASHRAE Handbook: Fundamentals*: American Society of Heating, Refrigerating & Air Conditioning Engineers, Incorporated.
- ASHRAE. (2010). 62.1-2010 Ventilation And Indoor Air Quality. Atlanta, GA: ASHRAE.
- ASHRAE. (2014). BACnet - A Data Communication Protocol for Building Automation and Control Networks. Retrieved September 24, 2014, from <http://www.bacnet.org/index.html>
- Atkeson, C. G., Moore, A. W., and Schaal, S. (1999). Locally weighted learning *Artificial Intelligence Review*.
- AutomatedLogic. (2012). AutomatedLogic System Architecture. Retrieved September 24, 2014, from <http://www.automatedlogic.com/system-architecture/>
- Bauereiss, S. (2013). *Indoor positioning of mobile devices using ultrasonic positioning and the blackboard architectural pattern*. (Master), Technische Universität München.
- Bentley. (2013a). AECOsim Compliance Manager. from <http://www.bentley.com/en-US/Promo/AECOsim/aecosim+compliance+manager.htm>
- Bentley. (2013b). AECOsim Energy Simulator. from <http://www.bentley.com/en-US/Promo/AECOsim/aecosim+energy+simulator.htm>
- Bernal, W., Behl, M., Nghiem, T., and Mangharam, R. (2012). *MLE+: A Tool for Integrated Design and Deployment of Energy Efficient Building Controls*. Paper presented at the 4th ACM Workshop On Embedded Sensing Systems For Energy-Efficiency In Buildings, (BuildSys '12), Toronto.
- Bonte, M., Thellier, F., and Lartigue, B. (2014). Impact of occupant's actions on energy building performance and thermal sensation. *Energy and Buildings*, 76(0), 219-227.

- Boser, B. E., Guyon, I. M., and Vapnik, V. N. (1992). *A training algorithm for optimal margin classifiers*. Paper presented at the Proceedings of the fifth annual workshop on Computational learning theory, Pittsburgh, Pennsylvania, USA.
- Braun, J. E. (1990). Reducing energy costs and peak electrical demand through optimal control of building thermal storage. *ASHRAE transactions*, 96(2), 876-888.
- Buck, J. T., Ha, S., Lee, E. A., and Messerschmitt, D. G. (1994). Ptolemy: A framework for simulating and prototyping heterogeneous systems.
- Buhl, F. (2007). Energy Performance of Underfloor Air Distribution Systems. Berkeley, CA: California Energy Commission.
- Campbell. (2014). Measurement & Control Products for Long-term Monitoring. Retrieved September 24, 2014, from <http://www.campbellsci.com/>
- Candau, Y., and Piar, G. (1993). An application of spectral decomposition to model validation in the thermal analysis of buildings. *International Journal of Heat and Mass Transfer*, 36(3), 645-650.
- Carletta, J. (1996). Assessing agreement on classification tasks: the kappa statistic. *Computational linguistics*, 22(2), 249-254.
- Carrico, A. R., and Riemer, M. (2011). Motivating energy conservation in the workplace: An evaluation of the use of group-level feedback and peer education. *Journal of Environmental Psychology*, 31(1), 1-13.
- Castilla, M., Alvarez, J. D., Berenguel, M., Rodriguez, F., Guzman, J. L., and Perez, M. (2011). A comparison of thermal comfort predictive control strategies. *Energy and Buildings*, 43, 2737-2746.
- Choi, J. H. (2010). CoBi: Bio-Sensing Building Mechanical System Controls for Sustainably Enhancing Individual Thermal Comfort (PhD Dissertation). Pittsburgh: Carnegie Mellon University.
- Clarke, J. A., Cockroft, J., Conner, S., Hand, J. W., Kelly, N. J., Moore, R., . . . Strachan, P. (2002). Simulation-assisted control in building energy management systems. *Energy and Buildings*, 34, 933-940.
- Cleveland, W. S. (1979). Robust Locally Weighted Regression and Smoothing Scatterplots. *Journal of the American Statistical Association*, 74(368), 829-836.
- Coffey, B., Haghighat, F., Morofsky, E., and Kutrowski, E. (2010). A software framework for model predictive control with GenOpt. *Energy and Buildings*, 42, 1084-1092.
- Cohn, D. A., Ghahramani, Z., and Jordan, M. I. (1996). Locally Weighted Regression. Retrieved April 16, 2014, from <http://www.cs.cmu.edu/afs/cs/project/jair/pub/volume4/cohn96a-html/statmodels.html>
- Corbin, C. D., Henze, G. P., and May-Ostendorp, P. (2012). A model predictive control optimization environment for real-time commercial building application. *Journal of Building Performance Simulation*, 6(3), 159-174.
- Cortes, C., and Vapnik, V. (1995). Support-Vector Networks. *Mach. Learn.*, 20(3), 273-297.

- Crawley, D. B., Lawrie, L. K., Winkelmann, F. C., Buhl, W. F., Huang, Y. J., Pedersen, C. O., . . . Glazer, J. (2001). EnergyPlus: creating a new-generation building energy simulation program. *Energy and Buildings*, 319-331.
- Daum, D., Haldi, F., and Morel, N. (2011). A personalized measure of thermal comfort for building controls. *Building and Environment*, 46, 3-11.
- DesignBuilder. (2012). DesignBuilder. *DesignBuilder*. from <http://www.designbuilder.co.uk/>
- Dietterich, T. G. (2000). An experimental comparison of three methods for constructing ensembles of decision trees: Bagging, boosting, and randomization. *Machine learning*, 40(2), 139-157.
- DOE. (2008). Federal Energy Management Program's M&V Guidelines: Measurement and Verification for Federal Energy Projects, Version 3.0.
- DOE. (2010). The Encyclopedic Reference to EnergyPlus Input and Output.
- DOE. (2012, May 25). About EnergyPlus. Retrieved April 27, 2014, from [http://apps1.eere.energy.gov/buildings/energyplus/energyplus\\_about.cfm](http://apps1.eere.energy.gov/buildings/energyplus/energyplus_about.cfm)
- DOE. (2013a). External Interface(s) Application Guide - Guide for using EnergyPlus with External Interface(s) (pp. 25).
- DOE. (2013b). Tips & Tricks for Using EnergyPlus (pp. 58).
- DOE. (2014a, April 17, 2014). Commercial Prototype Building Models. Retrieved April 18, 2014, from [https://www.energycodes.gov/development/commercial/90.1\\_models](https://www.energycodes.gov/development/commercial/90.1_models)
- DOE. (2014b). Commercial Reference Buildings. Retrieved April 14, 2014, from <http://energy.gov/eere/buildings/commercial-reference-buildings>
- DOE. (2014c). Simergy. Retrieved December 1, 2014, from <http://simergy.lbl.gov/index.html>
- Dong, B. (2010). *Integrated Building Heating, Cooling and Ventilation Control (PhD Dissertation)*. Carnegie Mellon University, Pittsburgh.
- Dong, B., Chen, C., and Lee, S. E. (2005). Applying support vector machines to predict building energy consumption in the tropics. *Energy and Buildings*, 37(5), 545-553.
- Dong, B., and Lam, K. P. (2011). Building energy and comfort management through occupant behaviour pattern detection based on a large-scale environmental sensor network. *Journal of Building Performance Simulation*, 4(4), 359-369.
- Drucker, H., Burges, C. J., Kaufman, L., Smola, A., and Vapnik, V. (1997). Support vector regression machines. *Advances in neural information processing systems*, 9, 155-161.
- Duarte, C., Van Den Wymelenberg, K., and Rieger, C. (2013). Revealing occupancy patterns in an office building through the use of occupancy sensor data. *Energy and Buildings*, 67, 587-595.
- E-Mon. (2010). Energy Monitoring Products. Retrieved September 24, 2014, from <http://www.emon.com/commercial.html>
- EIA. (2012). Commercial Buildings Energy Consumption Survey (CBECS) *U.S. Energy Information Administration (USEIA)*.

- Elith, J., Leathwick, J. R., and Hastie, T. (2008). A working guide to boosted regression trees. *Journal of Animal Ecology*, 77(4), 802-813.
- Erbs, D., Klein, S., and Duffie, J. (1982). Estimation of the diffuse radiation fraction for hourly, daily and monthly-average global radiation. *Solar energy*, 28(4), 293-302.
- Esen, H., Inalli, M., Sengur, A., and Esen, M. (2008). Modeling a ground-coupled heat pump system by a support vector machine. *Renewable Energy*, 33(8), 1814-1823.
- ESP-r. (2000). ESP-r Overview. from <http://www.esru.strath.ac.uk/Programs/ESP-r.htm>
- EVO. (2003). International Performance Measurement & Verification Protocol (IPMVP) Volume III: Concepts and Options for Determining Energy Savings in New Construction.
- Fitbit. (2013a). Fitbit Flex. Retrieved April 27, 2014, from <https://www.fitbit.com/flex/specs>
- Fitbit. (2013b). Fitbit Zip. *Fitbit*. Retrieved April 27, 2014, from <http://www.fitbit.com/zip/specs>
- Frank, E., Hall, M., and Pfahringer, B. (2002). *Locally weighted naive bayes*. Paper presented at the Proceedings of the Nineteenth conference on Uncertainty in Artificial Intelligence.
- Frankel, M., and Turner, C. (2008). *How Accurate is Energy Modeling in the Market?* Paper presented at the ACEEE Summer Study on Energy Efficiency in Buildings, Pacific Grove.
- Freire, R. Z., Oliveira, G. H. C., and Mendes, N. (2008). Predictive controllers for thermal comfort optimization and energy savings. *Energy and Buildings*, 1353-1365.
- Garcia, C. E., Prett, D. M., and Morari, M. (1989). Model Predictive Control: Theory and Practice - a Survey. *International Federation of Automatic Control*, 25(3), 335-348.
- Glicksman, L. R., and Taub, S. (1997). Thermal and behavioral modeling of occupant-controlled heating, ventilating and air conditioning systems. *Energy and Buildings*, 25, 243-249.
- Goins, J., and Moezzi, M. (2013). Linking occupant complaints to building performance. *Building Research & Information*, 41(3), 361-372.
- Gu, Y. (2011). *The Impacts of Real-time Knowledge Based Personal Lighting Control on Energy Consumption, User Satisfaction and Task Performance in Offices (PhD Dissertation)*. Carnegie Mellon University, Pittsburgh.
- Gu, Y., Lo, A., and Niemegeers, I. (2009). A survey of indoor positioning systems for wireless personal networks. *Communications Surveys & Tutorials, IEEE*, 11(1), 13-32.
- Gyalistras, D. (2010). Use of Weather and Occupancy Forecasts for Optimal Building Climate Control (OptiControl). Zurich: swisselectric research.
- Hallberg, J., Nilsson, M., and Synnes, K. (2003, 23 Feb.-1 March 2003). *Positioning with Bluetooth*. Paper presented at the Telecommunications, 2003. ICT 2003. 10th International Conference on.



- Hartkopf, V. H., Loftness, V. E., and Mill, A. D. P. (1986). The Concept of Total Building Performance and Building Diagnostics *Building Performance: Function, Preservation, and Rehabilitation* (pp. 5-22). West Conshohocken, PA: American Society for Testing and Materials.
- Henze, G. P., Dodier, R. H., and Krarti, M. (1997). Development of a Predictive Optimal Controller for Thermal Energy Storage Systems. *HVAC&R Research*, 3(3), 233-264.
- Hong, T., and Lin, H.-W. (2012). *Occupant Behavior: Impact on Energy Use of Private Offices*. Paper presented at the ASim 2012.
- ILFI. (2013). Living Building Challenge. Retrieved April 27, 2014, from <http://living-future.org/lbc>
- Irizarry, R. (2001). Local Regression. Retrieved April 16, 2014, from <http://www.biostat.jhsph.edu/~ririzarr/Teaching/754/>
- Jayada, B. (2003). A Model-Based Approach To Ventilation Control in Buildings (PhD Dissertation). Pittsburgh: Carnegie Mellon University.
- Jensen, S. O. (1995). Validation of building energy simulation programs a methodology. *Energy and Buildings*, 22, 133-144.
- Judkoff, R., Wortman, D., O'Doherty, B., and Burch, J. (2008). A Methodology for Validating Building Energy Analysis Simulation. Kansas City: National Renewable Energy Laboratory.
- Kandil, A.-E., and Love, J. A. (2013). Signature analysis calibration of a school energy model using hourly data. *Journal of Building Performance Simulation*, 1-20.
- Karaguzel, O. T. (2013). *Simulation-Based Parametric Analysis of Building Systems Integrative Solar Photovoltaics*. (PhD), Carnegie Mellon University.
- Karlsson, F., Rohdin, P., and Persson, M.-L. (2007). Measured and predicted energy demand of a low energy building: important aspects when using Building Energy Simulation. *Building Services Engineering Research and Technology*, 28(3), 223-235.
- Kelly, G. (1988). Control system simulation in North America. *Energy and Buildings*, 10, 193-202.
- Klein, L., Kwak, J.-y., Kavulya, G., Jazizadeh, F., Becerik-Gerber, B., Varakantham, P., and Tambe, M. (2012). Coordinating occupant behavior for building energy and comfort management using multi-agent systems. *Automation in Construction*, 22, 525-536.
- Kolda, T. G., Lewis, R. M., and Torczon, V. (2003). Optimization by direct search: new perspectives on some classical and modern methods. *Society for Industrial and Applied Mathematics*, 45(3), 385-482.
- Kolokotsa, D., Pouliezos, A., Stavrakakis, G., and Lazos, C. (2009). Predictive control techniques for energy and indoor environmental quality management in buildings. *Building and Environment*, 44, 1850-1863.
- Kotsiantis, S. B. (2007). Supervised Machine Learning: A Review of Classification Techniques.

- Kummert, M., Leduc, M.-A., and Moreau, A. (2011). *Using MPC to reduce the peak demand associated with electric heating*. Paper presented at the Model predictive control in buildings workshop, Montreal, CA.
- Lam, J. C., and Hui, S. C. M. (1996). Sensitivity Analysis of Energy Performance of Office Buildings. *Building and Environment*, 31(1), 27-39.
- Lam, K. P., Zhang, R., Wang, H., Dong, B., and Zhang, R. (2013). Development of web-based information technology infrastructures and regulatory repositories for green building codes in China (iCodes). *Building Simulation*, 1-11.
- Lee, Y. S., and Malkawi, A. M. (2014). Simulating multiple occupant behaviors in buildings: An agent-based modeling approach. *Energy and Buildings*, 69, 407-416.
- Li, Q., Meng, Q., Cai, J., Yoshino, H., and Mochida, A. (2009). Applying support vector machine to predict hourly cooling load in the building. *Applied Energy*, 86(10), 2249-2256.
- Liao, C., Lin, Y., and Barooah, P. (2011). Agent-based and graphical modelling of building occupancy. *Journal of Building Performance Simulation*, 5(1), 5-25.
- Liu, H., Darabi, H., Banerjee, P., and Liu, J. (2007). Survey of wireless indoor positioning techniques and systems. *Systems, Man, and Cybernetics, Part C: Applications and Reviews, IEEE Transactions on*, 37(6), 1067-1080.
- Loftness, V., Aziz, A., Choi, J., Kampschroer, K., Powell, K., Atkinson, M., and Heerwagen, J. (2009). The value of post-occupancy evaluation for building occupants and facility managers. *Intelligent Buildings International*, 1(4), 249-268.
- Lomas, K. J., Eppel, H., Martin, C. J., and Bloomfield, D. P. (1997). Empirical validation of building energy simulation programs. *Energy and Buildings*, 26, 253-275.
- Lucid-Design. (2010). Elon University Strives to Meet Carbon Commitment Through Behavior Change. Retrieved April 27, 2014, from <http://www.luciddesigngroup.com/download.php?id=20100701>
- Lutron. (2014). Whole Building solutions. Retrieved September 24, 2014, from <http://www.lutron.com/en-US/Residential-Commercial-Solutions/Pages/Commercial-Solutions/WholeBuildingSolutions.aspx>
- Mahdavi, A. (2001). Simulation-based control of building systems operation. *Building and Environment*, 36, 789-796.
- Mahdavi, A., and Pröglhöf, C. (2008). A model-based approach to natural ventilation. *Building and Environment*, 43(4), 620-627.
- Masoso, O. T., and Grobler, L. J. (2010). The dark side of occupants' behaviour on building energy use. *Energy and Buildings*, 42, 173-177.
- Mathworks. (2012). Matlab. *Matlab*. Retrieved July 10, 2012, from <http://www.mathworks.com/products/matlab/>
- May-Ostendorp, P., Henze, G. P., Corbin, C. D., Rajagopalan, B., and Felsmann, C. (2011). Model-predictive control of mixed-mode buildings with rule extraction. *Building and Environment*, 46, 428-437.
- Mertz, K. B. (2003). A Representational Framework for Building Systems Control (PhD Dissertation). Pittsburgh: Carnegie Mellon University.

- Microsoft. (2014). What is Microsoft Azure? Retrieved November 12, 2014, from <http://azure.microsoft.com/en-us/overview/what-is-azure/>
- Minitab. (2014). Minitab. Retrieved April 17, 2014, from <http://www.minitab.com/en-us/>
- Mitchell, T. M. (2010). Generative and Discriminative Classifiers: Naive Bayes and Logistic Regression. *Machine Learning*. Retrieved April 16, 2014, from <http://www.cs.cmu.edu/~tom/mlbook/NBayesLogReg.pdf>
- Mo, Z. (2003). An Agent-based Simulation-assisted Approach to Bi-lateral Building Systems Control (PhD Dissertation). Pittsburgh: Carnegie Mellon University.
- Moore, A. (2003). Information Gain. Retrieved April 15, 2014, from <http://www.autonlab.org/tutorials/infogain11.pdf>
- Murakami, Y., Terano, M., Mizutani, K., Harada, M., and Kuno, S. (2007). Field experiments on energy consumption and thermal comfort in the office environment controlled by occupants' requirements from PC terminal. *Building and Environment*, 42, 4022-4027.
- NBI. (2013, July). The COMNET Energy Modeling Portal. Retrieved August 29, 2014, from <http://www.comnet.org/about-comnet-portal>
- Neto, A. H., and Fiorelli, F. A. S. (2008). Comparison between detailed model simulation and artificial neural network for forecasting building energy consumption. *Energy and Buildings*, 40(12), 2169-2176.
- Nghiem, T. X. (Producer). (2012, June 26). MLE+: a Matlab-EnergyPlus Co-simulation Interface. *MLE+: a Matlab-EnergyPlus Co-simulation Interface*. Retrieved from <http://www.seas.upenn.edu/~nghiem/mleplus.html>
- Onset. (2014). Weather Stations. Retrieved November 4, 2014, from <http://www.onsetcomp.com/products/data-loggers/weather-stations>
- Oracle. (2014). MySQL. Retrieved April 27, 2014, from <http://www.mysql.com/>
- OSIsoft. (2014a). PI Data Access. Retrieved November 5, 2014, from [http://www.osisoft.com/software-support/products/PI\\_Data\\_Access.aspx](http://www.osisoft.com/software-support/products/PI_Data_Access.aspx)
- OSIsoft. (2014b). PI Interface for Universal File and Stream Loading (UFL) (pp. 65).
- OSIsoft. (2014c). The PI System - the industry standard in enterprise infrastructure for management of real-time data and events. Retrieved September 24, 2014, from [http://www.osisoft.com/software-support/what-is-pi/what\\_is\\_pi.aspx](http://www.osisoft.com/software-support/what-is-pi/what_is_pi.aspx)
- Page, J., Robinson, D., Morel, N., and Scartezzini, J.-L. (2008). A generalised stochastic model for the simulation of occupant presence. *Energy and Buildings*, 40, 83-98.
- Pan, Y., Huang, Z., and Wu, G. (2007). Calibrated building energy simulation and its application in a high-rise commercial building in Shanghai. *Energy and Buildings*, 39(6), 651-657.
- Pang, X., Bhattacharya, P., O'Neill, Z., Haves, P., Wetter, M., and Bailey, T. (2011). *Real-time building energy simulation using EnergyPlus and the Building Controls Virtual Test Bed*. Paper presented at the Proceedings of Building Simulation 2011, Sydney.
- Paris, B., Eynard, J., Grieu, S., Talbert, T., and Polit, M. (2010). Heating control schemes for energy management in buildings. *Energy and Buildings*, 42, 1908-1917.

- Park, J. (2013). *Post-occupancy Evaluation for Energy Conservation, Superior IEQ & Increased Occupant Satisfaction*. Paper presented at the World Workplace 2013.
- Pedrini, A., Westphal, F. S., and Lamberts, R. (2002). A methodology for building energy modelling and calibration in warm climates. *Building and Environment*, 37(8–9), 903-912.
- Perez, R. (1993). Phantom Loads. *Home Power*, 37, 46-48.
- Peters, S., Loftness, V., and Hartkopf, V. (2011). *The intuitive control of smart home and office environments*. Paper presented at the Proceedings of the 10th SIGPLAN symposium on New ideas, new paradigms, and reflections on programming and software, Portland, Oregon, USA.
- Phipps. (2012). Center for Sustainable Landscapes. *Phipps Conservatory*. from <http://hipps.conservatory.org/project-green-heart/green-heart-at-hipps/center-for-sustainable-landscapes.aspx>
- Platt, J. (1998). *Sequential minimal optimization: A fast algorithm for training support vector machines*.
- Plugwise. (2013). Circle. Retrieved April 27, 2014, from <http://www.plugwise.com/idplugtype-b/circle>
- Privara, S., Siroky, J., Ferkl, L., and Cigler, J. (2011). Model predictive control of a building heating system: the first experience. *Energy and Buildings*, 43, 564-572.
- Python. (2012, January 20). Python Programming Language – Official Website. *Python Programming Language – Official Website*. Retrieved January, 20, 2012, from <http://python.org/>
- Quinlan, J. R. (1993). *C4. 5: programs for machine learning* (Vol. 1): Morgan kaufmann.
- Raftery, P., Keane, M., and Costa, A. (2011). Calibrating whole building energy models: Detailed case study using hourly measured data. *Energy and Buildings*, 43(12), 3666-3679.
- Raftery, P., Keane, M., and O'Donnell, J. (2011). Calibrating whole building energy models: An evidence-based methodology. *Energy and Buildings*, 43(9), 2356-2364.
- Raja, I. A., Nicol, J. F., McCartney, K. J., and Humphreys, M. A. (2001). Thermal comfort: use of controls in naturally ventilated buildings. *Energy and Buildings*, 33, 235-244.
- Reddy, A. T. (2006). Literature review on calibration of building energy simulation programs: uses, problems, procedures, uncertainty, and tools. *ASHRAE transactions*, 226-240.
- Schiavon, S., Lee, K. H., Bauman, F., and Webster, T. (2010). Simplified calculation method for design cooling loads in underfloor air distribution (UFAD) systems. *Energy and Buildings*, 43(2-3), 517-528.
- Seo, D., Huang, J., and Krarti, M. (2009). Evaluation of Typical Weather Year Selection Approaches for Energy Analysis of Buildings. *ASHRAE Transactions*, 115(2).
- Shih, H.-C. (2014). A robust occupancy detection and tracking algorithm for the automatic monitoring and commissioning of a building. *Energy and Buildings*, 77(0), 270-280.

- Sinha, S. (2008). Exhaustive search - Introduction to Bioinformatics.  
<http://veda.cs.uiuc.edu/courses/fa08/cs466/schedule.html>
- Solomon, D. M., Winter, R. L., Boulanger, A. G., Anderson, R. N., and Wu, L. L. (2011). Forecasting energy demand in large commercial buildings using support vector machine regression.
- Sorensen, S. (2013). Smart Power Strip. Retrieved June 14, 2014, from  
<http://scholarworks.montana.edu/xmlui/handle/1/593>
- Stoppel, C. M., and Leite, F. (2014). Integrating probabilistic methods for describing occupant presence with building energy simulation models. *Energy and Buildings*, 68, 99-107.
- Swook, H., Jung-Hun, K., Soo-Yong, J., and Chang-Soo, P. (2010, 19-23 Sept. 2010). *White LED ceiling lights positioning systems for optical wireless indoor applications*. Paper presented at the Optical Communication (ECOC), 2010 36th European Conference and Exhibition on.
- Tanimoto, J., Hagishima, A., and Sagara, H. (2008). A methodology for peak energy requirement considering actual variation of occupants' behavior schedules. *Building and Environment*, 43, 610-619.
- Torcellini, P., Pless, S., Deru, M., and Crawley, D. (2006). *Zero Energy Buildings: A Critical Look at the Definition*. Paper presented at the ACEEE Summer Study, Pacific Grove, CA.
- TRANE. (2013). TRACE™ 700 and LEED®. from  
<http://www.trane.com/COMMERCIAL/DNA/View.aspx?i=2396>
- TRNSYS. (2012, June). TRNSYS. from  
<http://sel.me.wisc.edu/trnsys/features/features.html>
- UO-SRML. (2012). Solar radiation basics. Retrieved November 3, 2014, from  
<http://solardat.uoregon.edu/SolarRadiationBasics.html>
- USGBC. (2011a). Advanced Energy Modeling for LEED. Washington D.C.: U.S. Green Building Council.
- USGBC. (2011b). *LEED 2009 for New Construction and Major Renovation*. Washington, DC: United States Green Building Council.
- USGBC. (2013). LEED v4 for Building Design and Construction (pp. 145): USGBC.
- Vaughn, K. (2011, June 23). The "Push and Pull" of Energy Modeling Demand. from  
<http://blog.rmi.org/ThePushPullEnergyModelingDemand>
- Veitch, J. A., Charles, K. E., Farley, K. M. J., and Newsham, G. R. (2007). A model of satisfaction with open-plan office conditions: COPE field findings. *Journal of Environmental Psychology*, 27(3), 177-189.
- Virote, J., and Neves-Silva, R. (2012). Stochastic models for building energy prediction based on occupant behavior assessment. *Energy and Buildings*, 53, 183-193.
- Wang, C., Yan, D., and Jiang, Y. (2011). A novel approach for building occupancy simulation. *Building Simulation*, 4, 149-167.
- Wang, S., and Jin, X. (2000). Model-based optimal control of VAV air-conditioning system using genetic algorithm. *Building and Environment*, 35, 471-487.



- WBT. (2013). White Box Technologies (WBT). from <http://weather.whiteboxtechnologies.com/>
- Weather-Underground. (2014a). About Our Data. Retrieved November 5, 2014, from <http://www.wunderground.com/about/data.asp>
- Weather-Underground. (2014b). A weather API designed for developers. Retrieved November 5, 2014, from <http://www.wunderground.com/weather/api/>
- Weka. (2011). Weka 3: Data Mining Software in Java. Retrieved April 22, 2014, from <http://www.cs.waikato.ac.nz/ml/weka/>
- Wetter, M. (2011a). Co-simulation of building energy and control systems with the Building Controls Virtual Test Bed. *Journal of Building Performance Simulation*, 185-203.
- Wetter, M. (2011b). GenOpt(R) Generic Optimization Program User Manual. Berkeley: Lawrence Berkeley National Laboratory.
- Witten, I. H., Frank, E., and Hall, M. A. (2011). *Data Mining Practical Machine Learning Tools and Techniques - 3rd ed.* Amsterdam: Morgan Kaufmann.
- Yahiaoui, A., Hensen, J., Soethout, L., and Paassen, A. H. C. (2006). *Model based optimal control for integrated building systems*. Paper presented at the Proceedings of the 6th International Postgraduate Research Conference in the Built and Human Environment, Delft, Netherlands.
- Yang, K. H., and Su, C. H. (1997). An Approach to Building Energy Savings Using the PMV Index. *Building and Environment*, 32(1), 25-30.
- Yu, Y., Loftness, V., and Yu, D. (2013). Multi-structural fast nonlinear model-based predictive control of a hydronic heating system. *Building and Environment*, 69(0), 131-148.
- Yu, Z., Fung, B. C., and Haghighat, F. (2013). *Extracting knowledge from building-related data—A data mining framework*. Paper presented at the Building Simulation.
- Yu, Z., Haghighat, F., Fung, B. C. M., and Yoshino, H. (2010). A decision tree method for building energy demand modeling. *Energy and Buildings*, 42(10), 1637-1646.
- Yuan, S., and Ronald, P. (2006). Multiple-zone ventilation and temperature control of a single-duct VAV system using model predictive control. *Energy and Buildings*, 38, 1248-1261.
- Yun, R., Lasternas, B., Aziz, A., Loftness, V., Scupelli, P., Rowe, A., . . . Zhao, J. (2013). *Toward the Design of a Dashboard to Promote Environmentally Sustainable Behavior among Office Workers*. Paper presented at the 8th International Conference, PERSUASIVE 2013, Sydney, Australia.
- Yun, R., Scupelli, P., Aziz, A., and Loftness, V. (2013). *Sustainability in the Workplace: Nine Intervention Techniques for Behavior Change*. Paper presented at the 8th International Conference, PERSUASIVE 2013, Sydney, Australia.
- Zandbergen, P. A. (2009). Accuracy of iPhone Locations: A Comparison of Assisted GPS, WiFi and Cellular Positioning. *Transactions in GIS*, 13, 5-25.

- Zhang, R., Lam, K. P., Chiou, Y.-S., and Dong, B. (2012). Information-theoretic environment features selection for occupancy detection in open office spaces. *Building Simulation*, 5, 179-189.
- Zhao, J., and Lam, K. P. (2012). Influential factors analysis on LEED building markets in U.S. East Coast cities by using Support Vector Regression. *Sustainable Cities and Society*, 5(0), 37-43.
- Zhao, J., Lam, K. P., Ydstie, B. E., and Karaguzel, O. T. (2014). EnergyPlus model-based predictive control within design–build–operate energy information modelling infrastructure. *Journal of Building Performance Simulation*, 1-14.
- Zhao, J., Lasternas, B., Lam, K. P., Yun, R., and Loftness, V. (2014). Occupant behavior and schedule modeling for building energy simulation through office appliance power consumption data mining. *Energy and Buildings*, 82(0), 341-355.
- Zhao, J., Yun, R., Lasternas, B., Wang, H., Lam, K. P., Aziz, A., and Loftness, V. (2013). *Occupant Behavior And Schedule Prediction Based on Office Appliance Energy Consumption Data Mining*. Paper presented at the CISBAT 2013 Conference - Clean Technology for Smart Cities and Buildings, Lausanne, Switzerland.
- ZigBee. (2014). ZigBee Control your world. Retrieved April 27, 2014, from <https://www.zigbee.org/>

# Appendices

---

## A. Modeling process at the design stage

In order to make a better design decision for the purpose of energy efficiency at the design stage, the DBO-EIM infrastructure should be completed by following the steps as shown below.

At the schematic design (SD) stage, building systems have not yet been designed in detail, so it is important to setup baseline and perform parametric design on building orientation, geometry, and other architectural features to optimize the loads of building heating, cooling, lighting, and equipment rather than the actual energy consumption. At this stage, for benchmarking purposes, ASHRAE 90.1 standards should be used to establish baseline HVAC, lighting, and equipment systems. All the parametric design models should also use the same assumptions as the baseline model. DesignBuilder and other software programs can be used to establish baseline model and perform basic parametric designs for architectural features.

At the detailed design (DD) stage, minimum adjustment should be made to the design of building orientation, geometry, program, and other architectural features in the BEM models. The focus at this stage should be on building envelope material, thermal zoning, lighting zoning, HVAC, lighting, and equipment systems. Detailed EnergyPlus model can be created with the best available input information of the systems according to the design drawings. The parametric modeling of different systems can be done in EnergyPlus to achieve a better whole building energy performance.



At the construction drawings (CD) stage, adjustment should be made to reflect the final design of the architectural features in DesignBuilder. When exporting to EnergyPlus, some system inputs, such as material properties and mechanical system parameters, can be updated based on the available information provided by the manufacturer's product data sheet.

**Table 25 Energy modeling objectives and tasks.**

Modeling objectives to assist designers	Modeling tasks (software)		
	Schematic Design (SD)	Detailed Design (DD)	Construction Drawings (CD)
Building orientation, geometry, program, and other architectural features.	Parametric modeling to determine the optimized building loads. (DesignBuilder)	Minimum adjustment. (DesignBuilder)	Minimum adjustment. (DesignBuilder)
Building envelope materials.	ASHRAE 90.1 baseline (DesignBuilder)	Parametric modeling to assist architects and engineers to choose proper zones and systems for an optimized energy performance. (EnergyPlus)	Update the model inputs based on the final construction drawings. (EnergyPlus)
Thermal and lighting zoning.			
HVAC, lighting, and equipment systems.			

Table 25 shows a summary of different modeling objectives and tasks at sequential stages of the design process. The tasks may involve manual and iterative efforts between DesignBuilder and EnergyPlus programs. For example, the geometry updates can be executed in the DesignBuilder program effortlessly, however, the program has limited capability to choose and customize advanced HVAC systems. Therefore, in some cases, after the building geometry information is updated in DesignBuilder, the model needs to be exported to EnergyPlus to update the HVAC system. If somehow the geometry is updated again after the HVAC system has been updated in

EnergyPlus, there is no way to import the updated EnergyPlus model back into DesignBuilder again. The user has to go back to the original DesignBuilder model to update the geometry, and then export it to EnergyPlus, and then do the HVAC system update again. This iterative process may have high temporal and financial costs, which can be a difficulty for industry to adopt this method. To solve this problem, recently, DesignBuilder and other software vendors, such as Simergy (DOE, 2014c) have made tremendous effort in integrating EnergyPlus HVAC system modules in their software's graphical interface, so that users can update both geometry and HVAC system in one program. One can expect that in future, the cost of doing parametric designs on building systems would decrease dramatically.

## **B. Model calibration process at the construction, commissioning and early operation stages**

This dissertation has presented a whole building energy model calibration method using empirical data. Many of the procedures in the method have been streamlined, but a few manual procedures could benefit from further streamlining in future work. However, the most critical and probably the most difficult step for future researchers to complete the model calibration study is to get the real-time measured data. It is not common that the test-bed building in this dissertation has a very comprehensive building automation system (BAS) system and can closely monitor their indoor/outdoor environmental quality and energy use in real time. In order to facilitate future researchers to retrieve real-time measured data, the author summarizes all the necessary steps that have to be taken to setup the data collection scheme for the purpose of the BEM model calibration.

1. Design an integrated BAS with the help from manufacturers. The manufacturers should work with the client, architect and mechanical electrical and plumbing (MEP) engineers to design a proper and integrated BAS system to cover all aspects of building systems.
2. The integrated BAS should be able to stream the following data points at least on the hourly basis as shown in Table 26. The “Required” column includes all the necessary data points for implementing the model calibration method. The “Recommended” column includes the data points that are important to the model calibration and model-based control, but may be only suitable for some projects.

**Table 26 Data points should be streamed via BAS on the hourly basis.**

	Required	Recommended
Indoor environmental data	<ul style="list-style-type: none"> <li>• Air temperature (could be part of HVAC)</li> <li>• CO<sub>2</sub> (could be part of HVAC)</li> <li>• Humidity (could be part of HVAC)</li> <li>• Daylight illuminance (part of lighting system)</li> </ul>	<ul style="list-style-type: none"> <li>• Mean radiant temperature</li> <li>• Air quality (O<sub>3</sub>, CO, particles, etc.)</li> </ul>
Outdoor environmental data	<ul style="list-style-type: none"> <li>• Air temperature</li> <li>• Humidity</li> <li>• Global solar radiation</li> <li>• Wind direction/speed</li> <li>• Rain/Snow gauge</li> </ul>	<ul style="list-style-type: none"> <li>• Illuminance</li> <li>• Diffuse solar radiation</li> <li>• Direct solar radiation</li> </ul>
System energy/water consumption metering data	<ul style="list-style-type: none"> <li>• HVAC components: fans, pumps, heating, cooling, etc.</li> <li>• Lighting, plug load, and other system energy consumption by panel (at least floor by floor)</li> <li>• Individual water system consumption (black, gray, portable, etc.)</li> </ul>	<ul style="list-style-type: none"> <li>• Individual plug load meter (by appliance) for typical office spaces</li> </ul>
System operation status data	<ul style="list-style-type: none"> <li>• AHU supply air temperature/flow rate</li> <li>• AHU return air temperature/flow rate</li> <li>• Outdoor air temperature/flow rate</li> <li>• Exhaust air temperature/flow rate</li> <li>• Window opening status (for mixed-mode ventilated buildings)</li> </ul>	<ul style="list-style-type: none"> <li>• Plant-side system node status</li> </ul>

3. The data collection period should last at least one year after the building is occupied in order to cover all the seasonal differences. As a matter of fact, LEED, Living Building Challenge and other green building rating systems already require one year post-occupancy energy consumption data collection as prerequisites or to get credits. The difference here is that current requirements in the rating systems are not as rigorous or specific as what are shown in Table 26.

## **C. OME<sup>+</sup>PC development process at the operation stage**

After the EnergyPlus model is calibrated, it can be used to develop OME<sup>+</sup>PC, or its simplified versions of E<sup>+</sup>PC, or ME<sup>+</sup>PC, depending on the systems availability in the EnergyPlus model. The following sections will demonstrate a set of generic procedures of developing OME<sup>+</sup>PC using a DOE prototype medium office building EnergyPlus model.

### ***C.1. Software platform***

The following software programs need to be installed on a computer with Windows 7 operation system in the given order.

- Java: version 7 update 55
- Matlab R2012a (7.14.0.739)
- EnergyPlus Version 6.0.0.023
- BCVTB Version 1.1.0, January 13 2012
- MLE+ Version 1.0 (copy all the MLE+ files into the execution folder)

## ***C.2. Configure EnergyPlus model***

In order to demonstrate a generic EnergyPlus model configuration process, in this section, the author will replace the original test-bed EnergyPlus model with a DOE prototype medium office building EnergyPlus model and will document step-by-step processes and the time spent. Figure 90 shows the renderings of the prototype model in realistic view and X-Ray view. The building has three stories and 15 zones. The total floor area is 4,982m<sup>2</sup>. The building is designed based on ASHRAE Standards 90.1-2004, including one packaged Multi-zone VAV (MZVAV) with plenum zones, gas furnaces, and electric reheat for each floor. Windows are not operable in the building. The five zones on the first floor of the building will be controlled with OME<sup>+</sup>PC (The passive cooling module in the control algorithm will be disabled). The simulation will demonstrate the procedures to remake the model with the same control algorithm as the ones used in the original OME<sup>+</sup>PC for the test-bed building. Since there are major differences in the HVAC system design and input assumptions, the same control algorithm could run without error, but may not generate the optimal performance. New algorithms could be developed specifically for the MZVAV system in future work.

Here are the step-by-step guide to configure the EnergyPlus model:

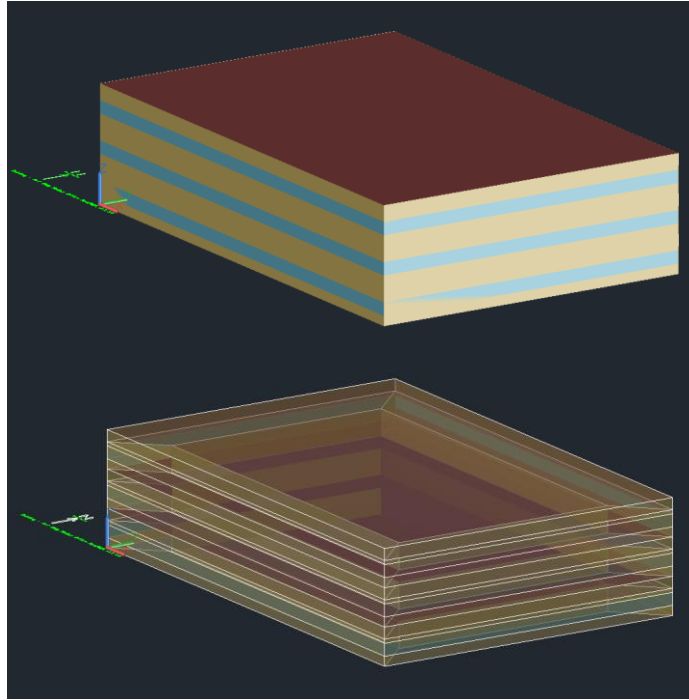


**Figure 90 DOE prototype medium office building model.**

- Timestep -> Number of Timesteps per Hour = 3
- Run period -> one week & Number of Times Run Period to be Repeated = 4538 (1 week of simulation)
- External Interface
  - ExternalInterface -> PtolemyServer
  - ExternalInterface:Schedule
    - AHUAirSetpoint
    - ZoneCoolingSetpoint\_1
    - ZoneHeaingSetpoint\_1
    - ZoneCoolingSetpoint\_2
    - ZoneHeaingSetpoint\_2
    - ZoneCoolingSetpoint\_3
    - ZoneHeaingSetpoint\_3
    - ZoneCoolingSetpoint\_4
    - ZoneHeaingSetpoint\_4
    - ZoneCoolingSetpoint\_Core
    - ZoneHeaingSetpoint\_Core
    - LightingSchedule
    - PeopleSchedule
  - ExternalInterface:Actuator
    - Outdoor Dry Bulb
    - Outdoor Relative Humidity

- Wind Speed
  - Wind Direction
  - Diffuse Solar
  - Direct Solar
  - EquipmentCore
  - EquipmentOne
  - EquipmentTwo
  - EquipmentThree
  - EquipmentFour
- Zone HVAC Controls and Thermostats
  - ThermostatSetpoint: DualSetpoint
    - Core\_bottom DualSPSched
      - ZoneHeatingSetpoint\_Core
      - ZoneCoolingSetpoint\_Core
    - Perimeter\_bot\_ZN\_1 DualSPSched
      - ZoneHeatingSetpoint\_1
      - ZoneCoolingSetpoint\_1
    - Perimeter\_bot\_ZN\_2 DualSPSched
      - ZoneHeatingSetpoint\_2
      - ZoneCoolingSetpoint\_2
    - Perimeter\_bot\_ZN\_3 DualSPSched
      - ZoneHeatingSetpoint\_3
      - ZoneCoolingSetpoint\_3
    - Perimeter\_bot\_ZN\_4 DualSPSched
      - ZoneHeatingSetpoint\_4
      - ZoneCoolingSetpoint\_4
- Setpoint Managers
  - SetpointManager: Scheduled
    - VAV\_1 SAT setpoint -> AHUAirSetpoint
- Output Reporting
  - OutputControl: Table: Style
    - JtoKWH
  - Output: Variable
    - Outdoor Dry Bulb
    - Outdoor Relative Humidity
    - Wind Speed
    - Wind Direction
    - Diffuse Solar
    - Direct Solar
    - Zone/Sys Air Temperature
      - Core\_bottom
      - Perimeter\_bot\_ZN\_1
      - Perimeter\_bot\_ZN\_2
      - Perimeter\_bot\_ZN\_3
      - Perimeter\_bot\_ZN\_4

- Zone/Sys Air Relative Humidity
    - Core\_bottom
    - Perimeter\_bot\_ZN\_1
    - Perimeter\_bot\_ZN\_2
    - Perimeter\_bot\_ZN\_3
    - Perimeter\_bot\_ZN\_4
  - Zone Mean Radiant Temperature
    - Core\_bottom
    - Perimeter\_bot\_ZN\_1
    - Perimeter\_bot\_ZN\_2
    - Perimeter\_bot\_ZN\_3
    - Perimeter\_bot\_ZN\_4
  - DX Cooling Coil Electric Power
  - Pump Electric Power
  - Fan Electric Power
  - Heating Coil Gas Consumption Rate
- Internal Gains
  - People: PeopleSchedule
    - Core\_bottom People
    - Perimeter\_bot\_ZN\_1 People
    - Perimeter\_bot\_ZN\_2 People
    - Perimeter\_bot\_ZN\_3 People
    - Perimeter\_bot\_ZN\_4 People
  - Lights: LightingSchedule
    - Core\_bottom People
    - Perimeter\_bot\_ZN\_1 Lights
    - Perimeter\_bot\_ZN\_2 Lights
    - Perimeter\_bot\_ZN\_3 Lights
    - Perimeter\_bot\_ZN\_4 Lights

### ***C.3. Configure BCVTB files***

After the EnergyPlus model is configured, an XML file (socket.cfg) has to be created in the same folder with the EnergyPlus IDF file. The socket should be configured as following,

- `<?xml version="1.0" encoding="ISO-8859-1"?>`
- `<BCVTB-client>`
- `<ipc>`
- `<socket port="52212" hostname="JieZhao-PC"/>`
- `</ipc>`



- `</BCVTB-client>`

In addition, another XML file (variables.cfg) that defines all the communicating variables between EnergyPlus and BCVTB (Matlab/Simulink) should also be created as following,

- `<?xml version="1.0" encoding="ISO-8859-1"?>`
- `<!DOCTYPE BCVTB-variables SYSTEM "variables.dtd">`
- `<BCVTB-variables>`
- `<!-- The next 15 elements receive zone air temperature, relative humidity, radiant temperature from E+ -->`
  - `<variable source="EnergyPlus">`
  - `<EnergyPlus name="Core_bottom" type="Zone/Sys Air Temperature"/>`
  - `</variable>`
  - `<variable source="EnergyPlus">`
  - `<EnergyPlus name="Core_bottom" type="Zone Air Relative Humidity"/>`
  - `</variable>`
  - `<variable source="EnergyPlus">`
  - `<EnergyPlus name="Core_bottom" type="Zone Mean Radiant Temperature"/>`
  - `</variable>`
  - `<variable source="EnergyPlus">`
  - `<EnergyPlus name="Perimeter_bot_ZN_1" type="Zone/Sys Air Temperature"/>`
  - `</variable>`
  - `<variable source="EnergyPlus">`
  - `<EnergyPlus name="Perimeter_bot_ZN_1" type="Zone Air Relative Humidity"/>`
  - `</variable>`
  - `<variable source="EnergyPlus">`
  - `<EnergyPlus name="Perimeter_bot_ZN_1" type="Zone Mean Radiant Temperature"/>`
  - `</variable>`
  - `<variable source="EnergyPlus">`
  - `<EnergyPlus name="Perimeter_bot_ZN_2" type="Zone/Sys Air Temperature"/>`
  - `</variable>`
  - `<variable source="EnergyPlus">`
  - `<EnergyPlus name="Perimeter_bot_ZN_2" type="Zone Air Relative Humidity"/>`
  - `</variable>`
  - `<variable source="EnergyPlus">`
  - `<EnergyPlus name="Perimeter_bot_ZN_2" type="Zone Mean Radiant Temperature"/>`
  - `</variable>`
  - `<variable source="EnergyPlus">`
  - `<EnergyPlus name="Perimeter_bot_ZN_3" type="Zone/Sys Air Temperature"/>`
  - `</variable>`
  - `<variable source="EnergyPlus">`

- <EnergyPlus name="Perimeter\_bot\_ZN\_3" type="Zone Air Relative Humidity"/>
- </variable>
- <variable source="EnergyPlus">
- <EnergyPlus name="Perimeter\_bot\_ZN\_3" type="Zone Mean Radiant Temperature"/>
- </variable>
- <variable source="EnergyPlus">
- <EnergyPlus name="Perimeter\_bot\_ZN\_4" type="Zone/Sys Air Temperature"/>
- </variable>
- <variable source="EnergyPlus">
- <EnergyPlus name="Perimeter\_bot\_ZN\_4" type="Zone Air Relative Humidity"/>
- </variable>
- <variable source="EnergyPlus">
- <EnergyPlus name="Perimeter\_bot\_ZN\_4" type="Zone Mean Radiant Temperature"/>
- </variable>
- <!-- The next 3 elements receive the air loop supply temperature, mass flow rate and humidity information from E+ -->
  - <variable source="EnergyPlus">
  - <EnergyPlus name="VAV\_1 Supply Equipment Outlet Node" type="System Node Temp"/>
  - </variable>
  - <variable source="EnergyPlus">
  - <EnergyPlus name="VAV\_1 Supply Equipment Outlet Node" type="System Node Humidity Ratio"/>
  - </variable>
  - <variable source="EnergyPlus">
  - <EnergyPlus name="VAV\_1 Supply Equipment Outlet Node" type="System Node MassFlowRate"/>
  - </variable>
- <!-- The next 4 elements receive VAV fan, pumps, cooling, and heating power data from E+ -->
  - <variable source="EnergyPlus">
  - <EnergyPlus name="VAV\_1\_Fan" type="Fan Electric Power"/>
  - </variable>
  - <variable source="EnergyPlus">
  - <EnergyPlus name="SWHSys1 Pump" type="Pump Electric Power"/>
  - </variable>
  - <variable source="EnergyPlus">
  - <EnergyPlus name="VAV\_1\_HeatC" type="Heating Coil Gas Consumption Rate"/>
  - </variable>
  - <variable source="EnergyPlus">

- <EnergyPlus name="VAV\_1\_CoolC DXCoil" type="DX Cooling Coil Electric Power"/>
  - </variable>
- <!-- The next 1 element send the set points to the HVAC system in E+ -->
  - <variable source="Ptolemy">
  - <EnergyPlus schedule="AHUAirSetpoint"/>
  - </variable>
- <!-- The next 6 elements send the weather condition in E+ -->
  - <variable source="Ptolemy">
  - <EnergyPlus actuator="DryBulb"/>
  - </variable>
  - <variable source="Ptolemy">
  - <EnergyPlus actuator="RelativeHumidity"/>
  - </variable>
  - <variable source="Ptolemy">
  - <EnergyPlus actuator="WindSpeed"/>
  - </variable>
  - <variable source="Ptolemy">
  - <EnergyPlus actuator="WindDirection"/>
  - </variable>
  - <variable source="Ptolemy">
  - <EnergyPlus actuator="DiffuseSolar"/>
  - </variable>
  - <variable source="Ptolemy">
  - <EnergyPlus actuator="DirectSolar"/>
  - </variable>
- <!-- The next 10 elements send the setpoints to the 5 zones in E+ -->
  - <variable source="Ptolemy">
  - <EnergyPlus schedule="ZoneCoolingSetpoint\_Core"/>
  - </variable>
  - <variable source="Ptolemy">
  - <EnergyPlus schedule="ZoneHeatingSetpoint\_Core"/>
  - </variable>
  - <variable source="Ptolemy">
  - <EnergyPlus schedule="ZoneCoolingSetpoint\_1"/>
  - </variable>
  - <variable source="Ptolemy">
  - <EnergyPlus schedule="ZoneHeatingSetpoint\_1"/>
  - </variable>
  - <variable source="Ptolemy">
  - <EnergyPlus schedule="ZoneCoolingSetpoint\_2"/>
  - </variable>
  - <variable source="Ptolemy">

- <EnergyPlus schedule="ZoneHeatingSetpoint\_2"/>
- </variable>
- <variable source="Ptolemy">
- <EnergyPlus schedule="ZoneCoolingSetpoint\_3"/>
- </variable>
- <variable source="Ptolemy">
- <EnergyPlus schedule="ZoneHeatingSetpoint\_3"/>
- </variable>
- <variable source="Ptolemy">
- <EnergyPlus schedule="ZoneCoolingSetpoint\_4"/>
- </variable>
- <variable source="Ptolemy">
- <EnergyPlus schedule="ZoneHeatingSetpoint\_4"/>
- </variable>
- <!-- The next 2 elements send lighting and people schedules to E+ -->
  - <variable source="Ptolemy">
  - <EnergyPlus schedule="lightingSchedule"/>
  - </variable>
  - <variable source="Ptolemy">
  - <EnergyPlus schedule="peopleSchedule"/>
  - </variable>
- <!-- The next 5 elements send equipment schedules to E+ -->
  - <variable source="Ptolemy">
  - <EnergyPlus actuator="EquipmentCore"/>
  - </variable>
  - <variable source="Ptolemy">
  - <EnergyPlus actuator="EquipmentOne"/>
  - </variable>
  - <variable source="Ptolemy">
  - <EnergyPlus actuator="EquipmentTwo"/>
  - </variable>
  - <variable source="Ptolemy">
  - <EnergyPlus actuator="EquipmentThree"/>
  - </variable>
  - <variable source="Ptolemy">
  - <EnergyPlus actuator="EquipmentFour"/>
  - </variable>
- </BCVTB-variables>

#### C.4. Configure data transfer in Matlab/Simulink

After the EnergyPlus model and BCVTB files are configured, one should update the data transfer in Matlab/Simulink. The first step is to configure the MLE+ co-simulation function block in Simulink. Configurations are shown in Figure 91. For “Weather Profile”, you can use any weather file available, since the weather data will be overridden by outside data input. The “Number of Real Outputs” should be equal to the number of variables with the label <variable source="EnergyPlus"> in the “variables.cfg” file.

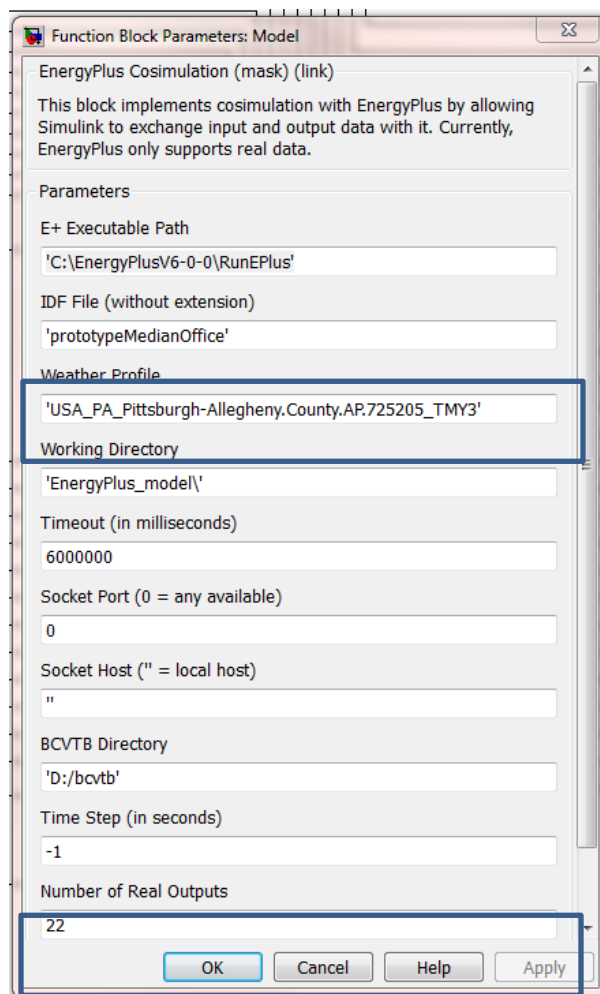


**Figure 91 MLE+ co-simulation function block.**

The second step is to configure input and output variables of EnergyPlus in Simulink. In this case study, EnergyPlus has 24 inputs and 22 outputs. The sequence of the variables in Simulink has to be the same as in the “variables.cfg” file, as following,

- EnergyPlus inputs:
  - AHUAirSetpoint
  - DryBulb
  - RelativeHumidity
  - WindSpeed
  - WindDirection
  - DiffuseSolar
  - DirectSolar
  - ZoneCoolingSetpoint\_Core
  - ZoneHeatingSetpoint\_Core
  - ZoneCoolingSetpoint\_1
  - ZoneHeatingSetpoint\_1
  - ZoneCoolingSetpoint\_2
  - ZoneHeatingSetpoint\_2
  - ZoneCoolingSetpoint\_3
  - ZoneHeatingSetpoint\_3
  - ZoneCoolingSetpoint\_4
  - ZoneHeatingSetpoint\_4
  - lightingSchedule
  - peopleSchedule
  - EquipmentCore
  - EquipmentOne
  - EquipmentTwo
  - EquipmentThree
  - EquipmentFour
- EnergyPlus outputs:
  - Zone Air Temperature\_Core
  - Zone Air Relative Humidity\_Core
  - Zone Mean Radiant Temperature\_Core
  - Zone Air Temperature\_1
  - Zone Air Relative Humidity\_1
  - Zone Mean Radiant Temperature\_1
  - Zone Air Temperature\_2
  - Zone Air Relative Humidity\_2
  - Zone Mean Radiant Temperature\_2
  - Zone Air Temperature\_3

- Zone Air Relative Humidity\_3
- Zone Mean Radiant Temperature\_3
- Zone Air Temperature\_4
- Zone Air Relative Humidity\_4
- Zone Mean Radiant Temperature\_4
- Supply Air Node Temp
- Supply Air Node Humidity Ratio
- Supply Air Node Mass Flow Rate
- Fan Electric Power
- Pump Electric Power
- Heating Coil Gas Consumption Rate
- DX Cooling Coil Electric Power

### ***C.5. Configure outside data input sources in Matlab/Simulink***

First, weather data needs to be provided to the control system. A CSV-format file with seven (or eight, including outdoor CO<sub>2</sub> data) variables as listed below should be created.

- Timestamp (20 minutes time interval, corresponding to the time step of EnergyPlus simulation.)
- DryBulb
- RelativeHumidity
- WindSpeed
- WindDirection
- DiffuseSolar
- DirectSolar
- OutdoorCO2 (optional)

Second, occupancy, lighting, and equipment schedules should be created for the same time interval and duration. One should note that these schedules are in fraction format, so the control algorithm should calculate the actual number of occupants, lighting power, and equipment power by multiplying the schedules with the densities of occupancy, lighting, and equipment, respectively. The CSV file column variables are listed below.

- Timestamp (the same as in the weather file.)

- Occupancy
- Lighting
- Equipment

Third, as discussed in the section of “4.5.4. OME+PC design and implementation”, Python scripts should be included in the control system in order to acquire real-time occupant thermal feedback from the internet-based dashboard. The following steps should be followed to achieve the goal.

- A “python.m” file, developed by the author for executing Python script in Matlab has to be put into the installation folder of Matlab. In this case, the file path should be:
  - C:\Program Files\MATLAB\R2012a\toolbox\matlab\general
- A “Python” folder, including two scripts: “getCloAdjustmentValue.py” and “getComfortAdjustmentValue.py”, should be included in the Matlab/Simulink execution folder.
- A “getComfortAndClo.m” file, to transfer data from Python script to Matlab program, should be put in the same Matlab/Simulink execution folder.
- In Simulink “PMV Adjustment” block, use the following codes to read the occupant thermal comfort feedback data:
  - coder.extrinsic('getComfortAndClo');
  - [originalComfort, clo] = getComfortAndClo();

### ***C.6. Update control algorithms in Matlab/Simulink***

In this demo, the original OME<sup>+</sup>PC control algorithm is updated according to the HVAC system of the prototype model without changing the whole control system structure. As shown in Figure 92, Block A is the EnergyPlus interface, Block B contains the AHU control algorithm, and Block



C contains the individual zone control algorithm. One difference between the original OME<sup>+</sup>PC and the demo is that in Block B, some of the inputs of EnergyPlus, such as “coolingCoilSchedule”, “heatingCoilSchedule”, “coolingCoilSetpoint”, “heatingCoilSetpoint”, and “realCO2”, are not connected to the EnergyPlus interface. The same changes are made to the EnergyPlus outputs, due to the difference of the HVAC systems used in the two building models.

Inside Block B, as shown in Figure 93, there are four blocks: Block B-1 takes care of receding horizon mechanism for the entire control system. Block B-2 finds the correct EnergyPlus occupancy, lighting, and equipment input values based on the receding horizon calculation results. Block B-3 finds the correct weather input values based on the receding horizon calculation results. Block B-4 optimizes the supply air temperature setpoints based on all the EnergyPlus system outputs as well as the five zone PMV outputs. All the four blocks are written in Matlab language inside Simulink.

Inside Block C, There are four sub-blocks: Block C-1 is a multiport selector to specify EnergyPlus output vector into separated arrays. Block C-2 calculates total power consumption of the HVAC system at each time stamp. Simple mathematical functions are used in Block C-2. Block C-3 calculates zone setpoints as EnergyPlus inputs, which contains five sub-blocks C-3-1, C-3-2, C-3-3, C-3-4, and C-3-5 representing five different zones in the prototype building, as shown in Figure 95. The occupant thermal feedback is collected in each of the five sub-blocks and then averaged in sub-block C-3-6.

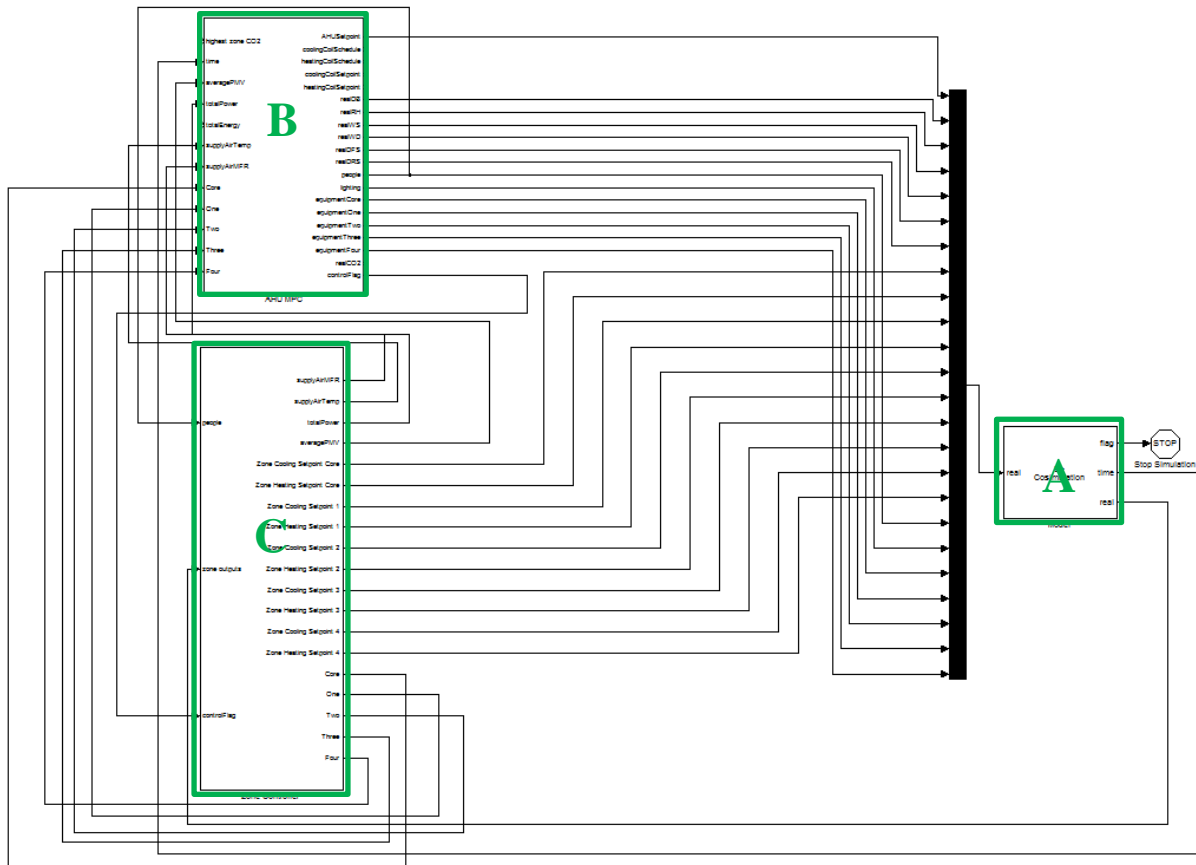


**Figure 92 Complete control system model in Simulink.**



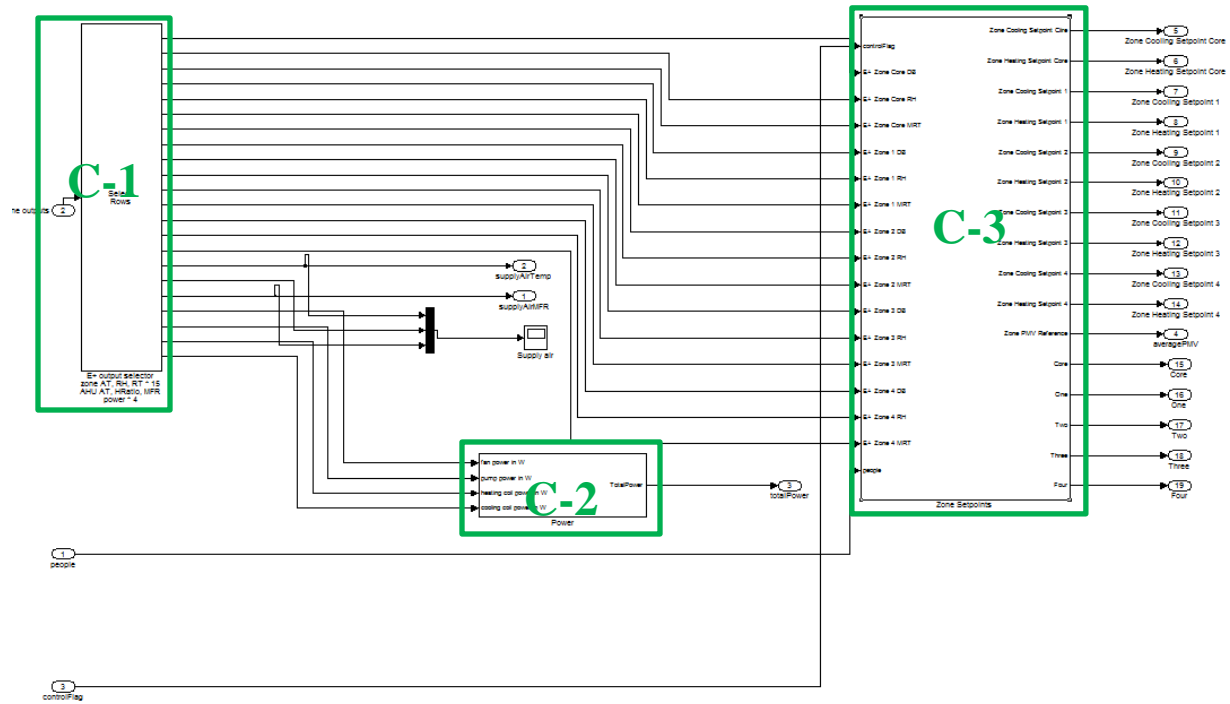


Figure 94 Block C of the control system model in Simulink.



- Delete all the files in “files” and “optimization” folders, which are the simulation results from the previous simulation.
- Go to <http://csl.intelligentworkplace.org> (contact the author for username and password) to adjust occupant thermal comfort and clothing feedback in real-time.

After the simulation is finished, all the control performance results are recorded in the “files”

folder of the Matlab execution folder, including:

- Final results
  - files/adjustedPMVUpperNE.csv
  - files/adjustedPMVUpperNM.csv
  - files/adjustedPMVUpperNW.csv
  - files/adjustedPMVUpperSW.csv
  - files/cloNE.csv
  - files/cloNM.csv
  - files/cloNW.csv
  - files/cloSW.csv
  - files/controlAirMFR.csv
  - files/controlCoolingCoilSchedule.csv
  - files/controlDB.csv
  - files/controlDFS.csv
  - files/controlEnergy.csv
  - files/controlEquipmentNE.csv
  - files/controlPeople.csv
  - files/controlPMV.csv
  - files/controlPMV\_NE.csv
  - files/controlPMV\_NM.csv
  - files/controlPMV\_NW.csv
  - files/controlPMV\_SW.csv
  - files/controlPower.csv
  - files/controlSetpoint.csv
  - files/controlSupplyAirTemp.csv
  - files/PMVAdjustmentNE.csv
  - files/PMVAdjustmentNM.csv
  - files/PMVAdjustmentNW.csv
  - files/PMVAdjustmentSW.csv
- Interim results
  - files/dayOfSimulation.csv
  - files/hourOfSimulation.csv

- files/hourOfSimulationContinuous.csv
- files/optimizationStep.csv
- files/optimizationStepContinuous.csv
- files/predictStep.csv
- files/realControlCO2.csv
- files/realControlDB.csv
- files/realControlDFS.csv
- files/realControlDRS.csv
- files/realControlEquipmentCore.csv
- files/realControlEquipmentFour.csv
- files/realControlEquipmentOne.csv
- files/realControlEquipmentThree.csv
- files/realControlEquipmentTwo.csv
- files/realControlLighting.csv
- files/realControlPeople.csv
- files/realControlRH.csv
- files/realControlWD.csv
- files/realControlWS.csv

All the optimization performance results for debugging are recorded in the “optimization” folder of the Matlab execution folder, including:

- optimization/AHUCoolingSetpointDatabase.csv
- optimization/AHUHeatingSetpointDatabase.csv
- optimization/eachPosition.csv
- optimization/firstPosition.csv
- optimization/lastPosition.csv
- optimization/predictAHUSetpoint.csv
- optimization/predictCoolingCoilSchedule.csv
- optimization/predictEnergy.csv
- optimization/predictMFR.csv
- optimization/predictNE.csv
- optimization/predictNM.csv
- optimization/predictNW.csv
- optimization/predictPMV.csv
- optimization/predictPower.csv
- optimization/predictSupplyAirTemp.csv
- optimization/predictSW.csv

### C.8. Demo development results

Following the steps above, the demo is developed and simulated Table 27 shows a summary of the demo development process.

**Table 27 Summary of the demo development process.**

Step	Task	Time spent	Challenges
1	Configure EnergyPlus model	1 <sup>st</sup> round: 8 hours.	<ul style="list-style-type: none"> <li>• Iterative heavy manual work.</li> <li>• Cannot test and debug without completing all the steps of 1 to 6.</li> </ul>
		2 <sup>nd</sup> round: 3 hours.	
		3 <sup>rd</sup> round: 2 hours.	
2	Configure BCVTB files	1 <sup>st</sup> round: 1 hour.	Human errors in XML file editing.
		2 <sup>nd</sup> round: 1 hour.	
		3 <sup>rd</sup> round: 1 hour.	
3	Configure data transfer in Matlab/Simulink	6 hours.	Human errors when configuring links in different layers of the Simulink blocks.
4	Configure outside data input sources in Matlab/Simulink	1 hour.	The compatibility among different file medias and software programs.
5	Update control algorithms in Matlab/Simulink	3 hours.	Control algorithms are system-specific. It is really difficult to develop one generic algorithm that can fit all the systems. This demo only provides minimum updates in order to run the HVAC system in the prototype model, which may not result in good control performance. Future work can develop other control algorithms for other types of HVAC systems.
6	Simulating and reporting	22 hours (for one week of simulation)	High computational and temporal costs
Total time spent:		48 hours (from creating the model based on the existing OME <sup>+</sup> PC to receiving the results of the simulation)	

The first two steps actually include three iterations, because the author has to go back-and-forth from EnergyPlus to BCVTB files, then to Matlab/Simulink codes in order to make the consistent changes to the variables. In total, configuring EnergyPlus model took 13 hours, and configuring



BCVTB files took three hours, during which the biggest challenge is that human errors may happen easily due to the tedious and text-based editing process.

Step 3 to step 5 needs to be completed in the Matlab/Simulink environment. It only took the author 10 hours to complete this part, mainly because only minimum updates are made to the original OME<sup>+</sup>PC control algorithm to ensure the MZVAV system can operate under the predictive control algorithm. Figure 96 shows the PMV simulation results of the demo model which meets the boundary requirements, but is not well optimized. This is mainly because the purpose of this demo is not creating an optimized control model that has been demonstrated fully in Chapter 4, but to provide a meaningful summary of the detailed steps that one can follow to recreate the OME<sup>+</sup>PC model for future studies and applications. Researching and developing new algorithm (such as distributed MPC algorithms) for the MZVAV system and other HVAC systems could be achieved in future work.

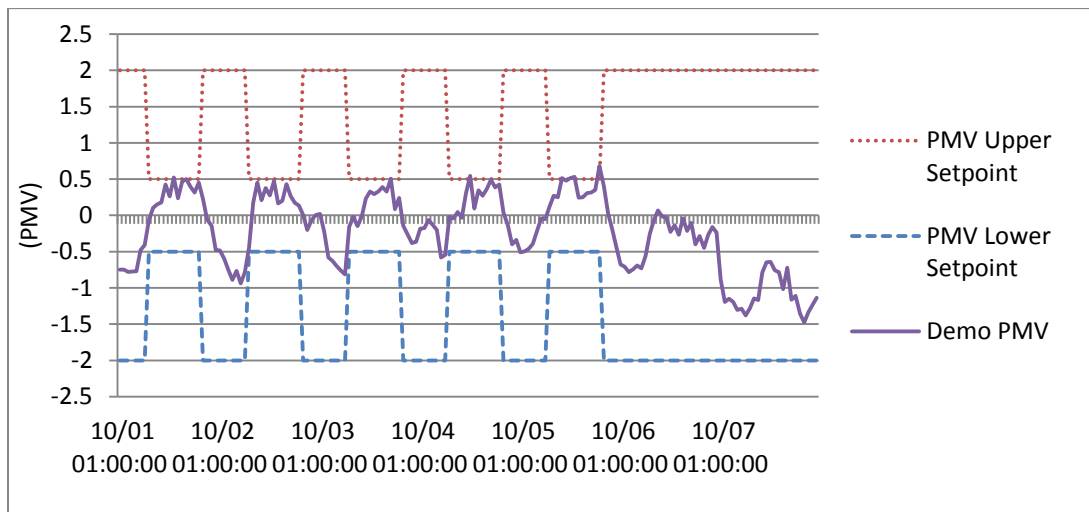


**Figure 96 PMV simulation results of the demo model.**

The last step of running the co-simulation model took 22 hours, and generated one week (168 hours) of simulation results. On average, it takes about seven minutes to run one hour of simulation. The computation time is acceptable for the purpose of real-time building controls.